

DISSERTATION

DESIGN OF CONVERGING  
STEPPED SPILLWAYS

Submitted by

Sherry Lynn Hunt

Civil and Environmental Engineering Department

In partial fulfillment of the requirements

For the Degree of Doctor of Philosophy

Colorado State University

Fort Collins, Colorado

Fall 2008

UMI Number: 3346441

## INFORMATION TO USERS

The quality of this reproduction is dependent upon the quality of the copy submitted. Broken or indistinct print, colored or poor quality illustrations and photographs, print bleed-through, substandard margins, and improper alignment can adversely affect reproduction.

In the unlikely event that the author did not send a complete manuscript and there are missing pages, these will be noted. Also, if unauthorized copyright material had to be removed, a note will indicate the deletion.

**UMI**<sup>®</sup>

---

UMI Microform 3346441

Copyright 2009 by ProQuest LLC.

All rights reserved. This microform edition is protected against unauthorized copying under Title 17, United States Code.

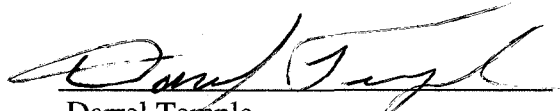
ProQuest LLC  
789 E. Eisenhower Parkway  
PO Box 1346  
Ann Arbor, MI 48106-1346

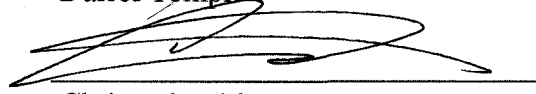
COLORADO STATE UNIVERSITY

October 10, 2008

WE HEREBY RECOMMEND THAT THE DISSERTATION PREPARED UNDER OUR SUPERVISION BY SHERRY LYNN HUNT ENTITLED DESIGN OF CONVERGING STEPPED SPILLWAYS BE ACCEPTED AS FULFILLING IN PART REQUIREMENTS FOR THE DEGREE OF DOCTOR OF PHILOSOPHY.

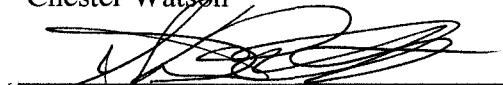
Committee on Graduate Work

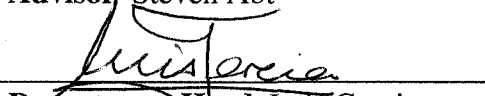
  
\_\_\_\_\_  
Darrel Temple

  
\_\_\_\_\_  
Christopher Thornton

  
\_\_\_\_\_  
Reagan Waskom

  
\_\_\_\_\_  
Chester Watson

  
\_\_\_\_\_  
Advisor: Steven Abt

  
\_\_\_\_\_  
Department Head Luis Garcia

ABSTRACT OF DISSERTATION  
DESIGN OF CONVERGING  
STEPPED SPILLWAYS

Roller compacted concrete (RCC) stepped spillways are growing in popularity for providing overtopping protection for aging watershed dams with inadequate auxiliary spillway capacity and for the construction of new dams. Unobtainable land rights, topographic features, and land use changes caused by urbanization limit the ability to construct new dams or modify the dimensions of existing embankments and spillways. The advantages of stepped spillways are 1) they can be placed over the top of an existing embankment without causing significant changes to the dam or spillway dimensions, 2) they provide considerable energy dissipation in the chute, potentially reducing the size of the stilling basin, and 3) they permit shorter, more efficient, and feasible construction schedules than other design options.

Currently, limited design guidelines are available in the literature for the design of stepped spillways constructed on flat slopes ( $\theta < 30^\circ$ ). Auxiliary spillways are designed to safely pass exceptionally large flood events to the downstream channel. In structural auxiliary spillways, spillway chute and stilling basin training walls are typically designed to prevent overtopping. However, the aspect of converging training walls increases the flow depth in the chute near the

walls, and it changes the hydraulic parameters for designing the stilling basin. To assist with the design of converging stepped spillways having similar design parameters (i.e. chute slope, step height, etc.), a study utilizing a three-dimensional, 1:22 scale physical model was conducted to evaluate the flow characteristics in the spillway. This study is the first known attempt at developing generalized design criteria for converging stepped spillways having vertical training walls.

Conclusions drawn from this study are that as the convergence of the training wall increases the flow depth near the wall also increases. A simplified control volume momentum analysis was used to predict the minimum training wall height necessary to prevent overtopping. The equation developed slightly under-predicted the results. This under-prediction may be a result of the assumptions made in the development of the prediction equation. Other design aids for determining training wall height were developed based on observations with the data. The results of the study will be discussed further herein.

Sherry Lynn Hunt  
Civil and Environmental Engineering Department  
Colorado State University  
Fort Collins, CO 80523  
Fall 2008

## ACKNOWLEDGEMENTS

This research was supported by funds provided by the U. S. Department of Agriculture (USDA), Agricultural Research Service (ARS) and the USDA-Natural Resources Conservation Service (NRCS). I would like to extend my gratitude to Dr. Greg Hanson, Location Coordinator and Research Leader; and Mr. Darrel Temple, retired Location Coordinator and Research Leader of the USDA-ARS Hydraulics Engineering Research Laboratory; for providing the research funds and facilities that made this research possible. The research topic for this dissertation is an outgrowth of specific needs by the NRCS for the rehabilitation of nearly 1,100 aging watershed dams that are expected to use the technology described herein. I would also like to extend my thanks to Mr. Henry McFarland, State Conservation Engineer for the Georgia NRCS and Mr. Bill Irwin, retired NRCS National Design Engineer, for providing research funds and the opportunity for me to carry out this research on behalf of the NRCS.

I would like to express my sincere appreciation to Dr. Steven Abt, my doctoral advisor, for his advice, encouragement, and direction. The countless hours he spent, especially during his wartime duties, reading draft after draft of this dissertation will never be forgotten. He has been a true mentor, and I cannot thank him enough for his endless support throughout my graduate studies at Colorado State University. My gratitude is also extended to Mr. Darrel Temple, my research mentor and doctoral committee member, for his continued support,

guidance, and insight in this project. The countless hours spent with Darrel discussing momentum analysis and the development of equations presented in this dissertation is greatly appreciated. I would also like to thank Dr. Chris Thornton, Dr. Chester Watson, and Dr. Reagan Waskom for serving on my graduate committee and for their time and support throughout this research effort.

I would especially like to thank Mr. Kem Kadavy for his assistance during the construction, testing, and data analysis of this project as well as his continuous support and guidance. My gratitude also goes to Dr. Greg Hanson for his helpful advice and to Mr. Ray Cox for his contributions during the construction phase of this project. The assistance of Mr. David Bevill and Mr. Tyler Selvey during testing and data processing is also greatly appreciated.

My sincere appreciation also goes to the faculty, staff, and students in the Civil Engineering Department for their continued support during my stay at Colorado State University.

Finally, I would like to thank my family, especially my husband, Brad, for his unconditional love and support during this long journey. His patience, encouragement, and belief in my abilities made this work a reality. I also want to thank my little girl, Jaley, for putting up with a crazy mommy during the writing of this dissertation. I also owe a debt of gratitude to my parents, Buddy and Janet Britton, for being a constant source of inspiration. They planted the seeds of self-motivation and desire to learn more, and taught me the true meaning of hard work. To my family, I sincerely dedicate this dissertation.

## TABLE OF CONTENTS

<u>Chapter</u>	<u>Page</u>
ABSTRACT.....	iii
ACKNOWLEDGEMENTS.....	v
LIST OF FIGURES.....	ix
LIST OF TABLES.....	xii
LIST OF SYMBOLS.....	xx
I INTRODUCTION.....	1
Problem Statement.....	1
Goals Objectives.....	5
II LITERATURE REVIEW.....	6
Stepped Spillways.....	6
Function of Stepped Chutes.....	8
Design and Construction of Stepped Spillways.....	8
<i>Spillway Crest</i> .....	11
<i>Stepped Spillway Chute</i> .....	13
<u>Training Walls</u> .....	13
<u>Step Size</u> .....	17
<u>Stepped Spillway Slope</u> .....	18
<i>Stilling Basin</i> .....	19
<i>Summary</i> .....	21
Basic Hydraulic Concepts for Stepped Spillways.....	21
Types of Flow.....	22
<i>Nappe Flow</i> .....	22
<i>Skimming Flow</i> .....	23
<i>Transitional Flow</i> .....	25
Air Entrainment.....	26
Scale Effects Associated with Physical Modeling of Stepped Spillways.....	29

III	THEORY DEVELOPMENT FOR TRAINING WALL	
	HEIGHT DESIGN CRITERIA.....	31
	Modeling and Similitude.....	31
	Momentum Principles.....	34
	Momentum Principles for Open Channel Flow.....	34
	Simplified Momentum Analysis for a Converging RCC Stepped Spillway and Equation Development For Training Wall Height.....	36
IV	EXPERIMENTAL EQUIPMENT.....	43
	Testing Facility.....	43
	Measuring Devices.....	47
V	METHODS AND PROCEDURES.....	52
VI	RESULTS AND DISCUSSION.....	57
	Air Entrainment.....	58
	Stepped Spillway Design for Converging Training Walls.....	62
	General Observations and Trends Captured during Testing through Data Collection and Digital Imagery.....	63
	Training Wall Influence on Flow.....	70
	Evaluation of a Simplified Momentum Equation for Determining Training Wall Height.....	76
	Application of the Simplified Momentum Equation for Determining Minimum Training Wall Height for Converging Stepped Spillways.....	82
	Limitations of the Application of the Simplified Momentum Equation for Predicting Training Wall Height for Converging Stepped Spillways.....	85
VII	SUMMARY OF RESULTS AND CONCLUSIONS.....	87
	REFERENCES.....	90
	APPENDIX A – DATA SUMMARY.....	93
	APPENDIX B – DESIGN EXAMPLE.....	270

## LIST OF FIGURES

<u>FIGURE</u>	<u>PAGE</u>
1.1 RCC stepped spillway under construction.....	4
2.1 a). RCC stepped spillway.....	7
2.1 b). Chute spillway.....	7
2.2 Schematic of a typical RCC stepped spillway.....	10
2.3 a). Ogee crested weir.....	12
2.3 b). Broad crested weir.....	12
2.4 Air entrainment inception point.....	15
2.5 Photographic view of nappe flow.....	23
2.6 Photographic view of skimming flow with injected dye highlighting recirculating vortices within the flow.....	24
3.1 a). Top view of the control volume illustrating that it is perpendicular to the training wall.....	38
3.1 b). Side view of the control volume showing that it is perpendicular to the chute floor.....	38
3.2 Chute profile: Section A-A as shown in Figure 3.1.....	38
3.3 Wall profile C-C as shown in Figure 3.1a.....	39
3.4 Wall profile: Section B-B as shown in Figure 3.1a.....	39
4.1 Aerial view of the USDA-ARS Hydraulic Engineering Research Unit...	43
4.2 Site map of the USDA-ARS Hydraulics Engineering Research Laboratory.....	44
4.3 Photograph of stepped spillway model with 52° convergence.....	44
4.4 Schematic top view of the stepped spillway provided by Golder.....	45
4.5 Schematic profile of the stepped spillway.....	45
4.6 Siphons located in the dam with a 0.46 m (18 inch) diameter pipe tapped into siphon one for flow delivery to the test facility.....	48
4.7 Water supplied to the test facility through a 0.46 m (18 inch) diameter pipe.....	48
4.8 Air-water differential manometer.....	49
4.9 Adjustable overflow weir.....	49
4.10 Water surface profile measurement.....	50
4.11 Air concentration and velocity measurement.....	51
5.1 Pipe for downstream filling of the test basin.....	54
5.2 Strip chart recorder for verification of stabilized inflow.....	54

5.3	Physical model with 52° convergence tested at $q_{\text{proto}} = 7.58 \text{ m}^3/(\text{s}\cdot\text{m})$ (81.6 cfs/ft) and design tailwater.....	55
6.1	Observed inception point and differences in flow characteristics.....	60
6.2	Centerline water surface profiles and water surface profiles near the training wall having a convergence angle of 52° tested under minimum tailwater depth.....	64
6.3	Centerline water surface profiles and water surface profiles near the training wall having a convergence angle of 30° tested under minimum tailwater depth. ....	64
6.4	Centerline water surface profiles and water surface profiles near the training wall having a convergence angle of 15° tested under minimum tailwater depth.....	65
6.5	Flow run-up overtopping the 52° converging training wall with prototype PMF ( $7.58 \text{ m}^3/(\text{s}\cdot\text{m})$ and 81.6 cfs/ft) and minimum tailwater depth.....	65
6.6	Water surface profiles along the training wall with varying convergence angles, PMF ( $7.58 \text{ m}^3/(\text{s}\cdot\text{m})$ and 81.6 cfs/ft), and minimum tailwater depth.....	67
6.7	Flow depth comparison for convergences 15°, 30°, and 52° at station 7.4 m (24.2 ft) for PMF ( $7.58 \text{ m}^3/(\text{s}\cdot\text{m})$ and 81.6 cfs/ft) flow conditions.....	67
6.8	Flow run-up along a 70° converging training wall with prototype 2/3 PMF ( $2.52 \text{ m}^3/(\text{s}\cdot\text{m})$ (27.1 cfs/ft)) and minimum tailwater depth.....	68
6.9	Turbulent flow run-up along a 70° converging training wall with prototype 1/3 PMF ( $2.52 \text{ m}^3/(\text{s}\cdot\text{m})$ (27.1 cfs/ft)) and minimum tailwater depth.....	69
6.10	Turbulent flow impeding on the spillway crest caused by a 70° converging training wall with prototype 1/3 PMF ( $2.52 \text{ m}^3/(\text{s}\cdot\text{m})$ (27.1 cfs/ft)) and minimum tailwater depth.....	69
6.11	Training wall influence observed constant down the spillway chute.....	71
6.12	Cross-sectional profile normalized by critical depth indicating that the training wall influences the flow approximately $1.8d_c$ horizontally away from the training wall for 15° convergence under full PMF ( $7.58 \text{ m}^3/(\text{s}\cdot\text{m})$ and 81.6 cfs/ft) flow.....	72
6.13	Cross-sectional profile normalized by critical depth indicating that the training wall influences the flow approximately $2.9d_c$ away from the training wall for 30° convergence under full PMF ( $7.58 \text{ m}^3/(\text{s}\cdot\text{m})$ and 81.6 cfs/ft) flow.....	72
6.14	Cross-sectional profile normalized by critical depth indicating that the training wall influences the flow approximately $7.3d_c$ away from the training wall for 52° convergence under full PMF ( $7.58 \text{ m}^3/(\text{s}\cdot\text{m})$ and 81.6 cfs/ft) flow.....	73

6.15	Bulking zone width or distance from the wall the training wall influences the flow horizontally normalized by critical depth versus the convergence angle.....	73
6.16	Bulking zone width prediction.....	74
6.17	Flow depth at the training wall normalized by critical depth at the spillway crest versus the normalized distance downstream of the spillway crest.....	75
6.18	Flow depth at the training wall normalized by critical depth at the spillway crest divided by $\sin(\phi)$ for all tested flows versus the normalized distance downstream of the spillway crest.....	76
6.19	Predicted versus measured flow depth near the training wall for a stepped spillway for $\phi$ 's ranging from 0 to 70 degrees.....	78
6.20	Predicted versus measured flow depth near the training wall for a stepped spillway for $\phi$ 's ranging from 0 to 52 degrees.....	79
6.21	$H_{w\text{-measured}}$ versus $H_{w\text{-predicted}}$ for convergences $0^\circ$ , $15^\circ$ , $30^\circ$ , and $52^\circ$ resulting in linear relationships with slopes of 1.0, 1.01, 0.99, and 1.1, respectively.....	81
6.22	$H_{w\text{-measured}}$ versus a corrected $H_{w\text{-predicted}}$ , for convergences ranging from 0 to $52^\circ$ resulting in a linear relationship with a slope of 0.99 and a coefficient of determination of 0.98.....	81

## LIST OF TABLES

<u>TABLE</u>	<u>PAGE</u>
5.1 Summary of Testing Program.....	52
6.1 Calculated distances to inception point and locations of inception point in the spillway as compared to the model observations.....	60
A1. Summary of prototype testing program.....	94
A2. Prototype centerline water surface profile for test # 1.....	95
A3. Model centerline water surface profile for test # 1.....	96
A4. Prototype water surface profile along the right wall looking downstream for test # 1.....	97
A5. Model water surface profiles along the right wall looking downstream for test # 1.....	98
A6. Prototype water surface profile along the left wall looking downstream for test #1.....	99
A7. Model water surface profile along the left wall looking downstream for test #1.....	100
A8. Prototype cross-sectional water surface profile along step 1, station 4.6 m for test #1.....	101
A9. Model cross-sectional water surface profile along step 1, station 4.6 m for test #1.....	102
A10. Prototype cross-sectional water surface profile along step 8, station 11 m for test #1.....	103
A11. Model cross-sectional water surface profile along step 8, station 0.5 m for test #1.....	104
A12. Prototype cross-sectional water surface profile along step 12, station 14.8 m for test #1.....	105
A13. Model cross-sectional water surface profile along step 12, station 0.67 m for test #1.....	106
A14. Prototype cross-sectional water surface profile along step 18, station 20.3 m for test #1.....	107
A15. Model cross-sectional water surface profile along step 18, station 0.92 m for test #1.....	108
A16. Prototype cross-sectional water surface profile along step 21, station 23.1 m for test #1.....	109
A17. Model cross-sectional water surface profile along step 21, station 1.05 m for test #1.....	110

A18. Prototype cross-sectional water surface profile along step 25, station 26.8 m for test #1.....	111
A19. Model cross-sectional water surface profile along step 25, station 1.22 m for test #1.....	112
A20. Prototype centerline water surface profile for test #2.....	113
A21. Model centerline water surface profile for test #2.....	114
A22. Prototype water surface profile along the right wall looking downstream for test #2.....	115
A23. Model water surface profile along the right wall looking downstream for test #2.....	116
A24. Prototype water surface profile along the left wall looking downstream for test #2.....	117
A25. Model water surface profile along the left wall looking downstream for test #2.....	118
A26. Prototype cross-sectional water surface profile at step 1, station 4.6 m for test #2.....	119
A27. Model cross-sectional water surface profile at step 1, station 0.21 m for test #2.....	120
A28. Prototype cross-sectional water surface profile at step 8, station 11 m for test #2.....	121
A29. Model cross-sectional water surface profile at step 8, station 0.5 m for test #2.....	122
A30. Prototype cross-sectional water surface profile at step 12, station 14.8 m for test #2.....	123
A31. Model cross-sectional water surface profile at step 12, station 0.67 m for test #2.....	124
A32. Prototype cross-sectional water surface profile at step 18, station 20.3 m for test #2.....	125
A33. Model cross-sectional water surface profile at step 18, station 0.92 m for test #2.....	126
A34. Prototype cross-sectional water surface profile at step 21, station 23.1 m for test #2.....	127
A35. Model cross-sectional water surface profile at step 21, station 1.05 m for test #2.....	128
A36. Prototype cross-sectional water surface profile at step 25, station 26.8 m for test #2.....	129
A37. Model cross-sectional water surface profile at step 25, station 1.22 m for test #2.....	129
A38. Prototype centerline water surface profile for test #3.....	130
A39. Model centerline water surface profile for test #3.....	131
A40. Prototype water surface profile along the right wall looking downstream for test #3.....	132
A41. Model water surface profile along the right wall looking downstream for test #3.....	133
A42. Prototype water surface profile along the left wall looking downstream for test #3.....	134

A43. Model water surface profile along the left wall looking downstream for test #3.....	135
A44. Prototype cross-sectional water surface profile at step 1, station 4.6 m for test #3.....	136
A45. Model cross-sectional water surface profile at step 1, station 0.21 m for test #3.....	137
A46. Prototype cross-sectional water surface profile at step 8, station 11 m for test #3.....	138
A47. Model cross-sectional water surface profile at step 8, station 0.5 m for test #3.....	139
A48. Prototype cross-sectional water surface profile at step 12, station 14.8 m for test #3.....	140
A49. Model cross-sectional water surface profile at step 12, station 0.67 m for test #3.....	141
A50. Prototype cross-sectional water surface profile at step 18, station 20.3 m for test #3.....	142
A51. Model cross-sectional water surface profile at step 18, station 0.92 m for test #3.....	143
A52. Prototype cross-sectional water surface profile at step 21, station 23.1 m for test #3.....	144
A53. Model cross-sectional water surface profile at step 21, station 1.05 m for test #3.....	145
A54. Prototype cross-sectional water surface profile at step 25, station 26.8 m for test #3.....	146
A55. Model cross-sectional water surface profile at step 25, station 1.22 m for test #3.....	147
A56. Prototype centerline water surface profile for test #4.....	148
A57. Model centerline water surface profile for test #4.....	149
A58. Prototype water surface profile along the right wall looking downstream for test #4.....	150
A59. Model water surface profile along the right wall looking downstream for test #4.....	151
A60. Prototype water surface profile along the left wall looking downstream for test #4.....	152
A61. Model water surface profile along the left wall looking downstream for test #4.....	153
A62. Prototype cross-sectional water surface profile at step 1, station 4.6 m for test #4.....	154
A63. Model cross-sectional water surface profile at step 1, station 0.21 m for test #4.....	155
A64. Prototype cross-sectional water surface profile at step 8, station 11 m for test #4.....	156
A65. Model cross-sectional water surface profile at step 8, station 0.5 m for test #4.....	157
A66. Prototype cross-sectional water surface profile at step 12, station 14.8 m for test #4.....	158

A67. Model cross-sectional water surface profile at step 12, station 0.67 m for test #4.....	159
A68. Prototype cross-sectional water surface profile at step 18, station 20.3 m for test #4.....	160
A69. Model cross-sectional water surface profile at step 18, station 0.92 m for test #4.....	161
A70. Prototype cross-sectional water surface profile at step 21, station 23.1 m for test #4.....	162
A71. Model cross-sectional water surface profile at step 21, station 1.05 m for test #4.....	163
A72. Prototype cross-sectional water surface profile at step 25, station 26.8 m for test #4.....	164
A73. Model cross-sectional water surface profile at step 25, station 1.22 m for test #4.....	165
A74. Prototype centerline water surface profile for test #24.....	166
A75. Model centerline water surface profile for test #24.....	167
A76. Prototype water surface profile along the right wall looking downstream for test #24.....	168
A77. Model water surface profile along the right wall looking downstream for test #24.....	169
A78. Prototype water surface profile along the left wall looking downstream for test #24.....	170
A79. Model water surface profile along the left wall looking downstream for test #24.....	171
A80. Prototype cross-sectional water surface profile at step 1, station 4.6 m for test #24.....	172
A81. Model cross-sectional water surface profile at step 1, station 0.21 m for test #24.....	173
A82. Prototype cross-sectional water surface profile at step 8, station 11 m for test #24.....	174
A83. Model cross-sectional water surface profile at step 8, station 0.5 m for test #24.....	175
A84. Prototype cross-sectional water surface profile at step 12, station 14.8 m for test #24.....	176
A85. Model cross-sectional water surface profile at step 12, station 0.67 m for test #24.....	177
A86. Prototype cross-sectional water surface profile at step 18, station 20.3 m for test #24.....	178
A87. Model cross-sectional water surface profile at step 18, station 0.92 m for test #24.....	179
A88. Prototype cross-sectional water surface profile at step 21, station 23.1 m for test #24.....	180
A89. Model cross-sectional water surface profile at step 21, station 1.05 m for test #24.....	181
A90. Prototype cross-sectional water surface profile at step 25, station 26.8 m for test #24.....	182

A91. Model cross-sectional water surface profile at step 25, station 1.22 m for test #24.....	183
A92. Prototype centerline water surface profile for test #25.....	184
A93. Model centerline water surface profile for test #25.....	185
A94. Prototype water surface profile along the right wall looking downstream for test #25.....	186
A95. Model water surface profile along the right wall looking downstream for test #25.....	187
A96. Prototype water surface profile along the left wall looking downstream for test #25.....	188
A97. Model water surface profile along the left wall looking downstream for test #25.....	189
A98. Prototype cross-sectional water surface profile at step 1, station 4.6 m for test #25.....	190
A99. Model cross-sectional water surface profile at step 1, station 0.21 m for test #25.....	191
A100. Prototype cross-sectional water surface profile at step 8, station 11 m for test #25.....	192
A101. Model cross-sectional water surface profile at step 8, station 0.5 m for test #25.....	193
A102. Prototype cross-sectional water surface profile at step 12, station 14.8 m for test #25.....	194
A103. Model cross-sectional water surface profile at step 12, station 0.67 m for test #25.....	195
A104. Prototype cross-sectional water surface profile at step 18, station 20.3 m for test #25.....	196
A105. Model cross-sectional water surface profile at step 18, station 0.92 m for test #25.....	196
A106. Prototype cross-sectional water surface profile at step 21, station 23.1 m for test #25.....	197
A107. Model cross-sectional water surface profile at step 21, station 1.05 m for test #25.....	198
A108. Prototype cross-sectional water surface profile at step 25, station 26.8 m for test #25.....	199
A109. Model cross-sectional water surface profile at step 25, station 1.22 m for test #25.....	200
A110. Prototype centerline water surface profile for test #26.....	201
A111. Model centerline water surface profile for test #26.....	202
A112. Prototype water surface profile along the right wall looking downstream for test #26.....	203
A113. Model water surface profile along the right wall looking downstream for test #26.....	204
A114. Prototype water surface profile along the left wall looking downstream for test #26.....	205
A115. Model water surface profile along the left wall looking downstream for test #26.....	206

A116. Prototype cross-sectional water surface profile at step 1, station 4.6 m for test #26.....	207
A117. Model cross-sectional water surface profile at step 1, station 0.21 m for test #26.....	208
A118. Prototype cross-sectional water surface profile at step 8, station 11 m for test #26.....	209
A119. Model cross-sectional water surface profile at step 8, station 0.5 m for test #26.....	210
A120. Prototype cross-sectional water surface profile at step 12, station 14.8 m for test #26.....	211
A121. Model cross-sectional water surface profile at step 12, station 0.67 m for test #26.....	212
A122. Prototype cross-sectional water surface profile at step 18, station 20.3 m for test #26.....	213
A123. Model cross-sectional water surface profile at step 18, station 0.92 m for test #26.....	214
A124. Prototype cross-sectional water surface profile at step 21, station 23.1 m for test #26.....	215
A125. Model cross-sectional water surface profile at step 21, station 1.05 m for test #26.....	216
A126. Prototype cross-sectional water surface profile at step 25, station 26.8 m for test #26.....	217
A127. Model cross-sectional water surface profile at step 25, station 1.22 m for test #26.....	218
A128. Prototype centerline water surface profile for test #27.....	219
A129. Model centerline water surface profile for test #27.....	220
A130. Prototype water surface profile along right wall looking downstream for test #27.....	221
A131. Model water surface profile along right wall looking downstream for test #27.....	222
A132. Prototype cross-sectional water surface profile at step 1, station 4.6 m for test #27.....	223
A133. Model cross-sectional water surface profile at step 1, station 0.21 m looking downstream for test #27.....	224
A134. Prototype cross-sectional water surface profile at step 8, station 11 m for test #27.....	225
A135. Model cross-sectional water surface profile at step 8, station 0.5 m for test #27.....	226
A136. Prototype cross-sectional water surface profile at step 12, station 14.8 m for test #27.....	227
A137. Model cross-sectional water surface profile at step 12, station 0.67 m for test #27.....	228
A138. Prototype cross-sectional water surface profile at step 18, station 20.3 m for test #27.....	229
A139. Model cross-sectional water surface profile at step 18, station 0.92 m for test #27.....	230

A140. Prototype cross-sectional water surface profile at step 21, station 23.1 m for test #27. ....	231
A141. Model cross-sectional water surface profile at step 21, station 1.05 m for test #27.....	232
A142. Prototype cross-sectional water surface profile at step 25, station 26.8 m for test #27.....	233
A143. Model cross-sectional water surface profile at step 25, station 1.22 m for test #27. ....	234
A144. Prototype centerline water surface profile for test #32.....	235
A145. Model centerline water surface profile for test #32.....	236
A146. Prototype centerline water surface profile along right wall looking downstream for test #32.....	237
A147. Model centerline water surface profile along right wall looking downstream for test #32.....	238
A148. Prototype centerline water surface profile along left wall looking downstream for test #32.....	239
A149. Model centerline water surface profile along left wall looking downstream for test #32. ....	240
A150. Prototype cross-sectional water surface profile at step 1, station 4.6 m for test #32. ....	241
A151. Model cross-sectional water surface profile at step 1, station 0.21 m for test #32.....	242
A152. Prototype cross-sectional water surface profile at step 8, station 11 m for test #32.....	243
A153. Model cross-sectional water surface profile at step 8, station 0.5 m for test #32.....	244
A154. Prototype cross-sectional water surface profile at step 12, station 14.8 m for test #32.....	245
A155. Model cross-sectional water surface profile at step 12, station 0.67 m for test #32.....	246
A156. Prototype cross-sectional water surface profile at step 18, station 20.3 m for test #32. ....	247
A157. Model cross-sectional water surface profile at step 18, station 0.92 m for test #32. ....	248
A158. Prototype cross-sectional water surface profile at step 21, station 23.1 m for test #32. ....	248
A159. Model cross-sectional water surface profile at step 21, station 1.05 m for test #32.....	249
A160. Prototype cross-sectional water surface profile at step 25, station 23.1 m for test #32. ....	249
A161. Prototype cross-sectional water surface profile at step 25, station 1.22 m for test #32. ....	250
A162. Prototype centerline water surface profile for test #33.....	250
A163. Model centerline water surface profile for test #33.....	251
A164. Prototype water surface profile along the right wall looking downstream for test #33.....	252

A165. Model water surface profile along the right wall looking downstream for test #33.....	253
A166. Prototype water surface profile along the left wall looking downstream for test #33.....	254
A167. Model water surface profile along the left wall looking downstream for test #33.....	255
A168. Prototype cross-sectional water surface profile at step 1, station 4.6 m for test #33.....	256
A169. Model cross-sectional water surface profile at step 1, station 0.21 m for test #33.....	257
A170. Prototype cross-sectional water surface profile at step 8, station 11 m for test #33.....	258
A171. Model cross-sectional water surface profile at step 8, station 0.5 m for test #33.....	259
A172. Prototype cross-sectional water surface profile at step 12, station 14.8 m for test #33.....	260
A173. Model cross-sectional water surface profile at step 12, station 0.67 m for test #33.....	261
A174. Prototype cross-sectional water surface profile at step 18, station 20.3 m for test #33.....	262
A175. Model cross-sectional water surface profile at step 18, station 0.92 m for test #33.....	263
A176. Prototype cross-sectional water surface profile at step 21, station 23.1 m for test #33.....	264
A177. Model cross-sectional water surface profile at step 21, station 1.05 m for test #33.....	264
A178. Prototype cross-sectional water surface profile at step 25, station 26.8 m for test #33.....	265
A179. Prototype cross-sectional water surface profile at step 25, station 1.22 m for test #33.....	265
A180. Prototype centerline bed surface profile.....	266
A181. Model centerline bed surface profile.....	267
A182. Prototype bed surface profile along the right wall looking downstream.....	268
A183. Model bed surface profile along the right wall looking downstream.....	268
A184. Prototype bed surface profile along the left wall looking downstream.....	269
A185. Model bed surface profile along the left wall looking downstream.....	269
B1. Centerline water surface profile.....	271
B2. Stepped spillway chute bed surface profile.....	272

## LIST OF SYMBOLS

A	area of the control volume
C	mean air concentration
$C_l$	coefficient associated with the control volume shape
d	centerline flow depth measured mutually perpendicular to the velocity vector and the water surface in the undisturbed section of the chute
d.s.	downstream
$d_b$	bulked flow depth
$d_c$	critical depth
$d_{ds}$	horizontal distance downstream from the center point of the crest
$d_w$	predicted flow depth at the wall measured mutually perpendicular to the velocity vector along the training wall and the local water surface of the chute
f	friction factor
F	Froude number
$F_f$	total external force of friction and resistance acting along the surface of contact between the water and the channel
$F_*$	Froude number in terms of roughness height
$\bar{F}$	forces applied to the control volume
$\bar{F}_{cvt}$	pressure force on the control volume in the undisturbed flow
$\bar{F}_{pw}$	pressure force on the wall
$\bar{F}_w$	force on the control volume associated with the weight of water

$g$	gravitational constant
$h$	step height
$h_d$	training wall height
$H_{\text{dam}}$	dam height
$H_o$	maximum head available
$H_w$	training wall height measured above the surface formed by connecting the steps
$H_{w\text{-measured}}$	observed training wall height measured above the surface formed by connecting the steps
$H_{w\text{-predicted}}$	predicted training wall height measured above the surface formed by connecting the steps
$h_{90, u}$	uniform characteristic mixing depth
$\ell$	characteristic length
$L_i$	inception point location
$\bar{M}$	momentum flux into the control volume through the upstream face
$P$	pressure force
$Q$	discharge
$q_{\text{proto}}$	prototype unit discharge
$q_w$	unit discharge
$TW$	tailwater
$TW_{\text{proto}}$	prototype tailwater
$\hat{u}_{\text{cf}}$	unit vector perpendicular to the chute face
$\hat{u}_{\text{cvi}}$	unit vector representing the upstream face of the control volume
$\hat{u}_{\text{pw}}$	unit vector lying in the plane of the wall perpendicular to the velocity vector along the wall

$\hat{U}_{vel}$	unit vector parallel to the velocity down the chute face
$\hat{U}_{vw}$	unit vector representing the velocity along the wall, which is perpendicular to the wall vector and is the vector entering the control volume on the upstream side and exiting the control volume on the downstream side
$\hat{U}_{wall}$	unit vector representing wall face
$v$	centerline velocity at the water surface
$V_{water}$	volume of water
$W$	weight of water
$w$	unit weight of water
$X_m, Y_m, Z_m$	model coordinates
$X_p, Y_p, Z_p$	prototype coordinates
$\beta$	momentum coefficient
$\Delta H$	total head loss
$\phi$	convergence angle
$\gamma$	specific weight of water
$\lambda_e$	length scale
$\mu$	dynamic viscosity
$\eta$	safety factor
$\theta$	spillway chute slope
$\rho$	fluid density
$\sigma$	surface tension
$\psi$	angle formed by the x-y plane with the vector parallel to the chute floor and perpendicular to the training wall

$\psi_2$

angle formed by the x-y plane with the vector lying in the plane of the wall and the chute floor

## **CHAPTER 1**

### **INTRODUCTION**

#### **Problem Statement**

The Congressional passage of the Flood Control Act of 1944 and the Watershed Protection and Flood Control Act of 1953 provided the necessary funds to the United States Department of Agriculture (USDA) Natural Resources Conservation Service (NRCS) to assist in the design and construction of more than 11,000 small watershed dams (USDA-NRCS, 2005). These dams offer over \$1.5 billion in benefits each year by providing flood control, wildlife habitat, recreation, irrigation and livestock water, and municipal and rural water supplies. Most of these dams were constructed with a planned service life of 50 years, and in recent reports, the NRCS declared that more than half of those dams are more than 30 years old (USDA-NRCS, 2005). In fact, it is projected that over 3,000 of these structures will reach the end of their planned service life by 2016 (USDA-NRCS, 2005).

In recognition of these aging structures, United States Congress passed the Watershed Rehabilitation Amendments of 2000, which amended the Watershed Protection and Flood Prevention Act of 1953 (USDA-NRCS, 2005). Similar in some ways to the previous legislation passed, these amendments authorized the NRCS to provide technical and financial assistance to watershed

project sponsors for the rehabilitation of these aging structures. Rehabilitation in the dam safety community is defined as the change, improvement, repair, and/or restoration of the planned service life of an existing embankment so that these structures continue to function properly and safely. If ignored, these dams could place life and property at risk.

Due to the age of the embankments, some dams begin to exhibit dam safety concerns. For example, some dams show evidence of sediment deposition in flood pools, which in turn limits the flood capacity of the reservoir and could lead to inadequate spillway capacity or even overtopping of the embankment in extreme cases. Additionally, several of these structures were originally constructed in rural environments, but residential communities and infrastructure now surround them. In these situations, the hydrology and flood storage of the dam is affected, and hazard classification changes are often required. The hazard classification of dams is based on the potential loss of life and property damage that may occur during a flood event. As described, a single or combination of problems with the aging embankment often leads to inadequate spillway capacity, one of the key deficiencies for these structures. The function of the spillway is to convey flow from extreme flood events downstream with limited property damage and/or loss of life.

Options are available to design engineers for earth dam rehabilitation including 1) raising the dam, 2) increasing the auxiliary spillway capacity, 3) providing overtopping protection (i.e. structurally), 4) allowing limited overtopping of the existing earth embankment, 5) combining any of the previously mentioned

options, and/or 6) decommissioning the structure. Selecting the preferred design option depends on the site conditions and the economical impact (i.e. development within the watershed and right-of-way issues) related to each of the options. Providing additional spillway capacity is often the preferred choice in dam rehabilitation. The alternatives available for providing additional spillway capacity are 1) widening the existing auxiliary spillway, 2) providing multiple auxiliary spillways, and/or 3) allowing the embankment to overtop. Widening the existing auxiliary spillway and/or providing multiple auxiliary spillways are in many cases limited by development within the watershed and/or right-of-way issues. Allowing the embankment to overtop is frequently the only practical option available for engineers to address the dam safety and rehabilitation of the structure.

Because of the threat of failure, overtopping embankments is generally restricted to those that are protected by a structurally sound design such as a roller compacted concrete (RCC) stepped spillway (Figure 1.1) or other lined chutes. Factors including flow duration, flow depth, downstream slope, and the erodibility of the embankment materials may result in serious erosion and/or failure of the embankment if the embankment is left unprotected. RCC stepped spillways are becoming a more viable option in dam rehabilitation and the construction of new dams because of the added protection provided, spillway capacity available, energy dissipation created, and shorter, more efficient construction schedules offered (Chanson, 2002 and Portland Cement Association, 2006).

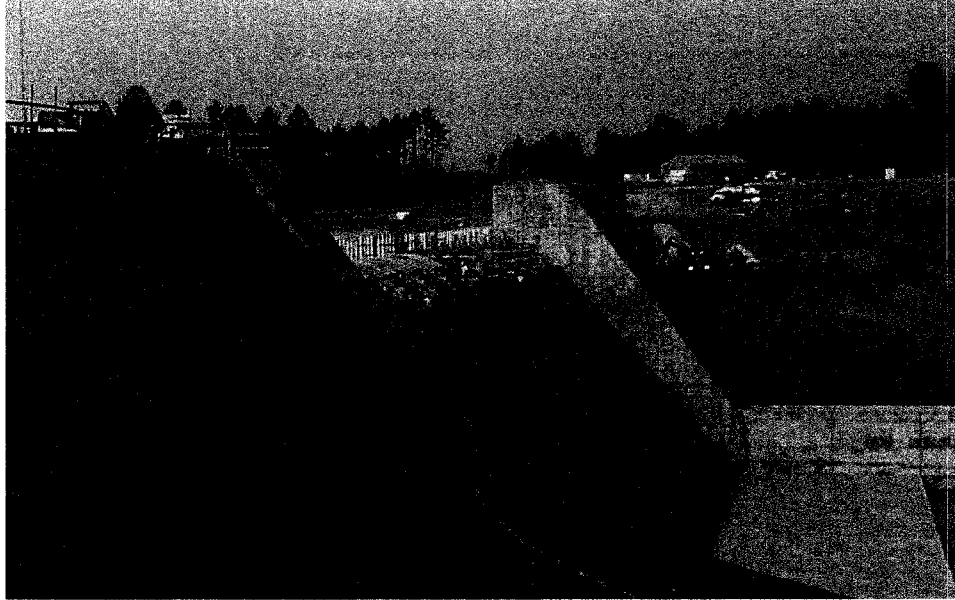


Figure 1.1 RCC stepped spillway under construction.

Research interest among the engineering community has increased due to the potential number of RCC stepped spillways projected for implementation. Topics of interest include energy dissipation characteristics on flat slopes (i.e. typically defined as slopes  $< 30^\circ$ ) versus steep slopes (i.e. often characterized as slopes  $> 30^\circ$ ), high unit discharges (i.e. typically  $> 14 \text{ m}^3/(\text{s}\cdot\text{m})$  (150 cfs/ft)) versus low flow capacities (i.e. defined as  $< 14 \text{ m}^3/(\text{s}\cdot\text{m})$  (150 cfs/ft)), chute convergence; and variable step heights. Previous research studies addressed the design of straight, steep (i.e.  $> 30^\circ$ ), stepped chutes under low flow conditions (i.e.  $< 14 \text{ m}^3/(\text{s}\cdot\text{m})$  (150 cfs/ft)), such that the flow is highly turbulent and air entrained. Research conducted thus far is limited in the investigation of the trials and tribulations associated with the design of converging stepped spillways located on relatively flat spillway chute slopes ( $< 30^\circ$ ).

## **Goals Objectives**

The goal of this research is to provide design guidance for the application of converging stepped spillway technology. Specifically, this study examines the hydraulic performance of converging stepped spillways under a conservative probable maximum design. The specific objective of this research is to develop a predictive equation to approximate the flow depth near the training walls of converging and non-converging stepped spillways. The predictive equation will provide design engineers with a minimum training wall design height criterion for containing the maximum expected flood event. The application of this predictive equation is limited to non-air entrained flows or flows where the turbulent boundary layer reaching the free surface is not well established. This research can potentially lead to improved design criteria and an enhanced understanding for stepped spillway implementation.

**CHAPTER II**  
**LITERATURE REVIEW**  
**Stepped Spillways**

A spillway is a channel or passageway around or over a dam that conveys or releases excess water downstream without causing major damage to the dam. A spillway must be capable of discharging extreme flood events in a safe manner that would limit the loss of life and damage to property. Several types of spillways exist including chute spillways, straight-drop spillways, stepped spillways, and vegetated auxiliary spillways. The selection of a spillway for a specific dam and reservoir is typically based on the discharge requirements, topography, geology, dam safety, and the feasibility of the project.

Many of the aging earthen embankments were originally constructed to protect agricultural land from flooding. Through the years, these embankments have been engulfed by infrastructure and urbanization, causing a change in hazard classification. In these situations, the embankment dams are still necessary for flood protection, so removing the dam is not an option. Increasing the flood storage or the spillway capacity is often required. Flood storage can be increased by raising the top of dam, yet the design engineer and the public must live with the consequences. Raising the top of dam can lead to increased flooding upstream of the embankment. Land owners must make sacrifices as well by giving up some property rights. Making modifications to the existing

auxiliary spillway is often limited by topography, infrastructure, and/or land right constraints.

Stepped spillways for NRCS sponsored structures are becoming a popular choice for addressing rehabilitation and dam safety issues related to hazard classification changes. Stepped spillways are typically selected over other designs to increase spillway capacity because stepped spillway provides a safe and economic means for conveying extreme flood events over the dam. In many instances, these structures can be placed over the existing embankment without the requirement of additional land rights. A stepped spillway is similar to a chute spillway in that it conveys flow over the spillway crest down a steep-sloped, open chute into an outlet energy dissipation basin. The major difference between a stepped spillway (Figure 2.1a) and a chute spillway (Figure 2.1b) is that the stepped spillway provides a stepped surface within the open chute whereas a chute spillway consists of a smooth open chute. The steps in the spillway provide energy dissipation of the flow, and thereby reduce the energy dissipation requirements for the outlet basin.

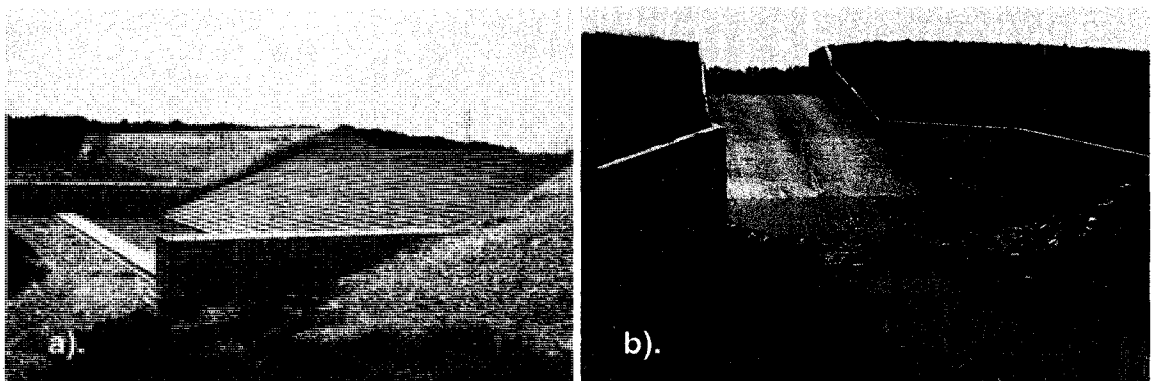


Figure 2.1 a). RCC stepped spillway and b). Chute spillway.

This chapter is intended to present comprehensive information about stepped spillways. The following subsections provide details about the function of stepped spillways or stepped chutes throughout history, the design and construction of stepped spillways, the basic hydraulic concepts of stepped spillways, and the scale effects associated with modeling stepped spillways.

### **Function of Stepped Chutes**

Throughout history, stepped channels have served in a variety of capacities including canals for irrigation water; spillways for flood control structures; aesthetically, pleasing fountain displays; and the creation of waterpower. In fact, stepped surfaces for hydraulic applications dates back to 1300 B. C. in Akarnania, Greece, where the world's oldest stepped spillway can be found (Chanson, 2002). The most common use of stepped chutes today is for spillway design and storm water runoff systems (Chanson, 2002).

### **Design and Construction of Stepped Spillways**

Little design guidance is available for stepped spillways, particularly those constructed on relatively flat slopes of less than  $30^\circ$  and those that converge due to landscape and/or land right concerns. Most of these designs rely on the experience of the design engineer of what has worked in the past. Safety is key for developing design for these structures as well.

Roller compacted concrete (RCC) is typically the material of choice over other construction materials like conventional concrete or gabion rock baskets when building stepped structures. The advantages of RCC over conventional concrete are 1) steps are a "natural" feature of construction, 2) its ability to be

placed by conventional paving equipment, 3) its drier than usual mix of cement, water and aggregates allows it to be placed without the use of forms and reinforced steel while allowing it to have similar strength characteristics to conventional concrete, and 4) the economical feasibility of the material and its placement permits shorter than usual construction schedules to be met (Portland Cement Association, 2002). Likewise, RCC has advantages over gabion rock baskets. Gabion rock baskets are very labor intensive, and implementing gabion baskets are often not practical.

There are three key components in designing stepped spillways: the spillway crest; the stepped spillway chute including the training walls, step sizes, spillway slope, and spillway shape; and the stilling basin and downstream channel stabilization materials. Figure 2.2 illustrates a schematic of a typical stepped spillway and depicts the key features of the spillway. The stepped spillway crest is typically an uncontrolled overflow crest that automatically releases excess water whenever the reservoir water surface rises above the crest level. The stepped spillway chute is the section of the spillway that consists of an open channel extending from the spillway crest down the slope of the dam, or some defined slope, to the stilling basin at the base. The stepped spillway chute has several design features including training walls, step size, and spillway slope. Training walls are defined as the walls that extend from the outer edges of the spillway entrance down the outer sides of the spillway chute to the stilling basin. Training walls are typically designed to retain some specific flood event such as the probable maximum flood (PMF). The variables that may impact

training wall sizing include the discharge through the spillway or flow depth, step height, spillway slope, spillway shape (i.e. converging or non-converging), and flow aeration. For example, step height, spillway slope, and spillway shape (i.e. converging or straight) can affect the amount of energy dissipated in the spillway, and thereby affect the flow depth at the training wall. Additionally, these spillway chute characteristics may have an effect on other hydraulic parameters that are necessary for designing the energy dissipating stilling basin and the downstream channel protection. The stilling basin is a structure meant to dissipate the energy of the flow exiting the spillway chute before the flow is allowed to discharge and return to the downstream channel.

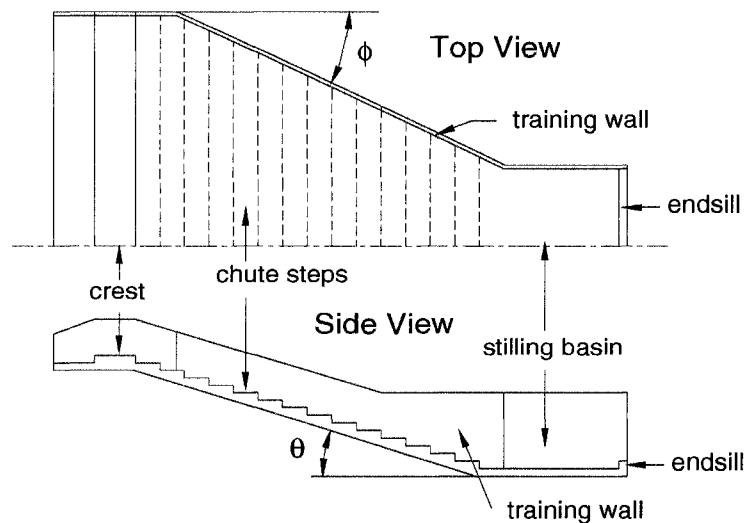


Figure 2.2 Schematic of a typical RCC stepped spillway.

The specific design of each of these key stepped spillway features will be further discussed in subsequent sections; however, some of the factors that have an effect on the design of the stepped spillway that should be identified include

- 1) the hydraulic parameters necessary to design each element

- 2) the techniques and equipment used to construct each of the components
- 3) the public and environmental safety of conveying flow through the stepped spillway
- 4) the public safety of the stepped spillway when not in use
- 5) and the topography and infrastructure surrounding the spillway.

Additional information concerning these influencing factors of the stepped spillway design will be provided.

### ***Spillway Crest***

The stepped spillway crest is most commonly an uncontrolled overflow crest that releases excess water whenever the reservoir water surface rises above the crest level. Stepped spillways are generally constructed with ogee shaped crested weirs or broad crested weirs (Figure 2.3a and 2.3b) (Chanson, 2002). A weir is a structure used for measuring or regulating the flow of water through a spillway. An ogee shaped weir, otherwise known as an S-shaped weir, is designed such that the upper curve of the weir conforms to the underneath profile of the nappe (Figure 2.3a). A broad crested weir is a long raised overflow crest that is normally shaped as a flat horizontal block (Figure 2.3b). The selection of the crest shape is based on a balance of cost, construction, maintenance, and safety. Most often, the shape of the spillway crest is ogee shaped because it provides the most optimum and efficient discharge of the flow down the chute.

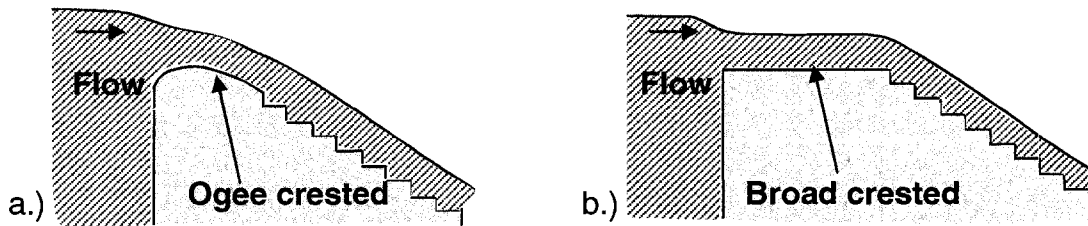


Figure 2.3 a.) Ogee crested weir and b.) Broad crested weir (not to scale).

Many factors including the effective length of the crest, the approach depth, the approach velocity, and the limitations of spillway location have some bearing on the selection of the spillway crest. The effective length of the crest may be affected by piers and abutments, causing side contractions of the overflow. If piers and abutments are manipulating the flow, then the effective length of the crest will be less than the actual length of the crest. The flow over an ogee shaped crested weir typically glides over the crest, allowing it to attain near-maximum discharge efficiency with lower approach depths than other types of crests (United States Bureau of Reclamation (USBR), 1973). A broad shaped crest is found to reduce the efficiency of discharge; whereas, a sharper shaped crest section creates negative pressure effects that will increase the effective head or the approach depth over the crest, and thereby increase the discharge. Since maximum discharge efficiency is achieved with an ogee crested weir, most uncontrolled spillways will have these types of crest sections (USBR, 1973).

Many factors play a role in the selection of the type or design of the spillway crest section. These factors include site limitations of where the spillway is to be placed and simplicity and feasibility of the design. For instance, an ogee

crested approach section may be preferred for spillways located in highly urbanized settings because it requires a lower approach depth over the crest in order to achieve the maximum discharge as compared to other crest types (Chanson, 2002). Selecting a broad crested weir over an ogee crested approach can potentially increase the flooding in the upper watershed because it requires a higher approach depth as compared to an ogee crested weir. A broad crested weir is normally selected for the design over other alternatives due to the ease of construction and simplicity of its design.

### ***Stepped Spillway Chute***

The stepped spillway chute is an open channel that extends from spillway crest down the slope of the dam or down another defined slope to the entrance of the stilling basin usually located at the toe of the dam. The stepped spillway chute has several design features including training walls, step size, and spillway slope. The components of the stepped spillway are further described in the following sub-sections.

### **Training Walls**

Spillway training walls extend from the outside edges of the spillway entrance (i.e. crest) down the outside edges of the spillway chute to the stilling basin. The training walls are sufficiently high to contain an extreme flood event. Factors affecting the height of the training walls are the flow depth/discharge, the aeration or flow bulking in the water, the convergence of the training walls, step height, and spillway chute slope.

Flow bulking is the term attributed to the air entrainment within the flow that causes an increase in flow depth. An example of the air entrainment within the flow is the visually observed “white water” action above the normal flow depth, but it can occur prior to this obvious disturbance in the flow. Sorenson (1985) found that the non-aerated flow depth down the chute decreases as the flow descends down the chute until it reaches the point of impacting air entrained flow. As the non-aerated flow intersects the aerated flow, the depth continually increases until reaching the toe of the spillway (Sorenson, 1985). Chanson (2002) further explains this flow interaction through the concept of an air entrainment inception point. The inception point of air entrainment is a characteristic term used to describe the location where the turbulent boundary layer reaches the free surface. Figure 2.4 illustrates the inception point concept. Chanson (2002) defines the boundary layer as the thin layer of fluid near the boundary surface, in this case the spillway surface, that has a changing velocity of zero near the spillway surface to a free-stream value velocity as it moves up through the flow profile. The boundary layer is characterized as turbulent when the friction on the spillway surface creates unsteady flows in the form of eddies or vortices within the boundary layer. Air entrainment inception point and the variables involved in its determination will be discussed in further detail in the sub-section entitled “Basic Hydraulic Concepts of Stepped Spillways.”

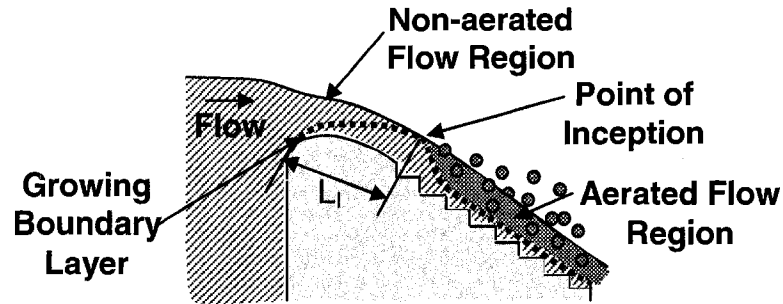


Figure 2.4 Air entrainment inception point.

Although flow bulking can occur prior to the turbulent boundary layer reaching the free surface, the majority of flow bulking can be visually observed during a stepped spillway flow event as “white water” action in the flow. Flow bulking is related to the flow aeration, discharge, step height, spillway convergence, and spillway chute slope; all factors necessary for determining the proper training wall height to contain the flow down the chute. Boes and Hager (2003a) relate each of these terms with exception of spillway convergence to the training wall height. Boes and Minor (2002) and Boes and Hager (2003b) propose that the training wall design height ( $h_d$ ) is a function of a safety factor ( $\eta$ ) ranging from 1.2 to 1.5 (dependent on the erosion of the downstream face of the spillway) and the uniform characteristic mixing depth ( $h_{90,u}$ ). The uniform characteristic mixing depth is a function of step height ( $h$ ), unit discharge ( $q_w$ ), and spillway slope ( $\theta$ ). Boes and Hager (2003b) propose the training wall design height to be written as follows:

$$h_d = \eta(h_{90,u}) \quad (2.1)$$

where:  $h_d$  = training wall design height,  $\eta$  = safety factor, and  $h_{90,u} = 0.50s[(q_w/\{g(\sin \theta h^3)\}^{0.5})^{(0.1\tan\theta+0.5)}$ . Equation 2.1 was developed for non-

converging stepped spillway designs, and it is a starting point for engineers faced with designing these structures.

The convergence of the training walls has an effect in determining the training wall height (Hanna and Pugh, 1997; Robinson, et al. 1998; Hunt, et al. 2005 and 2006; Hunt, et al. 2008; Woolbright, et al. 2008). The convergence angle of the training walls is measured in the x-y plane such that an angle of zero indicates that the training walls are parallel to the flow (Figure 2.2). The effects convergence has on the training wall height are relatively unknown except for a few specific model studies conducted. Robinson et al. (1998) and Hanna and Pugh (1997) evaluated converging stepped spillways. Robinson, et al. (1998) conducted both two- and three-dimensional physical model studies on a steep (0.7H:1V), stepped chute to be located at the Randleman Lake Dam in North Carolina. The three-dimensional model evaluated vertical training walls with convergence angles of 0°, 20.9°, and 32.5°, respectively. Robinson, et al. (1998) concluded that the hydraulic performance of the converging spillway was satisfactory for the given flow and tailwater conditions. Additional findings showed that as the degree of convergence increased, the flow depth at the wall increased. Consequently, the findings indicate that as flow convergence increased; the training wall height necessary to contain the design flow increased.

Hanna and Pugh (1997) conducted research on a relatively steep (0.8H:1V) spillway with vertical training walls converging at 16°. Flow depths at the training walls were among the measurements taken by Hanna and Pugh

(1997) during the study. However, they recognized that the Froude scaling used in their modeling approach could not accurately simulate the expected aeration in the flow because of viscous forces and surface tension effects. To address these influences, Hanna and Pugh (1997) determined the bulked or aerated flow depth in the spillway using a procedure developed by the United States Bureau of Reclamation (USBR) (Falvey, 1980). The aerated (bulked) flow depth is based on the mean air concentration and the non-aerated flow depth measured in stepped spillway model such that

$$d_b = \frac{1}{(1-C)} d \quad (2.2)$$

where  $d_b$  = bulked flow depth,  $C$  = mean air concentration, and  $d$  = measured flow depth. The air concentration is described in the USBR Engineering Monograph No. 41 (Falvey, 1980) as the air concentration related to some distance down the spillway slope. The bulked flow depth resolved by Equation 2.2 indicates the required training wall height necessary to prevent overtopping (Hanna and Pugh, 1997). In this particular case, the bulked flow depth was expected to be higher than the flow depth actually observed and measured in the physical model. Consequently, this increased flow depth resulted in an increase of the training wall height essential to prevent overtopping.

### **Step Size**

Step size in the spillway chute can play a critical role in the energy dissipation of the flow. Step size (i.e. height) for stepped spillway chute design is often based on the construction technique and feasibility rather than its ability to dissipate energy (Chanson, 2002 and Frizell, 2005). For this reason, most

operating stepped spillways constructed today will have step heights ranging from 0.3 m (1 ft) to 0.91 m (3 ft); however, some stepped spillways have larger step heights due to safety concerns.

Several physical model studies, primarily on steep ( $\theta > 30^\circ$ ) stepped spillway applications, have been conducted to evaluate the effect the step height has on the energy dissipation of the flow. Studies by Robinson, et al. (1998); Rice and Kadavy (1996); and Rice and Kadavy (1997) have indicated that the step size had little impact on the amount of energy dissipated. However, according to Chanson (2002), stepped spillways with large steps are expected to create more energy dissipation as compared to stepped spillways with small steps designed for the same flood event.

### **Stepped Spillway Slope**

The stepped spillway slope is another key parameter in the stepped spillway design. The spillway slope is the angle created by taking the arctangent of the ratio of the vertical height of the spillway to the horizontal distance between the spillway crest and the spillway toe (Figure 2.2). The spillway slope is often dictated by the location constraints and the foundation underlying the spillway. For example, if the stepped spillway is being placed over an existing embankment, then the slope will take on the slope of the existing downstream face of the embankment if the foundation is suitable for construction. If the stepped spillway is new, then the slope may be dictated by available land rights, existing topography, expected flood inundation areas, and/or soil/geology foundation materials.

The spillway slope may have a significant affect on other design components of the spillway. For instance, the slope can play a role in the development of air-entrained flow. Spillway slope is a critical element in determining the location of the inception point of air-entrained flow; and therefore, it may provide insight on whether flow bulking should be considered in the design of the training walls. The variables involved for calculating the air entrainment inception point location will be discussed in further details in subsequent sections.

### ***Stilling Basin***

To reduce the attack on the downstream channel, stilling basins or other hydraulic jump basins (Figure 2.2) are used to reduce the exit velocity from the spillway to a calming state (USBR, 1973). The jump created in the stilling basin has distinct characteristics that can be related to the Froude number,  $v/(gd)^{0.5}$ ; unit discharge,  $q_w$ ; the kinetic flow factor,  $v^2/gd$ ; or critical depth,  $d_c$  (USBR, 1973). Currently, little is known about designing stilling basins for stepped spillways; except that a non-converging stepped spillway can reduce the size of the energy dissipating stilling basin when compared to a stilling basin designed for a non-converging smooth spillway (Rice and Kadavy, 1996; Rice and Kadavy, 1997; and Robinson, et al., 1998).

Stilling basin design for stepped spillways can be challenging due to the design of the spillway chute. Spillway convergence and the energy dissipation of the flow created by the steps in the spillway affect the velocity entering the stilling basin. The velocity entering the stilling basin is a variable in determining the

Froude number, and the Froude number is a parameter used in selecting the type and dimensions of stilling basin used (USBR, 1973). When determining the velocity entering the stilling basin, the engineer must account for the energy dissipated or energy loss in the spillway chute. Since a stepped spillway is expected to have more energy dissipation than a smooth spillway (Rice and Kadavy, 1996; Rice and Kadavy, 1997; and Robinson, et al., 1998), the velocity entering the stilling basin is expected to decrease for stepped spillways as compared to smooth spillways. More energy dissipation in the spillway chute means less energy dissipation needed in the stilling basin. Consequently, stilling basins for stepped spillways are typically shorter than stilling basins for smooth spillways. Although extensive research has been conducted on the energy dissipation on steep ( $\theta > 30^\circ$ ) stepped spillways (Chanson, 2002), little research has been conducted on determining the energy dissipation in flatter ( $\theta < 30^\circ$ ) stepped spillways; thereby, making it complicated to design stilling basins for these particular spillways.

In addition to the energy dissipation in the stepped spillway, the convergence of the stepped spillway can also play a role in the stilling basin design. Researchers have found that as a spillway converges the flow depth at the training wall is more than the flow depth in the center of the spillway (Robinson, et al. 1998; Hunt, et al. 2005 and 2006; Hunt, et al. 2008; Woolbright, et al. 2008). Consequently, the flow is no longer uniform as it enters the stilling basin, meaning the flow depth at the stilling basin wall is deeper than the flow depth in the center of the stilling basin. This variation in flow conditions may

affect the velocity entering the stilling basin since the assumption can no longer be made that the velocity exiting the spillway and entering the stilling basin is the same throughout the cross-sectional profile of the structure. Since the velocity is a parameter in determining the stilling basin type and dimensions, researchers have found it taxing to design stilling basins for converging stepped spillways.

### ***Summary***

The key components of a stepped spillway are the spillway crest, spillway chute, and the energy dissipating stilling basin (Figure 2.2). In some cases, engineers select some of the design attributes (i.e. type of spillway crest, step height, spillway chute slope) based on constraints of the location (i.e. topography, available land rights, foundation materials, and expected flood inundation areas), the design feasibility, construction ease of the design, and/or safety. Other design features like training wall heights are affected by other design aspects like step sizes, flow aeration or flow bulking, spillway slope, and the convergence of the spillway. Additionally, research on converging stepped spillways and energy dissipation on flatter ( $\theta < 30^\circ$ ) stepped spillways has been limited. Subsequently, design guidelines are incomplete for these types of specific stepped spillways.

### **Basic Hydraulic Concepts for Stepped Spillways**

This section is intended to identify basic hydraulic concepts for stepped spillways. These concepts include types of flow phenomenon that can occur in stepped spillways and detailed information pertaining to air entrainment and energy dissipation of the flow that occurs in stepped spillways.

## **Types of Flow**

The flow in stepped spillways may be described in one of three ways: 1) nappe flow, 2) skimming flow, or 3) transitional flow. When stepped chutes experience low flow events, water is observed to plunge from one step to the next in free falling nappes, classifying the flow as nappe flow (Chanson, 2002). Jets of water impacting each step, jets of water breaking up in the air, and/or the formation of hydraulic jumps within the flow regime are commonly observed as “white water” action during nappe flow events (Chanson, 2002). When stepped chutes are subjected to large flow events, flow is typically observed to skim over the step edges with recirculating vortices developing between the main stream and the step edges (Chanson, 2002). This is known as skimming flow and is observed to have a glassy appearance. Transitional flow is defined when nappe flow is attempting to cross the boundary into skimming flow such that the turbulent action of the water located near the surface begins to decrease and exhibits signs of a glassy skimming flow. Regardless of the type of flow observed, flow characteristics are related to discharge, chute slope, step geometry, and local flow properties at each step with energy dissipation occurring in each (Chanson, 2002).

### ***Nappe Flow***

Nappe flow is commonly referred to as “white water” flow in stepped chutes. Flow is highly turbulent throughout the water profile during low flow events, but it is distinguishable from its counterpart, skimming flow, due to the

“white water” action or water-air interface that is observed near the surface of the water. Figure 2.5 illustrates nappe flow photographically.

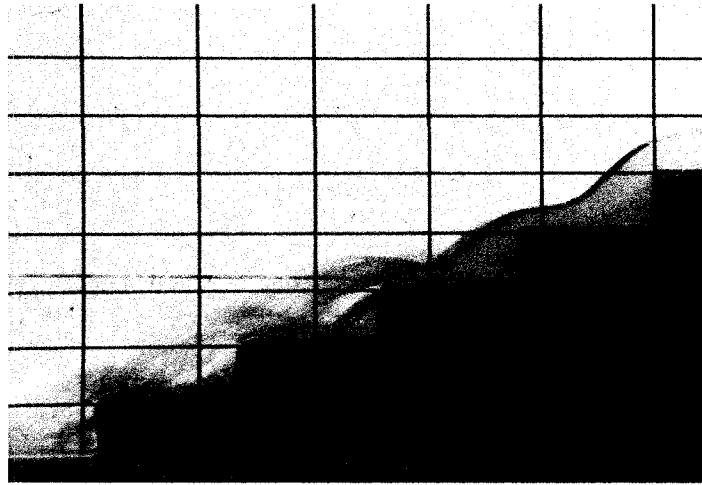


Figure 2.5 Photographic view of nappe flow.

Efforts have been conducted to evaluate the energy dissipation associated with nappe flow events. Rajaratnam (1990) investigated skimming flow and concluded that nappe flow exists when the ratio of critical depth to step height,  $d_c/h$ , is less than 0.8. Sorenson (1985) found that nappe flow occurred when  $d_c/h = 0.16$ . It is recognized that these observations are based on experiments involving relatively steep slopes (i.e.  $\theta > 25^\circ$ ).

### ***Skimming Flow***

Skimming flow most commonly occurs during larger flow events such that the flow is observed to skim over the step edges and has a glassy appearance. Although energy dissipation occurs during these events, it is less apparent to the naked eye as the high turbulent, air entrained flow is not observed at the water surface like nappe flow. Instead, recirculating vortices develop between the main stream and the step edges (Chanson, 2002). Figure 2.6 illustrates skimming flow

photographically with dye injected to highlight the recirculating vortices within the flow.

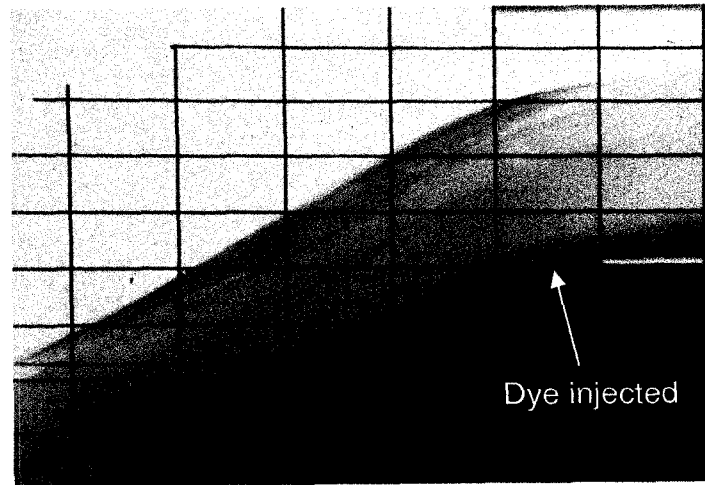


Figure 2.6 Photographic view of skimming flow with injected dye highlighting recirculating vortices within the flow.

Numerous researchers including Rajaratnam (1990), Chanson (1995), Chamani and Rajaratnam (1999), Matos, et al. (1999), and Pegram, et al. (1999) have conducted in-depth investigations into skimming flow in stepped spillways. Rajaratnam (1990) investigated the skimming flow regime in stepped spillways to predict shear stress and frictional energy loss. To determine the shear stress, Rajaratnam (1990) set out to establish the coefficient for fluid friction for a given set of flow conditions. To estimate the energy loss for skimming flow on a stepped spillway, Rajaratnam (1990) compared the energy loss caused by the steps to the energy loss created by a smooth spillway. He concluded that a considerable amount of energy is lost due to steps compared to the energy loss created by a smooth spillway. He further concluded that skimming flow can be characterized based on critical flow depth ( $y_c$ ) to vertical step height ( $h$ ) ratio is greater than 0.8. Chanson (1993, 1995) additionally proposed that the total head

loss could be estimated for skimming flow conditions in steep ( $\theta > 50^\circ$ ), stepped spillways such that it is a function of friction factor, the spillway slope, the critical depth, and dam height such that it is written as follows:

$$\frac{\Delta H}{H_o} = 1 - \frac{\left(\frac{f}{8 \sin \theta}\right)^{1/3} * \cos \theta + \frac{1}{2} \left(\frac{f}{8 \sin \theta}\right)^{-2/3}}{\frac{H_{dam}}{d_c} + \frac{3}{2}} \quad (2.3)$$

where:  $\Delta H$  = total head loss,  $H_o$  = maximum head available,  $f$  = friction factor,  $\theta$  = channel slope,  $H_{dam}$  = dam height, and  $d_c$  = critical flow depth (Chanson, 1995). Chanson (1995) advises that Equation 2.3 be used with caution as it does not address flow aeration. Additional vigilance should be taken with this information, so it is not applied outside the ranges (i.e. steep ( $\theta > 30^\circ$ ), stepped spillways) for which it was developed.

### ***Transitional Flow***

Transitional flow is the point where nappe flow attempts to shift into skimming flow characteristics. The high turbulence “white water” observed at the water surface begins to decrease, and a more glassy appearance begins to emerge of the water surface. Little information has been obtained in research about transitional flow. For a relatively flat slope ( $\theta < 30^\circ$ ), Yasuda and Ohtsu (1999) reports observations in which transitional flow regime occurs between a critical depth ( $d_c$ ) to step height ( $h$ ) ratio of 0.78 and 1.05, respectively. The work by Chanson (2002) supports these findings.

## **Air Entrainment and Energy Dissipation**

One of the advantages of a stepped chute in spillway applications is its ability to dissipate energy, potentially reducing the size of the energy dissipating stilling basin and therefore making stepped spillway applications more feasible. Energy dissipation that occurs in stepped spillways can be visually observed by the high turbulence or “white water” action occurring on the steps; however, energy dissipation occurs in stepped spillways before this aerated region is fully developed. This “white water” action is typically characterized as air entrainment within the flow. Although not visually apparent, air entrainment begins to develop prior to it reaching the water surface. Air-entrained flows in stepped spillways occurs when the water jet impacts the steps; when the water-air interface such that the jet of water breaks up in the air; or when the water is recirculated causing the undissolved air to become trapped (Chanson, 2002). Chanson (2002) states that air entrainment is caused by the unstable flow fluctuations that occur next to the air-water free surface. Consequently, this instability causes an increase in flow bulking within the spillway chute and in turn affects design parameters of the spillway chute and stilling basin.

Air-entrained flow is not typically visible to the naked eye until it reaches the free surface. The visually apparent air-entrained flow is normally described as “white water.” The location where the “white water” begins or where the air-entrained flow reaches the free surface is known as the air entrainment inception point (Chanson, 2002) (Figure 2.4). Air entrainment within the flow initiates flow bulking, a variable in determining the training wall height in the spillway chute.

For conditions upstream of the inception point, the role of air entrainment is expected to be minimal, and therefore, accountability of it in the design height of the training walls may be insignificant (Hunt and Kadavy, 2008). Air entrainment is expected to be more of a factor in determining training wall height when the length of the spillway chute extends beyond the inception point into the aerated flow region. Therefore, the location of the inception point within the spillway may dictate whether the air entrainment within the flow is sufficiently significant for engineers to account for it in the design height of the training walls.

Although questions are often raised with respect to scale effects in modeling air entrained flows, Chanson (1994, 2002) and Boes and Hager (2003a) provide insight in determining the point at which air entrainment starts within a stepped spillway. Chanson (1994, 2002) relied on model and prototype data to numerically determine the distance the inception point of air entrainment is from the spillway crest:

$$L_I = 9.719(\sin \theta)^{0.0796} (F_*)^{0.713} h (\cos \theta) \quad (2.4)$$

where  $L_I$  = distance from the start of growth of boundary layer to the inception point of air entrainment (Figure 2.4),  $\theta$  = spillway slope,  $F_*$  = Froude number defined in terms of the roughness height:  $F_* = q_w / [g (\sin \theta) \{h (\cos \theta)\}^3]^{0.5}$ ,  $h$  = step height,  $q_w$  = discharge per unit width, and  $g$  = gravitational constant. Chanson (2002) notes that the development of Equation 2.4 was based on spillway slopes ranging from 6.8 to 55°. However, most of the data for the equation development represented the steeper end ( $\theta > 50^\circ$ ) of the slope spectrum. Therefore, Chanson (2002) recommends that caution be used when applying this equation to flatter

slope conditions. Hunt and Kadavy (2008) has conducted an extensive generalized model study showing that Chanson's relationship, Equation 2.4, is suitable for slopes as flat as 14°.

Boes and Hager (2003a) likewise developed equations based on model studies for determining the location of the air entrainment inception point. Based on spillway slopes ranging from 26 to 75°, Boes and Hager (2003a) estimated that the distance from the spillway crest to the inception point as they define it as

$$L_I = \frac{5.90d_c^{6/5}}{(\sin \theta)^{7/5} h^{1/5}} \quad (2.5)$$

where  $d_c$  = critical depth,  $\theta$  = spillway slope, and  $h$  = step height.

Air entrainment within the flow plays a vital role in determining flow depth and velocity in stepped spillways. In modeling stepped spillways, it is often difficult to measure the flow depth with a point gauge and velocity with a pitot tube because of the "white water" nature of the flow in the stepped spillway. Even though a point gauge remains the instrument of choice in collecting water surface profiles, instrumentation such as a fiber-optical probe (Boes and Hager, 2003a) is an alternative method used in data collection of air concentrations and flow velocities. The ability to determine air concentrations within the flow can lead to an improved estimation of flow depth and therefore a better approximation of the training wall height necessary to retain the design flow (Boes and Hager, 2003a).

When water becomes infiltrated with air, water properties such as the specific weight of water may be affected, and these water properties may play an important role in developing design criteria for stepped spillways. The specific

weight of water is defined as the weight of water per unit volume. The specific weight of water at 15.6 °C (60 °F) is typically reported as 9.81 kN/m<sup>3</sup> (62.4 lb/ft<sup>3</sup>). For stepped spillways, the volume of water in this example becomes permeated with air, and therefore, decreases the weight of water within the volume. Consequently, the specific weight of water for the flows in stepped spillways is expected to be less than the normally reported value. Current literature has not reported what the specific weight of water for air-entrained flows is; instead, most stepped spillway research involving the specific study of air entrainment reports air concentrations and air bubble properties.

#### **Scale Effects Associated with Physical Modeling of Stepped Spillways**

Measurement techniques in physical modeling may create errors within the data collected; however, additional problems can arise from physically modeling stepped spillway surfaces because of scale effects. Scale effect is a term given when slight distortions that are introduced by the forces (i.e. gravity, viscosity, surface tension) involved in the modeling of a structure. Scale effects are typically apparent when the scale of the model is small. For instance, air entrainment in stepped spillways is not fully developed when modeled at small scales; consequently, energy dissipation may be overestimated within the chute.

Scale relationships between model and prototype are typically based on Froude similarity, a method that provides replication of gravitational forces (USBR, 1980). When scaling the model according to Froude similarity, it is assumed that the effects of gravity usually outweigh the effects of viscosity and surface tension (USBR, 1980). It has been documented; however, that scale

effects associated with highly air-entrained flows are expected because viscosity and surface tension are not as outweighed by gravitational forces as one might think (Chanson, 2002 and Boes and Hager 2003a).

In Froude similarity, the Reynolds number, a non-dimensional term that is a measure of the ratio of the inertia force on an element of fluid to the viscous force on an element, is different in the prototype than in the model because the fluid in the model is typically the same as the fluid in the prototype (Munson, et al. 1994). A model Reynolds number greater than  $10^4$  is normally accepted in the practice of hydraulic modeling because it is deemed that the scale effects associated with viscous forces are relatively insignificant (USBR, 1980). However, according to Boes and Hager (2003a), the Froude, Reynolds, and Weber similarity laws must be satisfied to approximate similarity for air entrained processes between models and prototypes. To satisfy these laws, Boes and Hager (2003a) as outlined in studies by Kobus (1984) and Rutschmann (1988) recommend that the minimum limits for the Reynolds and Weber numbers be  $10^5$  and 100, respectively, to achieve minimal scale effects in physical modeling of stepped spillways. Takahashi, et al. (2006) recommends that Froude, Reynolds, and Morton similarity be satisfied for modeling highly air-entrained flow, but they recognize that this can only be achieved at full-scale. Chanson (2002) recommends that scales no smaller than 10:1 be used in order to avoid scale effects; otherwise, smaller scales may lead to overestimation of energy dissipation and flow depth.

**CHAPTER III**  
**THEORY DEVELOPMENT FOR TRAINING WALL HEIGHT DESIGN CRITERIA**  
**Modeling and Similitude**

Models are a scaled representation of a physical system that may be used to predict the prototype behavior of the system in some desired respect. Models may be mathematical, computer, and/or physical depending what is known about the system or what information about the system is of interest. From a hydraulic engineering standpoint, larger physical models are more expensive to construct and test to the point where large scale models may be cost prohibitive; therefore, a physical model is usually constructed and tested at small-scale. The disadvantage of using a smaller scale; however, is misinterpreting data such that it does not reproduce the design behavior of a prototype. Therefore, it is vitally important that a physical model is properly designed and tested within the cost constraints and physical limitations of the model, so the results are correctly interpreted.

The theory of models is based on the principles of dimensional analysis. Dimensional analysis is a problem solving method used to check the validity of equations such that the dimensions on one side of the equation must equal the dimensions on the other side of the equation (Munson, et al. 1994). It has been shown that any given problem can be expressed in terms of a set of

dimensionless products known as “pi” terms that arise from dimensional analysis. For example, free surface flow that occurs in canals, rivers, spillways, stepped chutes, and stilling basins can be described by a set of dimensionless groups that include the Froude number ( $\frac{V}{\sqrt{g\ell}}$ ), Reynolds number ( $\frac{\rho V\ell}{\mu}$ ), and Weber number ( $\frac{\rho V^2\ell}{\sigma}$ ) where  $V$  is the velocity,  $g$  is gravitational acceleration,  $\ell$  is some characteristic length in the system,  $\rho$  is the density of the fluid,  $\mu$  is the dynamic viscosity, and  $\sigma$  is the surface tension (Munson, et al. 1994). Dimensionless numbers such as Froude, Reynolds, and Weber numbers represent force ratios, usually with inertial forces in the numerator. The Froude number accounts for both gravitational and inertial forces within the free surface flow. Reynolds number is the ratio of inertial forces to viscous forces, and in addition to inertial forces, Weber number accounts for surface tension forces. Large values of the ratios represented by the Froude, Reynolds, and Weber numbers suggest that the forces represented in the numerator are much greater than those represented in the denominator for the condition of interest. For that condition, exact matching of the ratio for model and prototype may not be required as long as the ratio remains large for both (that is, the same type of force retains dominance). When the relative importance of the forces are similar such that the value of the ratio is on the order of 1.0, then the ratio should be matched between model and prototype, so the influence of both force systems are correctly represented. Yet, it is impossible to satisfy exact equality of all ratios in

a scaled model using prototype fluid and prototype gravitational field in the model.

Because the Froude number between model and prototype can be closely matched such that the Froude number in typical physical systems of interest is on the order of one, Froude modeling is most commonly chosen method for modeling free surface flows. Froude number similarity between models and prototypes is thus described by the following relationship:

$$\frac{V_m}{\sqrt{g_m \ell_m}} = \frac{V}{\sqrt{g \ell}} \quad (3.1)$$

where the subscript  $m$  denotes the model. Since the model and prototype are expected to operate in the same gravitational field ( $g_m = g$ ), Equation 3.1 can be further simplified to the following relationship:

$$\frac{V_m}{V} = \sqrt{\frac{\ell_m}{\ell}} = \sqrt{\lambda_\ell} \quad (3.2)$$

where  $\lambda_\ell$  is the length scale. Froude modeling, with respect to the continuity equations, yields the following relationships for discharge and unit discharge:

$$\frac{Q_m}{Q} = (\lambda_\ell)^{5/2} \quad (3.3)$$

$$\frac{q_m}{q} = (\lambda_\ell)^{3/2} \quad (3.4)$$

where  $Q$  is the discharge and  $q$  is unit discharge.

Satisfying both the Weber number and Reynolds number similarity for free surface flow adds an element of complexity in modeling free surface flow in stepped spillways. In many problems involving free surface flow, surface tension

and viscous forces are small in comparison to gravitational and inertial forces, so Weber number and Reynolds number similarity are not always necessary. However, when dealing with small-scale models of stepped spillways where the flow depths are often small, viscous forces and air entrainment become dominating, and viscous effects and surface tension become important factors in relation to scale (Chanson, 2005 and Boes and Hager, 2003a). In the literature, Boes and Hager (2003a) recommend that the minimum limits for the Reynolds and Weber numbers be  $10^5$  and 100, respectively. Boes and Hager (2003a) believe these values will minimize the scale effects associated with viscosity and surface tension. Many researchers advise that the scale be 10:1 or larger to achieve minimal scale effects (Chanson, 2002). The research community has yet to reach a consensus on the limits of scale and/or Reynolds and Weber numbers to minimize scale effects in physical models of stepped spillways when air entrainment may become an important factor.

## **Momentum Principles**

### **Momentum Principles for Open Channel Flow**

The classical definition of momentum is mass times velocity or otherwise defined as mass in motion. Newton's second law of motion relates momentum to open channel flow parallel to the channel bed by stating that the time rate change of momentum in a body of water in a flowing channel is equal to the resultant of all the external forces that are acting on the body (Chow, 1959). Applying Newton's second law of motion to a large channel slope, the momentum equation can be written as follows:

$$\frac{Qw}{g}(\beta_2 V_2 - \beta_1 V_1) = P_1 - P_2 + W \sin \theta - F_f \quad (3.5)$$

where  $Q$  = discharge,  $w$  = the unit weight of water,  $\beta$  = the momentum coefficient,  $V$  = velocity,  $P$  = pressure force,  $W$  = weight of water,  $\theta$  = channel slope, and  $F_f$  = the total external force of friction and resistance acting along the surface of contact between the water and the channel. The subscripts refer to two points along the channel as described by Chow (1959).

To simplify Equation 3.5, some assumptions may be made about the flow in the channel. First, the flow may be assumed parallel or gradually varied. Gradually varied flow is defined as a steady flow whose depth varies gradually down the length of the channel. Since the term gradually varied flow signifies a steady flow condition, the flow can be considered constant for a time interval under consideration. Gradually varied flow is already established in Equation 3.5 since it does not include a time derivative. Additionally, the flow is considered parallel; consequently, the flow may be assumed to have a hydrostatic pressure distribution such that the pressure in Equation 3.5 may be computed (Chow, 1959). For a slope angle,  $\theta$ , that is large, pressure may be determined as

$$P = \frac{1}{2} w d^2 \cos \theta \quad (3.6)$$

where  $d$  = the depth of flow measured perpendicularly from the bed surface and the other terms were previously defined. Parallel flow also implies that the momentum coefficient,  $\beta$ , is equivalent to one. Equations 3.5 and 3.6 are vital in the development of prediction equations for spillway training wall height using a momentum analysis approach.

## Simplified Momentum Analysis for a Converging RCC Stepped Spillway and Equation Development for Training Wall Height

A control volume vector approach to momentum analysis for a converging RCC stepped spillway is used to develop a prediction equation for the flow depth along the training wall and consequently the minimal height necessary to prevent overtopping of the training wall. Equation 3.5 defines a momentum relationship as it relates to a simple condition in an open channel. For a converging spillway, a more complex control volume is required to determine the wall height; therefore, the classical force balance of the control volume is

$$\Sigma \vec{F} = \int_{cs} \rho \vec{v} \vec{v} \cdot d\vec{A} \quad (3.7)$$

In order to apply Equation 3.7, the control volume must be defined in relation to location within the converging spillway chute. The control volume is placed in the spillway chute such that it is perpendicular to the wall and to the face of the chute. Figures 3.1a and 3.1b illustrate the placement of the control volume in the spillway. Further definition of the control volume is necessary, so the direction of forces acting on the control volume can ultimately and reasonably be resolved. Therefore, the unit vector perpendicular to the chute face is defined as

$$\hat{u}_{cf} = \sin(\theta)\hat{i} + 0\hat{j} + \cos(\theta)\hat{k} \quad (3.8)$$

where  $\theta$  = chute slope. Figure 3.2 illustrates the chute profile section A-A as depicted in Figure 3.1a.

The unit vector parallel to the velocity down the chute face is

$$\hat{u}_{vel} = \cos(\theta)\hat{i} + 0\hat{j} - \sin(\theta)\hat{k} \quad (3.9)$$

Figure 3.2 also depicts the orientation of the velocity unit vector in relation to the control volume.

The unit vector representing the upstream face of the control volume is

$$\hat{u}_{cvt} = -\cos(\psi)\sin(\phi)\hat{i} + \cos(\psi)\cos(\phi)\hat{j} + \sin(\psi)\hat{k} \quad (3.10)$$

where  $\psi = \tan^{-1}(\sin(\phi)\tan(\theta))$  (i.e. angle formed by the x-y plane with the vector parallel to the chute floor and perpendicular to the training wall) and  $\phi$  is the angle of convergence (i.e. angle measured in the x-y plane such that zero indicates training walls parallel with flow). Figure 3.3 illustrates the orientation of  $\hat{u}_{cvt}$  in the wall profile section C-C as defined in Figure 3.1a.

The unit vector representing the wall face is

$$\hat{u}_{wall} = -\sin(\phi)\hat{i} + \cos(\phi)\hat{j} + 0\hat{k} \quad (3.11)$$

Figure 3.3 also depicts  $\hat{u}_{wall}$ .

The unit vector representing the velocity along the wall, which is perpendicular to the wall vector and is the vector entering the control volume on the upstream side and exiting the control volume on the downstream side is

$$\hat{u}_{vw} = \cos(\psi_2)\cos(\phi)\hat{i} + \cos(\psi_2)\sin(\phi)\hat{j} - \sin(\psi_2)\hat{k} \quad (3.12)$$

where  $\psi_2 = \tan^{-1}(\cos(\phi)\tan(\theta))$  (i.e. angle formed by the x-y plane with the vector lying in the plane of the wall and the chute floor). Figure 3.4 demonstrates the location of  $\hat{u}_{vw}$  in the wall profile section B-B as defined in Figure 3.1a.

The unit vector lying in the plane of the wall perpendicular to the velocity vector along the wall is

$$\hat{u}_{pw} = \sin(\psi_2) \cos(\phi) \hat{i} + \sin(\psi_2) \sin(\phi) \hat{j} + \cos(\psi_2) \hat{k} \quad (3.13)$$

Figures 3.3 and 3.4 illustrates the orientation of  $\hat{u}_{pw}$  in the wall profile.

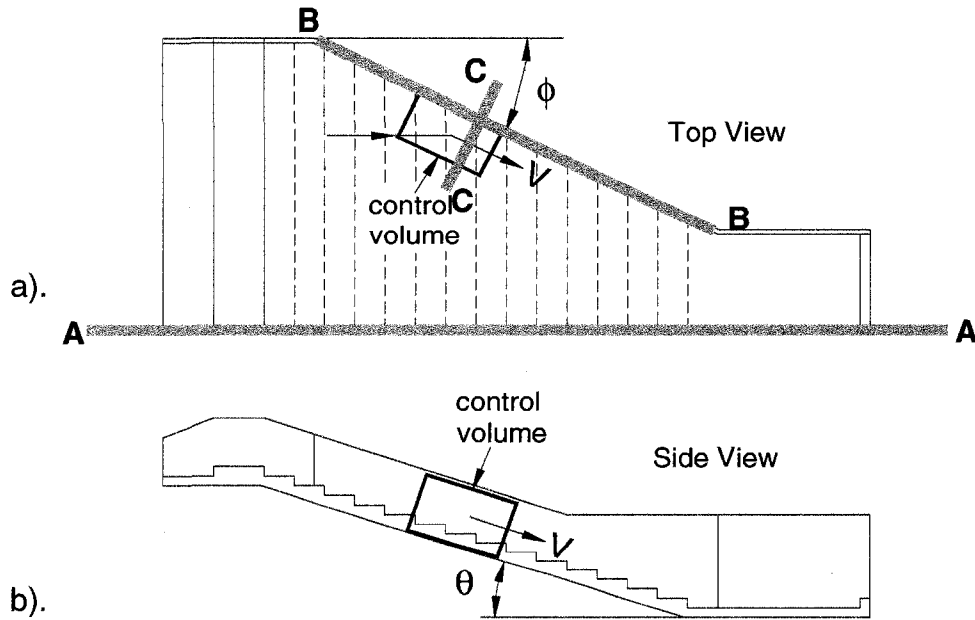


Figure 3.1 a). Top view of the control volume illustrating that the upstream face is perpendicular to the training wall. b). Side view of the control volume showing that the upstream face is perpendicular to the chute floor.

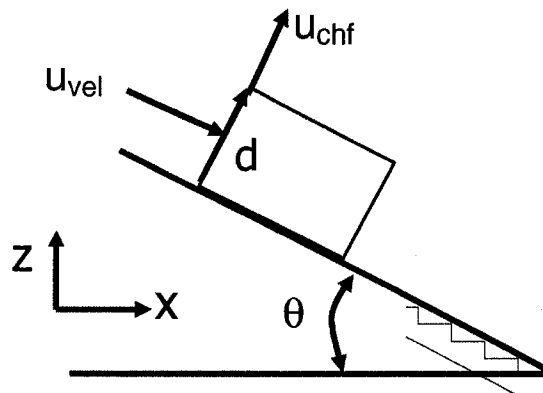


Figure 3.2 Chute profile: Section A-A as shown in Figure 3.1a.

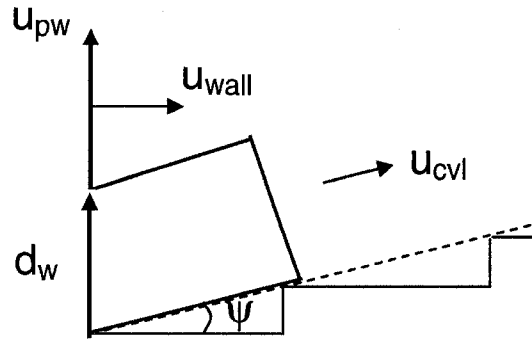


Figure 3.3 Wall profile C-C as shown in Figure 3.1a.

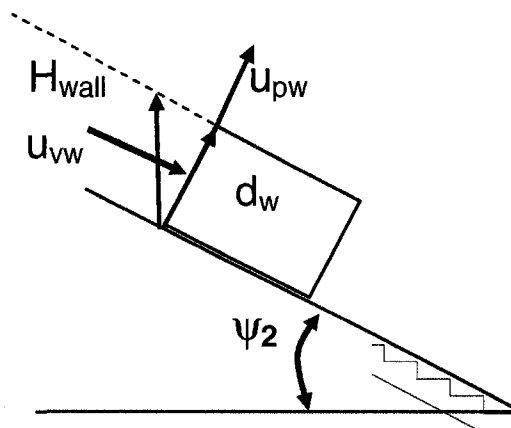


Figure 3.4 Wall profile: Section B-B as shown in Figure 3.1a.

With the control volume defined, the basic force balance as written in Equation 3.6 must be satisfied. The resulting scalar relations derived from Equation 3.6 must then be satisfied in any selected direction such that the forces on the control volume balance. Application of the analysis to the selected control volume is complicated because all dominant forces and velocities must be determined. Despite the direction chosen to resolve the forces and momentum flux, assumptions about the pressure and velocity distributions must be chosen. These assumptions implied by the selected control volume are 1) velocity distribution on the face of the chute is uniform in the direction implied by the unit vector parallel to the velocity down the chute face, and this is the velocity seen by

the face of the control volume away from the wall, 2) velocity direction changes suddenly at the shock within the control volume such that the sides of the control volume see only velocity aligned with the unit vector representing the velocity along the training wall, and 3) the pressure distribution is implied by the assumed velocity vectors and is assumed to be hydrostatic relative to the implied water surfaces at both the training wall and in the undisturbed chute. The first assumption implies that there is no shear component on the face of the control volume in the undisturbed flow. The second assumption concerned with the rapid change of flow direction at the shock implies that the direction of the shear on the bed and the shear stress on the wall is in the direction of  $-u_{vw}$ . For this assumption, the magnitude of flow depth, velocity, and roughness would have to be estimated. An additional implication is that the velocity of the flow up the wall is negligible.

An attempt was made to resolve the forces along the unit vector representing the upstream face of the control volume,  $\hat{u}_{cvi}$ . By assuming a control volume of unit width, the pressure force on the wall is

$$\bar{F}_{pw} = \gamma d_w^2 \cos(\psi_2) / 2\hat{u}_{wall} \quad (3.14)$$

where  $\gamma$  = specific weight of water and  $d_w$  = the predicted flow depth at the wall measured mutually perpendicular to the velocity vector along the training wall and the local water surface of the chute (along the unit vector lying in the plane of the wall perpendicular to the velocity vector along the wall). The pressure force on the control volume in the undisturbed flow is

$$\bar{F}_{cvi} = -\gamma d^2 \cos(\theta) / 2\hat{u}_{cvi} \quad (3.15)$$

where  $d$  = the flow depth measured mutually perpendicular to the velocity vector and the water surface in the undisturbed section of the chute (along the unit vector perpendicular to the chute face). The weight of water in the control volume acts vertically downward yielding

$$\vec{F}_w = -\mathcal{W}_{water} \hat{k} \quad (3.16)$$

$\vec{F}_w$  is computed knowing the distance from the wall as well as the shape of the upper surface. Additionally, the value  $d_w$  appears in the relation. However, one could assume a control volume shape for computing water volume that would not affect the pressure terms; thereby allowing the weight force to be determined as follows:

$$\vec{F}_w = -\gamma d_w^2 \left( C_i - C_i^2 \frac{\tan(\psi)}{2} + (1 - C_i \tan(\psi))^2 \frac{\sin(\psi) \cos(\psi)}{2} \right) \hat{k} \quad (3.17)$$

The momentum flux into the control volume through the upstream face is then given by:

$$\vec{M} = \rho v^2 (\hat{u}_{vel} \bullet \hat{u}_{cv1}) \hat{u}_{vel} \quad (3.18)$$

or 
$$\vec{M} = \rho v^2 d (\cos(\theta) \cos(\psi) \sin(\phi) + 0 - \sin(\theta) \sin(\phi)) \hat{u}_{vel} \quad (3.19)$$

To reduce each of these vectors to scalar form along the vector  $u_{cv1}$  requires the dot product of each of the force momentum flux vectors. Some relationships may be identified as perpendicular, and therefore, the dot product would be zero. If the weight of water in the control volume in the direction of the forces being resolved is considered small compared to the other terms in the momentum analysis, then the above relations would be expected to yield the following equation:

$$\frac{\gamma d_w^2 \cos(\psi_2) \cos(\psi)}{2} = \frac{\gamma d^2 \cos \theta}{2} + \rho v^2 d (\cos(\theta) \cos(\psi) \sin(\phi) + \sin(\theta) \sin(\phi))^2 \quad (3.20)$$

To specifically solve for  $d_w$ , Equation 3.20 was rearranged into Equation 3.21.

$$d_w = \sqrt{\frac{\left[ \frac{\gamma d^2 \cos \theta}{2} + \rho v^2 d (\cos(\theta) \cos(\psi) \sin(\phi) + \sin(\theta) \sin(\phi))^2 \right] * 2}{\gamma \cos(\psi_2) \cos(\psi)}} \quad (3.21)$$

Equation 3.21 has the potential for collapsing data for various discharges, slopes, and convergence angles to yield a minimum training wall height necessary to retain the desired design discharge, where the wall height above the surface formed by connecting the step would be:

$$H_{wall} = \frac{d_w}{\cos(\psi_2)} \quad (3.22)$$

Figure 3.4 illustrates the wall height in relation to the control volume along the wall profile. Caution must be exercised when using Equations 3.21 and 3.22 because air entrainment within the flow is not considered.

**CHAPTER IV**  
**EXPERIMENTAL EQUIPMENT**

**Testing Facility**

An experimental program was conducted in a testing facility at the USDA-ARS Hydraulics Engineering Research Laboratory. Figure 4.1 shows an aerial view of the USDA-ARS Hydraulic Engineering Research Laboratory. The laboratory is located near Lake Carl Blackwell approximately 7 miles west of Stillwater, Oklahoma (Figure 4.2). A three-dimensional, 1:22-scale physical model replica of a proposed converging RCC stepped spillway design was constructed in a test basin and used to evaluate the flow characteristics in the spillway. Figure 4.3 photographically illustrates the physical model. The dimensions of the test basin were 19.8 m (65 ft) long, 6.7 m (22 ft) wide, and 1.2 m (4 ft) deep, respectively.

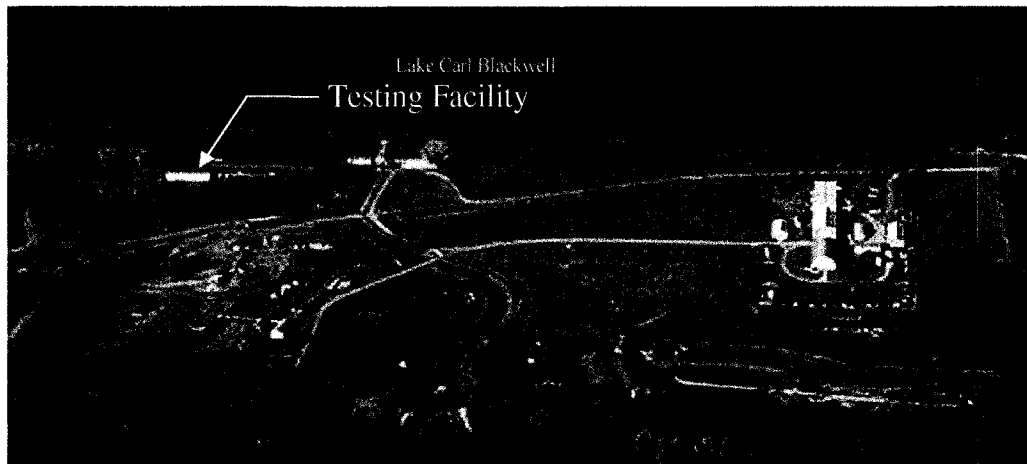


Figure 4.1 Aerial view of the USDA-ARS Hydraulic Engineering Research Unit.

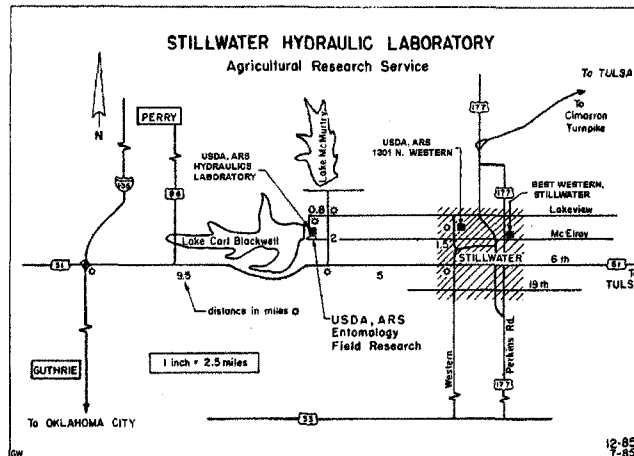


Figure 4.2 Site map of the USDA-ARS Hydraulics Engineering Research Laboratory.

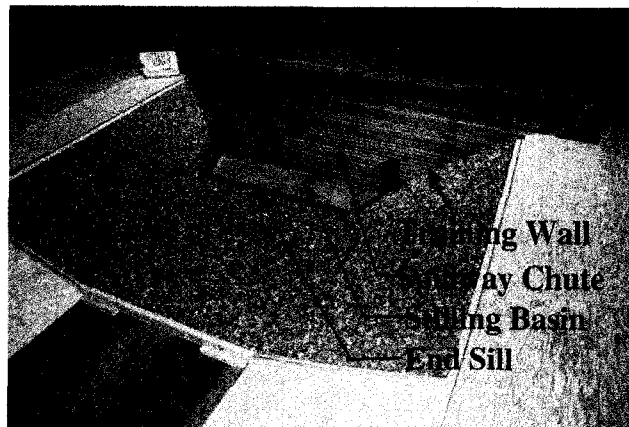


Figure 4.3 Photograph of stepped spillway model with  $52^\circ$  convergence.

The model dimensions were based on a prototype design of a stepped spillway planned for Big Haynes Creek watershed site 3 (H-3) in Gwinnett County, Georgia. The prototype design was provided by Golder Associates Inc. (Golder) and Gwinnett County Department of Public Utilities (GCDPU) (Golder, 2003) (Figure 4.4). Golder is a contracted architecture and engineering firm for the Georgia NRCS, and GCDPU is the sponsor responsible for the flood retarding structure. The prototype entrance to the spillway consists of a 100-m

(330 ft) wide ogee crested weir (Figure 4.4), with flow continuing down a 3(H):1(V) ( $\theta = 18.4^\circ$ ) chute with 0.3 m (1 ft) prototype size steps (Figure 4.5). The spillway walls converged down the chute with angles ( $\phi$ )  $0^\circ$ ,  $15^\circ$ ,  $30^\circ$ ,  $52^\circ$ , and  $70^\circ$  tested. Figure 2.2 as well as Figure 3.1a illustrates  $\phi$ . The point of convergence commenced at station 3.72 m (12.2 ft) (Figure 4.5). The approximate prototype spillway drop was 9.7 m (32 ft).

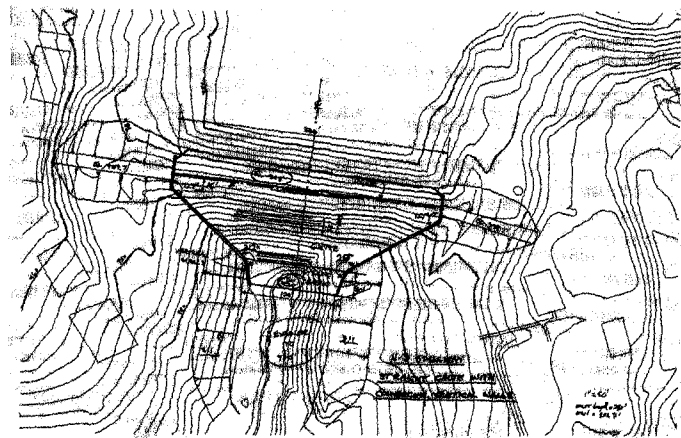


Figure 4.4 Schematic top view of the stepped spillway provided by Golder.

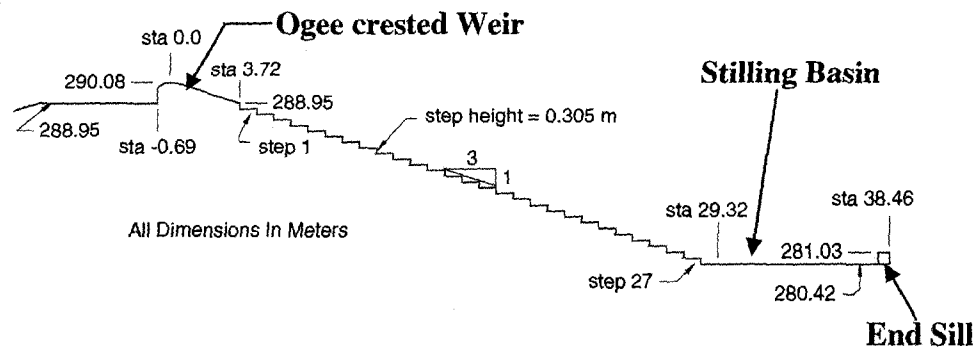


Figure 4.5 Schematic profile of the stepped spillway.

The original design of the structure required a training wall height of 3.7 m (12 ft) (Golder, 2003). To ensure that the flow would be contained in the model,

the training walls in the model were constructed to represent a prototype height of 4.3 m (14 ft). The stilling basin length and wall height provided in the design proposal were 9.1 m (30 ft) and 6.7 m (22 ft), respectively (Golder, 2003). The stilling basin length for all tested flows in the model was later modified to an 18.2 m (60 ft) prototype representation based on performance observations in the early stages of the testing. The stilling basin end sill height as indicated by the proposed design was 0.6 m (2 ft prototype) (Golder, 2003). For the 52° convergence test, the prototype stilling basin entrance and exit widths were 36.6 m (120 ft) and 30.5 m (100 ft), respectively.

Since the training wall design was the primary point of interest for this particular study, it was verified during the testing of the 52° convergence that the flow behaved similarly on both sides of the model. Therefore, subsequent tests included testing two convergence angles at once. For example, during a series of tests, one training wall convergence was 30°, and one training wall convergence was 15°. By conducting the experiments in this manner, testing could be conducted over a larger range of convergence angles in a more timely fashion.

The model steps were constructed of sanded redwood that was coated in polyurethane. The ogee crest section was comprised of a PVC material, and the training walls were constructed with clear acrylic material that allowed visual observations of the flow within the chute.

## Measuring Devices

The flow to the test facility and subsequently to the model was delivered through a 0.46 m (18 inch) diameter pipe that tapped into a 0.46 m (18 inch) diameter siphon. The siphon is one of five siphons that are located within the embankment dam of Lake Carl Blackwell; consequently, water for all tests was lake water (Figure 4.6). Figure 4.7 photographically depicts the test facility as the water delivery pipes enter the building. Test flows were controlled using a combination of an orifice meter (Figure 4.7) and air-water differential manometer (Figure 4.8). The accuracy of the flow measurement for the facility is within  $\pm 1\%$ . The water temperature was taken for each test using a thermometer. The thermometer was read to the nearest degree. The outflow and tailwater was controlled with an adjustable overflow weir (Figure 4.9). Tailwater conditions were tracked regularly during testing using a manually operated point gauge attached to the downstream end of the test basin. The point gauge is read within  $\pm 0.0003$  m ( $\pm 0.001$  ft). Once the flow exited the model basin, it exited the facility and was discharged into Stillwater Creek downstream of the facility and Lake Carl Blackwell.

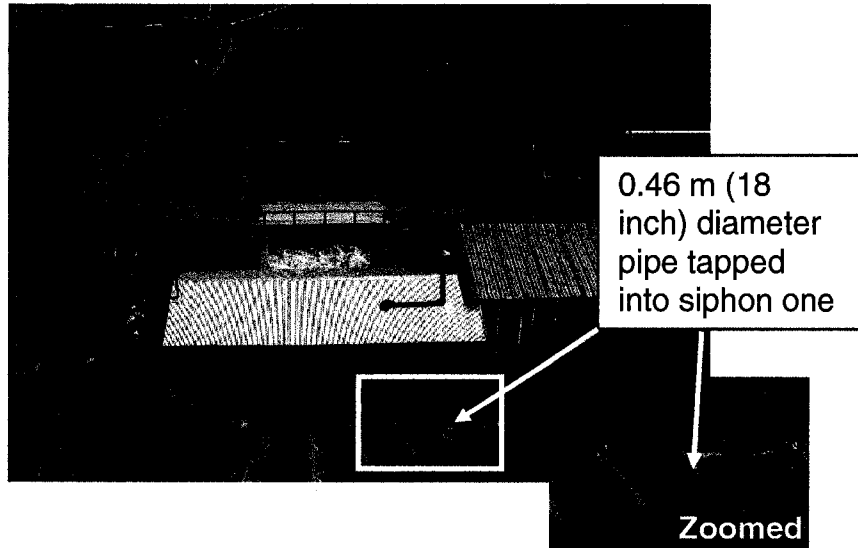


Figure 4.6 Siphons located in the dam with a 0.46 m (18 inch) diameter pipe tapped into siphon one for flow delivery to the test facility.

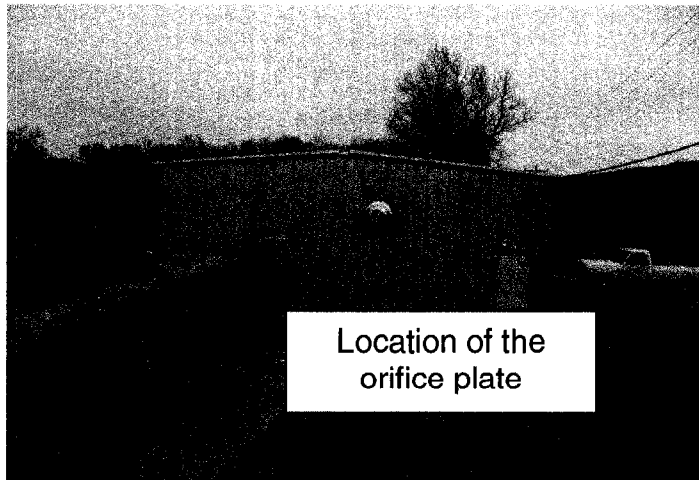


Figure 4.7 Water supplied to the test facility through a 0.46 m (18 inch) diameter pipe.



Figure 4.8 Air-water differential manometer.



Figure 4.9 Adjustable overflow weir.

Data including bed elevations, water surface elevations, velocities, and air concentrations were collected during testing, and digital photography documented each test visually. A manually operated carriage mounted point gauge was used to take cross-sectional and lateral bed profiles and water level measurements from the approach section of the spillway to downstream of the stilling basin (Figure 4.10). The point gauge is read within  $\pm 0.0003$  m ( $\pm 0.001$  ft). Velocities and air concentrations were taken only for the specific design

configuration of interest. These measurements were taken with a two-tip fiber-optical probe attached to a data acquisition system similar to that described by Boes and Hager (2003a, b) (Figure 4.11). The accuracy of the velocity and the air concentration measurements as reported by RBI Instrumentation et mesure (2004) is  $\pm 10^{-5}$ . Other flow measurement devices like a pitot tube coupled with a pressure transducer could have been used to measure velocity; however, these tools were not used for data collection because the flow depth at times was so small that the pitot tube would have caused flow disruption and inaccurate measurements to be collected. Digital photos and digital video documented the changes in flow characteristics during each test.

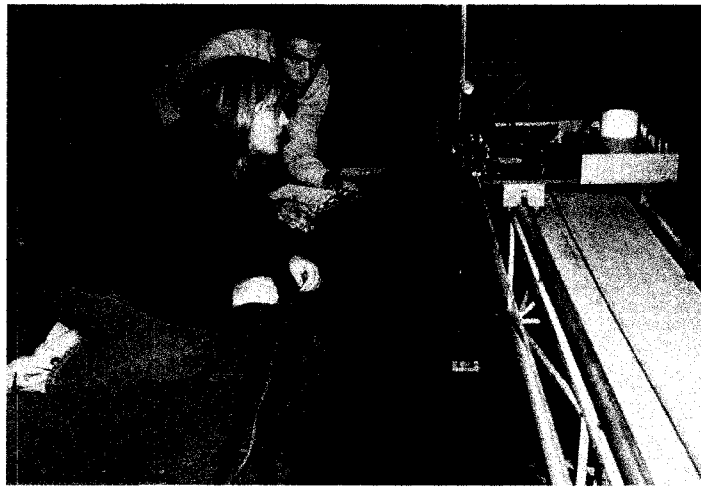


Figure 4.10 Water surface profile measurement.

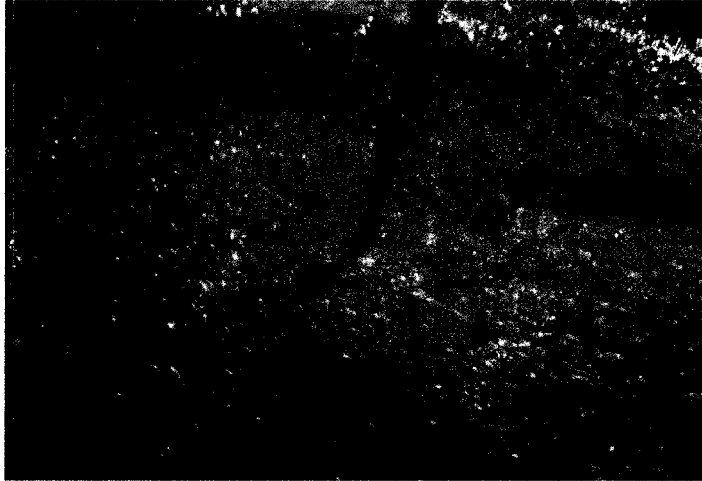


Figure 4.11 Air concentration and velocity measurement.

**CHAPTER V**  
**METHODS AND PROCEDURES**

Once the model was prepared in accordance with the testing program presented in Table 5.1, data were taken prior to testing, during each test, and at the conclusion of each test. Prior to initiating flow, base line model conditions were documented. The documentation included centerline channel profiles of the model; spillway profiles along the steps against the training wall; and cross-sectional profiles of the crest section, the spillway chute at stations 4.6, 11.1, 14.8, 20.3, 23.1, and 26.8 m, and stilling basin were taken.

Table 5.1 Summary of Testing Program.

Test #	$\phi$ (°) Left, Right	$q_{\text{proto}}$ ( $\text{m}^3/(\text{s}\cdot\text{m})$ )	$TW_{\text{proto}}$ (m)	$d_c$ (m)
1	52, 52	5.05	286.2	1.37
2	52, 52	7.58	287.1	1.80
3	52, 52	1.26	283.7	0.55
4	52, 52	2.52	284.9	0.87
24	15, 30	7.58	-	1.80
25	15, 30	5.05	-	1.37
26	15, 30	2.52	-	0.87
27	15, 30	1.26	-	0.55
32	0, 70	1.26	-	0.55
33	0, 70	2.52	-	0.87

After the base line model conditions were recorded, testing began. Test initiation started with the downstream filling of the test basin with water to the desired tailwater level. This allowed the majority of the test basin to be filled with water without exposing the model to unnecessary flow that could cause the model to prematurely deteriorate. Water for the downstream end of the test basin was delivered through a 0.1 m (4 inch) pipe located in the downstream end of the test basin. The line taps into the original pipe entering the facility (Figure 5.1). Once the tailwater conditions were established, the inflow to the model was initiated, and the 0.1 m (4 inch) pipe in the downstream test basin was shut off. The inflow was allowed to stabilize, which was verified through a strip-chart recorder (Figure 5.2). A strip chart recorder is a device used to measure and record water level over time. This particular strip-chart recorder consists of a float pulley, a float, a counterweight, a rotating drum, a six-hour chart, and pen. As the water level changes, the float and counterweight will rise and fall according to the water level. This action rotates the pulley wheel to mimic the rise and fall of the water level, subsequently moving the pen that is attached to the pulley wheel. The pen records the changes in water level on the chart that is attached to the rotating drum. Once the water level reached a steady state condition as indicated by a continuous line on the chart, the flow was deemed stabilized. Stabilization typically occurred within 20 minutes of the initiation of inflow. Once the desired inflow was established, the air-water differential manometer and the chart recorder were routinely checked during the test to

insure a constant flow rate. Additionally, a manually operated point gauge was checked regularly to insure the preferred tailwater conditions were set.

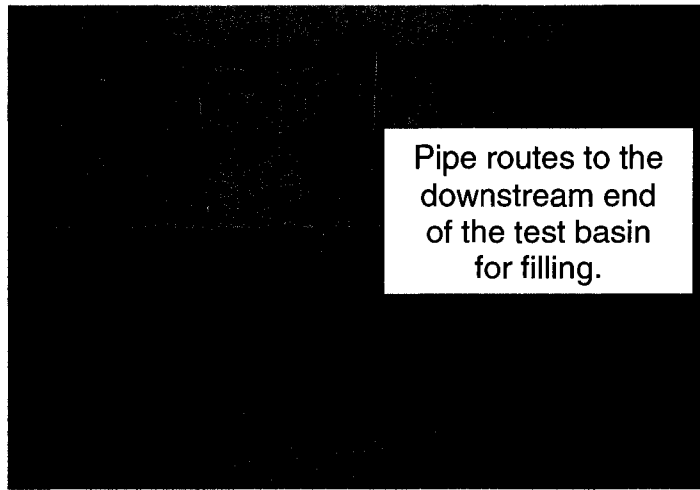


Figure 5.1 Pipe for downstream filling of the test basin.

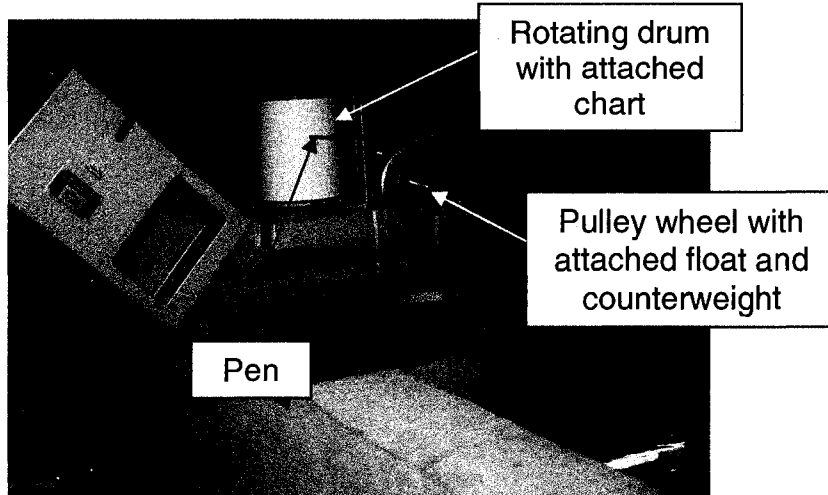


Figure 5.2 Strip chart recorder for verification of stabilized inflow.

Each model configuration was tested under four inflow conditions. The largest prototype flow,  $7.58 \text{ m}^3/(\text{s}\cdot\text{m})$  (81.6 cfs/ft), was set based on the expected spillway discharge or probable maximum flood (PMF) for the specific site for which the spillway was being designed. Additional flow rates were selected for testing based on this PMF ( $7.58 \text{ m}^3/(\text{s}\cdot\text{m})$ ) and are summarized in Table 5.1

along with the prototype tailwater elevations, and the critical depth along the spillway crest. Figure 5.3 illustrates the model with 52° convergence tested at the PMF (7.58 m<sup>3</sup>/(s·m)) and design tailwater. As previously mentioned, the model was constructed at a 1:22 scale. Equation 3.4 provides the relationship necessary for determining model flow conditions given prototype flow conditions summarized in Table 5.1.



Figure 5.3 Physical model with 52° convergence tested at  $q_{\text{proto}} = 7.58$  m<sup>3</sup>/(s·m) (81.6 cfs/ft) and design tailwater.

Each model configuration was tested under two tailwater conditions. The first tailwater condition was that indicated by the specific location for the original design as summarized in Table 5.1. The second set of tailwater conditions was the minimum tailwater conditions for the structures in order to obtain a spectrum of data. The minimum tailwater is the tailwater on the chute that is controlled by the basin end sill.

The flow through the model was characterized by taking water level measurements, noting qualitative changes or disturbances within the flow, and photographing and videoing each test. Water level measurements included centerline water profiles, training wall water profiles, and cross-sectional profiles

taken at the downstream edge of steps one, eight, twelve, eighteen, twenty-one, and twenty-five. The steps are designated in Figure 4.5 with step one beginning at the top of the spillway chute next to the ogee crest and step 27 ending at the bottom of the spillway chute. Step one, eight, twelve, eighteen, twenty-one, and twenty-five correspond to horizontal stations 4.6, 11.1, 14.8, 20.3, 23.1, and 26.8 m, respectively. All water surface profiles, velocity measurement, and photographs were collected once the flow stabilized.

Velocity and air concentrations measurements were taken during the testing of the 52° convergence, which was the specific configuration of interest. Tests one thru four were specifically conducted to collect water surface profiles. Tests five thru eight were conducted similarly to tests one thru four; however, the specific data of interest were the velocity and air concentration measurements at step 21 (i.e. sta. 23.1 m) under minimal tailwater conditions. No water level profiles except for some spot check locations were taken during tests five thru eight. Additionally, velocity and air concentration measurements were not recorded for other test configurations due to the lack of air entrainment. The extrapolation of these data to prototype conditions is unreliable until an appropriate scaling factor can be determined.

Each test was documented photographically through the use of both digital photography and digital videography. The digital images were taken towards the conclusion of each test to document flow characteristics.

## **CHAPTER VI**

### **RESULTS AND DISCUSSION**

Several components play a role in the design of a converging stepped spillway. To name a few, these elements include air entrainment, discharge, and convergence angle of the training wall. Chapter VI outlines an empirical approach based on measurements collected during testing for designing a converging stepped spillway of similar design (i.e. chute slope and step height). An inception point relationship developed by Chanson (1994) may be used to determine whether air entrainment should be considered in the design height of the training walls. The convergence of the training wall also plays a significant role in the flow depth at the training wall as well as the bulking width. These observations are detailed in the sub-sections of this chapter.

As outlined in Chapter III, a simplified, momentum analysis approach to predict the flow depth at the training wall was developed. This theoretical approach could provide minimum height requirements for the training wall necessary to retain the design flow. The measured flow depth at the training wall is compared to the predicted flow depth at the training wall as described herein. The simplified, momentum analysis method provides design engineers an alternative for determining the training wall height requirements for converging stepped spillways.

## Air Entrainment

Air entrainment within a stepped spillway chute must be accounted in determining training wall height. It is believed that air entrainment is expected to be a factor in determining training wall height when the length of the chute extends beyond the point of significant air entrainment, referred to as the inception point. Therefore, the inception point location may dictate whether air entrainment must be integrated into the spillway design of the training walls. For conditions upstream of the inception point, air entrainment at the free surface is expected to be minimal. For long chutes, air entrainment is expected to impact the design of the training wall height as the turbulent boundary layer approaches the free surface prior to the flow reaching the stilling basin. Flow bulking, an increase in flow depth, is expected to occur as this turbulent boundary layer reaches the free surface. Figure 2.4 in Chapter II illustrates the approach of the turbulent boundary layer to the free surface and the resulting air entrainment inception point.

Although questions are often raised with respect to scale effects in modeling air entrained flows, Chanson (1994, 2001, 2002) and Boes and Hager (2003a) provide insight in determining the point at which air entrainment reaches the free surface within a stepped spillway as indicated by Equations 2.4 and 2.5 (as outlined in Chapter II sub-section Air Entrainment and Energy Dissipation). The air entrainment inception point relationship developed by Chanson (1994, 2001, 2002) is applicable for spillway chute slopes ranging from  $6.8^\circ$  to  $55^\circ$ , with the majority of the data in the steeper spectrum of  $22^\circ$  or greater. Equation 2.4,

in fact, incorporates two data points for slopes less than  $22^\circ$ . The air entrainment inception point equation developed by Boes and Hager (2003a) was developed for stepped spillway chute slopes greater than  $26^\circ$ . The spillway chute slope of  $18.4^\circ$  studied in this investigation can be used as additional data in determining the suitability of Equations 2.4 and 2.5 for flatter sloped stepped spillways.

Detection of the air entrainment inception point is difficult to ascertain. A change in the flow appearance is an indicator of the air entrainment inception point. As Figure 2.4 illustrates, the flow appears smooth above the air entrainment inception point. The flow becomes irregular and often displays an appearance of “white water” beyond the air entrainment inception point, depending on the development of the turbulent boundary layer for the given flow conditions. Visually observed changes in water surface from a smooth, glassy appearance to a rougher, irregular flow appearance were noted during the tests for the four flow rates (Table 5.1, Chapter V, Methods and Procedures) tested. Figure 6.1 depicts the change in the water surface. Fully developed white water is not expected at the free surface for this scale of 1:22; however, these slight changes in flow appearance were determined to be the location of the air entrainment inception point or where the turbulent boundary layer was apparently intersecting the free surface. Table 6.1 summarizes the step location (steps descend the spillway chute beginning at the crest section) and the distance from the spillway crest section where the visually observed air entrainment inception point was observed for each flow tested. Table 6.1 also summarizes the predicted location (i.e. step location and distance from the spillway crest) of the

air entrainment inception point according to equations developed by Chanson (1994, 2002) and Boes and Hager (2003a).

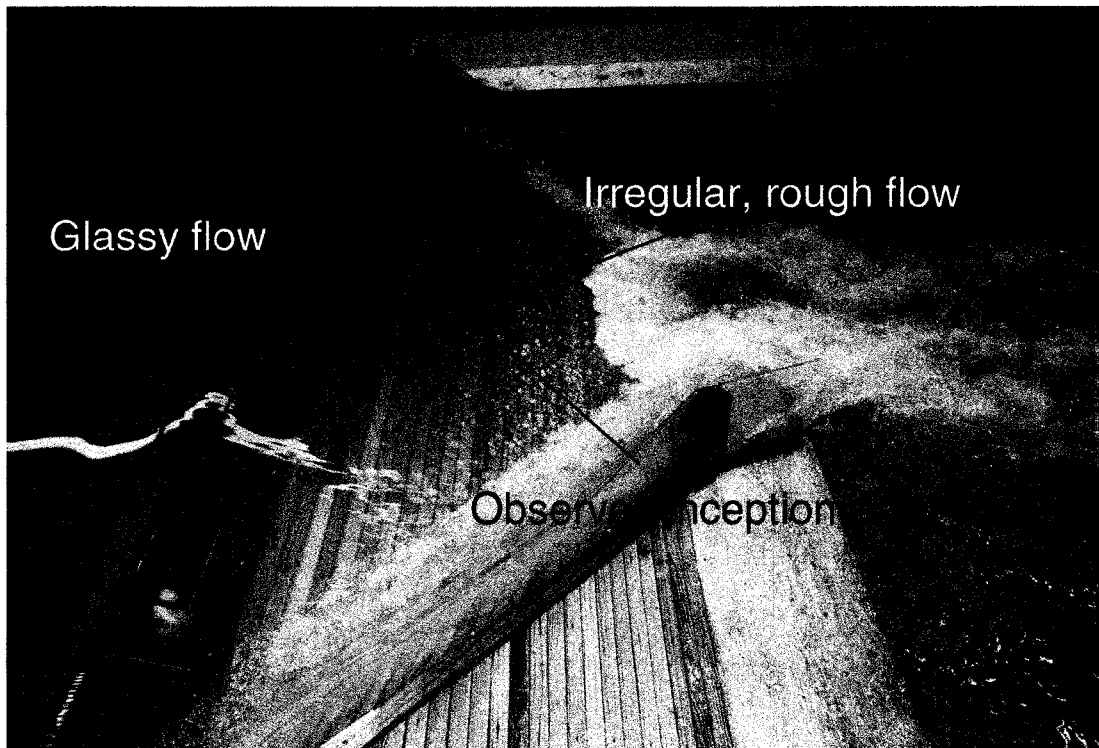


Figure 6.1 Observed inception point and differences in flow characteristics.

Table 6.1. Calculated distances to inception point and locations of inception point in the spillway as compared to the model observations.

			Chanson (1994, 2001, and 2002)		Boes and Hager (2003a)		Observed	
	$Q_{w\text{-proto}}$ (m <sup>2</sup> /s)	$Q_{w\text{-proto}}$ (cfs/ft)	$L_i$ (m)	Inc. pt. (step) <sup>a</sup>	$L_i$ (m)	Inc. pt. (step) <sup>a</sup>	$L_i$ (m)	Inc. pt. (step) <sup>a</sup>
PMF	7.58	81.6	27.37	25	76.10	-	-	-
2/3 PMF	5.05	54.4	20.50	17	55.02	-	16.5	14
1/3 PMF	2.52	27.1	12.51	9	31.6	-	10.1	7
1/6 PMF	1.26	13.6	7.63	4	18.15	15	7.38	4

<sup>a</sup>Inception point relative to step location in the spillway defined in Figure 4.5.

Table 6.1 compares the visual observations of the air entrainment inception point to the air entrainment inception point locations predicted by Chanson (Equation 2.4) and Boes and Hager (Equation 2.5). As Table 6.1 indicates, Equation 2.4 predicts the observed air entrainment inception point for the lowest discharge, 1/6 PMF (1.26 m<sup>3</sup>/(s·m) and 13.6 cfs/ft), tested, with step 4

specified as the location of the air entrainment inception point for both the observed and the predicted condition. For the 1/3 PMF ( $2.52 \text{ m}^3/(\text{s}\cdot\text{m})$  and 27.1 cfs/ft) flow, the observed and predicted air entrainment inception point locations (as calculated by Equation 2.4) were within approximately -6%. As flow discharge increases, the difference between the predicted and the observed air entrainment inception point increases. Equation 2.4 prediction for flows lower than 1/3 PMF ( $2.52 \text{ m}^3/(\text{s}\cdot\text{m})$  and 27.1 cfs/ft) showed less variation in the inception point location than at flows higher than 1/3 PMF ( $2.52 \text{ m}^3/(\text{s}\cdot\text{m})$  and 27.1 cfs/ft) because the air entrainment was more developed at the free surface and more visible at lower flows than higher flows. Table 6.1 shows that Equation 2.5 over predicts the distance of the inception point from the spillway crest for all tested flows by as by an average 150% as compared to the observed location of inception.

Another observation is that there was no inception point in the spillway chute at the highest discharge (PMF =  $7.58 \text{ m}^3/(\text{s}\cdot\text{m})$  and 81.6 cfs/ft) tested such that the turbulent boundary layer did not appear to reach the free surface. The design tailwater elevation was noted near step 13, station 15.6 m (51.3 ft) when collecting water surface data in the centerline of the spillway chute for the PMF ( $7.58 \text{ m}^3/(\text{s}\cdot\text{m})$  and 81.6 cfs/ft) flow. Based on the predicted location of the inception point for the PMF ( $7.58 \text{ m}^3/(\text{s}\cdot\text{m})$  and 81.6 cfs/ft), the inception point would occur below the design tailwater at step 25, station 27.37 m (89.8 ft). Therefore, air entrainment does not appear to influence training wall height design for the PMF ( $7.58 \text{ m}^3/(\text{s}\cdot\text{m})$  and 81.6 cfs/ft) discharge and design tailwater

elevation of 287 m (942 ft) for the spillway described in this model study. If the design tailwater for this spillway were lower than the elevation of 281 m (923 ft) at step 25, then air entrainment at the water surface would be expected as summarized by Equation 2.4 in Table 6.1. As a result, the design engineer would need to consider the flow bulking aspect caused by the air entrainment in the height design of the training walls for this portion of the spillway. Additionally for flows less than the PMF ( $7.58 \text{ m}^3/(\text{s}\cdot\text{m})$  and 81.6 cfs/ft), air entrainment is expected, so a design engineer must consider this as well in the design of the training walls.

### **Stepped Spillway Design for Converging Training Walls**

Most spillway designs require that the training walls retain a specified design storm (i.e. a 100-year flood, the probable maximum flood, etc.). According to the USDA-NRCS (2005), the design height of training walls for structural spillways should be of sufficient height to prevent overtopping during the passage of the full maximum freeboard discharge. The Portland Cement Company, PCA (2002), indicates that the critical areas of the dam where the training walls are located can result in high concentrated flow; therefore, high training walls are recommended to prevent erosion of the embankment dam that these RCC stepped spillways overlay. The following sub-sections summarize the general observations and trends captured during testing. These observed results are also compared to results determined through a simplified momentum equation as outlined and developed in Chapter III.

## **General Observations and Trends Captured during Testing through Data Collections and Digital Imagery**

Challenges associated in the design of converging stepped spillways include the high concentrated flow near the training walls, containment of highly air entrained flow, and the containment of concentrated flow or flow run-up along converging training walls. Flow run-up is the additional depth of water extending up the training wall created by flow convergence, compared to non-converging flow or the undisturbed flow in the center of the chute. During testing, the flow depth at the training wall increased at the point of convergence, station 3.7 m (12 ft), when compared to the centerline flow depth for each training wall convergence. Figures 6.2, 6.3, and 6.4 graphically illustrate flow run-up. For example, the water surface at the training wall as a result of the 52° convergences as portrayed in Figure 6.2 is approximately 4.5 m (15 ft) greater than the water surface in the center of the spillway chute at station 29 m (95 ft), an increase over 500%. Additionally, Figures 6.2 and 6.3 representing the 52° and 30° convergences, respectively, show a gradual increase in the flow depth along the training wall as it descends though the spillway chute, whereas Figure 6.4 graphically displays a more constant flow depth along the training wall for the 15° convergence. It is observed in Figure 6.2 that the flow overtops the 52° converging training walls with a PMF ( $7.58 \text{ m}^3/(\text{s}\cdot\text{m})$  and 81.6 cfs/ft) flow condition near station 9.6 m (32 ft). Figure 6.5 depicts the training wall overtopping photographically. Figures 6.3 and 6.4 show that there was no

overtopping for the 30° and 15° convergences under PMF (7.58 m<sup>3</sup>/(s·m) and 81.6 cfs/ft) flow conditions.

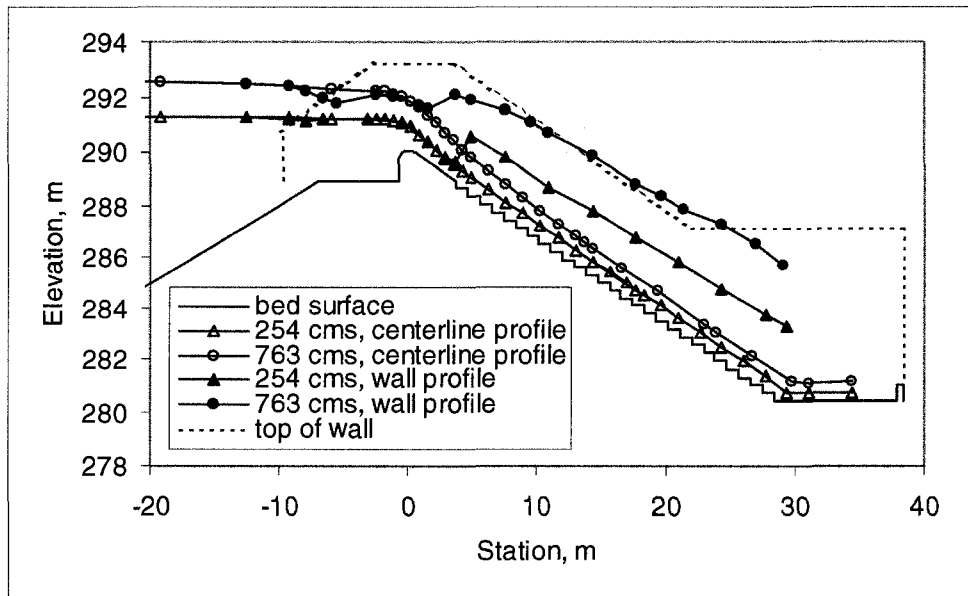


Figure 6.2 Centerline water surface profiles and water surface profiles near the training wall having a convergence angle of 52° tested under minimum tailwater depth.

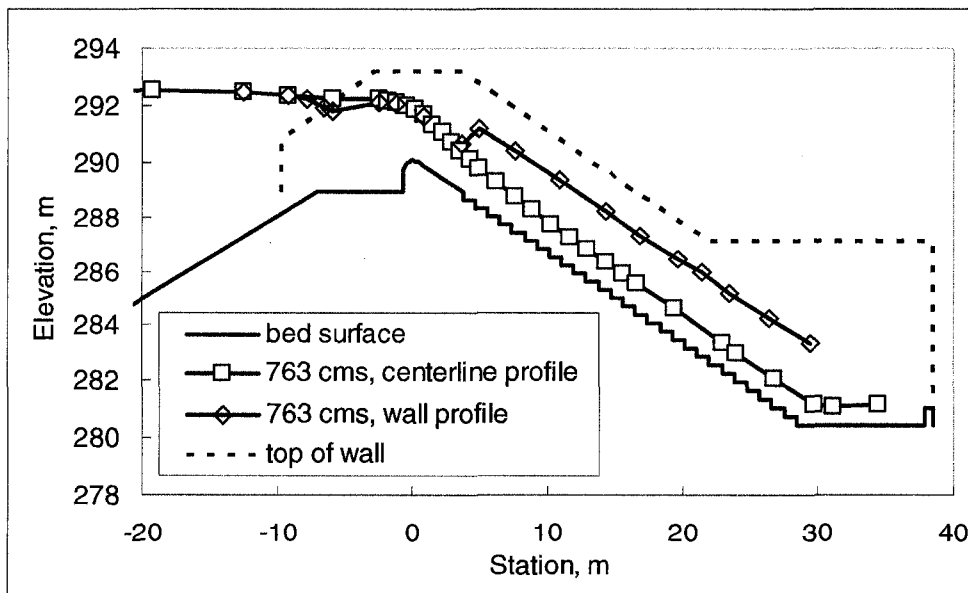


Figure 6.3 Centerline water surface profiles and water surface profiles near the training wall having a convergence angle of 30° tested under minimum tailwater depth.

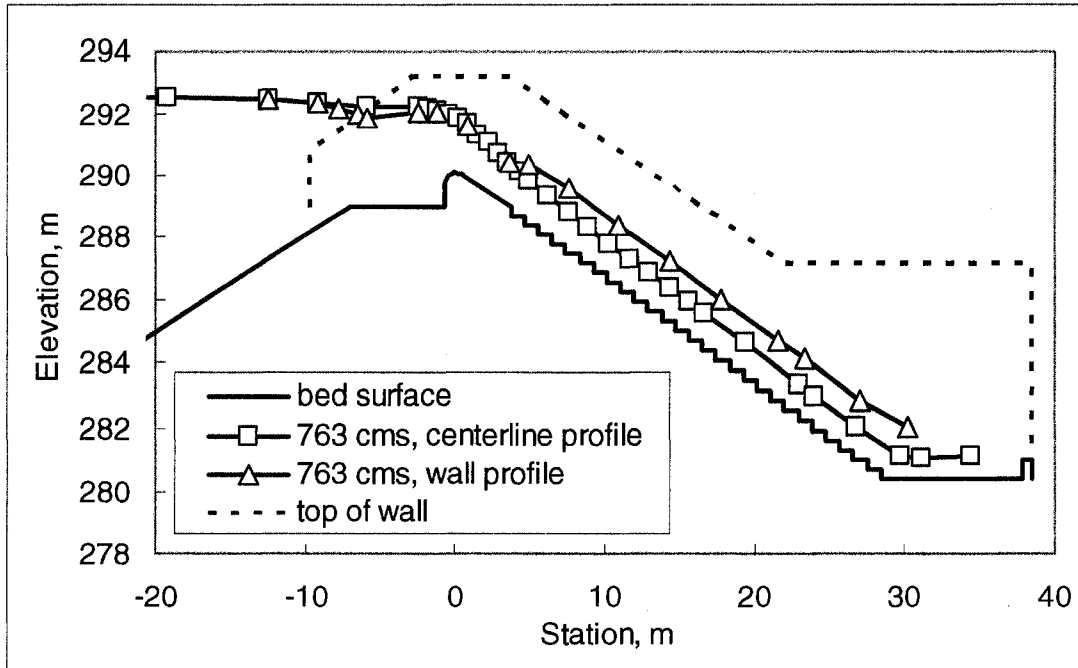


Figure 6.4 Centerline water surface profiles and water surface profiles near the training wall having a convergence angle of  $15^\circ$  tested under minimum tailwater depth.

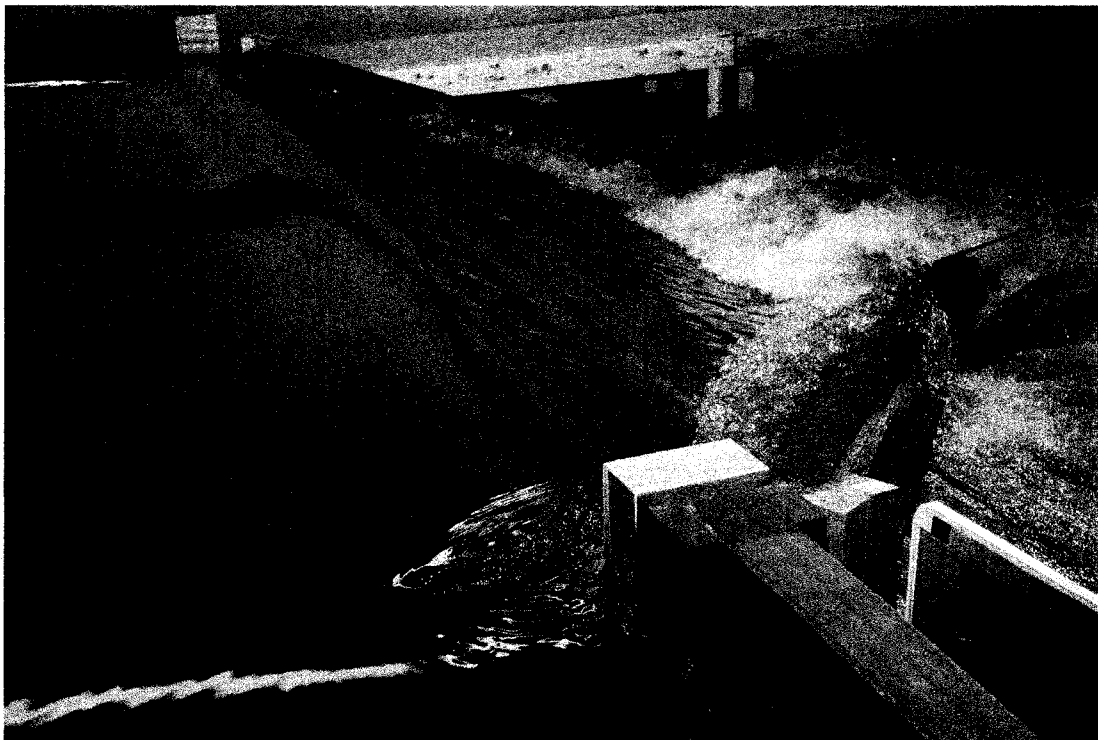


Figure 6.5 Flow run-up overtopping the  $52^\circ$  converging training wall with prototype PMF ( $7.58 \text{ m}^3/(\text{s}\cdot\text{m})$  and  $81.6 \text{ cfs/ft}$ ) and minimum tailwater depth.

A comparison of the water surface profiles along the training walls with convergence angles ranging from  $0^\circ$  to  $52^\circ$  for the PMF ( $7.58 \text{ m}^3/(\text{s}\cdot\text{m})$  and  $81.6 \text{ cfs/ft}$ ) flow rate with minimum tailwater depths is shown in Figure 6.6. At station  $3.7 \text{ m}$  ( $12 \text{ ft}$ ), the point of convergence, Figure 6.6 illustrates a dramatic increase in the water surface for each of the tested convergence under the same flow conditions. Figure 6.6 also shows the gradual increase in the flow depth near the training wall as it descends the chute for each of the convergences. As the convergence increases, the flow depth at the training wall also increases. For instance, the flow depth along the  $52^\circ$  converging training wall at station  $22 \text{ m}$  ( $72.6 \text{ ft}$ ) is nearly 3.2 times greater than the flow depth generated along the  $15^\circ$  converging training wall at the same station as more directly illustrated in Figure 6.7. Figure 6.6 also demonstrates symmetry in the flow patterns on both sides of the spillway as shown by the left and right water surfaces plotted on top of one another for the  $52^\circ$  convergence. Chanson (1994) indicated that shock waves would develop across converging spillways, so symmetry was not totally expected for the extreme convergence case of  $52^\circ$ .

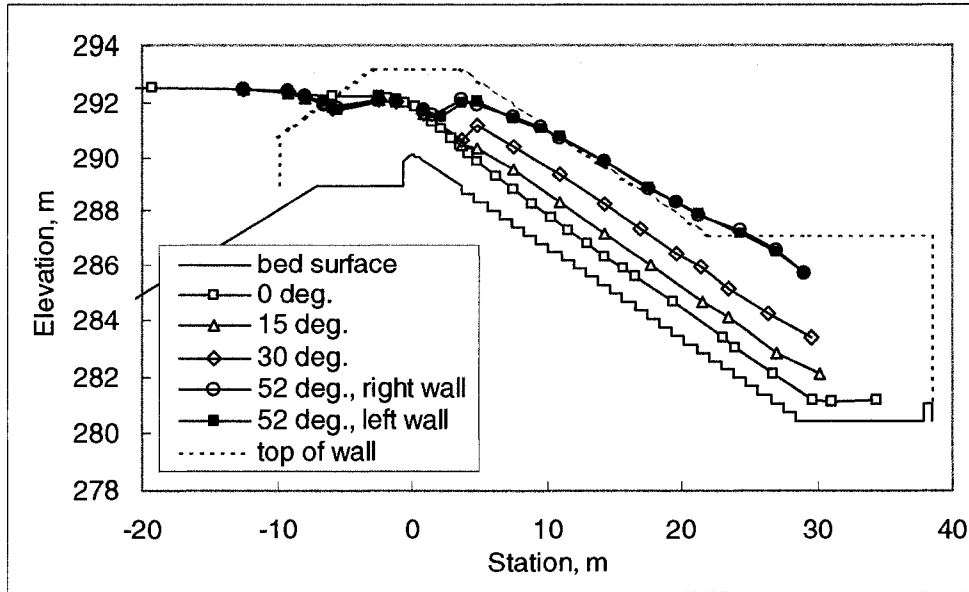


Figure 6.6 Water surface profiles along the training wall with varying convergence angles, PMF ( $7.58 \text{ m}^3/(\text{s}\cdot\text{m})$  and  $81.6 \text{ cfs/ft}$ ), and minimum tailwater depth.

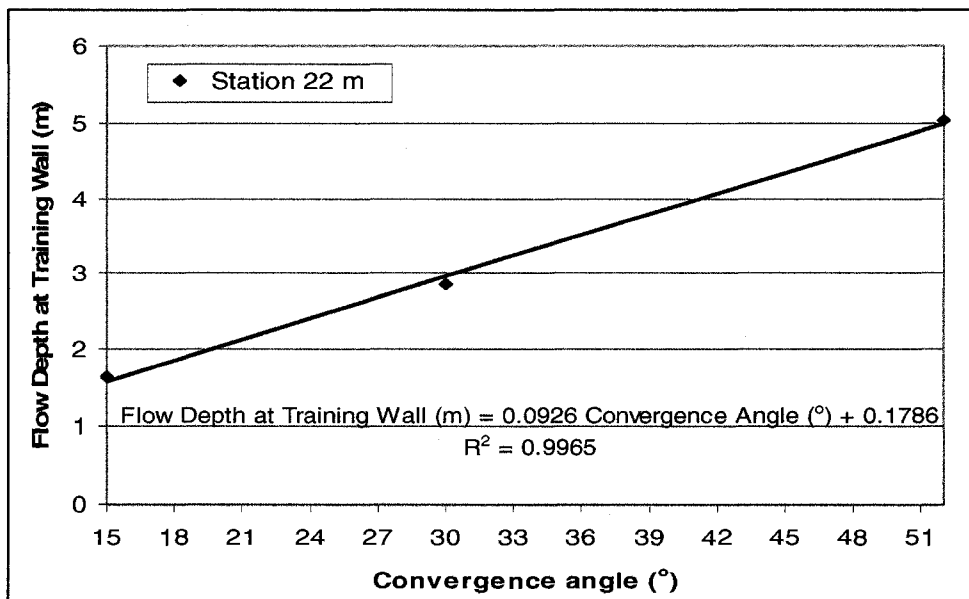


Figure 6.7 Flow depth comparison for convergences  $15^\circ$ ,  $30^\circ$ , and  $52^\circ$  at station  $7.4 \text{ m}$  ( $24.2 \text{ ft}$ ) for PMF ( $7.58 \text{ m}^3/(\text{s}\cdot\text{m})$  and  $81.6 \text{ cfs/ft}$ ) flow conditions.

The stepped spillway was also examined with a training wall convergence of  $70^\circ$ . The two lowest flow conditions,  $1/6 \text{ PMF}$  ( $1.26 \text{ m}^3/(\text{s}\cdot\text{m})$  and  $13.6 \text{ cfs/ft}$ ) and  $1/3 \text{ PMF}$  ( $2.52 \text{ m}^3/(\text{s}\cdot\text{m})$  and  $27.1 \text{ cfs/ft}$ ), were tested for this configuration.

Turbulent flow behavior was observed as the flow descended the spillway chute as illustrated in Figures 6.8 and 6.9. Erratic flow conditions made data collection difficult and subject to measurement errors. Another undesirable attribute of the 70° convergence during low flow testing revealed that the training walls disrupted the flow over the spillway crest such that backwater effect occurred as a result of the flow bulking at the training walls. Figure 6.10 portrays the training wall impeding the flow near the crest of the spillway during 1/3 PMF (2.52 m<sup>3</sup>/(s·m) and 27.1 cfs/ft) flow. Consequently, higher flows were not tested for the 70° convergence as a result of these observations. Further testing at higher discharges exceeded the limits of the test basin and the spillway model for the configuration of 70° convergence.

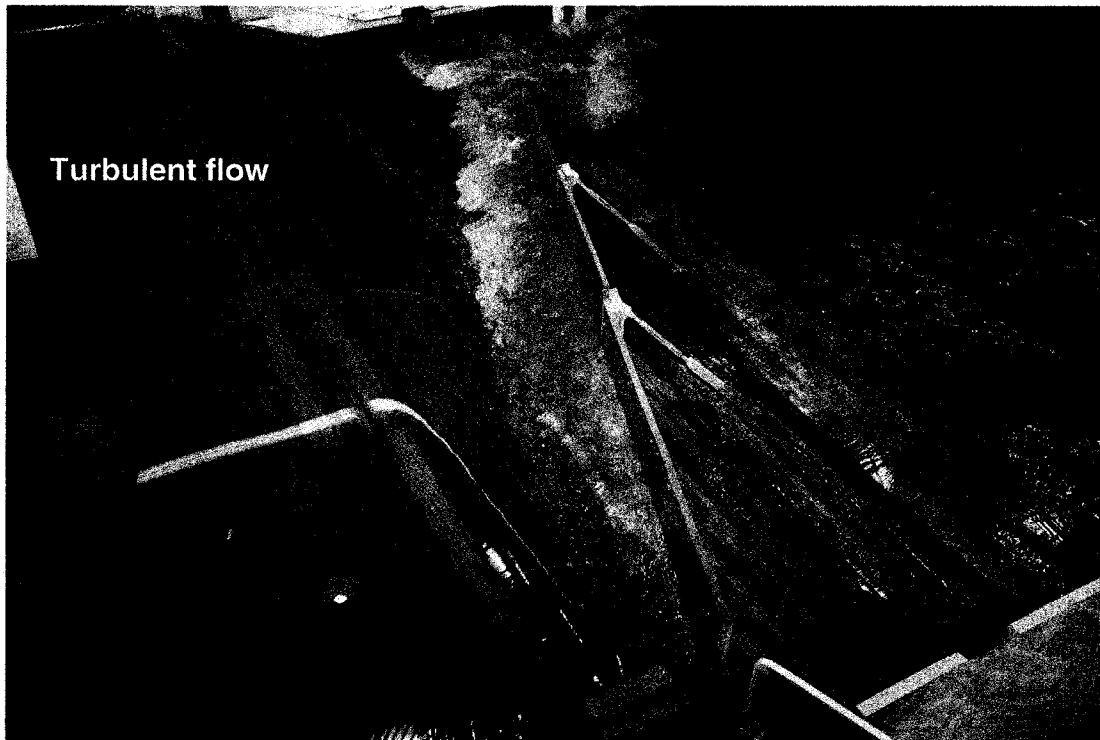


Figure 6.8 Flow run-up along a 70° converging training wall with prototype 2/3 PMF (2.52 m<sup>3</sup>/(s·m) (27.1 cfs/ft)) and minimum tailwater depth.

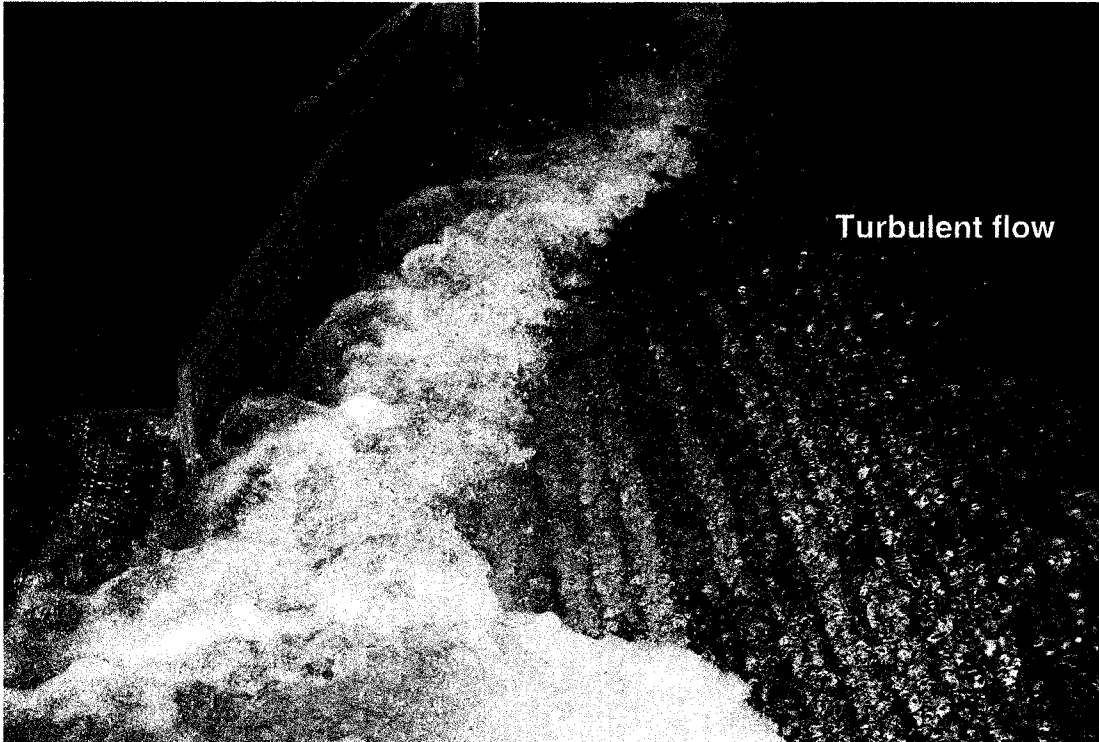


Figure 6.9 Turbulent flow run-up along a 70° converging training wall with prototype 1/3 PMF ( $2.52 \text{ m}^3/(\text{s}\cdot\text{m})$ ) ( $27.1 \text{ cfs/ft}$ ) and minimum tailwater depth.

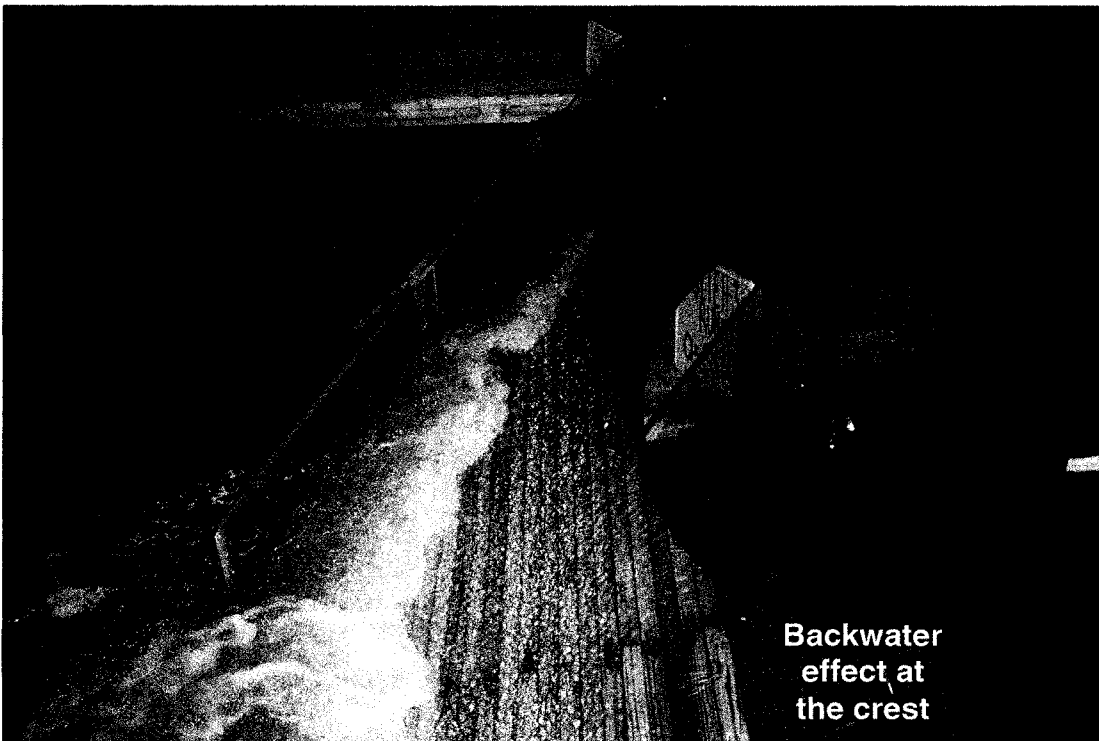


Figure 6.10 Turbulent flow impeding on the spillway crest caused by a 70° converging training wall with prototype 1/3 PMF ( $2.52 \text{ m}^3/(\text{s}\cdot\text{m})$ ) ( $27.1 \text{ cfs/ft}$ ) and minimum tailwater depth.

## Training Wall Influence on Flow

Observations were made with respect to the training walls influence on the flow. Flow bulking extended horizontally from the training wall along the entire length of the spillway chute as it entered the tailwater as shown in Figure 6.11. Cross-sectional profiles were taken at steps one, eight, twelve, and twenty-one. These profiles were normalized by the critical depth with the profiles presented graphically in Figures 6.12, 6.13, and 6.14 for the PMF flow. Tabular data is summarized in Appendix A. Figure 6.12 illustrates the horizontal width of  $1.8d_c$  for the bulking zone created as a result of the training wall converging  $15^\circ$ . Figures 6.13 and 6.14 show similar patterns in the bulking zone with horizontal widths of  $2.9d_c$ , and  $7.3d_c$  for  $30^\circ$  and  $52^\circ$  convergences, respectively. Other flow rates produce similar relationships as those illustrated in Figures 6.12, 6.13, and 6.14. These relationships are summarized graphically in Figure 6.15 where the convergence angle is plotted against the bulking zone width or the horizontal distance from the wall normalized by the critical depth. Figure 6.15 shows that as the flow rate increases, the bulking zone width increases. Additionally, the bulking width increases with increasing convergence. A distinct pattern in the bulking width is observed in Figure 6.15, and the square root of the Froude number determined from the depth at step one and the unit discharge through the chute was determined to collapse the family of curves in Figure 6.15 into one that is illustrated in Figure 6.16. The bulking width, or distance from the wall the flow is influenced, can be determined by the following expression:

$$\text{Bulking width (Distance from the wall)} = \frac{e^{(\phi+5.78)/24.4} d_c}{Fr^{0.5}} \quad (6.1)$$

where  $\phi$  = convergence angle,  $d_c$  = critical depth, and  $Fr$  = Froude number.

Equation 6.1 provides a means to determine the bulking width of the flow that enters the stilling basin as a function of convergence angle, critical depth, and Froude number. Equation 6.1 provides specific information about the flow as it enters the stilling basin; consequently, this information may provide insight in establishing specific design criteria of stilling basins and downstream riprap for converging stepped spillways.

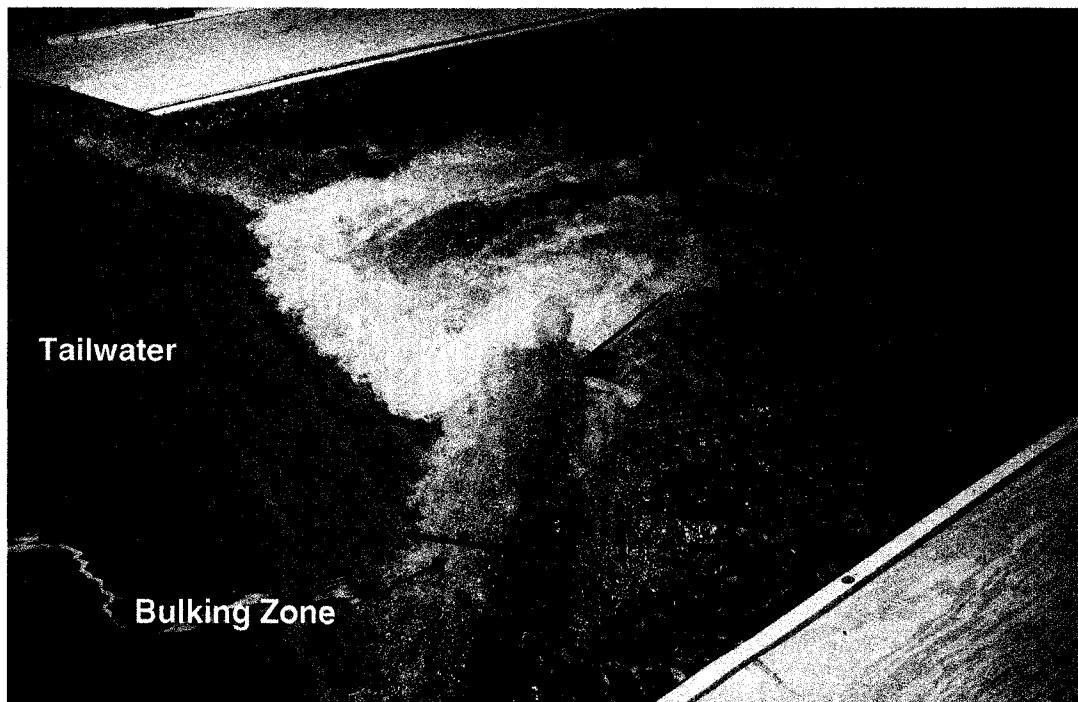


Figure 6.11 Training wall influence observed constant down the spillway chute.

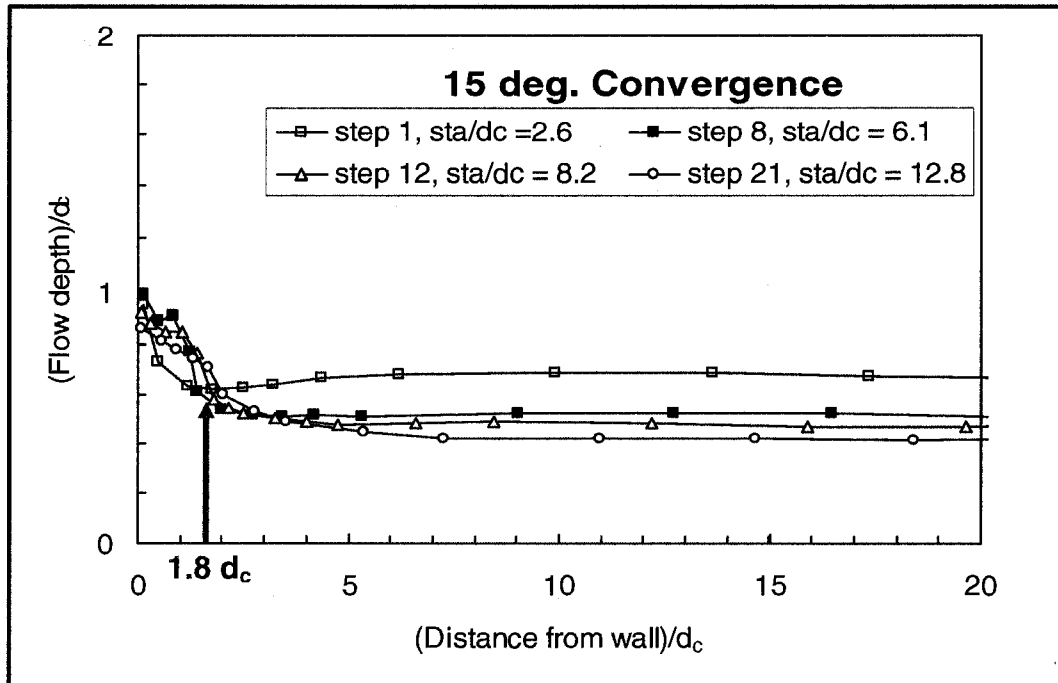


Figure 6.12 Cross-sectional profile normalized by critical depth indicating that the training wall influences the flow approximately  $1.8d_c$  horizontally away from the training wall for  $15^\circ$  convergence under full PMF ( $7.58 \text{ m}^3/(\text{s}\cdot\text{m})$  and  $81.6 \text{ cfs/ft}$ ) flow.

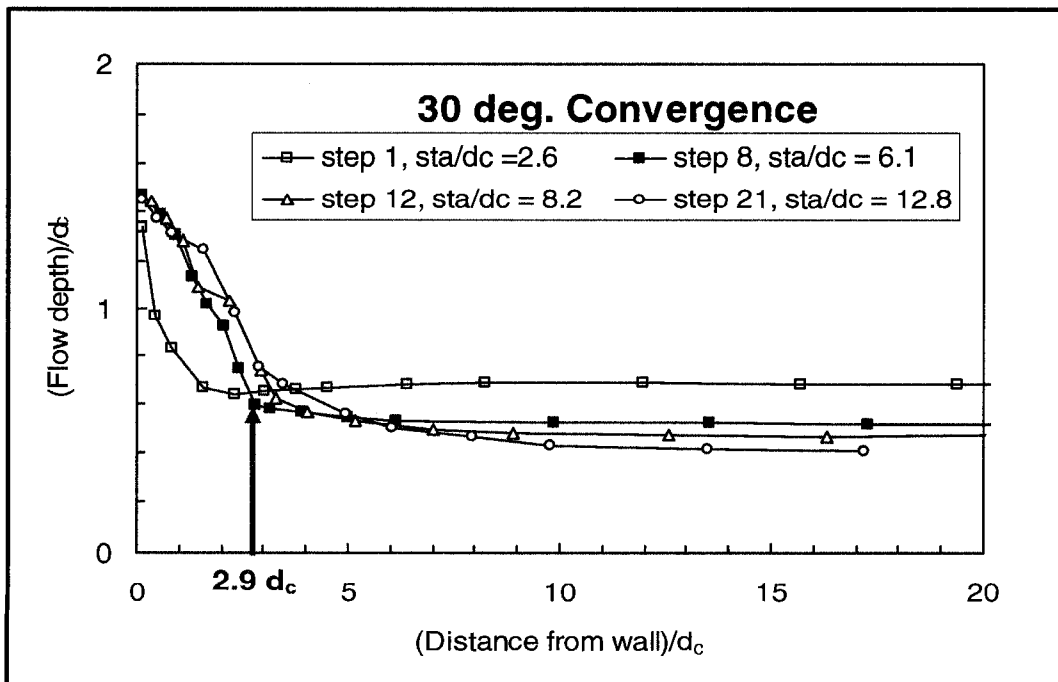


Figure 6.13 Cross-sectional profile normalized by critical depth indicating that the training wall influences the flow approximately  $2.9d_c$  away from the training wall for  $30^\circ$  convergence under full PMF ( $7.58 \text{ m}^3/(\text{s}\cdot\text{m})$  and  $81.6 \text{ cfs/ft}$ ) flow.

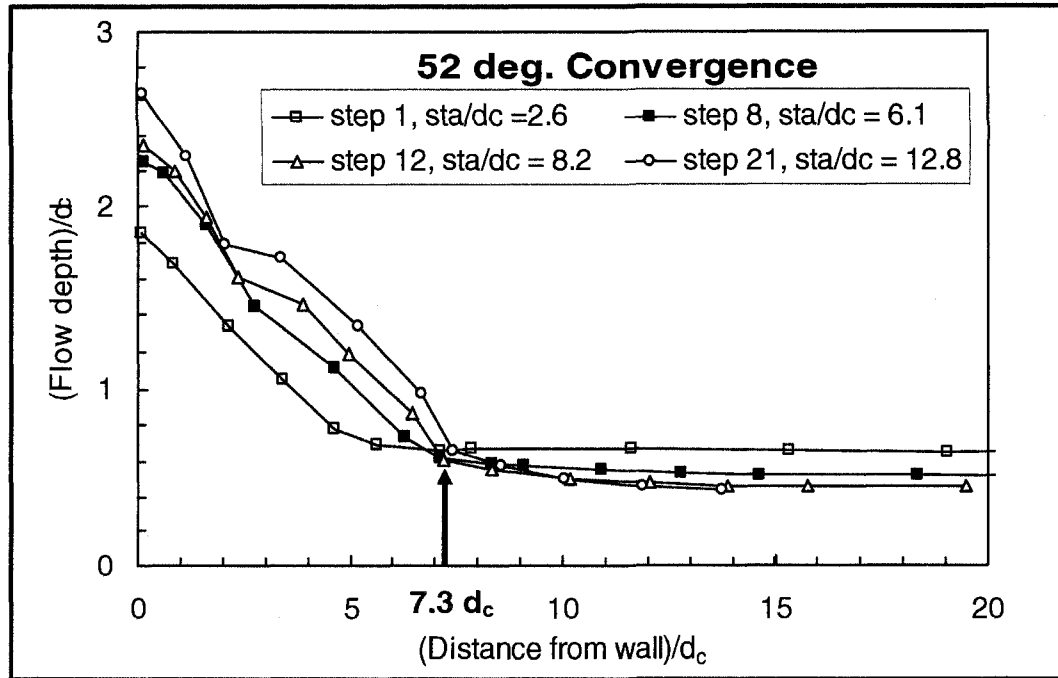


Figure 6.14 Cross-sectional profile normalized by critical depth indicating that the training wall influences the flow approximately  $7.3d_c$  away from the training wall for  $52^\circ$  convergence under full PMF ( $7.58 \text{ m}^3/(\text{s}\cdot\text{m})$  and  $81.6 \text{ cfs/ft}$ ) flow.

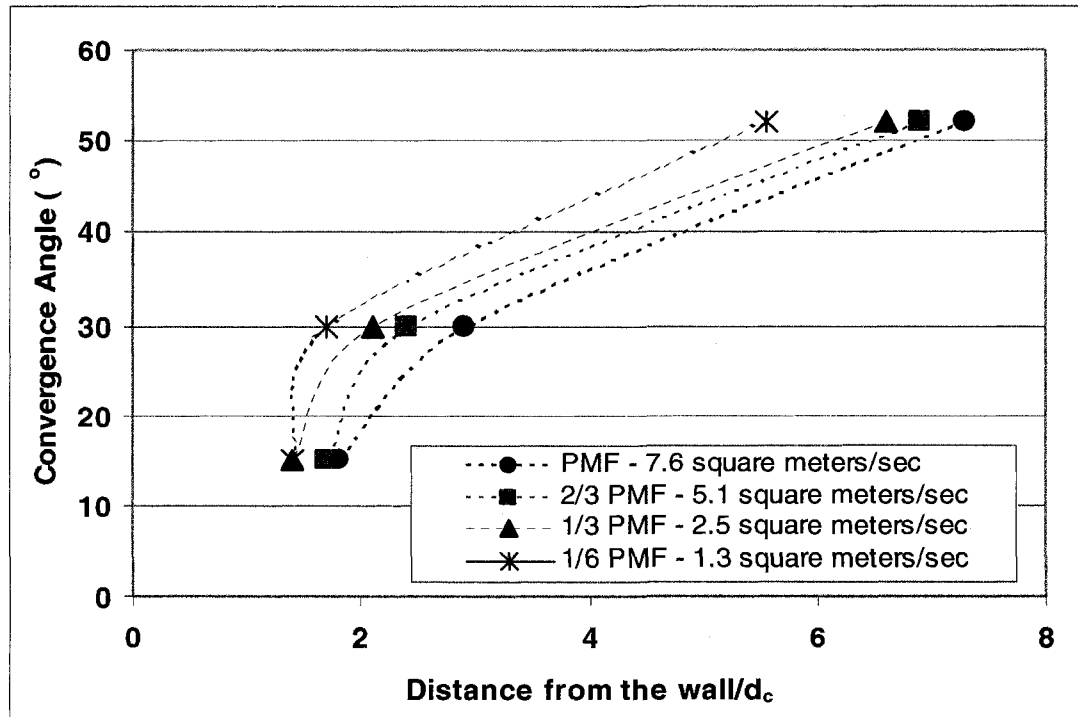


Figure 6.15 Bulking zone width or distance from the wall the training wall influences the flow horizontally normalized by critical depth versus the convergence angle.

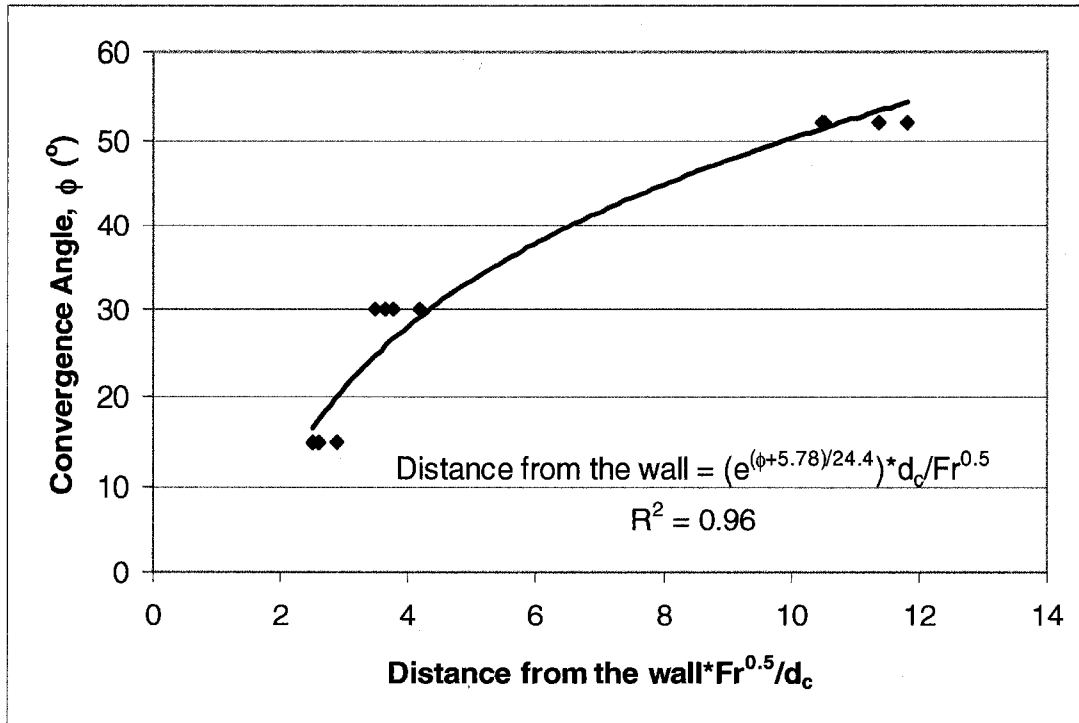


Figure 6.16 Bulking zone width prediction.

The flow depth at the training wall as illustrated in Figures 6.12, 6.13, and 6.14 was also evaluated over the series of stations located at steps one, eight, twelve, and twenty-one. In addition to the width of the bulking zone, Figures 6.12, 6.13, and 6.14 also present the maximum depth of the flow at the training wall normalized by critical depth for the different convergences at PMF (7.58 m<sup>3</sup>/(s·m) and 81.6 cfs/ft) flow. The normalized flow depth at the training wall was determined for all flow rates, convergences, and cross-section. These results are illustrated in Figure 6.17 where the normalized flow depth is plotted versus the distance downstream from the crest or station normalized by critical depth. Figure 6.17 presents the collective normalized flow depths at the training wall as 1.0d<sub>c</sub>, 1.5d<sub>c</sub>, 3.0d<sub>c</sub>, and 5.0d<sub>c</sub> for convergence angles 15°, 30°, 52°, and 70°.

respectively. The four data sets illustrated in Figure 6.17 were collapsed, with the exception of the 70° convergence data, by dividing the normalized flow depth at the training wall by the by  $\sin(\phi)$ , where  $\phi$  is the convergence angle and is presented in Figure 6.18.

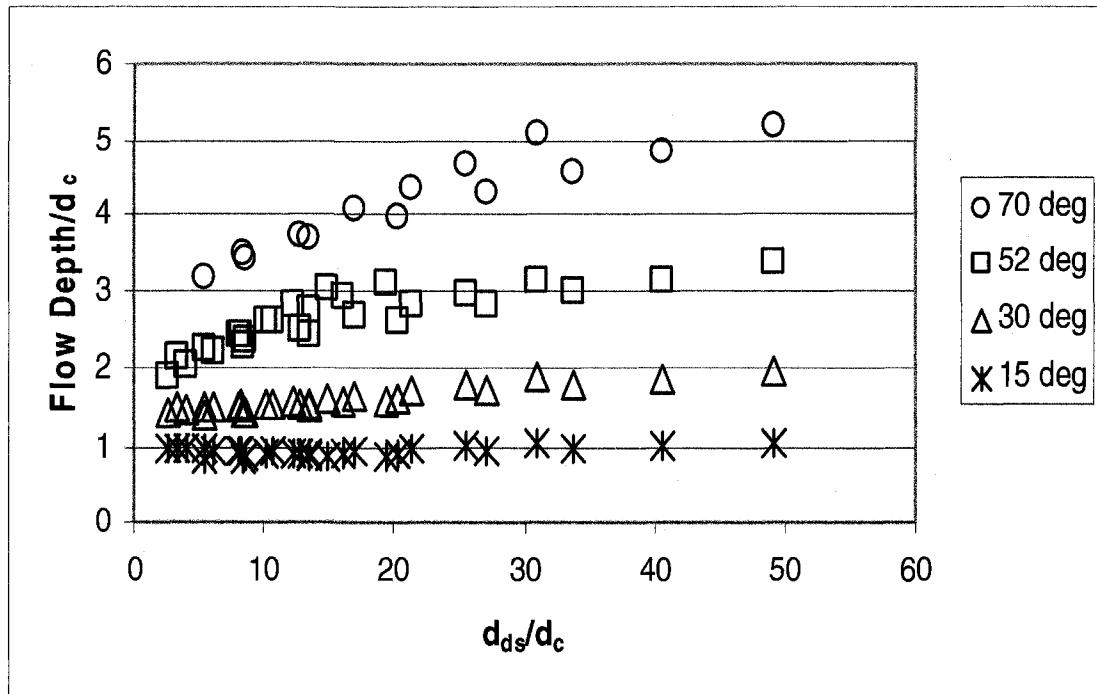


Figure 6.17. Flow depth at the training wall normalized by critical depth at the spillway crest versus the normalized distance downstream of the spillway crest.

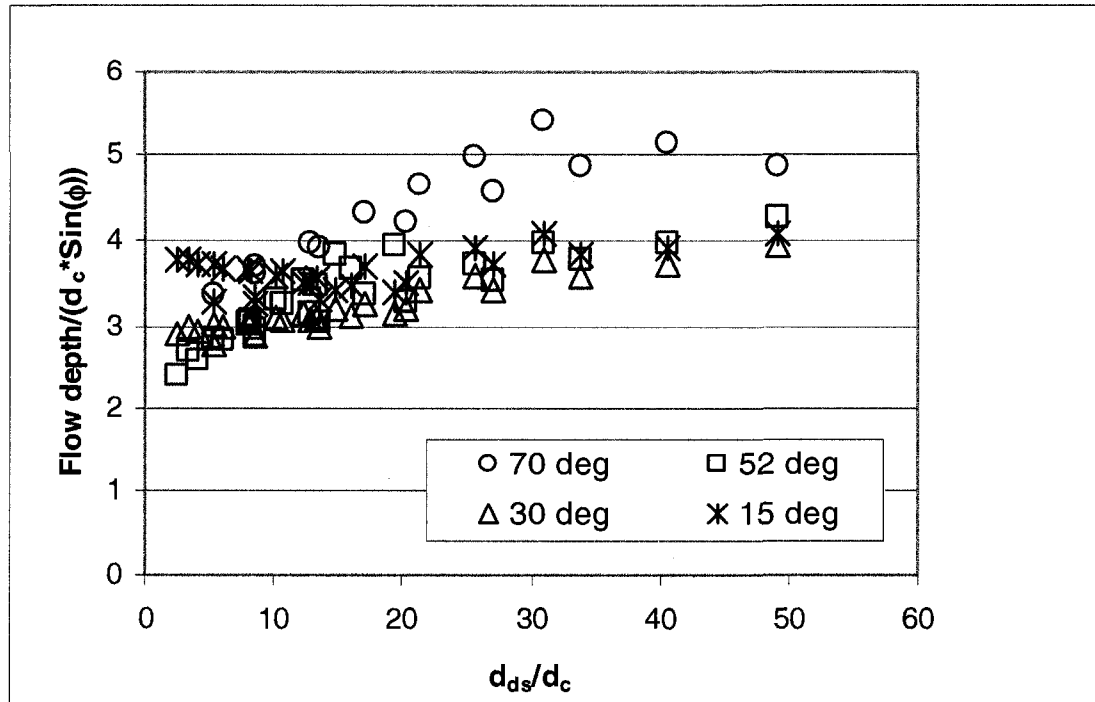


Figure 6.18. Flow depth at the training wall normalized by critical depth at the spillway crest divided by  $\sin(\phi)$  for all tested flows versus the normalized distance downstream of the spillway crest.

### Evaluation of a Simplified Momentum Equation for Determining Training Wall Height

As outlined in Chapter III, a simplified, momentum analysis approach can be used to predict the flow depth at the training wall. It was theorized that this approach would provide minimum height requirements for the training wall necessary to retain the design flow. Figure 6.19 illustrates a comparison of the predicted training wall height,  $H_{w\text{-predicted}}$  as calculated by Equation 3.22, and the measured training wall height necessary to contain the measured flow depth at the training wall,  $H_{w\text{-measured}}$ , for the stepped spillway described herein. Equation 3.22 as presented in Chapter III is:

$$H_w = \frac{d_w}{\cos(\psi_2)} \quad (3.22)$$

$H_{\text{wall-predicted}}$  requires the centerline flow depth, the velocity of the flow in the spillway chute, the training wall convergence, and the spillway chute slope for calculation through the term,  $d_w$ . The data presented in Figure 6.19 represents the data obtained from the four flow conditions, the four convergence angles, and for stations 4.6, 11.1, 14.8, 20.3, 23.1, and 26.8 m, respectively. As presented in Figure 6.19,  $H_{w\text{-predicted}}$  and  $H_{w\text{-measured}}$  are relatively close with approximately 11% error between the predicted and measured results for all tested convergence angles. A coefficient of determination of 0.91 and a linear relationship of

$$H_{w\text{-measured}} = 1.11H_{w\text{-predicted}} \quad (6.2)$$

are illustrated in Figure 6.19. The majority of the outliers depicted in Figure 6.16 represent the data from the 70° convergence configuration. These outliers may be a result of questionable water surface measurements because of the extreme turbulence of the flow near the wall. The severity of the convergence also impacted the depth over the spillway crest, which subsequently affected the unit discharge and velocity used in Equation 3.21.

Additionally, Equation 6.2 indicates that the predicted training wall height under-predicted the actual training wall height necessary to retain the design flow. This under-prediction may show weaknesses in the development of Equation 3.21. For instance, an assumption was made that the force with regard to the weight of water was negligible. However, it was evident that as the convergence angle increased the volume of water near the training wall increased. Ultimately, this impacts the prediction of the training wall height

necessary to retain the design flow at higher degrees of convergences because as the volume of water increases, the force with regards to the weight of water also increases, making it more significant in the overall prediction of the training wall height at the 70° convergence.

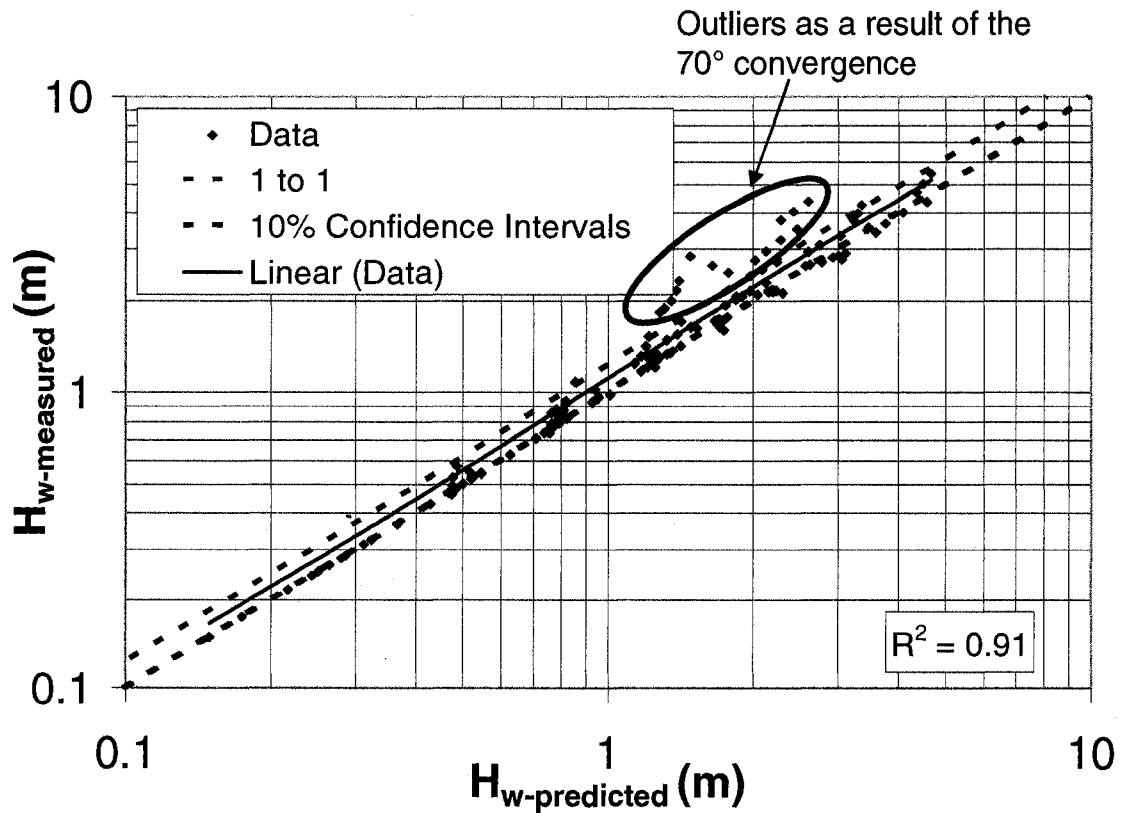


Figure 6.19. Predicted versus measured flow depth near the training wall for a stepped spillway for  $\phi$ 's ranging from 0 to 70 degrees.

The 70° convergence data was subsequently removed, and the data for the 0°, 15°, 30°, and 52° convergences were plotted for all flow conditions as presented in Figure 6.20. A linear regression analysis was performed to determine whether Equation 3.22 more closely predicts the observed data. As

shown in Figure 6.20, the data closely aligns with approximately 6% error, a coefficient of determination,  $R^2$ , of 0.98 and a linear relationship of

$$H_{w\text{-measured}} = 1.06H_{w\text{-predicted}} \quad (6.3)$$

The majority of the outliers in Figure 6.20 represent data points collected near the bottom of the chute near the energy dissipating stilling basin for the  $52^\circ$  convergence. The tailwater imposed by the end sill of the stilling basin may have influenced the measured results in this section of the stepped spillway, which resulted in the outliers depicted.

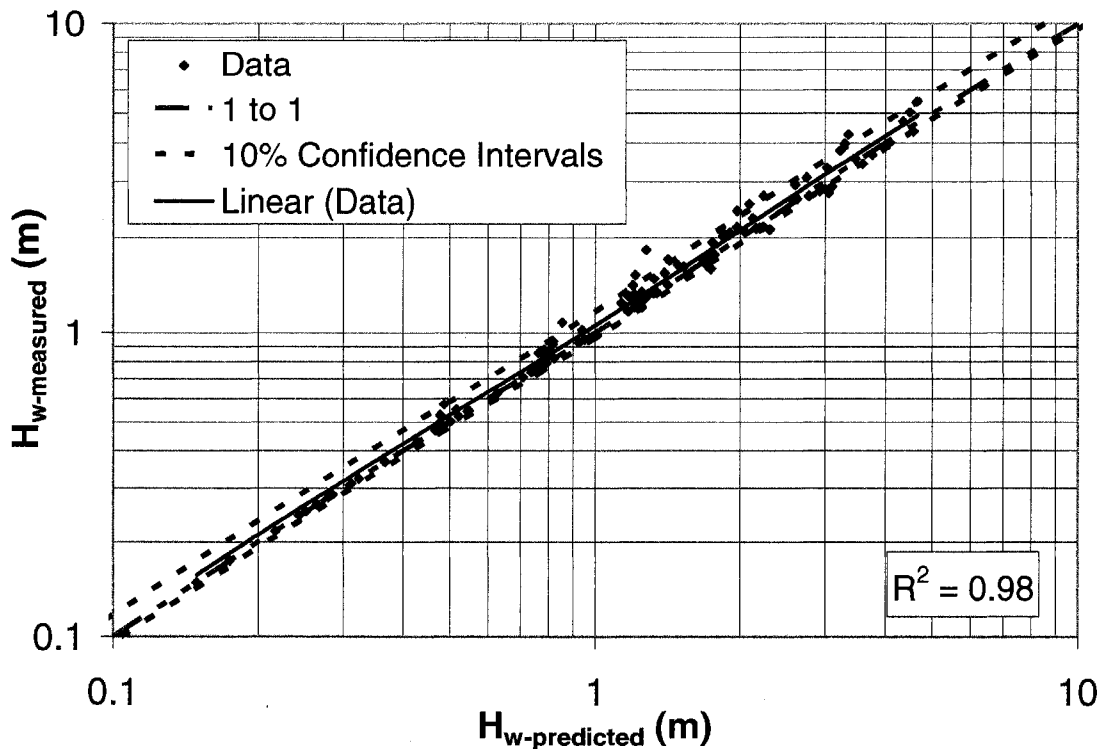


Figure 6.20. Predicted versus measured flow depth near the training wall for a stepped spillway for  $\phi$ 's ranging from 0 to  $52^\circ$ .

The linearity of the measured versus predicted training wall heights were further examined for each of the convergences. Figure 6.21 yields linear relationships for each set of convergence data. The resulting slopes for these

linear relationships for the 0°, 15°, 30°, and 52° convergences are 1.0, 1.01, 0.99, and 1.1 respectively. Based on this analysis, Equations 3.21 and 3.22 can be used directly to obtain the training wall height for convergences between 0° and 30° with approximately 1% error for a convergence of 30°. To expand the application of Equations 3.21 and 3.22 to slopes as large as 52°, the individual slopes from Figure 6.21 were examined as correction factors. Upon observation of the data, it appeared that the 0° to 52° data set could be enveloped using the slopes of the individual data sets. At first glance, it appeared that a  $1 + a \sin^b(\phi)$  relationship could be used to further refine Equations 3.21 and 3.22. In a trial and error method, “a” equal to 0.2 and “b” equal to 2.0 resulted in the best fit parameters. When  $1 + 0.2 \sin^2(\phi)$  was used as a multiplier of Equation 3.22, the linear relationship between the measured and this corrected predicted training wall height became

$$H_{w\text{-measured}} = 0.99 * (1 + 0.2 * \sin^2(\phi)) * H_{w\text{-predicted}} \quad (6.4)$$

Equation 6.4 presents a slightly more conservative relationship for determining the training wall height for convergences ranging from 0° to 52°.

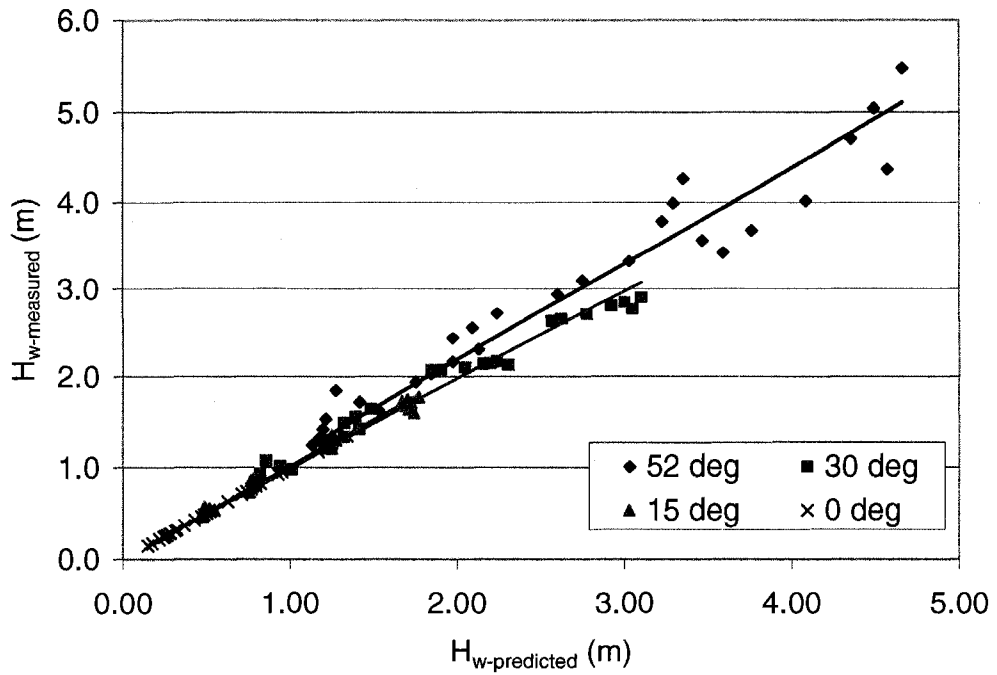


Figure 6.21  $H_{w\text{-measured}}$  versus  $H_{w\text{-predicted}}$  for convergences  $0^\circ$ ,  $15^\circ$ ,  $30^\circ$ , and  $52^\circ$  resulting in linear relationships with slopes of 1.0, 1.01, 0.99, and 1.1, respectively.

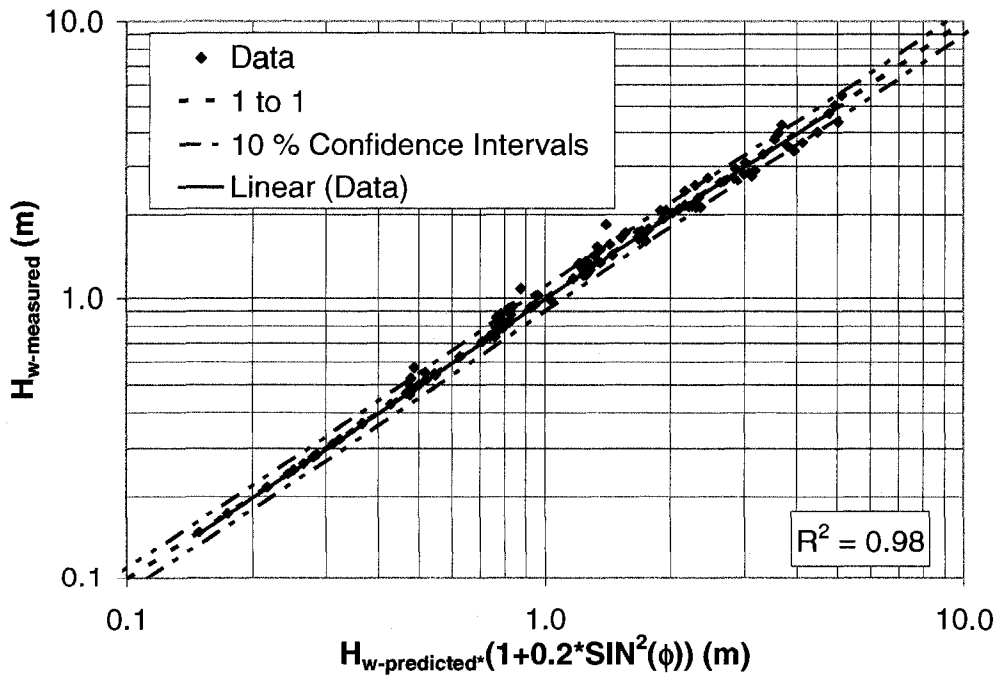


Figure 6.22  $H_{w\text{-measured}}$  versus a corrected  $H_{w\text{-predicted}}$ , for convergences ranging from  $0$  to  $52^\circ$  resulting in a linear relationship with a slope of 0.99 and a coefficient of determination of 0.98.

## Application of the Simplified Momentum Equation for Determining Minimum Training Wall for Converging Stepped Spillways

The simplified momentum equation presented in Equation 3.21

$$d_w = \sqrt{\frac{\left[ \frac{\gamma d^2 \cos \theta}{2} + \rho v^2 d (\cos(\theta) \cos(\psi) \sin(\phi) + \sin(\theta) \sin(\phi))^2 \right] * 2}{\gamma \cos(\psi_2) \cos(\psi)}} \quad (3.21)$$

requires known design elements of the stepped spillway. The design engineer must decide the spillway chute slope ( $\theta$ ) and the training wall convergence angle ( $\phi$ ). These two design parameters are used to determine the factors  $\psi = \tan^{-1}(\sin(\phi) \tan(\theta))$  and  $\psi_2 = \tan^{-1}(\cos(\phi) \tan(\theta))$ , which are necessary for determining the flow depth near the training wall,  $d_w$ .  $\psi$  and  $\psi_2$  were originally presented in Chapter III in the description of unit vector representing the upstream face of the control volume as presented in Equation 3.9 and in the description of unit vector representing the velocity along the wall as presented in Equation 3.11. As a word of caution, the flow depth near the wall in Equation 3.21, has only been applied to the spillway chute slope of 3(H):1(V), so further verification of its application to other spillway chute slopes configurations should be considered. Robinson and Kadavy (1998) reported that a change in step height in stepped spillways did not significantly impact the flow depth in the spillway; yet Chanson (2002) reported that the energy dissipation increased significantly with large step heights on relatively flat slopes. Therefore, Equation 3.21 may or may not be applicable to other step heights. More testing for verification is recommended.

In addition to the spillway parameters, flow conditions for the design of the spillway are necessary. One of the most important parameters for determining the necessary training wall height to retain the design flow is to estimate the flow depth,  $d_w$ , along the training wall in the spillway. Equation 3.21 as originally presented in Chapter III for  $d_w$  is expressed as

$$d_w = \sqrt{\frac{\gamma d^2 \cos \theta}{2} + \rho v^2 d (\cos(\theta) \cos(\psi) \sin(\phi) + \sin(\theta) \sin(\phi))^2} * 2 \quad (3.21)$$

$$\gamma \cos(\psi_2) \cos(\psi)$$

where the  $\gamma$  = specific weight of water,  $d$  = the flow depth in the center of spillway,  $\theta$  = chute slope,  $\rho$  = the density of water,  $v$  = velocity of the spillway flow as it descends the chute,  $\psi = \tan^{-1}(\sin(\phi) \tan(\theta))$ ,  $\phi$  = convergence angle, and  $\psi_2 = \tan^{-1}(\cos(\phi) \tan(\theta))$ . Additionally, the flow depth in the center of the spillway,  $d$ , and the velocity of the water as it descends the spillway chute,  $v$ , are required. The Portland Cement Association (2002) recommends that the design engineer follow classic spillway design procedures for determining training wall height for non-converging stepped spillways like that presented by the USBR (1987) as if the spillway was not stepped. The Portland Cement Association (2002) provides detailed examples for determining the flow depth in the center of a stepped spillway chute.

When considering the flow depth in the center of the spillway chute, the design engineer must decide if the flow depth in the center of the spillway chute will be affected by air entrainment. Equation 2.4, as presented in Chapter II, expressed as

$$L_I = 9.719(\sin \theta)^{0.0796} (F_*)^{0.713} h (\cos \theta) \quad (2.4)$$

where  $L_I$  = distance from the start of growth of boundary layer to the inception point of air entrainment (Figure 2.4),  $\theta$  = spillway slope,  $F_*$  = Froude number defined in terms of the roughness height:  $F_* = q_w / [g (\sin \theta) \{h (\cos \theta)\}^3]^{0.5}$ ,  $h$  = step height,  $q_w$  = discharge per unit width, and  $g$  = gravitational constant provides the design engineer a way of determining the location at which the air reaches the free surface. If it is determined that the air entrainment inception point occurs downstream of the expected length of the spillway chute, then the flow depth in the center of the spillway will not have to be adjusted for air entrainment. If the air entrainment inception point occurs downstream of the spillway crest and upstream of the expected design tailwater, then the design engineer must consider adjusting the flow depth to account for the bulking caused by the aeration in the flow from that point forward.

Once the flow depth in the center of the spillway chute is determined, the next step is to determine the velocity of the flow as it descends the spillway chute. Velocities at specific stations of interest were determined based on the unit design discharge per flow depth at that station. It was assumed that the unit design discharge remained constant through the stepped spillway chute.

The flow depth at the training wall as determined by Equation 3.21, and the  $\psi_2 = \tan^{-1}(\cos(\phi) \tan(\theta))$  are key components for estimating the training wall height necessary to retain the design flow in the spillway chute as presented in Equation 3.22. As presented in Equation 6.3 and Figure 6.20, the actual training wall height is approximately 1.06 of the predicted training wall height for spillway

convergences of 0° to 52°. To further refine the predicted relationship, a correction factor was determined to envelope the 0° to 52° data. A multiplier of  $1+0.2*\sin^2(\phi)$  improved the linear relationship between the measured training wall and the predicted training wall, so it is reasonable that Equation 3.22 with the  $1+0.2*\sin^2(\phi)$  adjustment can be used to determine the minimum training wall height for stepped spillways on a 3(H):1(V) slope with convergences ranging from 0° to 52° where air entrainment does not reach the free surface. Equation 6.5 would ultimately be used to determine the training wall height for converging stepped spillways ranging from 0° to 52° where air entrainment does not reach the free surface.

$$H_{wall} = \frac{(1 + 0.2 * \sin^2(\phi)) * \sqrt{\frac{\gamma d^2 \cos \theta}{2} + \rho v^2 d (\cos(\theta) \cos(\psi) \sin(\phi) + \sin(\theta) \sin(\phi))^2} * 2}{\gamma \cos(\psi_2) \cos(\psi) \cos(\psi_2)}$$

(6.5)

### **Limitations of the Application of the Simplified Momentum Equation for Predicting Training Wall Height for Converging Stepped Spillways**

The training wall height relationship outlined in Equation 6.5 has limitations in its use. First, Equation 6.5 does not account for air entrainment development at the free surface. Equation 6.5 evaluated the worse case scenario of a PMF flow condition for a relatively short spillway chute length. This was a conservative approach since these are flows that may only occur 500 or 1000 years. Additionally, if the design engineer finds that an aerated flow region

develops within the spillway, then another factor should be considered in the design of the spillway training walls to account for the bulked flow that occurs in this aerated region. This additional factor would increase the conservatism taken in this approach.

Secondly, Equation 6.5 has only been validated for one spillway chute slope. The equation is expected to predict the training wall height under similar flat slope conditions. Further investigation is recommended to evaluate the range of chute slopes that Equation 6.5 is valid.

Equation 6.5 is more suited for spillway convergences ranging from  $0^\circ$  to  $52^\circ$ . Application of Equation 6.5 begins to deteriorate for convergences greater than  $52^\circ$  as established by Figure 6.19. This limitation is a result of the assumptions made in developing Equation 3.21. The force related to the weight of water was assumed to be negligible when in all actuality there is value associated with this force. Increasing the convergence angle increases the volume of water along the training wall. As the volume of water increases, the force associated with the weight of water also increases. Therefore, large convergences angles, greater than  $52^\circ$ , are likely to under-predict the training wall height when considering Equation 3.21 because the volume of water and the force associated with the weight of water are expected to have a larger impact and can't be considered negligible at that point.

## CHAPTER VII

### SUMMARY OF RESULTS AND CONCLUSIONS

Stepped chutes are an established technology. In fact, some of these structures are centuries old. The majority of these chutes in spillway applications are designed for gravity dams where the spillway chute is expected to have a slope greater than  $30^\circ$ ; and therefore, the majority of the research to date has been in this arena. The NRCS is expected to design nearly 1,100 of these stepped chute spillways for the rehabilitation of existing embankment dams for the means of increasing spillway capacity. NRCS structures are typically placed over the existing embankment such that the spillway chute slope is the same as the downstream slope of the embankment face. These slopes are normally  $30^\circ$  or flatter. Some of these structures have further complications due to convergence of the spillway chute required to meet land right and/or topography constraints. Lack of design guidance available for stepped spillways applied in these situations was the reasoning for completing this research.

A practical approach in terms of design aids, Figures 6.16 and 6.18, and a theoretical simplified momentum relationship, Equations 3.21 and 3.22, was developed to determine minimum training wall heights for converging stepped spillways having a 3(H):1(V) chute slope, step heights of 0.3 m (1 ft), and a chute convergence up to  $70^\circ$ . The design aids, Figures 6.16 and 6.18,

provide a graphical approach for determining the bulking width and the flow depth at the training wall. Equations 3.21 and 3.22 provide an analytical approach to predict the flow depth near the training wall with 11% error expected to that of the measured flow depth for convergences up to 70°. The flow depth prediction for convergence angles up to 52° improves significantly with 6% reported error when applying Equations 3.11 and 3.22. Both the design aid and theoretical approach provide a conservative approach for estimating the training wall height because PMF flows were under consideration for the development of these approaches. Appendix B provides a design example using both the design aids and the theoretical equation.

When applying the empirical and theoretical approaches, the design engineer must consider the limitations of their development. First, the empirical and theoretical approaches do not account for air entrained flow. Chanson's (1994) relationship, Equation 2.4, may be used to determine inception point location for chute slopes as flat as 18.4°. This relationship has been further verified by Hunt and Kadavy (2007, 2008) such that it can be used on slopes as flat as 14°. Flows downstream of the inception point are expected to be aerated, causing an increase in flow depth. Flows upstream of the inception point are expected to be non-aerated at the surface. Therefore, it is anticipated that the flow depth will not be affected by air entrainment upstream of the inception point. In many cases, stepped spillways applied to earthen embankments are expected to have relatively short chute lengths with relatively high discharges; therefore, the air

entrainment is not expected to significantly impact the height of the training wall. However, using Chanson's (1994) relationship, the location of the inception point can verify whether air entrainment will become a consideration in the design of the training walls.

Additionally, the empirical and theoretical approaches were developed for a specific spillway chute slope of 3(H):1(V). Equations 3.21 and 3.22 were developed using the concepts of momentum and a control volume analysis, so this approach is expected to perform well over a range of chute slopes. Yet, the theoretical approach should be further investigated to determine the range of chute slopes it is applicable. The design aids were solely based on a chute slope of 3(H):1(V), and they are only applicable for this chute slope. Further testing may establish similar trends in the flow depth and bulking width at the training wall. To develop these design aids, additional testing is recommended to determine their applicability over a greater range of chute slopes.

## REFERENCES

- Boes, R. M. and W. H. Hager. (2003a). Two-phase flow characteristics of stepped spillways. *J. of Hydr. Engrg.*, ASCE, 129(9):661-670.
- Boes, R. M. and W. H. Hager. (2003b). Hydraulic design of stepped spillways. *J. of Hydr. Engrg.*, ASCE, 129(9):671-679.
- Boes, R., and H.-E. Minor. (2002). "Hydraulic design of stepped spillways for RCC dams." *Hydropower Dams*, 9(3), 87-91.
- Chamani, M. R. and N. Rajaratnam. (1999). "Characteristics of skimming flow over stepped spillways." *Jour. of Hydr. Engrg.*, ASCE, 125(4), 361-368.
- Chanson, H. (1993). "Stepped spillway flows and air entrainment." *Can. Jour. of Civil Eng*, 20(3), 422-435.
- Chanson, H. (1994). "Hydraulics of skimming flows over stepped channels and spillways." *Jour. of Hydr. Engrg. Research*, 32(3), 445-460.
- Chanson, H. (1995). *Hydraulic Design of Stepped Cascades, Channels, Weirs, and Spillways*. Pergamon, Oxford, UK.
- Chanson, H. (2001). "Hydraulic design of stepped spillways and downstream energy dissipators." *Dam Engineering*. 11(4): 205-242.
- Chanson, H. (2002). *The Hydraulics of Stepped Chutes and Spillways*. Steenwijk, The Netherlands: A. A. Balkema Publishers.
- Chow, V. T. (1959). *Open-Channel Hydraulics*. Boston, MA: McGraw-Hill, Book Company, Inc.
- Falvey, Henry T. (1980). "Air-water flow in hydraulic structures." *Engineering Monograph No. 41*. United States Department of the Interior, Water and Power Resources Service.
- Frizell, K. (2005). Research State-of-the Art and Needs for Hydraulic Design of Stepped Spillways. U. S. Department of Interior, Bureau of Reclamation, U. S. Government Printing Office, Denver, Colorado.

- Hanna, L. J. and C.A. Pugh. (1997). *Hydraulic Model Study of Pilar Dam*. U.S. Department of Interior, Bureau of Reclamation, U. S. Government Printing Office, Denver, Colorado.
- Hunt, S. L., K. C. Kadavy, S. R. Abt, and D. M. Temple. (2005). "Impact of converging chute walls for RCC stepped spillways." *In the Proc. 2005 World Environmental and Water Resources Congress, ASCE Conference, Anchorage, Alaska.*
- Hunt, S. L., K. C. Kadavy, and D. M. Temple. (2006). "Converging RCC stepped spillways." *In the Proc. 2006 World Environmental and Water Resources Congress, ASCE Conference, Omaha, Nebraska.*
- Hunt, S. L. and K. C. Kadavy. (2007). "Renwick dam RCC stepped spillway research." *In the Proceedings of the Association of State Dam Safety Officials Annual Conference. Austin, Texas.*
- Hunt, S. L. and K. C. Kadavy. (2008). "Velocities and energy dissipation on a flat-sloped stepped spillway." *ASABE Annual International Meeting. ASABE Paper No. 084151. Providence, RI.*
- Hunt, S. L., K. C. Kadavy, S. R. Abt, and D. M. Temple. (2008). "Impact of converging chute walls for RCC stepped spillways." *Jour. of Hydr. Engrg., ASCE, 134(7):1000-1003.*
- Kobus, H. (1984). "Local air entrainment and detrainment." *Proc., Symp. On Scale Effects in Modelling Hydraulic Structures, H. Kobus, ed., Esslingen, Germany, Vol. 4.10, 1-10.*
- Matos, J., M. Sanchez, A. Quintela, and J. Dolz. (1999). "Characteristic depth and pressure profiles in skimming flow over stepped spillways." *In the Proc. 28<sup>th</sup> IAHR Congress (CD-ROM), Theme B. Graz, Austria.*
- Munson, B. R., D. F. Young, and T. H. Okiishi. (1994). *Fundamentals of Fluid Mechanics*. New York, NY: John Wiley & Sons, Inc.
- Pegram, G. G. S., A. K. Officer, and S. R. Mottram. (1999). "Hydraulics of skimming flow on modeled stepped spillways." *Jour. of Hydr. Engrg., ASCE, 125(5), 500-510.*
- Portland Cement Association (PCA). (2006). "Roller-compacted concrete: the right choice for safe dams." (Accessed February 10, 2006: [http://www.cement.org/water/dams\\_rcc.asp](http://www.cement.org/water/dams_rcc.asp))
- Rajaratnam, N. (1990). "Skimming flow in stepped spillways." *Jour. of Hydr. Engrg., ASCE, 116(4), 587-591.*

- Rice, C. E. and K. C. Kadavy. (1996). "Model study of a roller compacted concrete stepped spillway." *Jour. of Hydraulic Engrg.*, ASCE, 122(6):292-297.
- Rice, C. E. and K. C. Kadavy. (1997). "Physical model study of the proposed spillway for Cedar Run Site 6, Fauquier County Virginia." *Appl. Eng. Agric.*, ASAE, 13(6), 723-729.
- Robinson, K. M., C. E. Rice, K. C. Kadavy, and J. R. Talbot. (1998). "Energy losses on roller compacted concrete stepped spillways." *In the Proc. 1998 Water Resources Engineering, ASCE Conference*, Memphis, TN 2:1434-1439.
- Rutschmann, P. (1988). "Belüftungseinbauten in Schussrinnen." PhD thesis, VAW, ETH Zurich, Switzerland (in German).
- Sorenson, R. M. (1985). "Stepped spillway hydraulic model investigation." *J. Hydr. Engrg.*, ASCE, 111(12), 1461-1472.
- Takahashi, M., C. A. Gonzalez, and H. Chanson. (2006). "Self-aeration and turbulence in a stepped Channel: influence of cavity surface roughness." *International Journal of Multiphase Flow*. 32:1370-1385.
- United States Department of Agriculture (USDA) Natural Resources Conservation Service. 2005. Watershed Rehabilitation: A Progress Report 2005. USDA, NRCS, Washington D. C.
- United States Department of the Interior Bureau of Reclamation (USBR). (1973). *Design of Small Dams*. U.S. Government Printing Office, Denver, Colorado.
- United States Bureau of Reclamation (USBR) (formerly the Water and Power Resources Service in the U.S. Department of the Interior). (1980). *Hydraulic Laboratory Techniques*. U.S. Government Printing Office, Denver, Colorado.
- Woolbright, R. W., S. L. Hunt, and G. J. Hanson. 2008. "Model study of RCC stepped spillways with sloped converging training walls." *ASABE Annual International Meeting*. ASABE Paper No. 084149. Providence, RI.
- Yasuda, Y. and I. Ohtsu. (1999). "Flow resistance of skimming flow in stepped channels." *Proc., 28<sup>th</sup> IAHR Congress*, Graz, Austria, Session B14.

## **APPENDIX A**

Table A1. Summary of prototype testing program.

Test #	$\phi$ (°) Left, Right	Flood Event	$q_{\text{proto}}$ ( $\text{m}^3/(\text{s}\cdot\text{m})$ )	$\text{TW}_{\text{proto}}$ (m)	$d_c$ (m)
1	52, 52	2/3 PMF	5.05	286.2	1.37
2	52, 52	PMF	7.58	287.1	1.80
3	52, 52	1/6 PMF	1.26	283.7	0.55
4	52, 52	1/3 PMF	2.52	284.9	0.87
24	15, 30	PMF	7.58	-	1.80
25	15, 30	2/3 PMF	5.05	-	1.37
26	15, 30	1/3 PMF	2.52	-	0.87
27	15, 30	1/6 PMF	1.26	-	0.55
32	0, 70	1/6 PMF	1.26	-	0.55
33	0, 70	1/3 PMF	2.52	-	0.87

Table A2. Prototype centerline water surface profile for test # 1.

Prototype Water Surface Profile		
Centerline Profile, $Y_p = 0.0$ m; 2/3 PMF		
station $X_p$ (m)	elev $Z_p$ (m)	Comments
-113.12	292.00	
-99.71	292.00	
-86.30	292.00	
-72.89	292.00	
-59.48	292.00	
-46.07	292.00	
-32.66	291.99	
-19.25	291.98	
-12.54	291.95	
-9.19	291.89	
-5.83	291.82	
-2.48	291.79	
-1.81	291.77	Ogee Crest
-1.14	291.71	Ogee Crest
-0.47	291.63	Ogee Crest
0.20	291.44	Ogee Crest
0.87	291.20	Ogee Crest
1.54	290.89	Ogee Crest
2.21	290.59	Ogee Crest
2.88	290.26	Ogee Crest
3.55	289.97	Ogee Crest
4.22	289.70	Steps Start
4.90	289.47	
6.24	288.97	
7.58	288.47	
8.92	287.97	
10.26	287.52	
11.60	287.03	
12.94	286.57	
14.28	286.12	
15.62	285.68	Edge of Tailwater
16.97	285.30	TW
19.65	285.63	TW
22.33	285.78	TW
25.01	285.81	TW
27.69	286.32	TW
30.38	286.61	Stilling Basin
33.06	286.63	Stilling Basin
37.75	286.61	Stilling Basin
41.11	286.50	Out of stilling basin
47.81	286.48	
54.52	286.48	
61.22	286.40	
74.63	286.34	
88.04	286.22	
101.46	286.32	
114.87	286.17	

Table A3. Model centerline water surface profile for test # 1.

Model Water Surface Profile		
Run #: Run 1		Centerline profile, $Y_m = 0.0$ m; 2/3 PMF
Date: 14 Oct 2004		
station $X_m$ (m)	elev $Z_m$ (m)	Comments
-5.14	13.27	
-4.53	13.27	
-3.92	13.27	
-3.31	13.27	
-2.70	13.27	
-2.09	13.27	
-1.48	13.27	
-0.87	13.27	
-0.57	13.27	
-0.42	13.27	
-0.27	13.26	
-0.11	13.26	
-0.08	13.26	Ogee Crest
-0.05	13.26	Ogee Crest
-0.02	13.26	Ogee Crest
0.01	13.25	Ogee Crest
0.04	13.24	Ogee Crest
0.07	13.22	Ogee Crest
0.10	13.21	Ogee Crest
0.13	13.19	Ogee Crest
0.16	13.18	Ogee Crest
0.19	13.17	Steps Start
0.22	13.16	
0.28	13.13	
0.34	13.11	
0.41	13.09	
0.47	13.07	
0.53	13.05	
0.59	13.03	
0.65	13.01	
0.71	12.99	Edge of Tailwater
0.77	12.97	TW
0.89	12.98	TW
1.01	12.99	TW
1.14	12.99	TW
1.26	13.01	TW
1.38	13.03	Stilling Basin
1.50	13.03	Stilling Basin
1.72	13.03	Stilling Basin
1.87	13.02	Out of stilling basin
2.17	13.02	
2.48	13.02	
2.78	13.02	
3.39	13.02	
4.00	13.01	
4.61	13.01	
5.22	13.01	

Table A4. Prototype water surface profile along the right wall looking downstream for test # 1.

<b>Prototype Water Surface Profile</b>			
WS along Rt. Wall looking d.s. 2/3 PMF			
<b>station X<sub>p</sub> (m)</b>	<b>station Y<sub>p</sub> (m)</b>	<b>elev Z<sub>p</sub>(m)</b>	<b>Comments</b>
-12.54	-49.62	291.96	Rt. Wall w.s. profile looking d.s.
-9.19	-49.62	291.85	
-7.85	-49.62	291.55	
-6.50	-49.62	291.64	
-3.15	-49.62	291.73	
-0.47	-49.62	291.56	
1.54	-49.62	290.92	
2.88	-49.62	290.54	
3.69	-49.62	291.27	joint - starts conv
4.90	-48.15	291.55	
7.58	-47.95	290.86	
10.93	-40.70	289.88	
14.28	-36.55	289.01	
17.64	-32.19	288.14	
19.65	-29.84	287.59	
21.32	-27.49	287.09	wall levels out
24.34	-23.47	286.25	
27.02	-20.79	285.82	
29.04	-17.77	285.92	
30.38	-17.57	284.22	Basin wall
34.40	-16.09	286.70	
38.22	-14.75	287.60	Basin exit

Table A5. Model water surface profiles along the right wall looking downstream for test # 1.

<b>Model Water Surface Profile</b>			
WS along Lt. Wall looking d.s. 2/3 PMF			
<b>station X<sub>m</sub> (m)</b>	<b>station Y<sub>m</sub> (m)</b>	<b>elev Z<sub>m</sub>(m)</b>	<b>Comments</b>
-0.57	-2.26	13.27	Rt. Wall w.s. profile looking d.s.
-0.42	-2.26	13.27	
-0.36	-2.26	13.25	
-0.30	-2.26	13.26	
-0.14	-2.26	13.26	
-0.02	-2.26	13.25	
0.07	-2.26	13.22	
0.13	-2.26	13.21	
0.17	-2.26	13.24	joint - starts conv
0.22	-2.19	13.25	
0.34	-2.18	13.22	
0.50	-1.85	13.18	
0.65	-1.66	13.14	
0.80	-1.46	13.10	
0.89	-1.36	13.07	
0.97	-1.25	13.05	wall levels out
1.11	-1.07	13.01	
1.23	-0.94	12.99	
1.32	-0.81	13.00	
1.38	-0.80	12.92	Basin wall
1.56	-0.73	13.03	
1.74	-0.67	13.07	Basin exit

Table A6. Prototype water surface profile along the left wall looking downstream for test #1.

<b>Prototype Water Surface Profile</b>			
WS along Lt. Wall looking d.s. 2/3 PMF			
<b>station X<sub>p</sub> (m)</b>	<b>station Y<sub>p</sub> (m)</b>	<b>elev Z<sub>p</sub> (m)</b>	<b>Comments</b>
-12.54	49.62	291.94	
-9.19	49.62	291.73	
-7.85	49.62	291.54	
-6.50	49.62	291.62	
-3.15	49.62	291.73	
-0.47	49.62	291.57	
1.54	49.62	290.94	
2.88	49.62	290.48	
3.69	49.62	291.09	
4.90	48.28	291.50	
7.58	44.93	290.82	
10.93	40.90	289.86	
14.28	36.55	289.01	
17.64	32.52	288.17	
19.65	29.84	287.60	
21.32	28.03	287.15	wall levels off
24.34	24.01	286.24	
27.02	20.45	285.65	
29.04	18.11	285.70	joint
30.38	17.64	284.51	
34.40	16.09	286.94	
38.22	15.02	287.36	basin exit

Table A7. Model water surface profile along the left wall looking downstream for test #1.

<b>Model Water Surface Profile</b>			
WS along Lt. Wall looking d.s. 2/3 PMF			
<b>station</b> <b>X<sub>m</sub> (m)</b>	<b>station</b> <b>Y<sub>m</sub> (m)</b>	<b>elev</b> <b>Z<sub>m</sub>(m)</b>	<b>Comments</b>
-0.57	-2.26	13.27	Rt. Wall w.s. profile looking d.s.
-0.42	-2.26	13.27	
-0.36	-2.26	13.25	
-0.30	-2.26	13.26	
-0.14	-2.26	13.26	
-0.02	-2.26	13.25	
0.07	-2.26	13.22	
0.13	-2.26	13.21	
0.17	-2.26	13.24	joint - starts conv
0.22	-2.19	13.25	
0.34	-2.18	13.22	
0.50	-1.85	13.18	
0.65	-1.66	13.14	
0.80	-1.46	13.10	
0.89	-1.36	13.07	
0.97	-1.25	13.05	wall levels out
1.11	-1.07	13.01	
1.23	-0.94	12.99	
1.32	-0.81	13.00	
1.38	-0.80	12.92	Basin wall
1.56	-0.73	13.03	
1.74	-0.67	13.07	Basin exit

Table A8. Prototype cross-sectional water surface profile along step 1, station 4.6 m for test #1.

<b>Prototype Water Surface Profile</b>		
Cross-Sectional Profile, $X_p = 4.6$ m - Step 1; 2/3 PMF		
<b>station</b>	<b>elev</b>	
<b><math>Y_p</math> (m)</b>	<b><math>Z_p</math>(m)</b>	<b>Comments</b>
-49.08	292.89	top of wall
-48.95	291.57	
-47.95	291.33	
-46.60	290.59	
-45.26	290.21	
-42.92	289.77	
-40.50	289.54	end of rough water
-37.55	289.55	
-34.87	289.55	
-28.16	289.55	
-21.46	289.55	
-14.75	289.55	
-8.05	289.55	
-1.34	289.55	
5.36	289.54	
12.07	289.54	
18.78	289.54	
25.48	289.56	
32.19	289.58	
35.54	289.58	
38.22	289.58	
39.56	289.58	
40.90	289.59	
42.25	289.62	start of rough water surface
44.26	290.06	
45.60	290.36	
46.94	290.65	
47.61	291.14	
48.28	291.49	
49.08	291.61	
49.22	292.90	top of wall

Table A9. Model cross-sectional water surface profile along step 1, station 4.6 m for test #1.

<b>Model Water Surface Profile</b>		
Cross-Sectional Profile, $X_m = 0.21$ m - Step 1; 2/3 PMF		
<b>station</b>	<b>elev</b>	
<b><math>Y_m</math> (m)</b>	<b><math>Z_m</math> (m)</b>	<b>Comments</b>
-2.23	13.31	top of wall
-2.23	13.25	
-2.18	13.24	
-2.12	13.21	
-2.06	13.19	
-1.95	13.17	
-1.84	13.16	end of rough water
-1.71	13.16	
-1.58	13.16	
-1.28	13.16	
-0.98	13.16	
-0.67	13.16	
-0.37	13.16	
-0.06	13.16	
0.24	13.16	
0.55	13.16	
0.85	13.16	
1.16	13.16	
1.46	13.16	
1.62	13.16	
1.74	13.16	
1.80	13.16	
1.86	13.16	
1.92	13.16	start of rough water surface
2.01	13.18	
2.07	13.20	
2.13	13.21	
2.16	13.23	
2.19	13.25	
2.23	13.26	
2.24	13.31	top of wall

Table A10. Prototype cross-sectional water surface profile along step 8, station 11 m for test #1.

<b>Prototype Water Surface Profile</b>		
Cross-Sectional Profile, $X_p = 11$ m - Step 8; 2/3 PMF		
<b>station</b> $Y_p$ (m)	<b>elev</b> $Z_p$ (m)	<b>Comments</b>
-41.11	290.78	top of wall
-40.90	289.87	
-39.90	289.68	
-38.22	288.93	
-36.88	288.96	
-35.54	288.53	
-34.20	288.23	
-31.85	287.68	end of rough water
-30.85	287.44	
-28.16	287.35	
-24.81	287.30	
-21.46	287.27	
-14.75	287.23	
-8.05	287.23	
-1.34	287.23	
5.36	287.23	
12.07	287.23	
18.78	287.24	
22.13	287.26	
25.48	287.30	
27.49	287.33	
30.51	287.42	
31.52	287.52	start of rough water surface
32.86	287.93	
34.20	288.23	
36.21	288.69	
38.56	288.99	
40.23	289.74	
41.04	289.84	
41.37	290.78	top of wall

Table A11. Model cross-sectional water surface profile along step 8, station 0.5 m for test #1.

<b>Model Water Surface Profile</b>		
Cross-Sectional Profile, $X_m = 0.5$ m - Step 8; 2/3 PMF		
<b>station</b> $Y_m$ (m)	<b>elev</b> $Z_m$ (m)	<b>Comments</b>
-1.87	13.22	top of wall
-1.86	13.18	
-1.81	13.17	
-1.74	13.13	
-1.68	13.13	
-1.62	13.11	
-1.55	13.10	
-1.45	13.08	end of rough water
-1.40	13.07	
-1.28	13.06	
-1.13	13.06	
-0.98	13.06	
-0.67	13.06	
-0.37	13.06	
-0.06	13.06	
0.24	13.06	
0.55	13.06	
0.85	13.06	
1.01	13.06	
1.16	13.06	
1.25	13.06	
1.39	13.06	
1.43	13.07	start of rough water surface
1.49	13.09	
1.55	13.10	
1.65	13.12	
1.75	13.14	
1.83	13.17	
1.87	13.17	
1.88	13.22	top of wall

Table A12. Prototype cross-sectional water surface profile along step 12, station 14.8 m for test #1.

<b>Prototype Water Surface Profile</b>		
Cross-Sectional Profile, $X_p = 14.8$ m - Step 12; 2/3 PMF		
<b>station</b>	<b>elev</b>	
<b><math>Y_p</math> (m)</b>	<b><math>Z_p</math> (m)</b>	<b>Comments</b>
-36.48	289.55	top of wall
-36.34	288.87	
-35.87	288.88	
-35.20	288.66	
-33.86	287.98	
-32.19	287.89	
-30.85	287.42	
-28.16	286.85	
-26.82	286.36	end of rough water
-25.48	286.19	
-24.14	286.13	
-22.80	286.08	
-21.46	286.04	
-18.11	285.98	
-14.75	285.95	
-8.05	285.95	
-1.34	285.94	
5.36	285.95	
12.07	285.95	
18.78	285.99	
22.13	286.05	
24.14	286.14	
25.48	286.23	
27.49	286.70	start of rough water surface
30.85	287.59	
32.86	287.99	
34.20	288.16	
35.54	288.70	
36.48	288.89	
36.75	289.54	top of wall

Table A13. Model cross-sectional water surface profile along step 12, station 0.67 m for test #1.

<b>Model Water Surface Profile</b>		
Cross-Sectional Profile, $X_m = 0.67$ m - Step 12; 2/3 PMF		
<b>station</b>	<b>elev</b>	
<b><math>Y_m</math> (m)</b>	<b><math>Z_m</math> (m)</b>	<b>Comments</b>
-1.66	13.16	top of wall
-1.65	13.13	
-1.63	13.13	
-1.60	13.12	
-1.54	13.09	
-1.46	13.09	
-1.40	13.06	
-1.28	13.04	
-1.22	13.02	end of rough water
-1.16	13.01	
-1.10	13.01	
-1.04	13.00	
-0.98	13.00	
-0.82	13.00	
-0.67	13.00	
-0.37	13.00	
-0.06	13.00	
0.24	13.00	
0.55	13.00	
0.85	13.00	
1.01	13.00	
1.10	13.01	
1.16	13.01	
1.25	13.03	start of rough water surface
1.40	13.07	
1.49	13.09	
1.55	13.10	
1.62	13.12	
1.66	13.13	
1.67	13.16	top of wall

Table A14. Prototype cross-sectional water surface profile along step 18, station 20.3 m for test #1.

<b>Prototype Water Surface Profile</b>		
Cross-Sectional Profile, $X_p = 20.3$ m - Step 18; 2/3 PMF		
<b>station</b> <b><math>Y_p</math> (m)</b>	<b>elev</b> <b><math>Z_p</math> (m)</b>	<b>Comments</b>
-29.50	287.68	top of wall
-29.37	287.46	
-28.83	287.39	
-26.82	286.52	
-25.48	286.26	
-22.13	285.71	
-19.45	284.81	Edge of Converging Jet
-18.11	284.89	TW
-14.75	285.38	TW
-8.05	285.65	TW
-1.34	285.73	TW
5.36	285.78	TW
12.07	285.46	TW
15.42	285.31	TW
18.78	284.91	TW
20.12	285.04	Edge of Converging Jet
22.13	285.80	
25.48	286.38	
27.49	286.74	
28.50	287.19	
29.17	287.39	
29.57	287.46	
29.77	287.68	top of wall

Table A15. Model cross-sectional water surface profile along step 18, station 0.92 m for test #1.

<b>Model Water Surface Profile</b>		
Cross-Sectional Profile, $X_m = 0.92$ m - Step 18; 2/3 PMF		
<b>station</b> $Y_m$ (m)	<b>elev</b> $Z_m$ (m)	<b>Comments</b>
-1.34	13.08	top of wall
-1.34	13.07	
-1.31	13.06	
-1.22	13.02	
-1.16	13.01	
-1.01	12.99	
-0.88	12.95	Edge of Converging Jet
-0.82	12.95	TW
-0.67	12.97	TW
-0.37	12.98	TW
-0.06	12.99	TW
0.24	12.99	TW
0.55	12.98	TW
0.70	12.97	TW
0.85	12.95	TW
0.91	12.96	Edge of Converging Jet
1.01	12.99	
1.16	13.02	
1.25	13.03	
1.30	13.05	
1.33	13.06	
1.34	13.07	
1.35	13.08	top of wall

Table A16. Prototype cross-sectional water surface profile along step 21, station 23.1 m for test #1.

<b>Prototype Water Surface Profile</b>		
Cross-Sectional Profile, $X_p = 23.1$ m - Step 21; 2/3 PMF - Low TW		
<b>station</b> $Y_p$ (m)	<b>elev</b> $Z_p$ (m)	<b>Comments</b>
-26.15	287.25	top of wall (level section)
-25.88	286.60	
-25.15	286.58	
-22.80	285.58	
-19.78	285.05	
-16.09	283.99	end of rough water
-14.75	283.57	
-13.41	283.51	
-11.40	283.37	
-8.05	283.23	
-1.34	283.13	
5.36	283.16	
8.72	283.23	
12.07	283.36	
14.42	283.53	
16.09	283.98	start of rough water surface
19.45	285.14	
22.13	285.62	
23.47	285.63	
25.15	286.47	
26.08	286.60	
26.29	287.25	top of wall (level section)

Table A17. Model cross-sectional water surface profile along step 21, station 1.05 m for test #1.

<b>Model Water Surface Profile</b>		
Cross-Sectional Profile, $X_m = 1.05$ m - Step 21; 2/3 PMF - Low TW		
<b>station</b>	<b>elev</b>	
<b><math>Y_m</math> (m)</b>	<b><math>Z_m</math> (m)</b>	<b>Comments</b>
-1.19	13.06	top of wall (level section)
-1.18	13.03	
-1.14	13.03	
-1.04	12.98	
-0.90	12.96	
-0.73	12.91	end of rough water
-0.67	12.89	
-0.61	12.89	
-0.52	12.88	
-0.37	12.87	
-0.06	12.87	
0.24	12.87	
0.40	12.87	
0.55	12.88	
0.66	12.89	
0.73	12.91	start of rough water surface
0.88	12.96	
1.01	12.98	
1.07	12.98	
1.14	13.02	
1.19	13.03	
1.19	13.06	top of wall (level section)

Table A18. Prototype cross-sectional water surface profile along step 25, station 26.8 m for test #1.

<b>Prototype Water Surface Profile</b>		
Cross-Sectional Profile, $X_p = 26.8$ m - Step 25; 2/3 PMF - Low TW		
<b>station</b>	<b>elev</b>	
<b><math>Y_p</math> (m)</b>	<b><math>Z_p</math> (m)</b>	<b>Comments</b>
-21.59	287.20	top of wall
-21.32	285.53	
-20.12	285.22	
-18.37	284.50	
-15.42	284.10	
-12.41	283.30	Edge of Converging Jet
-10.53	283.04	TW
-8.05	283.31	TW
-1.34	283.12	TW
5.36	283.23	TW
8.72	283.25	TW
10.73	282.92	TW
12.07	283.10	Edge of Converging Jet
14.08	283.75	
16.09	284.30	
18.78	284.61	
20.45	285.28	
21.46	285.51	
21.66	287.20	top of wall

Table A19. Model cross-sectional water surface profile along step 25, station 1.22 m for test #1.

<b>Model Water Surface Profile</b>		
Cross-Sectional Profile, $X_m = 1.22$ m - Step 25; 2/3 PMF - Low TW		
<b>station</b>	<b>elev</b>	
<b><math>Y_m</math> (m)</b>	<b><math>Z_m</math> (m)</b>	<b>Comments</b>
-0.98	13.05	top of wall
-0.97	12.98	
-0.91	12.96	
-0.84	12.93	
-0.70	12.91	
-0.56	12.88	Edge of Converging Jet
-0.48	12.87	TW
-0.37	12.88	TW
-0.06	12.87	TW
0.24	12.87	TW
0.40	12.88	TW
0.49	12.86	TW
0.55	12.87	Edge of Converging Jet
0.64	12.90	
0.73	12.92	
0.85	12.94	
0.93	12.97	
0.98	12.98	
0.98	13.05	top of wall

Table A20. Prototype centerline water surface profile for test #2.

<b>Prototype Water Surface Profile</b>		
Centerline Profile, $Y_p = 0.0$ m; PMF		
<b>station</b> <b><math>X_p</math> (m)</b>	<b>elev</b> <b><math>Z_p</math>(m)</b>	<b>Comments</b>
-113.12	292.57	
-99.71	292.57	
-86.30	292.56	
-72.89	292.55	
-59.48	292.56	
-46.07	292.55	
-32.66	292.55	
-19.25	292.53	
-12.54	292.48	
-9.19	292.38	
-5.83	292.26	
-2.48	292.22	
-1.81	292.20	Ogee Crest
-1.14	292.11	Ogee Crest
-0.47	292.02	Ogee Crest
0.20	291.86	Ogee Crest
0.87	291.68	Ogee Crest
1.54	291.33	Ogee Crest
2.21	291.07	Ogee Crest
2.88	290.70	Ogee Crest
3.55	290.43	Ogee Crest
4.22	290.08	Steps Start
4.90	289.83	
6.24	289.30	
7.58	288.77	
8.92	288.27	
10.26	287.78	
11.60	287.29	
12.94	286.85	
13.61	286.59	
14.28	286.33	
15.62	286.70	Edge of TW
16.97	286.61	TW
18.31	286.65	TW
19.65	286.69	TW
24.34	286.80	TW
27.69	287.26	Edge of Stilling Basin
31.05	287.72	Stilling Basin
34.40	287.80	Stilling Basin
41.11	287.57	Out of Stilling Basin
47.81	287.26	
54.52	287.37	
67.93	287.09	
81.34	286.90	
94.75	286.87	
108.16	286.89	

Table A21. Model centerline water surface profile for test #2.

Model Water Surface Profile		
Run #: Run 2		Centerline profile, $Y_m = 0.0$ m; PMF
Date: 14 Oct 2004		
station $X_m$ (m)	elev $Z_m$ (m)	Comments
-5.14	13.30	
-4.53	13.30	
-3.92	13.30	
-3.31	13.30	
-2.70	13.30	
-2.09	13.30	
-1.48	13.30	
-0.87	13.30	
-0.57	13.29	
-0.42	13.29	
-0.27	13.28	
-0.11	13.28	
-0.08	13.28	Ogee Crest
-0.05	13.28	Ogee Crest
-0.02	13.27	Ogee Crest
0.01	13.27	Ogee Crest
0.04	13.26	Ogee Crest
0.07	13.24	Ogee Crest
0.10	13.23	Ogee Crest
0.13	13.21	Ogee Crest
0.16	13.20	Ogee Crest
0.19	13.19	Steps Start
0.22	13.17	
0.28	13.15	
0.34	13.13	
0.41	13.10	
0.47	13.08	
0.53	13.06	
0.59	13.04	
0.62	13.03	
0.65	13.01	
0.71	13.03	Edge of TW
0.77	13.03	TW
0.83	13.03	TW
0.89	13.03	TW
1.11	13.04	TW
1.26	13.06	Edge of Stilling Basin
1.41	13.08	Stilling Basin
1.56	13.08	Stilling Basin
1.87	13.07	Out of Stilling Basin
2.17	13.06	
2.48	13.06	
3.09	13.05	
3.70	13.04	
4.31	13.04	
4.92	13.04	

Table A22. Prototype water surface profile along the right wall looking downstream for test #2.

<b>Prototype Water Surface Profile</b>			
WS along Rt. Wall looking d.s. PMF			
<b>station X<sub>p</sub> (m)</b>	<b>station Y<sub>p</sub> (m)</b>	<b>elev Z<sub>p</sub>(m)</b>	<b>Comments</b>
-12.54	-49.62	292.50	
-9.19	-49.62	292.39	
-7.85	-49.62	292.22	
-6.50	-49.62	291.95	
-5.50	-49.62	291.78	
-2.48	-49.62	292.08	
-1.14	-49.62	292.04	
0.87	-49.62	291.74	
1.54	-49.62	291.59	
3.69	-49.62	292.08	joint - start converge
4.90	-48.28	291.91	
7.58	-44.93	291.51	
9.59	-42.25	291.11	Flow over Wall
10.93	-40.37	290.70	
14.28	-36.55	289.89	
17.64	-29.50	288.88	
19.65	-29.77	288.35	
21.32	-27.96	287.95	wall levels out
24.34	-24.01	287.38	
27.69	-19.71	286.87	
30.38	-17.57	285.22	Basin wall - low point
34.40	-16.09	286.72	
38.22	-14.75	288.20	Basin exit

Table A23. Model water surface profile along the right wall looking downstream for test #2.

<b>Model Water Surface Profile</b>			
WS along Rt. Wall looking d.s. PMF			
<b>station X<sub>m</sub> (m)</b>	<b>station Y<sub>m</sub> (m)</b>	<b>elev Z<sub>m</sub> (m)</b>	<b>Comments</b>
-0.57	-2.26	13.30	
-0.42	-2.26	13.29	
-0.36	-2.26	13.28	
-0.30	-2.26	13.27	
-0.25	-2.26	13.26	
-0.11	-2.26	13.28	
-0.05	-2.26	13.27	
0.04	-2.26	13.26	
0.07	-2.26	13.25	
0.17	-2.26	13.28	joint - start converge
0.22	-2.19	13.27	
0.34	-2.04	13.25	
0.44	-1.92	13.23	Flow over Wall
0.50	-1.83	13.21	
0.65	-1.66	13.18	
0.80	-1.34	13.13	
0.89	-1.35	13.11	
0.97	-1.27	13.09	wall levels out
1.11	-1.09	13.06	
1.26	-0.90	13.04	
1.38	-0.80	12.96	Basin wall - low point
1.56	-0.73	13.03	

Table A24. Prototype water surface profile along the left wall looking downstream for test #2.

<b>Prototype Water Surface Profile</b>			
WS along Lt. Wall looking d.s.PMF			
<b>station</b> <b>X<sub>p</sub> (m)</b>	<b>station</b> <b>Y<sub>p</sub> (m)</b>	<b>elev</b> <b>Z<sub>p</sub> (m)</b>	<b>Comments</b>
-12.54	49.62	292.49	
-9.19	49.62	292.38	
-7.85	49.62	292.23	
-6.50	49.62	292.02	
-5.50	49.62	291.77	
-2.48	49.62	292.06	
-1.14	49.62	292.06	
0.87	49.62	291.73	
2.21	49.62	291.47	
3.69	49.62	291.98	
4.90	48.35	292.06	
7.58	44.79	291.45	
9.59	42.51	291.07	
10.93	40.97	290.79	
14.28	36.88	289.90	
17.64	32.59	288.91	wall levels off
19.65	30.04	288.30	
21.32	27.96	287.89	
24.34	23.94	287.34	joint
27.69	19.71	286.85	
30.38	17.50	285.31	
34.40	16.16	286.95	basin exit
38.22	15.09	288.23	

Table A25. Model water surface profile along the left wall looking downstream for test #2.

<b>Model Water Surface Profile</b>			
WS along Lt. Wall looking d.s. PMF			
<b>station</b> <b>X<sub>m</sub> (m)</b>	<b>station</b> <b>Y<sub>m</sub> (m)</b>	<b>elev</b> <b>Z<sub>m</sub> (m)</b>	<b>Comments</b>
-0.57	2.26	13.30	
-0.42	2.26	13.29	
-0.36	2.26	13.28	
-0.30	2.26	13.27	
-0.25	2.26	13.26	
-0.11	2.26	13.28	
-0.05	2.26	13.28	
0.04	2.26	13.26	
0.10	2.26	13.25	
0.17	2.26	13.27	
0.22	2.20	13.28	
0.34	2.04	13.25	
0.44	1.93	13.23	
0.50	1.86	13.22	
0.65	1.68	13.18	
0.80	1.48	13.13	wall levels off
0.89	1.37	13.10	
0.97	1.27	13.09	
1.11	1.09	13.06	joint
1.26	0.90	13.04	
1.38	0.80	12.97	
1.56	0.73	13.04	basin exit
1.74	0.69	13.10	

Table A26. Prototype cross-sectional water surface profile at step 1, station 4.6 m for test #2.

<b>Prototype Water Surface Profile</b>		
Cross-Sectional Profile, $X_p = 4.6$ m - Step 1; PMF		
<b>station</b> $Y_p$ (m)	<b>elev</b> $Z_p$ (m)	<b>Comments</b>
-49.08	292.89	top of wall
-48.95	292.18	
-47.61	291.85	
-45.26	291.18	
-42.92	290.64	
-40.77	290.13	End of rough water
-38.89	289.97	
-36.21	289.92	
-34.87	289.92	
-28.16	289.92	
-21.46	289.92	
-14.75	289.90	
-8.05	289.91	
-1.34	289.90	
5.36	289.89	
12.07	289.88	
18.78	289.90	
25.48	289.90	
32.19	289.92	
35.54	289.94	
38.89	289.97	
40.03	290.05	Start of rough water
41.57	290.41	
43.59	290.96	
44.86	291.33	
46.27	291.65	
47.54	291.86	
49.02	292.24	
49.29	292.89	top of wall

Table A27. Model cross-sectional water surface profile at step 1, station 0.21 m for test #2.

<b>Model Water Surface Profile</b>		
Cross-Sectional Profile, $X_m = 0.21$ m - Step 1; PMF		
<b>station</b> $Y_m$ (m)	<b>elev</b> $Z_m$ (m)	<b>Comments</b>
-2.23	13.31	top of wall
-2.23	13.28	
-2.16	13.27	
-2.06	13.24	
-1.95	13.21	
-1.85	13.19	End of rough water
-1.77	13.18	
-1.65	13.18	
-1.58	13.18	
-1.28	13.18	
-0.98	13.18	
-0.67	13.18	
-0.37	13.18	
-0.06	13.18	
0.24	13.18	
0.55	13.18	
0.85	13.18	
1.16	13.18	
1.46	13.18	
1.62	13.18	
1.77	13.18	
1.82	13.18	Start of rough water
1.89	13.20	
1.98	13.23	
2.04	13.24	
2.10	13.26	
2.16	13.27	
2.23	13.28	
2.24	13.31	top of wall

Table A28. Prototype cross-sectional water surface profile at step 8, station 11 m for test #2.

<b>Prototype Water Surface Profile</b>		
Cross-Sectional Profile, $X_p = 11$ m - Step 8; PMF		
<b>station</b> <b><math>Y_p</math> (m)</b>	<b>elev</b> <b><math>Z_p</math> (m)</b>	<b>Comments</b>
-41.17	290.80	top of wall
-40.97	290.78	
-40.10	290.67	
-38.22	290.11	
-36.21	289.25	
-32.86	288.64	
-29.84	287.93	End of rough water
-28.30	287.69	
-26.15	287.64	
-24.81	287.61	
-21.46	287.56	
-18.11	287.53	
-14.75	287.50	
-8.05	287.51	
-1.34	287.50	
5.36	287.50	
12.07	287.51	
15.42	287.50	
18.78	287.52	
22.13	287.55	
25.48	287.61	
27.49	287.66	
29.17	287.79	Start of rough water
32.19	288.58	
35.54	289.28	
37.55	289.72	
38.89	290.25	
40.23	290.65	
41.17	290.77	
41.37	290.79	top of wall

Table A29. Model cross-sectional water surface profile at step 8, station 0.5 m for test #2.

<b>Model Water Surface Profile</b>		
Cross-Sectional Profile, $X_m = 0.5$ m - Step 8; PMF		
<b>station</b> <b><math>Y_m</math> (m)</b>	<b>elev</b> <b><math>Z_m</math> (m)</b>	<b>Comments</b>
-1.87	13.22	top of wall
-1.86	13.22	
-1.82	13.21	
-1.74	13.19	
-1.65	13.15	
-1.49	13.12	
-1.36	13.09	End of rough water
-1.29	13.08	
-1.19	13.07	
-1.13	13.07	
-0.98	13.07	
-0.82	13.07	
-0.67	13.07	
-0.37	13.07	
-0.06	13.07	
0.24	13.07	
0.55	13.07	
0.70	13.07	
0.85	13.07	
1.01	13.07	
1.16	13.07	
1.25	13.08	
1.33	13.08	Start of rough water
1.46	13.12	
1.62	13.15	
1.71	13.17	
1.77	13.19	
1.83	13.21	
1.87	13.22	
1.88	13.22	top of wall

Table A30. Prototype cross-sectional water surface profile at step 12, station 14.8 m for test #2.

<b>Prototype Water Surface Profile</b>		
Cross-Sectional Profile, $X_p = 14.8$ m - Step 12; PMF		
<b>station</b> $Y_p$ (m)	<b>elev</b> $Z_p$ (m)	<b>Comments</b>
-36.48	289.55	top of wall
-36.21	289.75	
-34.87	289.47	
-33.53	288.99	
-32.19	288.35	
-29.50	288.07	
-27.49	287.56	
-24.81	286.94	
-23.47	286.46	End of rough water
-21.46	286.35	
-18.11	286.26	
-14.75	286.20	
-11.40	286.17	
-8.05	286.17	
-1.34	286.17	
5.36	286.18	
12.07	286.17	
15.42	286.21	
18.78	286.27	
22.13	286.39	
23.13	286.42	
24.14	286.65	Start of rough water
26.15	287.30	
28.83	287.83	
31.52	288.21	
32.86	288.54	
34.20	289.23	
35.54	289.64	
36.48	289.73	
36.75	289.54	top of wall

Table A31. Model cross-sectional water surface profile at step 12, station 0.67 m for test #2.

<b>Model Water Surface Profile</b>		
Cross-Sectional Profile, $X_m = 0.67$ m - Step 12; PMF		
<b>station</b>	<b>elev</b>	
<b><math>Y_m</math> (m)</b>	<b><math>Z_m</math> (m)</b>	<b>Comments</b>
-1.66	13.16	top of wall
-1.65	13.17	
-1.58	13.16	
-1.52	13.14	
-1.46	13.11	
-1.34	13.09	
-1.25	13.07	
-1.13	13.04	
-1.07	13.02	End of rough water
-0.98	13.02	
-0.82	13.01	
-0.67	13.01	
-0.52	13.01	
-0.37	13.01	
-0.06	13.01	
0.24	13.01	
0.55	13.01	
0.70	13.01	
0.85	13.01	
1.01	13.02	
1.05	13.02	
1.10	13.03	Start of rough water
1.19	13.06	
1.31	13.08	
1.43	13.10	
1.49	13.12	
1.55	13.15	
1.62	13.17	
1.66	13.17	
1.67	13.16	top of wall

Table A32. Prototype cross-sectional water surface profile at step 18, station 20.3 m for test #2.

<b>Prototype Water Surface Profile</b>		
Cross-Sectional Profile, $X_p = 20.3$ m - Step 18; PMF		
<b>station</b>	<b>elev</b>	
<b><math>Y_p</math> (m)</b>	<b><math>Z_p</math> (m)</b>	<b>Comments</b>
-29.71	287.70	top of wall
-29.50	288.07	
-28.50	288.03	
-26.82	287.40	
-24.81	286.72	
-22.80	286.52	
-19.45	285.90	
-18.11	285.50	Point of Conv jet & Tailwater
-16.76	285.91	Tailwater
-14.75	285.91	Tailwater
-8.05	286.24	Tailwater
-1.34	286.59	Tailwater
5.36	286.42	Tailwater
8.72	286.30	Tailwater
12.07	286.10	Tailwater
15.42	285.90	Tailwater
17.77	285.46	Point of Conv jet & Tailwater
19.45	285.87	
22.80	286.48	
25.48	286.81	
26.82	287.23	
28.16	287.84	
29.17	288.13	
29.71	288.15	
29.84	287.70	top of wall

Table A33. Model cross-sectional water surface profile at step 18, station 0.92 m for test #2.

<b>Model Water Surface Profile</b>		
Cross-Sectional Profile, $X_m = 0.92$ m - Step 18; PMF		
<b>station</b> <b><math>Y_m</math> (m)</b>	<b>elev</b> <b><math>Z_m</math>(m)</b>	<b>Comments</b>
-1.35	13.08	top of wall
-1.34	13.09	
-1.30	13.09	
-1.22	13.06	
-1.13	13.03	
-1.04	13.02	
-0.88	13.00	
-0.82	12.98	Point of Conv jet & Tailwater
-0.76	13.00	Tailwater
-0.67	13.00	Tailwater
-0.37	13.01	Tailwater
-0.06	13.03	Tailwater
0.24	13.02	Tailwater
0.40	13.01	Tailwater
0.55	13.00	Tailwater
0.70	13.00	Tailwater
0.81	12.98	Point of Conv jet & Tailwater
0.88	12.99	
1.04	13.02	
1.16	13.04	
1.22	13.06	
1.28	13.08	
1.33	13.10	
1.35	13.10	
1.36	13.08	top of wall

Table A34. Prototype cross-sectional water surface profile at step 21, station 23.1 m for test #2.

<b>Prototype Water Surface Profile</b>		
Cross-Sectional Profile, $X_p = 23.1$ m - Step 21; PMF - Low TW		
<b>station</b> <b><math>Y_p</math> (m)</b>	<b>elev</b> <b><math>Z_p</math>(m)</b>	<b>Comments</b>
-26.15	287.24	top of wall
-25.95	287.57	
-24.14	286.89	
-22.46	285.95	
-20.12	285.81	
-16.76	285.10	
-14.08	284.41	
-12.74	283.82	End of rough water
-10.73	283.65	
-8.05	283.51	
-4.69	283.42	
-1.34	283.39	
2.01	283.39	
5.36	283.43	
8.72	283.53	
10.73	283.63	
12.74	283.77	
14.08	284.24	Start of rough water
16.76	285.06	
20.12	285.77	
22.46	286.00	
24.81	287.11	
25.95	287.52	
26.22	287.25	top of wall

Table A35. Model cross-sectional water surface profile at step 21, station 1.05 m for test #2.

<b>Model Water Surface Profile</b>		
Cross-Sectional Profile, $X_m = 1.05$ m - Step 21; PMF - Low TW		
<b>station</b> $Y_m$ (m)	<b>elev</b> $Z_m$ (m)	<b>Comments</b>
-1.19	13.06	top of wall
-1.18	13.07	
-1.10	13.04	
-1.02	13.00	
-0.91	12.99	
-0.76	12.96	
-0.64	12.93	
-0.58	12.90	End of rough water
-0.49	12.89	
-0.37	12.89	
-0.21	12.88	
-0.06	12.88	
0.09	12.88	
0.24	12.88	
0.40	12.89	
0.49	12.89	
0.58	12.90	
0.64	12.92	Start of rough water
0.76	12.96	
0.91	12.99	
1.02	13.00	
1.13	13.05	
1.18	13.07	
1.19	13.06	top of wall

Table A36. Prototype cross-sectional water surface profile at step 25, station 26.8 m for test #2.

<b>Prototype Water Surface Profile</b>		
Cross-Sectional Profile, $X_p = 26.8$ m - Step 25; PMF - Low TW		
<b>station</b> $Y_p$ (m)	<b>elev</b> $Z_p$ (m)	<b>Comments</b>
-21.66	287.20	top of wall
-21.39	286.83	
-20.12	286.37	
-17.43	284.96	
-14.08	284.47	
-10.73	283.77	Point of Conv jet & Tailwater
-8.05	284.10	TW
-1.34	283.95	TW
5.36	283.82	TW
9.05	283.80	TW
10.39	283.45	Point of Conv jet & Tailwater
12.07	283.96	
15.42	284.77	
17.43	285.07	
19.45	285.88	
21.39	286.60	
21.73	287.19	top of wall

Table A37. Model cross-sectional water surface profile at step 25, station 1.22 m for test #2.

<b>Model Water Surface Profile</b>		
Cross-Sectional Profile, $X_m = 1.22$ m - Step 25; PMF - Low TW		
<b>station</b> $Y_m$ (m)	<b>elev</b> $Z_m$ (m)	<b>Comments</b>
-0.98	13.05	top of wall
-0.97	13.04	
-0.91	13.02	
-0.79	12.95	
-0.64	12.93	
-0.49	12.90	Point of Conv jet & Tailwater
-0.37	12.91	TW
-0.06	12.91	TW
0.24	12.90	TW
0.41	12.90	TW
0.47	12.88	Point of Conv jet & Tailwater
0.55	12.91	
0.70	12.94	
0.79	12.96	
0.88	12.99	
0.97	13.03	
0.99	13.05	top of wall

Table A38. Prototype centerline water surface profile for test #3.

<b>Prototype Water Surface Profile</b>		
Centerline Profile, $Y_p = 0.0$ m; 1/6 PMF		
<b>station</b> $X_p$ (m)	<b>elev</b> $Z_p$ (m)	<b>Comments</b>
-113.12	290.86	
-99.71	290.87	
-86.30	290.86	
-72.89	290.86	
-59.48	290.87	
-46.07	290.87	
-32.66	290.86	
-19.25	290.86	
-12.54	290.85	
-9.19	290.84	
-5.83	290.83	
-2.48	290.82	
-1.81	290.82	Ogee Crest
-1.14	290.82	Ogee Crest
-0.47	290.77	Ogee Crest
0.20	290.61	Ogee Crest
0.87	290.34	Ogee Crest
1.54	290.09	Ogee Crest
2.21	289.79	Ogee Crest
2.88	289.53	Ogee Crest
3.55	289.29	Ogee Crest
4.22	289.07	Steps Start
4.90	288.87	
6.24	288.44	
7.58	287.91	
8.92	287.48	
10.26	287.02	
11.60	286.59	
12.94	286.16	
14.28	285.73	
15.62	285.28	
16.97	284.84	
18.31	284.36	
19.65	283.96	
20.99	283.51	
22.33	283.59	Tailwater
24.34	283.49	Tailwater
27.69	283.80	Tailwater
31.05	283.91	Stilling Basin - Tailwater
34.40	283.90	Stilling Basin - Tailwater
37.75	283.91	Stilling Basin - Tailwater
41.11	283.71	Out of Stilling Basin
47.81	283.63	
61.22	283.63	
74.63	283.61	
88.04	283.61	
101.46	283.59	
114.87	283.60	

Table A39. Model centerline water surface profile for test #3.

<b>Model Water Surface Profile</b>		
Run #: Run 3		Centerline profile, $Y_m = 0.0$ m; 1/6 PMF
Date: 19 Oct 2004		
station	elev	Comments
$X_m$ (m)	$Z_m$ (m)	
-5.14	13.22	
-4.53	13.22	
-3.92	13.22	
-3.31	13.22	
-2.70	13.22	
-2.09	13.22	
-1.48	13.22	
-0.87	13.22	
-0.57	13.22	
-0.42	13.22	
-0.27	13.22	
-0.11	13.22	
-0.08	13.22	Ogee Crest
-0.05	13.22	Ogee Crest
-0.02	13.22	Ogee Crest
0.01	13.21	Ogee Crest
0.04	13.20	Ogee Crest
0.07	13.19	Ogee Crest
0.10	13.17	Ogee Crest
0.13	13.16	Ogee Crest
0.16	13.15	Ogee Crest
0.19	13.14	Steps Start
0.22	13.13	
0.28	13.11	
0.34	13.09	
0.41	13.07	
0.47	13.05	
0.53	13.03	
0.59	13.01	
0.65	12.99	
0.71	12.97	
0.77	12.95	
0.83	12.93	
0.89	12.91	
0.95	12.89	
1.01	12.89	Tailwater
1.11	12.89	Tailwater
1.26	12.90	Tailwater
1.41	12.90	Stilling Basin - Tailwater
1.56	12.90	Stilling Basin - Tailwater
1.72	12.90	Stilling Basin - Tailwater
1.87	12.90	Out of Stilling Basin
2.17	12.89	
2.78	12.89	
3.39	12.89	
4.00	12.89	
4.61	12.89	
5.22	12.89	

Table A40. Prototype water surface profile along the right wall looking downstream for test #3.

<b>Prototype Water Surface Profile</b>			
WS along Rt. Wall looking d.s. 1/6 PMF			
<b>station X<sub>p</sub> (m)</b>	<b>station Y<sub>p</sub> (m)</b>	<b>elev Z<sub>p</sub>(m)</b>	<b>Comments</b>
-12.54	-49.62	290.85	
-9.19	-49.62	290.82	
-7.85	-49.62	290.82	
-6.50	-49.62	290.82	
-3.15	-49.62	290.84	
-0.47	-49.62	290.74	
1.54	-49.62	290.03	
2.88	-49.62	289.53	
3.69	-49.62	289.27	Joint - starts to conv
4.90	-48.35	289.92	
7.58	-44.79	289.03	
10.93	-40.90	287.98	
14.28	-36.68	286.95	
17.64	-32.46	285.96	
21.32	-28.03	284.91	Wall levels off
24.34	-24.14	283.94	
26.82	-21.06	283.16	Edge of tw & conv jet
29.04	-18.11	283.89	Tailwater
30.38	-17.57	283.42	Tailwater - Basin
34.40	-16.23	283.80	Tailwater - Basin
38.22	-14.89	283.83	Basin exit

Table A41. Model water surface profile along the right wall looking downstream for test #3.

<b>Model Water Surface Profile</b>			
WS along Rt. Wall looking d.s. 1/6 PMF			
<b>station X<sub>m</sub> (m)</b>	<b>station Y<sub>m</sub> (m)</b>	<b>elev Z<sub>m</sub>(m)</b>	<b>Comments</b>
-0.57	-2.26	13.22	
-0.42	-2.26	13.22	
-0.36	-2.26	13.22	
-0.30	-2.26	13.22	
-0.14	-2.26	13.22	
-0.02	-2.26	13.22	
0.07	-2.26	13.18	
0.13	-2.26	13.16	
0.17	-2.26	13.15	Joint - starts to conv
0.22	-2.20	13.18	
0.34	-2.04	13.14	
0.50	-1.86	13.09	
0.65	-1.67	13.04	
0.80	-1.48	13.00	
0.97	-1.27	12.95	Wall levels off
1.11	-1.10	12.91	
1.22	-0.96	12.87	Edge of tw & conv jet
1.32	-0.82	12.90	Tailwater
1.38	-0.80	12.88	Tailwater - Basin
1.56	-0.74	12.90	Tailwater - Basin
1.74	-0.68	12.90	Basin exit

Table A42. Prototype water surface profile along the left wall looking downstream for test #3.

<b>Prototype Water Surface Profile</b>			
WS along Lt. Wall looking d.s.1/6 PMF			
<b>station X<sub>p</sub> (m)</b>	<b>station Y<sub>p</sub> (m)</b>	<b>elev Z<sub>p</sub>(m)</b>	<b>Comments</b>
-12.54	49.62	290.84	
-9.19	49.62	290.82	
-7.85	49.62	290.82	
-6.50	49.62	290.81	
-3.15	49.62	290.82	
-0.47	49.62	290.74	
1.54	49.62	290.05	
2.88	49.62	289.55	
3.69	49.62	289.29	joint - starts to conv
4.90	48.55	289.94	
7.58	45.33	288.98	
10.93	41.11	288.00	
14.28	36.81	286.93	
17.64	32.66	285.95	
21.32	28.16	284.91	wall levels off
24.34	24.27	283.86	
26.82	21.12	283.14	edge of tw & conv jet
29.04	17.90	283.80	TW
30.38	17.84	283.16	TW-Basin
34.40	16.43	283.77	TW-Basin
38.22	15.36	283.79	Basin exit

Table A43. Model water surface profile along the left wall looking downstream for test #3.

<b>Model Water Surface Profile</b>			
WS along Lt. Wall looking d.s. 1/6 PMF			
<b>station</b> <b>X<sub>m</sub> (m)</b>	<b>station</b> <b>Y<sub>m</sub> (m)</b>	<b>elev</b> <b>Z<sub>m</sub> (m)</b>	<b>Comments</b>
-0.57	2.26	13.22	
-0.42	2.26	13.22	
-0.36	2.26	13.22	
-0.30	2.26	13.22	
-0.14	2.26	13.22	
-0.02	2.26	13.22	
0.07	2.26	13.18	
0.13	2.26	13.16	
0.17	2.26	13.15	joint - starts to conv
0.22	2.21	13.18	
0.34	2.06	13.14	
0.50	1.87	13.09	
0.65	1.67	13.04	
0.80	1.48	13.00	
0.97	1.28	12.95	wall levels off
1.11	1.10	12.90	
1.22	0.96	12.87	edge of tw & conv jet
1.32	0.81	12.90	TW
1.38	0.81	12.87	TW-Basin
1.56	0.75	12.90	TW-Basin
1.74	0.70	12.90	Basin exit

Table A44. Prototype cross-sectional water surface profile at step 1, station 4.6 m for test #3.

<b>Prototype Water Surface Profile</b>		
Cross-Sectional Profile, $X_p = 4.6$ m - Step 1; 1/6 PMF		
<b>station</b> <b><math>Y_p</math> (m)</b>	<b>elev</b> <b><math>Z_p</math> (m)</b>	<b>Comments</b>
-49.08	292.89	Top of wall
-48.82	289.95	
-48.35	289.77	End of rough water
-47.95	289.01	Start of smooth water
-46.94	288.94	
-44.93	288.93	
-41.57	288.92	
-34.87	288.92	
-28.16	288.92	
-21.46	288.92	
-14.75	288.92	
-8.05	288.94	
-1.34	288.93	
5.36	288.92	
12.07	288.92	
18.78	288.92	
25.48	288.94	
32.19	288.95	
38.89	288.96	
44.26	288.94	
46.94	288.95	
48.08	288.99	
48.48	289.81	Start of rough water
49.02	289.90	
49.22	292.89	Top of wall

Table A45. Model cross-sectional water surface profile at step 1, station 0.21 m for test #3.

<b>Model Water Surface Profile</b>		
Cross-Sectional Profile, $X_m = 0.21$ m - Step 1; 1/6 PMF		
<b>station</b>	<b>elev</b>	
<b><math>Y_m</math> (m)</b>	<b><math>Z_m</math> (m)</b>	<b>Comments</b>
-2.23	13.31	Top of wall
-2.22	13.18	
-2.20	13.17	End of rough water
-2.18	13.14	Start of smooth water
-2.13	13.13	
-2.04	13.13	
-1.89	13.13	
-1.58	13.13	
-1.28	13.13	
-0.98	13.13	
-0.67	13.13	
-0.37	13.13	
-0.06	13.13	
0.24	13.13	
0.55	13.13	
0.85	13.13	
1.16	13.13	
1.46	13.13	
1.77	13.13	
2.01	13.13	
2.13	13.13	
2.19	13.14	
2.20	13.17	Start of rough water
2.23	13.18	
2.24	13.31	Top of wall

Table A46. Prototype cross-sectional water surface profile at step 8, station 11 m for test #3.

<b>Prototype Water Surface Profile</b>		
Cross-Sectional Profile, $X_p = 11$ m - Step 8; 1/6 PMF		
<b>station</b>	<b>elev</b>	
$Y_p$ (m)	$Z_p$ (m)	<b>Comments</b>
-41.11	290.79	top of wall
-40.84	287.96	
-39.56	287.67	
-38.42	287.36	
-37.82	287.07	
-36.21	286.89	
-34.87	286.83	End of rough water
-28.16	286.79	
-21.46	286.79	
-14.75	286.78	
-8.05	286.81	
-1.34	286.77	
5.36	286.80	
12.07	286.77	
18.78	286.81	
25.48	286.78	
32.19	286.82	
34.20	286.83	
35.54	286.89	
37.55	287.00	
38.56	287.29	
40.23	287.68	
41.04	287.95	Start of rough water
41.31	290.77	

Table A47. Model cross-sectional water surface profile at step 8, station 0.5 m for test #3.

<b>Model Water Surface Profile</b>		
Cross-Sectional Profile, $X_m = 0.5$ m - Step 8; 1/6 PMF		
<b>station</b>	<b>elev</b>	
<b><math>Y_m</math> (m)</b>	<b><math>Z_m</math> (m)</b>	<b>Comments</b>
-1.87	13.22	top of wall
-1.86	13.09	
-1.80	13.08	
-1.75	13.06	
-1.72	13.05	
-1.65	13.04	
-1.58	13.04	End of rough water
-1.28	13.04	
-0.98	13.04	
-0.67	13.04	
-0.37	13.04	
-0.06	13.04	
0.24	13.04	
0.55	13.04	
0.85	13.04	
1.16	13.04	
1.46	13.04	
1.55	13.04	
1.62	13.04	
1.71	13.05	
1.75	13.06	
1.83	13.08	
1.87	13.09	Start of rough water
1.88	13.22	

Table A48. Prototype cross-sectional water surface profile at step 12, station 14.8 m for test #3.

<b>Prototype Water Surface Profile</b>		
Cross-Sectional Profile, $X_p = 14.8$ m - Step 12; PMF		
<b>station</b> $Y_p$ (m)	<b>elev</b> $Z_p$ (m)	<b>Comments</b>
-36.61	289.57	Top of wall
-36.28	286.82	
-35.20	286.60	
-34.20	286.34	End of rough water
-33.53	286.05	Start of smooth water
-32.19	285.89	
-30.85	285.70	
-28.16	285.61	
-21.46	285.55	
-14.75	285.59	
-8.05	285.53	
-1.34	285.51	
5.36	285.53	
12.07	285.55	
18.78	285.57	
25.48	285.57	
28.83	285.62	
30.85	285.71	
32.19	285.82	
33.53	286.05	
34.20	286.30	Start of rough water
35.54	286.67	
36.48	286.83	
36.75	289.55	Top of wall

Table A49. Model cross-sectional water surface profile at step 12, station 0.67 m for test #3.

<b>Model Water Surface Profile</b>		
Cross-Sectional Profile, $X_m = 0.67$ m - Step 12; PMF		
<b>station</b>	<b>elev</b>	
<b><math>Y_m</math> (m)</b>	<b><math>Z_m</math> (m)</b>	<b>Comments</b>
-1.66	13.16	Top of wall
-1.65	13.04	
-1.60	13.03	
-1.55	13.02	End of rough water
-1.52	13.00	Start of smooth water
-1.46	12.99	
-1.40	12.99	
-1.28	12.98	
-0.98	12.98	
-0.67	12.98	
-0.37	12.98	
-0.06	12.98	
0.24	12.98	
0.55	12.98	
0.85	12.98	
1.16	12.98	
1.31	12.98	
1.40	12.99	
1.46	12.99	
1.52	13.00	
1.55	13.01	Start of rough water
1.62	13.03	
1.66	13.04	
1.67	13.16	Top of wall

Table A50. Prototype cross-sectional water surface profile at step 18, station 20.3 m for test #3.

<b>Prototype Water Surface Profile</b>		
Cross-Sectional Profile, $X_p = 20.3$ m - Step 18; 1/6 PMF		
<b>station</b>	<b>elev</b>	
<b><math>Y_p</math> (m)</b>	<b><math>Z_p</math>(m)</b>	<b>Comments</b>
-29.64	287.70	Top of wall
-29.37	285.24	
-28.50	285.06	
-27.49	284.71	End of rough water
-26.82	284.47	Start of smooth water
-24.81	284.18	
-22.80	283.92	
-21.46	283.86	
-14.75	283.75	
-8.05	283.73	
-1.34	283.75	
5.36	283.77	
12.07	283.76	
18.78	283.78	
22.13	283.86	
24.81	284.21	
26.82	284.44	Start of rough water
27.49	284.65	
28.83	285.00	
29.57	285.19	
29.84	287.70	Top of wall

Table A51. Model cross-sectional water surface profile at step 18, station 0.92 m for test #3.

<b>Model Water Surface Profile</b>		
Cross-Sectional Profile, $X_m = 0.92$ m - Step 18; 1/6 PMF		
<b>station</b>	<b>elev</b>	
$Y_m$ (m)	$Z_m$ (m)	<b>Comments</b>
-1.35	13.08	Top of wall
-1.34	12.97	
-1.30	12.96	
-1.25	12.94	End of rough water
-1.22	12.93	Start of smooth water
-1.13	12.92	
-1.04	12.91	
-0.98	12.90	
-0.67	12.90	
-0.37	12.90	
-0.06	12.90	
0.24	12.90	
0.55	12.90	
0.85	12.90	
1.01	12.90	
1.13	12.92	
1.22	12.93	Start of rough water
1.25	12.94	
1.31	12.95	
1.34	12.96	
1.36	13.08	Top of wall

Table A52. Prototype cross-sectional water surface profile at step 21, station 23.1 m for test #3.

<b>Prototype Water Surface Profile</b>		
Cross-Sectional Profile, $X_p = 23.1$ m - Step 21; 1/6 PMF - Low TW		
<b>station</b>	<b>elev</b>	
<b><math>Y_p</math> (m)</b>	<b><math>Z_p</math> (m)</b>	<b>Comments</b>
-26.15	287.25	Top of wall
-25.88	284.40	
-24.81	284.12	
-23.94	283.77	End of rough water
-23.13	283.51	
-21.46	283.42	
-18.11	282.95	
-14.75	282.91	
-14.08	283.37	TW
-8.05	283.57	TW
-1.34	283.53	TW
5.36	283.55	TW
12.07	283.52	TW
14.75	282.96	Out of Tailwater
17.43	282.89	
20.79	283.16	
23.13	283.50	
24.14	283.66	Start of rough water
25.15	284.04	
25.95	284.28	
26.29	287.25	Top of wall

Table A53. Model cross-sectional water surface profile at step 21, station 1.05 m for test #3.

<b>Model Water Surface Profile</b>		
Cross-Sectional Profile, $X_m = 1.05$ m - Step 21; 1/6 PMF - Low TW		
<b>station</b>	<b>elev</b>	
<b><math>Y_m</math> (m)</b>	<b><math>Z_m</math> (m)</b>	<b>Comments</b>
-1.19	13.06	Top of wall
-1.18	12.93	
-1.13	12.91	
-1.09	12.90	End of rough water
-1.05	12.89	
-0.98	12.88	
-0.82	12.86	
-0.67	12.86	
-0.64	12.88	TW
-0.37	12.89	TW
-0.06	12.89	TW
0.24	12.89	TW
0.55	12.89	TW
0.67	12.86	Out of Tailwater
0.79	12.86	
0.94	12.87	
1.05	12.89	
1.10	12.89	Start of rough water
1.14	12.91	
1.18	12.92	
1.19	13.06	Top of wall

Table A54. Prototype cross-sectional water surface profile at step 25, station 26.8 m for test #3.

<b>Prototype Water Surface Profile</b>		
Cross-Sectional Profile, $X_p = 26.8$ m - Step 25; 1/6 PMF - Low TW		
<b>station</b> <b><math>Y_p</math> (m)</b>	<b>elev</b> <b><math>Z_p</math> (m)</b>	<b>Comments</b>
-21.59	287.21	Top of wall
-21.32	283.16	
-20.45	282.97	
-19.45	282.68	End of rough water
-18.44	282.36	
-16.09	282.15	
-14.08	281.85	
-11.40	281.70	
-6.04	281.66	
-4.69	281.92	TW
-1.34	282.16	TW
4.02	282.07	TW
5.36	281.62	Out of Tailwater
8.72	281.62	
12.07	281.72	
15.42	281.97	
18.78	282.30	
19.78	282.60	Start of rough water
20.92	282.96	
21.46	283.08	
21.66	287.20	Top of wall

Table A55. Model cross-sectional water surface profile at step 25, station 1.22 m for test #3.

<b>Model Water Surface Profile</b>		
<b>Cross-Sectional Profile, <math>X_m = 1.22</math> m - Step 25; 1/6 PMF - Low TW</b>		
<b>station</b>	<b>elev</b>	
<b><math>Y_m</math> (m)</b>	<b><math>Z_m</math>(m)</b>	<b>Comments</b>
-0.98	13.05	Top of wall
-0.97	12.87	
-0.93	12.86	
-0.88	12.85	End of rough water
-0.84	12.83	
-0.73	12.82	
-0.64	12.81	
-0.52	12.80	
-0.27	12.80	
-0.21	12.81	TW
-0.06	12.83	TW
0.18	12.82	TW
0.24	12.80	Out of Tailwater
0.40	12.80	
0.55	12.81	
0.70	12.82	
0.85	12.83	
0.90	12.85	Start of rough water
0.95	12.86	
0.98	12.87	
0.98	13.05	Top of wall

Table A56. Prototype centerline water surface profile for test #4.

<b>Prototype Water Surface Profile</b>		
Centerline Profile, $Y_p = 0.0$ m; 1/3 PMF		
<b>station</b> $X_p$ (m)	<b>elev</b> $Z_p$ (m)	<b>Comments</b>
-113.12	291.28	
-99.71	291.28	
-86.30	291.28	
-72.89	291.28	
-59.48	291.29	
-46.07	291.29	
-32.66	291.28	
-19.25	291.28	
-12.54	291.27	
-9.19	291.24	
-5.83	291.21	
-2.48	291.20	
-1.81	291.19	ogee crest
-1.14	291.16	ogee crest
-0.47	291.10	ogee crest
0.20	290.92	ogee crest
0.87	290.65	ogee crest
1.54	290.39	ogee crest
2.21	290.06	ogee crest
2.88	289.78	ogee crest
3.55	289.54	ogee crest
4.22	289.28	steps start
4.90	289.06	
6.24	288.62	
7.58	288.12	
8.92	287.69	
10.26	287.23	
11.60	286.74	
12.94	286.27	
14.28	285.82	
15.62	285.40	
16.97	284.96	
18.31	284.51	
19.65	284.68	TW
20.99	284.63	TW
25.01	284.71	TW
27.69	285.05	TW
34.40	285.16	TW-stilling basin
41.11	285.03	out of stilling basin
47.81	284.96	
61.22	284.93	
74.63	284.83	
88.04	284.82	
101.46	284.87	
114.87	284.84	

Table A57. Model centerline water surface profile for test #4.

<b>Model Water Surface Profile</b>		
Run #: Run 4		Centerline profile, $Y_m = 0.0$ m; 1/3 PMF
Date: 19 Oct 2004		
station $X_m$ (m)	elev $Z_m$ (m)	Comments
-5.14	13.24	
-4.53	13.24	
-3.92	13.24	
-3.31	13.24	
-2.70	13.24	
-2.09	13.24	
-1.48	13.24	
-0.87	13.24	
-0.57	13.24	
-0.42	13.24	
-0.27	13.24	
-0.11	13.24	
-0.08	13.24	ogee crest
-0.05	13.23	ogee crest
-0.02	13.23	ogee crest
0.01	13.22	ogee crest
0.04	13.21	ogee crest
0.07	13.20	ogee crest
0.10	13.18	ogee crest
0.13	13.17	ogee crest
0.16	13.16	ogee crest
0.19	13.15	steps start
0.22	13.14	
0.28	13.12	
0.34	13.10	
0.41	13.08	
0.47	13.06	
0.53	13.03	
0.59	13.01	
0.65	12.99	
0.71	12.97	
0.77	12.95	
0.83	12.93	
0.89	12.94	TW
0.95	12.94	TW
1.14	12.94	TW
1.26	12.96	TW
1.56	12.96	TW-stilling basin
1.87	12.96	out of stilling basin
2.17	12.95	
2.78	12.95	
3.39	12.95	
4.00	12.95	
4.61	12.95	
5.22	12.95	

Table A58. Prototype water surface profile along the right wall looking downstream for test #4.

<b>Prototype Water Surface Profile</b>			
WS along Rt. Wall looking d.s. 1/3 PMF			
<b>station X<sub>p</sub> (m)</b>	<b>station Y<sub>p</sub> (m)</b>	<b>elev Z<sub>p</sub>(m)</b>	<b>Comments</b>
-12.54	-49.62	291.27	
-9.19	-49.62	291.22	
-7.85	-49.62	291.16	
-6.50	-49.62	291.20	
-3.15	-49.62	291.18	
-0.47	-49.62	291.08	
1.54	-49.62	290.37	
2.88	-49.62	289.80	
3.69	-49.62	289.64	wall joint
4.90	-48.35	290.59	
7.58	-45.06	289.81	
10.93	-40.77	288.69	
14.28	-36.55	287.75	
17.64	-32.32	286.73	
21.32	-27.83	285.71	wall levels off
24.34	-24.01	284.83	
26.35	-21.46	284.37	TW edge
29.04	-17.97	285.75	TW
30.38	-17.70	283.84	TW -basin
34.40	-16.29	285.24	Basin
38.22	-14.95	285.38	Basin exit

Table A59. Model water surface profile along the right wall looking downstream for test #4.

<b>Model Water Surface Profile</b>			
WS along Rt. Wall looking d.s. 1/3 PMF			
<b>station X<sub>m</sub> (m)</b>	<b>station Y<sub>m</sub> (m)</b>	<b>elev Z<sub>m</sub> (m)</b>	<b>Comments</b>
-0.57	-2.26	13.24	
-0.42	-2.26	13.24	
-0.36	-2.26	13.23	
-0.30	-2.26	13.24	
-0.14	-2.26	13.24	
-0.02	-2.26	13.23	
0.07	-2.26	13.20	
0.13	-2.26	13.17	
0.17	-2.26	13.17	wall joint
0.22	-2.20	13.21	
0.34	-2.05	13.17	
0.50	-1.85	13.12	
0.65	-1.66	13.08	
0.80	-1.47	13.03	
0.97	-1.26	12.99	wall levels off
1.11	-1.09	12.95	
1.20	-0.98	12.93	TW edge
1.32	-0.82	12.99	TW
1.38	-0.80	12.90	TW -basin
1.56	-0.74	12.97	Basin
1.74	-0.68	12.97	Basin exit

Table A60. Prototype water surface profile along the left wall looking downstream for test #4.

<b>Prototype Water Surface Profile</b>			
WS along Lt. Wall looking d.s.1/3 PMF			
<b>station X<sub>p</sub> (m)</b>	<b>station Y<sub>p</sub> (m)</b>	<b>elev Z<sub>p</sub>(m)</b>	<b>Comments</b>
-12.54	49.62	291.25	
-9.19	49.62	291.20	
-7.85	49.62	291.14	
-6.50	49.62	291.18	
-3.15	49.62	291.18	
-0.47	49.62	291.06	
1.54	49.62	290.35	
2.88	49.62	289.82	
3.69	49.62	289.60	wall joint
4.90	48.41	290.59	
7.58	45.13	289.86	
10.93	41.04	288.73	
14.28	36.81	287.74	
17.64	32.66	286.82	
21.32	27.90	285.69	wall levels off
24.34	24.14	284.69	
26.35	21.59	284.17	TW edge
29.04	18.11	285.60	TW
30.38	17.77	283.81	TW- basin
34.40	16.36	285.12	basin
38.22	15.09	285.22	basin exit

Table A61. Model water surface profile along the left wall looking downstream for test #4.

<b>Model Water Surface Profile</b>			
WS along Lt. Wall looking d.s. 1/3PMF			
<b>station</b> <b>X<sub>m</sub> (m)</b>	<b>station</b> <b>Y<sub>m</sub> (m)</b>	<b>elev</b> <b>Z<sub>m</sub> (m)</b>	<b>Comments</b>
-0.57	2.26	13.24	
-0.42	2.26	13.24	
-0.36	2.26	13.23	
-0.30	2.26	13.24	
-0.14	2.26	13.24	
-0.02	2.26	13.23	
0.07	2.26	13.20	
0.13	2.26	13.17	
0.17	2.26	13.16	wall joint
0.22	2.20	13.21	
0.34	2.05	13.18	
0.50	1.87	13.12	
0.65	1.67	13.08	
0.80	1.48	13.04	
0.97	1.27	12.99	wall levels off
1.11	1.10	12.94	
1.20	0.98	12.92	TW edge
1.32	0.82	12.98	TW
1.38	0.81	12.90	TW- basin
1.56	0.74	12.96	basin
1.74	0.69	12.96	basin exit

Table A62. Prototype cross-sectional water surface profile at step 1, station 4.6 m for test #4.

<b>Prototype Water Surface Profile</b>		
Cross-Sectional Profile, $X_p = 4.6$ m - Step 1; 1/3 PMF		
<b>station</b>	<b>elev</b>	
<b><math>Y_p</math> (m)</b>	<b><math>Z_p</math> (m)</b>	<b>Comments</b>
-49.15	292.91	top of wall
-48.82	290.65	
-48.28	290.51	
-47.27	289.27	
-45.60	289.17	
-41.57	289.11	
-34.87	289.13	
-28.16	289.13	
-21.46	289.13	
-8.05	289.13	
5.36	289.12	
18.78	289.12	
25.48	289.15	
32.19	289.16	
38.89	289.16	
42.25	289.13	
44.93	289.15	
46.94	289.17	
48.28	290.47	
48.95	290.63	
49.22	292.89	top of wall

Table A63. Model cross-sectional water surface profile at step 1, station 0.21 m for test #4.

<b>Model Water Surface Profile</b>		
Cross-Sectional Profile, $X_m = 0.21$ m - Step 1; 1/3 PMF		
<b>station</b>	<b>elev</b>	
<b><math>Y_m</math> (m)</b>	<b><math>Z_m</math> (m)</b>	<b>Comments</b>
-2.23	13.31	top of wall
-2.22	13.21	
-2.19	13.21	
-2.15	13.15	
-2.07	13.14	
-1.89	13.14	
-1.58	13.14	
-1.28	13.14	
-0.98	13.14	
-0.37	13.14	
0.24	13.14	
0.85	13.14	
1.16	13.14	
1.46	13.14	
1.77	13.14	
1.92	13.14	
2.04	13.14	
2.13	13.14	
2.19	13.20	
2.23	13.21	
2.24	13.31	top of wall

Table A64. Prototype cross-sectional water surface profile at step 8, station 11 m for test #4.

<b>Prototype Water Surface Profile</b>		
Cross-Sectional Profile, $X_p = 11$ m - Step 8; 1/3 PMF		
<b>station</b> <b><math>Y_p</math> (m)</b>	<b>elev</b> <b><math>Z_p</math> (m)</b>	<b>Comments</b>
-41.17	290.80	
-40.90	288.74	
-39.56	288.36	
-37.55	287.91	
-35.87	287.47	
-34.87	287.13	smooth water
-31.52	287.01	
-28.16	286.97	
-21.46	286.93	
-14.75	286.91	
-8.05	286.93	
-1.34	286.91	
5.36	286.93	
12.07	286.94	
18.78	286.94	
25.48	286.97	
28.83	287.00	
32.19	287.04	
35.20	287.14	
35.87	287.42	rough water
37.55	287.88	
38.89	288.13	
40.23	288.42	
41.04	288.72	
41.31	290.77	top of wall

Table A65. Model cross-sectional water surface profile at step 8, station 0.5 m for test #4.

<b>Model Water Surface Profile</b>		
Cross-Sectional Profile, $X_m = 0.5$ m - Step 8; 1/3 PMF		
<b>station</b> <b><math>Y_m</math> (m)</b>	<b>elev</b> <b><math>Z_m</math> (m)</b>	<b>Comments</b>
-1.87	13.22	
-1.86	13.12	
-1.80	13.11	
-1.71	13.09	
-1.63	13.07	
-1.58	13.05	smooth water
-1.43	13.05	
-1.28	13.04	
-0.98	13.04	
-0.67	13.04	
-0.37	13.04	
-0.06	13.04	
0.24	13.04	
0.55	13.04	
0.85	13.04	
1.16	13.04	
1.31	13.05	
1.46	13.05	
1.60	13.05	
1.63	13.06	rough water
1.71	13.09	
1.77	13.10	
1.83	13.11	
1.87	13.12	
1.88	13.22	top of wall

Table A66. Prototype cross-sectional water surface profile at step 12, station 14.8 m for test #4.

<b>Prototype Water Surface Profile</b>		
Cross-Sectional Profile, $X_p = 14.8$ m - Step 12; 1/3 PMF		
<b>station</b>	<b>elev</b>	
<b><math>Y_p</math> (m)</b>	<b><math>Z_p</math> (m)</b>	<b>Comments</b>
-36.48	289.55	top of wall
-36.21	287.90	
-35.54	287.54	
-34.87	287.22	
-34.20	287.17	
-33.53	287.13	
-32.86	287.03	
-32.19	286.81	
-31.52	286.56	
-30.38	285.98	smooth water
-28.16	285.83	
-21.46	285.70	
-14.75	285.67	
-8.05	285.67	
-1.34	285.69	
5.36	285.67	
12.07	285.67	
18.78	285.70	
24.14	285.76	
24.81	285.78	
26.82	285.88	
28.16	285.87	
29.50	286.00	
30.38	286.03	rough water
31.05	286.44	
32.19	286.98	
33.53	287.19	
34.87	287.52	
35.54	287.55	
36.41	287.70	
36.81	289.54	top of wall

Table A67. Model cross-sectional water surface profile at step 12, station 0.67 m for test #4.

<b>Model Water Surface Profile</b>		
Cross-Sectional Profile, $X_m = 0.67$ m - Step 12; 1/3 PMF		
<b>station</b>	<b>elev</b>	
<b><math>Y_m</math> (m)</b>	<b><math>Z_m</math> (m)</b>	<b>Comments</b>
-1.66	13.16	top of wall
-1.65	13.09	
-1.62	13.07	
-1.58	13.06	
-1.55	13.05	
-1.52	13.05	
-1.49	13.05	
-1.46	13.04	
-1.43	13.03	
-1.38	13.00	smooth water
-1.28	12.99	
-0.98	12.99	
-0.67	12.98	
-0.37	12.99	
-0.06	12.99	
0.24	12.99	
0.55	12.99	
0.85	12.99	
1.10	12.99	
1.13	12.99	
1.22	12.99	
1.28	12.99	
1.34	13.00	
1.38	13.00	rough water
1.41	13.02	
1.46	13.04	
1.52	13.05	
1.58	13.07	
1.62	13.07	
1.66	13.08	
1.67	13.16	top of wall

Table A68. Prototype cross-sectional water surface profile at step 18, station 20.3 m for test #4.

<b>Prototype Water Surface Profile</b>		
Cross-Sectional Profile, $X_p = 20.3$ m - Step 18; 1/3 PMF		
<b>station</b>	<b>elev</b>	
<b><math>Y_p</math> (m)</b>	<b><math>Z_p</math> (m)</b>	<b>Comments</b>
-29.77	287.73	top of wall
-29.50	286.11	
-28.83	286.00	
-28.16	285.80	
-26.82	285.67	
-25.48	285.38	
-24.54	285.14	last of rough water
-23.74	284.63	smooth water
-22.80	284.36	
-21.46	284.24	
-18.11	284.06	
-16.76	284.43	TW
-14.75	284.49	
-8.05	284.77	
-1.34	284.75	
5.36	284.73	
12.07	284.70	
15.42	284.59	
18.37	283.99	out of TW
20.12	284.16	
21.46	284.18	
22.80	284.37	last of smooth water
23.47	284.66	rough water
25.48	285.43	
26.82	285.81	
28.16	285.94	
28.83	285.97	
29.64	286.14	
29.91	287.72	top of wall

Table A69. Model cross-sectional water surface profile at step 18, station 0.92 m for test #4.

<b>Model Water Surface Profile</b>		
Cross-Sectional Profile, $X_m = 0.92$ m - Step 18; 1/3 PMF		
<b>station</b> $Y_m$ (m)	<b>elev</b> $Z_m$ (m)	<b>Comments</b>
-1.35	13.08	top of wall
-1.34	13.00	
-1.31	13.00	
-1.28	12.99	
-1.22	12.98	
-1.16	12.97	
-1.12	12.96	last of rough water
-1.08	12.94	smooth water
-1.04	12.93	
-0.98	12.92	
-0.82	12.91	
-0.76	12.93	TW
-0.67	12.93	
-0.37	12.94	
-0.06	12.94	
0.24	12.94	
0.55	12.94	
0.70	12.94	
0.84	12.91	out of TW
0.91	12.92	
0.98	12.92	
1.04	12.93	last of smooth water
1.07	12.94	rough water
1.16	12.97	
1.22	12.99	
1.28	13.00	
1.31	13.00	
1.35	13.01	
1.36	13.08	top of wall

Table A70. Prototype cross-sectional water surface profile at step 21, station 23.1 m for test #4.

<b>Prototype Water Surface Profile</b>		
Cross-Sectional Profile, $X_p = 23.1$ m - Step 21; 1/3 PMF - Low TW		
<b>station</b> <b><math>Y_p</math> (m)</b>	<b>elev</b> <b><math>Z_p</math> (m)</b>	<b>Comments</b>
-26.22	287.25	top of wall
-25.95	285.17	
-24.48	284.89	
-22.80	284.54	
-21.12	284.08	
-20.12	283.67	smooth water
-18.11	283.31	
-14.75	283.05	
-11.40	282.97	
-8.05	282.92	
-1.34	282.91	
5.36	282.92	
8.72	282.92	
12.07	282.98	
15.42	283.06	
18.78	283.35	
20.12	283.59	
20.79	283.89	rough water
22.80	284.56	
24.81	284.78	
26.02	285.12	
26.35	287.25	top of wall

Table A71. Model cross-sectional water surface profile at step 21, station 1.05 m for test #4.

<b>Model Water Surface Profile</b>		
Cross-Sectional Profile, $X_m = 1.05$ m - Step 21; 1/3 PMF - Low TW		
<b>station</b>	<b>elev</b>	
<b><math>Y_m</math> (m)</b>	<b><math>Z_m</math> (m)</b>	<b>Comments</b>
-1.19	13.06	top of wall
-1.18	12.96	
-1.11	12.95	
-1.04	12.93	
-0.96	12.91	
-0.91	12.89	smooth water
-0.82	12.88	
-0.67	12.87	
-0.52	12.86	
-0.37	12.86	
-0.06	12.86	
0.24	12.86	
0.40	12.86	
0.55	12.86	
0.70	12.87	
0.85	12.88	
0.91	12.89	
0.94	12.90	rough water
1.04	12.93	
1.13	12.94	
1.18	12.96	
1.20	13.06	top of wall

Table A72. Prototype cross-sectional water surface profile at step 25, station 26.8 m for test #4.

<b>Prototype Water Surface Profile</b>		
Cross-Sectional Profile, $X_p = 26.8$ m - Step 25; 1/3 PMF - Low TW		
<b>station</b> <b><math>Y_p</math> (m)</b>	<b>elev</b> <b><math>Z_p</math> (m)</b>	<b>Comments</b>
-22.06	287.20	top of wall
-21.73	284.21	
-20.12	283.88	
-17.77	283.33	
-16.09	282.72	smooth water
-14.08	282.32	
-11.40	282.02	
-8.05	282.42	tw
-1.34	282.49	
5.36	282.39	
8.72	282.38	
10.06	281.98	end tw/ smooth water begins
12.74	282.13	
15.42	282.51	
17.17	283.03	rough water
18.78	283.66	
20.79	283.86	
21.79	284.07	
22.13	287.21	top of wall

Table A73. Model cross-sectional water surface profile at step 25, station 1.22 m for test #4.

<b>Model Water Surface Profile</b>		
Cross-Sectional Profile, $X_m = 1.22$ m - Step 25; 1/3 PMF - Low TW		
<b>station</b>	<b>elev</b>	
<b><math>Y_m</math> (m)</b>	<b><math>Z_m</math> (m)</b>	<b>Comments</b>
-1.00	13.05	top of wall
-0.99	12.92	
-0.91	12.90	
-0.81	12.88	
-0.73	12.85	smooth water
-0.64	12.83	
-0.52	12.82	
-0.37	12.84	tw
-0.06	12.84	
0.24	12.84	
0.40	12.84	
0.46	12.82	end tw/ smooth water begins
0.58	12.82	
0.70	12.84	
0.78	12.87	rough water
0.85	12.89	
0.94	12.90	
0.99	12.91	
1.01	13.05	top of wall

Table A74. Prototype centerline water surface profile for test #24.

<b>Prototype Water Surface Profile</b>		
Centerline Profile, $Y_p = 0.0$ m; PMF		
<b>station</b> <b><math>X_p</math> (m)</b>	<b>elev</b> <b><math>Z_p</math> (m)</b>	<b>Comments</b>
-113.12	292.56	centerline profile
-99.71	292.56	
-86.30	292.56	
-72.89	292.55	
-59.48	292.55	
-46.07	292.55	
-32.66	292.53	
-19.25	292.52	
-12.54	292.47	
-9.19	292.37	
-5.83	292.24	
-2.48	292.22	
-1.81	292.18	ogee crest
-1.14	292.12	
-0.47	292.01	
0.20	291.86	
0.87	291.66	
1.54	291.33	
2.21	291.05	
2.88	290.72	
3.55	290.44	
4.22	290.13	
4.90	289.82	
6.24	289.30	
7.58	288.79	
8.92	288.26	
10.26	287.75	
11.60	287.28	
12.94	286.79	
14.28	286.33	
15.62	285.90	
16.29	285.65	edge of TW
16.97	285.91	TW
18.31	285.93	TW
20.99	286.16	TW
24.34	286.18	TW
27.69	286.20	Edge of stilling basin
31.05	286.45	stilling basin
34.40	286.58	stilling basin
41.11	286.98	out of stilling basin
47.81	286.88	
61.22	286.87	
74.63	286.89	
88.04	286.93	
101.46	286.91	
114.87	286.90	
141.69	286.88	TW reading d.s.

Table A75. Model centerline water surface profile for test #24.

<b>Model Water Surface Profile</b>		
Run #: 24		Centerline profile, $Y_m = 0.0$ m; PMF
Date: 4 Dec 2004		
<b>station</b>	<b>elev</b>	<b>Comments</b>
<b><math>X_m</math> (m)</b>	<b><math>Z_m</math> (m)</b>	
-5.14	13.30	centerline profile
-4.53	13.30	
-3.92	13.30	
-3.31	13.30	
-2.70	13.30	
-2.09	13.30	
-1.48	13.30	
-0.87	13.30	
-0.57	13.29	
-0.42	13.29	
-0.27	13.28	
-0.11	13.28	
-0.08	13.28	ogee crest
-0.05	13.28	
-0.02	13.27	
0.01	13.27	
0.04	13.26	
0.07	13.24	
0.10	13.23	
0.13	13.21	
0.16	13.20	
0.19	13.19	
0.22	13.17	
0.28	13.15	
0.34	13.13	
0.41	13.10	
0.47	13.08	
0.53	13.06	
0.59	13.04	
0.65	13.01	
0.71	13.00	
0.74	12.98	edge of TW
0.77	13.00	TW
0.83	13.00	TW
0.95	13.01	TW
1.11	13.01	TW
1.26	13.01	Edge of stilling basin
1.41	13.02	stilling basin
1.56	13.03	stilling basin
1.87	13.04	out of stilling basin
2.17	13.04	
2.78	13.04	
3.39	13.04	
4.00	13.04	
4.61	13.04	
5.22	13.04	
6.44	13.04	TW reading d.s.

Table A76. Prototype water surface profile along the right wall looking downstream for test #24.

<b>Prototype Water Surface Profile</b>			
WS along Rt. Wall looking d.s. PMF, $\phi = 30$ on rt, 15 on lt			
<b>station X<sub>p</sub> (m)</b>	<b>station Y<sub>p</sub> (m)</b>	<b>elev Z<sub>p</sub> (m)</b>	<b>Comments</b>
-12.54	-49.62	292.48	rt wall looking ds
-9.19	-49.62	292.38	
-7.85	-49.62	292.22	
-6.50	-49.62	291.96	
-5.83	-49.62	291.78	
-2.48	-49.62	292.10	
-1.14	-49.62	292.03	
0.87	-49.62	291.60	
3.69	-49.62	290.65	joint start converge
4.90	-49.29	291.18	
7.58	-47.61	290.42	
10.93	-45.80	289.37	
14.28	-43.85	288.25	
17.64	-41.91	287.12	
21.46	-39.63	285.87	wall starts to level of
24.34	-38.22	285.10	
25.01	-37.75	285.64	tw
27.69	-36.21	286.32	tw
29.50	-35.14	286.53	start st basin
31.05	-35.14	286.65	stilling basin
34.40	-35.14	287.05	stilling basin
38.22	-35.14	287.17	end stilling basin

Table A77. Model water surface profile along the right wall looking downstream for test #24.

<b>Model Water Surface Profile</b>			
WS along Rt. Wall looking d.s. PMF, $\phi = 30$ on rt, 15 on lt			
<b>station</b>	<b>station</b>	<b>elev</b>	<b>Comments</b>
<b>X<sub>m</sub> (m)</b>	<b>Y<sub>m</sub> (m)</b>	<b>Z<sub>m</sub> (m)</b>	
-0.57	-2.26	13.29	rt wall looking ds
-0.42	-2.26	13.29	
-0.36	-2.26	13.28	
-0.30	-2.26	13.27	
-0.27	-2.26	13.26	
-0.11	-2.26	13.28	
-0.05	-2.26	13.27	
0.04	-2.26	13.25	
0.17	-2.26	13.21	joint start converge
0.22	-2.24	13.24	
0.34	-2.16	13.20	
0.50	-2.08	13.15	
0.65	-1.99	13.10	
0.80	-1.91	13.05	
0.98	-1.80	12.99	wall starts to level of
1.11	-1.74	12.96	
1.14	-1.72	12.98	tw
1.26	-1.65	13.01	tw
1.34	-1.60	13.02	start st basin
1.41	-1.60	13.03	stilling basin
1.56	-1.60	13.05	stilling basin
1.74	-1.60	13.05	end stilling basin

Table A78. Prototype water surface profile along the left wall looking downstream for test #24.

<b>Prototype Water Surface Profile</b>			
WS along Lt. Wall looking d.s. PMF, $\phi = 30$ on rt, 15 on lt			
<b>station X<sub>p</sub> (m)</b>	<b>station Y<sub>p</sub> (m)</b>	<b>elev Z<sub>p</sub>(m)</b>	<b>Comments</b>
-12.54	49.62	292.48	lt wall looking ds
-9.19	49.62	292.36	
-7.85	49.62	292.16	
-6.50	49.62	292.00	
-5.83	49.62	291.87	
-2.48	49.62	292.08	
-1.14	49.62	292.06	
0.87	49.62	291.61	
3.69	49.62	290.43	joint starts to conv
4.90	49.82	290.32	
7.58	49.15	289.55	
10.93	48.28	288.34	
14.28	47.41	287.17	
17.64	46.54	286.01	edge of TW
19.98	45.80	285.24	TW
20.65	45.73	285.74	TW
21.46	45.40	285.87	wall begin to level off
24.34	44.73	286.20	TW
27.69	43.79	286.36	TW
29.50	43.25	286.59	start basin
31.05	43.25	286.73	stilling basin
34.40	43.25	286.26	stilling basin
38.22	43.25	286.97	end of basin

Table A79. Model water surface profile along the left wall looking downstream for test #24.

<b>Model Water Surface Profile</b>			
WS along Lt. Wall looking d.s. PMF, $\phi = 30$ on rt, 15 on lt			
<b>station</b>	<b>station</b>	<b>elev</b>	<b>Comments</b>
<b>X<sub>m</sub> (m)</b>	<b>Y<sub>m</sub> (m)</b>	<b>Z<sub>m</sub> (m)</b>	
-0.57	2.26	13.29	lt wall looking ds
-0.42	2.26	13.29	
-0.36	2.26	13.28	
-0.30	2.26	13.27	
-0.27	2.26	13.27	
-0.11	2.26	13.28	
-0.05	2.26	13.28	
0.04	2.26	13.26	
0.17	2.26	13.20	joint starts to conv
0.22	2.26	13.20	
0.34	2.23	13.16	
0.50	2.19	13.11	
0.65	2.15	13.05	
0.80	2.12	13.00	edge of TW
0.91	2.08	12.97	TW
0.94	2.08	12.99	TW
0.98	2.06	12.99	wall begin to level off
1.11	2.03	13.01	TW
1.26	1.99	13.02	TW
1.34	1.97	13.03	start basin
1.41	1.97	13.03	stilling basin
1.56	1.97	13.01	stilling basin
1.74	1.97	13.04	end of basin

Table A80. Prototype cross-sectional water surface profile at step 1, station 4.6 m for test #24.

<b>Prototype Water Surface Profile</b>		
Cross-Sectional Profile, $X_p = 4.6$ m - Step 1; PMF		
<b>station</b>	<b>elev</b>	
<b><math>Y_p</math> (m)</b>	<b><math>Z_p</math>(m)</b>	<b>Comments</b>
50.09	292.87	top of wall - step 1
49.89	290.45	
49.22	290.03	
47.95	289.84	
46.94	289.82	
45.60	289.84	
44.26	289.86	
42.25	289.92	
38.89	289.94	
32.19	289.96	
25.48	289.95	
18.78	289.93	
12.07	289.92	
5.36	289.93	
0.00	289.92	
-8.05	289.94	
-14.75	289.93	
-21.46	289.94	
-28.16	289.94	
-34.87	289.94	
-38.22	289.93	
-41.57	289.91	
-42.92	289.90	
-44.26	289.88	
-45.60	289.86	
-46.94	289.91	
-48.28	290.22	
-48.95	290.49	
-49.49	291.19	
-49.76	292.89	top of wall

Table A81. Model cross-sectional water surface profile at step 1, station 0.21 m for test #24.

<b>Model Water Surface Profile</b>		
Cross-Sectional Profile, $X_m = 0.21$ m - Step 1; PMF		
<b>station</b> $Y_m$ (m)	<b>elev</b> $Z_m$ (m)	<b>Comments</b>
2.28	13.31	top of wall - step 1
2.27	13.20	
2.24	13.18	
2.18	13.17	
2.13	13.17	
2.07	13.17	
2.01	13.18	
1.92	13.18	
1.77	13.18	
1.46	13.18	
1.16	13.18	
0.85	13.18	
0.55	13.18	
0.24	13.18	
0.00	13.18	
-0.37	13.18	
-0.67	13.18	
-0.98	13.18	
-1.28	13.18	
-1.58	13.18	
-1.74	13.18	
-1.89	13.18	
-1.95	13.18	
-2.01	13.18	
-2.07	13.18	
-2.13	13.18	
-2.19	13.19	
-2.23	13.20	
-2.25	13.24	
-2.26	13.31	top of wall

Table A82. Prototype cross-sectional water surface profile at step 8, station 11 m for test #24.

<b>Prototype Water Surface Profile</b>		
Cross-Sectional Profile, $X_p = 11$ m - Step 8; PMF		
<b>station</b>	<b>elev</b>	
<b><math>Y_p</math> (m)</b>	<b><math>Z_p</math>(m)</b>	<b>Comments</b>
48.48	290.70	top of wall - step 8
48.28	288.40	
47.61	288.19	
46.94	288.24	
46.27	287.97	
45.93	287.67	
44.93	287.54	
43.59	287.50	
42.25	287.48	
40.90	287.50	
38.89	287.48	
32.19	287.50	
25.48	287.50	
18.78	287.51	
12.07	287.48	
5.36	287.49	
0.00	287.48	
-8.05	287.49	
-14.75	287.49	
-21.46	287.50	
-28.16	287.50	
-34.87	287.52	
-36.88	287.54	
-38.89	287.58	
-40.23	287.62	
-40.90	287.64	
-41.57	287.93	rough water
-42.25	288.27	
-42.92	288.44	
-43.59	288.66	
-44.26	288.99	
-44.93	289.15	
-45.67	289.31	
-45.93	290.73	top of wall

Table A83. Model cross-sectional water surface profile at step 8, station 0.5 m for test #24.

<b>Model Water Surface Profile</b>		
Cross-Sectional Profile, $X_m = 0.5$ m - Step 8; PMF		
<b>station</b>	<b>elev</b>	
<b><math>Y_m</math> (m)</b>	<b><math>Z_m</math> (m)</b>	<b>Comments</b>
2.20	13.21	top of wall - step 8
2.19	13.11	
2.16	13.10	
2.13	13.10	
2.10	13.09	
2.09	13.08	
2.04	13.07	
1.98	13.07	
1.92	13.07	
1.86	13.07	
1.77	13.07	
1.46	13.07	
1.16	13.07	
0.85	13.07	
0.55	13.07	
0.24	13.07	
0.00	13.07	
-0.37	13.07	
-0.67	13.07	
-0.98	13.07	
-1.28	13.07	
-1.58	13.07	
-1.68	13.07	
-1.77	13.07	
-1.83	13.07	
-1.86	13.07	
-1.89	13.09	rough water
-1.92	13.10	
-1.95	13.11	
-1.98	13.12	
-2.01	13.14	
-2.04	13.14	
-2.08	13.15	
-2.09	13.21	top of wall

Table A84. Prototype cross-sectional water surface profile at step 12, station 14.8 m for test #24.

<b>Prototype Water Surface Profile</b>		
Cross-Sectional Profile, $X_p = 14.8$ m - Step 12; PMF		
<b>station</b> <b><math>Y_p</math> (m)</b>	<b>elev</b> <b><math>Z_p</math>(m)</b>	<b>Comments</b>
47.48	289.46	top of wall - step 12
47.34	287.05	
46.94	286.97	
46.27	286.90	
45.60	286.90	
44.93	286.74	
44.26	286.39	smooth water
43.59	286.32	
42.92	286.29	
41.57	286.24	
40.23	286.22	
38.89	286.20	
35.54	286.21	
32.19	286.22	
25.48	286.21	
18.78	286.18	
12.07	286.18	
5.36	286.20	
0.00	286.18	
-8.05	286.18	
-14.75	286.18	
-21.46	286.18	
-28.16	286.20	
-31.52	286.23	
-34.87	286.29	
-36.88	286.36	
-38.22	286.47	rough water
-38.89	286.70	
-40.23	287.26	
-41.57	287.37	
-42.25	287.73	
-42.92	287.91	
-43.59	288.03	
-44.19	289.47	top of wall

Table A85. Model cross-sectional water surface profile at step 12, station 0.67 m for test #24.

<b>Model Water Surface Profile</b>		
Cross-Sectional Profile, $X_m = 0.67$ m - Step 12; PMF		
<b>station</b>	<b>elev</b>	
<b><math>Y_m</math> (m)</b>	<b><math>Z_m</math> (m)</b>	<b>Comments</b>
2.16	13.16	top of wall - step 12
2.15	13.05	
2.13	13.04	
2.10	13.04	
2.07	13.04	
2.04	13.03	
2.01	13.02	smooth water
1.98	13.01	
1.95	13.01	
1.89	13.01	
1.83	13.01	
1.77	13.01	
1.62	13.01	
1.46	13.01	
1.16	13.01	
0.85	13.01	
0.55	13.01	
0.24	13.01	
0.00	13.01	
-0.37	13.01	
-0.67	13.01	
-0.98	13.01	
-1.28	13.01	
-1.43	13.01	
-1.58	13.01	
-1.68	13.02	
-1.74	13.02	
-1.77	13.03	rough water
-1.83	13.06	
-1.89	13.06	
-1.92	13.08	
-1.95	13.09	
-1.98	13.09	
-2.01	13.16	top of wall

Table A86. Prototype cross-sectional water surface profile at step 18, station 20.3 m for test #24.

<b>Prototype Water Surface Profile</b>		
Cross-Sectional Profile, $X_p = 20.3$ m - Step 18; PMF		
<b>station</b>	<b>elev</b>	
<b><math>Y_p</math> (m)</b>	<b><math>Z_p</math> (m)</b>	<b>Comments</b>
46.07	287.60	top of wall - step 18
45.87	285.21	coreflow
44.93	285.05	coreflow
43.92	285.04	coreflow
42.92	285.56	TW
32.19	285.83	TW
18.78	285.99	TW
5.36	285.99	TW
-8.05	285.99	TW
-21.46	286.01	TW
-31.52	285.49	TW
-33.53	284.66	coreflow
-35.20	284.94	coreflow
-36.21	285.28	coreflow
-37.55	285.70	coreflow
-38.89	285.77	coreflow
-39.90	286.14	coreflow
-40.43	286.25	coreflow
-40.64	287.62	top of wall

Table A87. Model cross-sectional water surface profile at step 18, station 0.92 m for test #24.

<b>Model Water Surface Profile</b>		
Cross-Sectional Profile, $X_m = 0.92$ m - Step 18; PMF		
<b>station</b> <b><math>Y_m</math> (m)</b>	<b>elev</b> <b><math>Z_m</math>(m)</b>	<b>Comments</b>
2.09	13.07	top of wall - step 18
2.08	12.96	coreflow
2.04	12.96	coreflow
2.00	12.96	coreflow
1.95	12.98	TW
1.46	12.99	TW
0.85	13.00	TW
0.24	13.00	TW
-0.37	13.00	TW
-0.98	13.00	TW
-1.43	12.98	TW
-1.52	12.94	coreflow
-1.60	12.95	coreflow
-1.65	12.97	coreflow
-1.71	12.99	coreflow
-1.77	12.99	coreflow
-1.81	13.01	coreflow
-1.84	13.01	coreflow
-1.85	13.07	top of wall

Table A88. Prototype cross-sectional water surface profile at step 21, station 23.1 m for test #24.

<b>Prototype Water Surface Profile</b>		
Cross-Sectional Profile, $X_p = 23.1$ m - Step 21; PMF - Low TW		
<b>station</b>	<b>elev</b>	
<b><math>Y_p</math> (m)</b>	<b><math>Z_p</math> (m)</b>	<b>Comments</b>
45.26	287.16	top of wall - step 21
45.13	284.18	
44.26	284.09	
43.59	284.02	
42.92	283.96	
42.25	283.90	
41.57	283.68	smooth water
40.23	283.56	
38.89	283.47	
35.54	283.40	
32.19	283.35	
25.48	283.35	
18.78	283.35	
12.07	283.34	
5.36	283.35	
0.00	283.34	
-8.05	283.31	
-14.75	283.33	
-21.46	283.37	
-24.81	283.43	
-28.16	283.50	
-30.18	283.61	
-32.86	283.84	
-33.86	283.98	smooth water
-34.87	284.41	
-36.21	284.92	
-37.55	285.04	
-38.22	285.16	
-38.89	285.30	
-39.09	287.23	top of wall

Table A89. Model cross-sectional water surface profile at step 21, station 1.05 m for test #24.

<b>Model Water Surface Profile</b>		
Cross-Sectional Profile, $X_m = 1.05$ m - Step 21; PMF - Low TW		
<b>station</b>	<b>elev</b>	
<b><math>Y_m</math> (m)</b>	<b><math>Z_m</math> (m)</b>	<b>Comments</b>
2.06	13.05	top of wall - step 21
2.05	12.92	
2.01	12.91	
1.98	12.91	
1.95	12.91	
1.92	12.90	
1.89	12.89	smooth water
1.83	12.89	
1.77	12.89	
1.62	12.88	
1.46	12.88	
1.16	12.88	
0.85	12.88	
0.55	12.88	
0.24	12.88	
0.00	12.88	
-0.37	12.88	
-0.67	12.88	
-0.98	12.88	
-1.13	12.88	
-1.28	12.89	
-1.37	12.89	
-1.49	12.90	
-1.54	12.91	smooth water
-1.58	12.93	
-1.65	12.95	
-1.71	12.96	
-1.74	12.96	
-1.77	12.97	
-1.78	13.06	top of wall

Table A90. Prototype cross-sectional water surface profile at step 25, station 26.8 m for test #24.

<b>Prototype Water Surface Profile</b>		
Cross-Sectional Profile, $X_p = 26.8$ m - Step 25; PMF - Low TW		
<b>station</b> $Y_p$ (m)	<b>elev</b> $Z_p$ (m)	<b>Comments</b>
44.39	287.15	top of wall - step 25
44.06	282.98	
42.92	282.86	
41.57	282.70	
40.23	282.45	
38.89	282.27	
35.54	282.16	smooth water
32.19	282.08	
25.48	282.08	
18.78	282.06	
12.07	282.05	
5.36	282.06	
0.00	282.07	
-8.05	282.06	
-14.75	282.09	
-21.46	282.15	
-24.81	282.29	
-28.16	282.46	
-30.18	282.64	
-31.92	282.84	smooth water
-32.52	283.20	
-33.53	283.50	
-34.87	283.83	
-35.87	283.95	
-36.81	284.12	
-37.01	287.17	top of wall

Table A91. Model cross-sectional water surface profile at step 25, station 1.22 m for test #24.

<b>Model Water Surface Profile</b>		
Cross-Sectional Profile, $X_m = 1.22$ m - Step 25; PMF - Low TW		
<b>station</b> <b><math>Y_m</math> (m)</b>	<b>elev</b> <b><math>Z_m</math>(m)</b>	<b>Comments</b>
2.02	13.05	top of wall - step 25
2.00	12.86	
1.95	12.86	
1.89	12.85	
1.83	12.84	
1.77	12.83	
1.62	12.83	smooth water
1.46	12.82	
1.16	12.82	
0.85	12.82	
0.55	12.82	
0.24	12.82	
0.00	12.82	
-0.37	12.82	
-0.67	12.82	
-0.98	12.82	
-1.13	12.83	
-1.28	12.84	
-1.37	12.85	
-1.45	12.86	smooth water
-1.48	12.87	
-1.52	12.89	
-1.58	12.90	
-1.63	12.91	
-1.67	12.91	
-1.68	13.05	top of wall

Table A92. Prototype centerline water surface profile for test #25.

<b>Prototype Water Surface Profile</b>		
Centerline Profile, $Y_p = 0.0$ m; 2/3 PMF		
<b>station</b> <b><math>X_p</math> (m)</b>	<b>elev</b> <b><math>Z_p</math>(m)</b>	<b>Comments</b>
-113.12	291.98	
-99.71	291.99	
-86.30	291.98	
-72.89	291.98	
-59.48	291.98	
-46.07	291.98	
-32.66	291.98	
-19.25	291.96	
-5.83	291.80	
-4.49	291.79	
-3.15	291.78	
-1.81	291.75	
-0.47	291.61	
0.87	291.20	
2.21	290.57	
3.55	289.97	
4.90	289.46	
6.24	288.94	
7.58	288.44	
10.93	287.23	
14.28	286.08	
17.64	284.97	edge of TW
18.98	285.35	TW
20.99	285.38	TW
24.34	285.52	TW
27.69	285.73	TW
31.05	285.85	stilling basin
34.40	285.92	stilling basin
41.11	286.03	out of stilling basin
47.81	286.03	
61.22	286.05	
74.63	286.05	
88.04	286.05	
101.46	286.04	
114.87	286.03	
141.69	285.99	TW reading d.s.

Table A93. Model centerline water surface profile for test #25.

Model Water Surface Profile		
Run #: 25		Centerline profile, $Y_m = 0.0$ m; 2/3 PMF
Date: 6 Dec 2004		
station $X_m$ (m)	elev $Z_m$ (m)	Comments
-5.14	13.27	
-4.53	13.27	
-3.92	13.27	
-3.31	13.27	
-2.70	13.27	
-2.09	13.27	
-1.48	13.27	
-0.87	13.27	
-0.27	13.26	
-0.20	13.26	
-0.14	13.26	
-0.08	13.26	
-0.02	13.26	
0.04	13.24	
0.10	13.21	
0.16	13.18	
0.22	13.16	
0.28	13.13	
0.34	13.11	
0.50	13.06	
0.65	13.00	
0.80	12.95	edge of TW
0.86	12.97	TW
0.95	12.97	TW
1.11	12.98	TW
1.26	12.99	TW
1.41	12.99	stilling basin
1.56	13.00	stilling basin
1.87	13.00	out of stilling basin
2.17	13.00	
2.78	13.00	
3.39	13.00	
4.00	13.00	
4.61	13.00	
5.22	13.00	
6.44	13.00	TW reading d.s.

Table A94. Prototype water surface profile along the right wall looking downstream for test #25.

Prototype Water Surface Profile			
WS along Rt. Wall looking d.s. 2/3 PMF, $\phi = 30$ on rt, 15 on lt			
station $X_p$ (m)	station $Y_p$ (m)	elev $Z_p$ (m)	Comments
-12.54	-49.62	291.94	rt wall look ds
-9.19	-49.62	291.86	
-7.85	-49.62	291.57	
-6.50	-49.62	291.64	
-5.83	-49.62	291.68	
-2.48	-49.62	291.71	
-1.14	-49.62	291.67	
0.87	-49.62	291.16	
3.69	-49.62	290.08	joint wall begins conv
4.90	-49.29	290.57	
7.58	-47.61	289.92	
10.93	-45.80	288.78	
14.28	-43.85	287.61	
17.64	-41.91	286.37	
21.46	-39.83	285.33	wall begins level off
24.34	-38.22	285.22	TW
27.69	-36.21	285.75	TW
29.50	-35.14	286.09	TW, stilling basin
31.05	-35.14	286.03	TW, stilling basin
34.40	-35.14	286.26	
38.22	-35.14	286.30	end of basin

Table A95. Model water surface profile along the right wall looking downstream for test #25.

<b>Model Water Surface Profile</b>			
WS along Rt. Wall looking d.s. 2/3 PMF, $\phi = 30$ on rt, 15 on lt			
<b>station X<sub>m</sub> (m)</b>	<b>station Y<sub>m</sub> (m)</b>	<b>elev Z<sub>m</sub>(m)</b>	<b>Comments</b>
-0.57	-2.26	13.27	rt wall look ds
-0.42	-2.26	13.27	
-0.36	-2.26	13.25	
-0.30	-2.26	13.26	
-0.27	-2.26	13.26	
-0.11	-2.26	13.26	
-0.05	-2.26	13.26	
0.04	-2.26	13.23	
0.17	-2.26	13.19	joint wall begins conv
0.22	-2.24	13.21	
0.34	-2.16	13.18	
0.50	-2.08	13.13	
0.65	-1.99	13.07	
0.80	-1.91	13.02	
0.98	-1.81	12.97	wall begins level off
1.11	-1.74	12.96	TW
1.26	-1.65	12.99	TW
1.34	-1.60	13.00	TW, stilling basin
1.41	-1.60	13.00	TW, stilling basin
1.56	-1.60	13.01	
1.74	-1.60	13.01	end of basin

Table A96. Prototype water surface profile along the left wall looking downstream for test #25.

Prototype Water Surface Profile			
WS along Lt. Wall looking d.s. 2/3 PMF, $\phi = 30$ on rt, 15 on lt			
station $X_p$ (m)	station $Y_p$ (m)	elev $Z_p$ (m)	Comments
-12.54	49.62	291.94	lt wall looking ds
-9.19	49.62	291.84	
-7.85	49.62	291.57	
-6.50	49.62	291.65	
-5.83	49.62	291.69	
-2.48	49.62	291.73	
-1.14	49.62	291.65	
0.87	49.62	291.18	
3.69	49.62	289.96	joint starts to conv
4.90	49.82	289.88	
7.58	49.15	289.15	
10.93	48.28	287.94	
14.28	47.41	286.75	
17.64	46.54	285.65	
19.98	45.80	285.18	TW
20.65	45.73	285.21	TW
21.46	45.40	285.19	wall begin to level off
24.34	44.73	285.50	TW
27.69	43.79	285.76	TW
29.50	43.25	285.94	start basin
31.05	43.25	285.93	stilling basin
34.40	43.25	286.10	stilling basin
38.22	43.25	286.15	stilling basin

Table A97. Model water surface profile along the left wall looking downstream for test #25.

<b>Model Water Surface Profile</b>			
WS along Lt. Wall looking d.s. 2/3 PMF, $\phi = 30$ on rt, 15 on lt			
<b>station</b> <b>X<sub>m</sub> (m)</b>	<b>station</b> <b>Y<sub>m</sub> (m)</b>	<b>elev</b> <b>Z<sub>m</sub>(m)</b>	<b>Comments</b>
-0.57	2.26	13.27	lt wall looking ds
-0.42	2.26	13.27	
-0.36	2.26	13.25	
-0.30	2.26	13.26	
-0.27	2.26	13.26	
-0.11	2.26	13.26	
-0.05	2.26	13.26	
0.04	2.26	13.24	
0.17	2.26	13.18	joint starts to conv
0.22	2.26	13.18	
0.34	2.23	13.14	
0.50	2.19	13.09	
0.65	2.15	13.03	
0.80	2.12	12.98	
0.91	2.08	12.96	TW
0.94	2.08	12.96	TW
0.98	2.06	12.96	wall begin to level off
1.11	2.03	12.98	TW
1.26	1.99	12.99	TW
1.34	1.97	13.00	start basin
1.41	1.97	13.00	stilling basin
1.56	1.97	13.00	stilling basin
1.74	1.97	13.01	stilling basin

Table A98. Prototype cross-sectional water surface profile at step 1, station 4.6 m for test #25.

<b>Prototype Water Surface Profile</b>		
Cross-Sectional Profile, $X_p = 4.6$ m - Step 1; 2/3 PMF		
<b>station</b> $Y_p$ (m)	<b>elev</b> $Z_p$ (m)	<b>Comments</b>
50.09	292.87	top of wall - step 1
49.89	289.92	
49.62	289.70	
48.95	289.62	
48.28	289.54	
46.94	289.53	
45.60	289.53	
42.25	289.56	
38.89	289.60	
32.19	289.60	
25.48	289.58	
18.78	289.56	
12.07	289.54	
5.36	289.56	
0.00	289.56	
-8.05	289.57	
-14.75	289.56	
-21.46	289.56	
-28.16	289.57	
-34.87	289.57	
-41.57	289.54	
-44.93	289.51	
-46.27	289.51	
-47.61	289.60	
-48.28	289.70	
-48.95	289.92	
-49.49	290.57	
-49.82	292.89	top of wall

Table A99. Model cross-sectional water surface profile at step 1, station 0.21 m for test #25.

<b>Model Water Surface Profile</b>		
Cross-Sectional Profile, $X_m = 0.21$ m - Step 1; 2/3 PMF		
<b>station</b> $Y_m$ (m)	<b>elev</b> $Z_m$ (m)	<b>Comments</b>
2.28	13.31	top of wall - step 1
2.27	13.18	
2.26	13.17	
2.23	13.16	
2.19	13.16	
2.13	13.16	
2.07	13.16	
1.92	13.16	
1.77	13.16	
1.46	13.16	
1.16	13.16	
0.85	13.16	
0.55	13.16	
0.24	13.16	
0.00	13.16	
-0.37	13.16	
-0.67	13.16	
-0.98	13.16	
-1.28	13.16	
-1.58	13.16	
-1.89	13.16	
-2.04	13.16	
-2.10	13.16	
-2.16	13.16	
-2.19	13.17	
-2.23	13.18	
-2.25	13.21	
-2.26	13.31	top of wall

Table A100. Prototype cross-sectional water surface profile at step 8, station 11 m for test #25.

<b>Prototype Water Surface Profile</b>		
Cross-Sectional Profile, $X_p = 11$ m - Step 8; 2/3 PMF		
<b>station</b> <b><math>Y_p</math> (m)</b>	<b>elev</b> <b><math>Z_p</math>(m)</b>	<b>Comments</b>
48.41	290.72	top of wall - step 8
48.28	287.92	
47.61	287.83	
46.94	287.75	
46.27	287.37	
45.60	287.30	
44.26	287.25	
42.25	287.24	
38.89	287.21	
32.19	287.25	
25.48	287.25	
18.78	287.24	
12.07	287.23	
5.36	287.23	
0.00	287.23	
-8.05	287.22	
-14.75	287.23	
-21.46	287.24	
-28.16	287.24	
-34.87	287.26	
-38.22	287.30	
-40.23	287.36	
-41.84	287.42	smooth water
-42.58	287.77	
-43.59	288.21	
-44.59	288.39	
-45.67	288.72	
-45.93	290.73	top of wall

Table A101. Model cross-sectional water surface profile at step 8, station 0.5 m for test #25.

<b>Model Water Surface Profile</b>		
Cross-Sectional Profile, $X_m = 0.5$ m - Step 8; 2/3 PMF		
<b>station</b> $Y_m$ (m)	<b>elev</b> $Z_m$ (m)	<b>Comments</b>
2.20	13.21	top of wall - step 8
2.19	13.09	
2.16	13.08	
2.13	13.08	
2.10	13.06	
2.07	13.06	
2.01	13.06	
1.92	13.06	
1.77	13.05	
1.46	13.06	
1.16	13.06	
0.85	13.06	
0.55	13.06	
0.24	13.06	
0.00	13.06	
-0.37	13.06	
-0.67	13.06	
-0.98	13.06	
-1.28	13.06	
-1.58	13.06	
-1.74	13.06	
-1.83	13.06	
-1.90	13.06	smooth water
-1.94	13.08	
-1.98	13.10	
-2.03	13.11	
-2.08	13.12	
-2.09	13.21	top of wall

Table A102. Prototype cross-sectional water surface profile at step 12, station 14.8 m for test #25.

<b>Prototype Water Surface Profile</b>		
Cross-Sectional Profile, $X_p = 14.8$ m - Step 12; 2/3 PMF		
<b>station</b> $Y_p$ (m)	<b>elev</b> $Z_p$ (m)	<b>Comments</b>
47.48	289.46	top of wall - step 12
47.34	286.62	
46.60	286.54	
45.60	286.44	
44.93	286.18	
43.59	286.07	
42.25	285.99	
40.90	285.97	
38.89	285.96	
32.19	285.97	
25.48	285.96	
18.78	285.94	
12.07	285.94	
5.36	285.95	
0.00	285.95	
-8.05	285.93	
-14.75	285.93	
-21.46	285.94	
-28.16	285.95	
-31.52	285.97	
-34.87	286.03	
-36.88	286.07	
-38.22	286.14	
-39.90	286.35	smooth water
-40.90	286.80	rough water
-41.57	287.21	
-42.92	287.20	
-43.59	287.43	
-43.79	289.47	top of wall

Table A103. Model cross-sectional water surface profile at step 12, station 0.67 m for test #25.

<b>Model Water Surface Profile</b>		
Cross-Sectional Profile, $X_m = 0.67$ m - Step 12; 2/3 PMF		
<b>station</b>	<b>elev</b>	
<b><math>Y_m</math> (m)</b>	<b><math>Z_m</math> (m)</b>	<b>Comments</b>
2.16	13.16	top of wall - step 12
2.15	13.03	
2.12	13.02	
2.07	13.02	
2.04	13.01	
1.98	13.00	
1.92	13.00	
1.86	13.00	
1.77	13.00	
1.46	13.00	
1.16	13.00	
0.85	13.00	
0.55	13.00	
0.24	13.00	
0.00	13.00	
-0.37	13.00	
-0.67	13.00	
-0.98	13.00	
-1.28	13.00	
-1.43	13.00	
-1.58	13.00	
-1.68	13.00	
-1.74	13.01	
-1.81	13.02	smooth water
-1.86	13.04	rough water
-1.89	13.06	
-1.95	13.05	
-1.98	13.06	
-1.99	13.16	top of wall

Table A104. Prototype cross-sectional water surface profile at step 18, station 20.3 m for test #25.

<b>Prototype Water Surface Profile</b>		
Cross-Sectional Profile, $X_p = 20.3$ m - Step 18; 2/3 PMF		
station	elev	
$Y_p$ (m)	$Z_p$ (m)	Comments
46.07	287.59	top of wall - step 18
45.87	285.19	tw
44.26	285.00	tw
38.89	285.20	tw
25.48	285.36	tw
12.07	285.46	tw
0.00	285.42	tw
-14.75	285.46	tw
-28.16	285.22	tw
-34.20	284.35	no tw
-35.87	284.53	no tw
-37.22	284.77	no tw
-38.22	285.29	no tw
-39.56	285.50	no tw
-40.50	285.67	no tw
-40.70	287.62	top of wall

Table A105. Model cross-sectional water surface profile at step 18, station 0.92 m for test #25.

<b>Model Water Surface Profile</b>		
Cross-Sectional Profile, $X_m = 0.92$ m - Step 18; 2/3 PMF		
station	elev	
$Y_m$ (m)	$Z_m$ (m)	Comments
2.09	13.07	top of wall - step 18
2.08	12.96	tw
2.01	12.95	tw
1.77	12.96	tw
1.16	12.97	tw
0.55	12.98	tw
0.00	12.97	tw
-0.67	12.98	tw
-1.28	12.96	tw
-1.55	12.93	no tw
-1.63	12.93	no tw
-1.69	12.94	no tw
-1.74	12.97	no tw
-1.80	12.98	no tw
-1.84	12.99	no tw
-1.85	13.07	top of wall

Table A106. Prototype cross-sectional water surface profile at step 21, station 23.1 m for test #25.

<b>Prototype Water Surface Profile</b>		
Cross-Sectional Profile, $X_p = 23.1$ m - Step 21; 2/3 PMF - Low TW		
<b>station</b>	<b>elev</b>	
<b><math>Y_p</math> (m)</b>	<b><math>Z_p</math> (m)</b>	<b>Comments</b>
45.33	287.15	top of wall - step 21
45.13	283.82	
44.26	283.73	
42.92	283.59	
41.57	283.35	
40.23	283.29	
38.89	283.23	smooth water
36.88	283.16	
35.54	283.16	
32.19	283.11	
25.48	283.13	
18.78	283.10	
12.07	283.10	
5.36	283.10	
0.00	283.10	
-8.05	283.10	
-14.75	283.11	
-21.46	283.12	
-28.16	283.23	
-31.52	283.39	
-33.53	283.55	
-35.20	283.75	
-36.21	284.20	
-37.55	284.50	
-38.22	284.69	
-38.89	284.97	
-39.16	287.22	top of wall

Table A107. Model cross-sectional water surface profile at step 21, station 1.05 m for test #25.

<b>Model Water Surface Profile</b>		
Cross-Sectional Profile, $X_m = 1.05$ m - Step 21; 2/3 PMF - Low TW		
<b>station</b>	<b>elev</b>	
<b><math>Y_m</math> (m)</b>	<b><math>Z_m</math>(m)</b>	<b>Comments</b>
2.06	13.05	top of wall - step 21
2.05	12.90	
2.01	12.90	
1.95	12.89	
1.89	12.88	
1.83	12.88	
1.77	12.87	
1.68	12.87	
1.62	12.87	
1.46	12.87	
1.16	12.87	
0.85	12.87	
0.55	12.87	
0.24	12.87	
0.00	12.87	
-0.37	12.87	
-0.67	12.87	
-0.98	12.87	
-1.28	12.87	
-1.43	12.88	
-1.52	12.89	
-1.60	12.90	
-1.65	12.92	
-1.71	12.93	
-1.74	12.94	
-1.77	12.95	
-1.78	13.06	top of wall

Table A108. Prototype cross-sectional water surface profile at step 25, station 26.8 m for test #25.

<b>Prototype Water Surface Profile</b>		
Cross-Sectional Profile, $X_p = 26.8$ m - Step 25; 2/3 PMF - Low TW		
<b>station</b>	<b>elev</b>	
<b><math>Y_p</math> (m)</b>	<b><math>Z_p</math> (m)</b>	<b>Comments</b>
44.32	287.14	top of wall - step 25
44.12	282.56	
43.59	282.55	
42.58	282.32	
41.11	282.15	
39.56	282.04	
38.22	281.96	
35.54	281.88	
32.19	281.88	
25.48	281.88	
18.78	281.87	
12.07	281.88	
5.36	281.89	
0.00	281.88	
-8.05	281.87	
-14.75	281.88	
-21.46	281.91	
-24.81	281.98	
-28.16	282.13	
-31.52	282.39	
-32.86	282.51	
-33.86	282.77	
-35.20	283.27	
-36.21	283.55	
-36.81	283.71	
-37.01	287.17	top of wall

Table A109. Model cross-sectional water surface profile at step 25, station 1.22 m for test #25.

<b>Model Water Surface Profile</b>		
Cross-Sectional Profile, $X_m = 1.22$ m - Step 25; 2/3 PMF - Low TW		
<b>station</b>	<b>elev</b>	
<b><math>Y_m</math> (m)</b>	<b><math>Z_m</math> (m)</b>	<b>Comments</b>
2.01	13.05	top of wall - step 25
2.01	12.84	
1.98	12.84	
1.94	12.83	
1.87	12.83	
1.80	12.82	
1.74	12.82	
1.62	12.81	
1.46	12.81	
1.16	12.81	
0.85	12.81	
0.55	12.81	
0.24	12.81	
0.00	12.81	
-0.37	12.81	
-0.67	12.81	
-0.98	12.81	
-1.13	12.82	
-1.28	12.82	
-1.43	12.84	
-1.49	12.84	
-1.54	12.85	
-1.60	12.88	
-1.65	12.89	
-1.67	12.90	
-1.68	13.05	top of wall

Table A1110. Prototype centerline water surface profile for test #26.

<b>Prototype Water Surface Profile</b>		
Centerline Profile, $Y_p = 0.0$ m; 1/3 PMF		
<b>station</b>	<b>elev</b>	
<b><math>X_p</math> (m)</b>	<b><math>Z_p</math>(m)</b>	<b>Comments</b>
-113.12	291.28	centerline profile
-99.71	291.28	
-86.30	291.28	
-72.89	291.27	
-59.48	291.27	
-46.07	291.27	
-32.66	291.27	
-19.25	291.27	
-5.83	291.20	
-4.49	291.19	
-3.15	291.20	
-1.81	291.18	
-0.47	291.06	
0.87	290.63	
2.21	290.04	
3.55	289.51	
4.90	289.05	
6.24	288.58	
7.58	288.11	
9.25	287.53	
10.93	286.96	
12.61	286.36	
14.28	285.82	
17.64	284.71	
18.84	284.30	edge of TW
19.65	284.69	TW
20.99	284.67	TW
24.34	284.74	TW
27.69	284.85	TW
34.40	284.94	TW
41.11	284.94	
47.81	284.95	
54.52	284.96	
61.22	284.95	
74.63	284.96	
101.46	284.96	
141.69	284.92	TW reading d.s.

Table A111. Model centerline water surface profile for test #26.

Model Water Surface Profile		
Run #: 26	Centerline profile, $Y_m = 0.0$ m; 1/3 PMF	
Date: 9 Dec 2004		
station	elev	Comments
$X_m$ (m)	$Z_m$ (m)	
-5.14	13.24	centerline profile
-4.53	13.24	
-3.92	13.24	
-3.31	13.24	
-2.70	13.24	
-2.09	13.24	
-1.48	13.24	
-0.87	13.24	
-0.27	13.24	
-0.20	13.24	
-0.14	13.24	
-0.08	13.24	
-0.02	13.23	
0.04	13.21	
0.10	13.18	
0.16	13.16	
0.22	13.14	
0.28	13.12	
0.34	13.10	
0.42	13.07	
0.50	13.04	
0.57	13.02	
0.65	12.99	
0.80	12.94	
0.86	12.92	edge of TW
0.89	12.94	TW
0.95	12.94	TW
1.11	12.94	TW
1.26	12.95	TW
1.56	12.95	TW
1.87	12.95	
2.17	12.95	
2.48	12.95	
2.78	12.95	
3.39	12.95	
4.61	12.95	
6.44	12.95	TW reading d.s.

Table A112. Prototype water surface profile along the right wall looking downstream for test #26.

<b>Prototype Water Surface Profile</b>			
WS along Rt. Wall looking d.s. 1/3 PMF, $\phi = 30$ on rt, 15 on lt			
<b>station <math>X_p</math> (m)</b>	<b>station <math>Y_p</math> (m)</b>	<b>elev <math>Z_p</math>(m)</b>	<b>Comments</b>
-12.54	-49.62	291.26	
-9.19	-49.62	291.22	
-7.85	-49.62	291.14	
-6.50	-49.62	291.19	
-5.83	-49.62	291.19	
-2.48	-49.62	291.18	
-1.14	-49.62	291.13	
0.87	-49.62	290.61	
3.69	-49.62	289.47	joint wall begins conv
4.90	-49.62	289.77	
7.58	-47.61	289.13	
10.93	-45.80	287.87	
14.28	-43.85	286.83	
17.64	-41.91	285.86	
21.46	-39.83	284.69	wall begins level off
24.34	-38.22	284.66	TW
27.69	-36.21	285.12	TW
31.05	-35.14	284.93	stilling basin
34.40	-35.14	285.02	stilling basin
38.22	-35.14	285.08	stilling basin end

Table A113. Model water surface profile along the right wall looking downstream for test #26.

Model Water Surface Profile			
WS along Rt. Wall looking d.s. 1/3 PMF, $\phi = 30$ on rt, 15 on lt			
station $X_m$ (m)	station $Y_m$ (m)	elev $Z_m$ (m)	Comments
-0.57	-2.26	13.24	
-0.42	-2.26	13.24	
-0.36	-2.26	13.23	
-0.30	-2.26	13.24	
-0.27	-2.26	13.24	
-0.11	-2.26	13.24	
-0.05	-2.26	13.23	
0.04	-2.26	13.21	
0.17	-2.26	13.16	joint wall begins conv
0.22	-2.26	13.17	
0.34	-2.16	13.14	
0.50	-2.08	13.08	
0.65	-1.99	13.04	
0.80	-1.91	12.99	
0.98	-1.81	12.94	wall begins level off
1.11	-1.74	12.94	TW
1.26	-1.65	12.96	TW
1.41	-1.60	12.95	stilling basin
1.56	-1.60	12.96	stilling basin
1.74	-1.60	12.96	stilling basin end

Table A114. Prototype water surface profile along the left wall looking downstream for test #26.

Prototype Water Surface Profile			
WS along Lt. Wall looking d.s. 1/3 PMF, $\phi = 30$ on rt, 15 on lt			
station $X_p$ (m)	station $Y_p$ (m)	elev $Z_p$ (m)	Comments
-12.54	49.62	291.24	
-9.19	49.62	291.19	
-7.85	49.62	291.14	
-6.50	49.62	291.19	
-5.83	49.62	291.20	
-2.48	49.62	291.17	
-1.14	49.62	291.13	
0.87	49.62	290.65	
3.69	49.62	289.54	joint wall begins conv
4.90	49.82	289.26	
7.58	49.15	288.58	
10.93	48.28	287.42	
14.28	47.41	286.27	
17.64	46.54	285.22	
20.32	45.80	284.28	TW edge
21.46	45.40	284.50	TW, wall levels off
24.34	44.73	284.69	TW
27.69	43.79	284.95	TW
29.50	43.25	284.96	start of stilling basin
31.05	43.25	284.98	stilling basin
34.40	43.25	285.00	stilling basin
38.22	43.25	285.01	stilling basin end

Table A115. Model water surface profile along the left wall looking downstream for test #26.

<b>Model Water Surface Profile</b>			
WS along Lt. Wall looking d.s. 1/3 PMF, $\phi = 30$ on rt, 15 on lt			
<b>station X<sub>m</sub> (m)</b>	<b>station Y<sub>m</sub> (m)</b>	<b>elev Z<sub>m</sub>(m)</b>	<b>Comments</b>
-0.57	2.26	13.24	
-0.42	2.26	13.24	
-0.36	2.26	13.23	
-0.30	2.26	13.24	
-0.27	2.26	13.24	
-0.11	2.26	13.24	
-0.05	2.26	13.23	
0.04	2.26	13.21	
0.17	2.26	13.16	joint wall begins conv
0.22	2.26	13.15	
0.34	2.23	13.12	
0.50	2.19	13.06	
0.65	2.15	13.01	
0.80	2.12	12.96	
0.92	2.08	12.92	TW edge
0.98	2.06	12.93	TW, wall levels off
1.11	2.03	12.94	TW
1.26	1.99	12.95	TW
1.34	1.97	12.95	start of stilling basin
1.41	1.97	12.95	stilling basin
1.56	1.97	12.95	stilling basin
1.74	1.97	12.95	stilling basin end

Table A116. Prototype cross-sectional water surface profile at step 1, station 4.6 m for test #26.

<b>Prototype Water Surface Profile</b>		
Cross-Sectional Profile, $X_p = 4.6$ m - Step 1; 1/3 PMF		
<b>station</b> <b><math>Y_p</math> (m)</b>	<b>elev</b> <b><math>Z_p</math> (m)</b>	<b>Comments</b>
50.09	292.87	top of wall - step 1
49.89	289.33	
49.62	289.21	
48.95	289.16	
48.28	289.14	
46.94	289.13	
45.60	289.14	
38.89	289.18	
32.19	289.18	
25.48	289.16	
18.78	289.15	
12.07	289.14	
5.36	289.14	
0.00	289.15	
-8.05	289.16	
-14.75	289.15	
-21.46	289.15	
-28.16	289.15	
-34.87	289.16	
-41.57	289.14	
-44.93	289.13	
-46.27	289.06	
-47.61	289.08	
-48.28	289.19	
-48.95	289.25	
-49.55	289.86	
-49.69	292.88	top of wall

Table A117. Model cross-sectional water surface profile at step 1, station 0.21 m for test #26.

<b>Model Water Surface Profile</b>		
Cross-Sectional Profile, $X_m = 0.21$ m - Step 1; 1/3 PMF		
<b>station</b> $Y_m$ (m)	<b>elev</b> $Z_m$ (m)	<b>Comments</b>
2.28	13.31	top of wall - step 1
2.27	13.15	
2.26	13.15	
2.23	13.14	
2.19	13.14	
2.13	13.14	
2.07	13.14	
1.77	13.14	
1.46	13.14	
1.16	13.14	
0.85	13.14	
0.55	13.14	
0.24	13.14	
0.00	13.14	
-0.37	13.14	
-0.67	13.14	
-0.98	13.14	
-1.28	13.14	
-1.58	13.14	
-1.89	13.14	
-2.04	13.14	
-2.10	13.14	
-2.16	13.14	
-2.19	13.15	
-2.23	13.15	
-2.25	13.18	
-2.26	13.31	top of wall

Table A118. Prototype cross-sectional water surface profile at step 8, station 11 m for test #26.

<b>Prototype Water Surface Profile</b>		
Cross-Sectional Profile, $X_p = 11$ m - Step 8; 1/3 PMF		
<b>station</b>	<b>elev</b>	
<b><math>Y_p</math> (m)</b>	<b><math>Z_p</math> (m)</b>	<b>Comments</b>
48.41	290.71	top of wall - step 8
48.28	287.34	
47.61	287.32	
46.94	287.11	
46.27	287.00	
45.60	286.98	
44.93	286.98	
43.59	286.95	
42.25	286.93	
38.89	286.91	
32.19	286.92	
25.48	286.93	
18.78	286.94	
12.07	286.93	
5.36	286.93	
0.00	286.92	
-8.05	286.92	
-14.75	286.93	
-21.46	286.94	
-28.16	286.95	
-34.87	286.95	
-38.22	286.97	
-40.23	287.00	
-41.57	287.03	
-42.92	287.10	
-43.59	287.26	
-44.26	287.58	
-44.93	287.79	
-45.67	287.82	
-45.93	290.72	top of wall

Table A119. Model cross-sectional water surface profile at step 8, station 0.5 m for test #26.

<b>Model Water Surface Profile</b>		
Cross-Sectional Profile, $X_m = 0.5$ m - Step 8; 1/3 PMF		
<b>station</b> <b><math>Y_m</math> (m)</b>	<b>elev</b> <b><math>Z_m</math>(m)</b>	<b>Comments</b>
2.20	13.21	top of wall - step 8
2.19	13.06	
2.16	13.06	
2.13	13.05	
2.10	13.05	
2.07	13.04	
2.04	13.04	
1.98	13.04	
1.92	13.04	
1.77	13.04	
1.46	13.04	
1.16	13.04	
0.85	13.04	
0.55	13.04	
0.24	13.04	
0.00	13.04	
-0.37	13.04	
-0.67	13.04	
-0.98	13.04	
-1.28	13.04	
-1.58	13.04	
-1.74	13.04	
-1.83	13.05	
-1.89	13.05	
-1.95	13.05	
-1.98	13.06	
-2.01	13.07	
-2.04	13.08	
-2.08	13.08	
-2.09	13.21	top of wall

Table A120. Prototype cross-sectional water surface profile at step 12, station 14.8 m for test #26.

<b>Prototype Water Surface Profile</b>		
Cross-Sectional Profile, $X_p = 14.8$ m - Step 12; 1/3 PMF		
<b>station</b> $Y_p$ (m)	<b>elev</b> $Z_p$ (m)	<b>Comments</b>
47.48	289.46	top of wall - step 12
47.34	286.15	
46.94	286.05	
46.27	286.03	
45.60	285.86	
44.93	285.77	
44.26	285.76	
42.92	285.71	
40.90	285.69	
38.89	285.66	
35.54	285.67	
38.89	285.69	
25.48	285.67	
18.78	285.65	
12.07	285.67	
5.36	285.68	
0.00	285.68	
-8.05	285.68	
-14.75	285.67	
-21.46	285.67	
-28.16	285.67	
-31.52	285.67	
-28.16	285.72	
-38.22	285.75	
-39.56	285.81	
-40.90	285.94	
-41.57	286.05	
-42.25	286.39	
-42.92	286.56	
-43.59	286.64	
-43.79	289.47	top of wall

Table A121. Model cross-sectional water surface profile at step 12, station 0.67 m for test #26.

<b>Model Water Surface Profile</b>		
Cross-Sectional Profile, $X_m = 0.67$ m - Step 12; 1/3 PMF		
<b>station</b> $Y_m$ (m)	<b>elev</b> $Z_m$ (m)	<b>Comments</b>
2.16	13.16	top of wall - step 12
2.15	13.01	
2.13	13.00	
2.10	13.00	
2.07	12.99	
2.04	12.99	
2.01	12.99	
1.95	12.99	
1.86	12.99	
1.77	12.98	
1.62	12.99	
1.77	12.99	
1.16	12.99	
0.85	12.98	
0.55	12.99	
0.24	12.99	
0.00	12.99	
-0.37	12.99	
-0.67	12.98	
-0.98	12.99	
-1.28	12.99	
-1.43	12.99	
-1.28	12.99	
-1.74	12.99	
-1.80	12.99	
-1.86	13.00	
-1.89	13.00	
-1.92	13.02	
-1.95	13.03	
-1.98	13.03	
-1.99	13.16	top of wall

Table A122. Prototype cross-sectional water surface profile at step 18, station 20.3 m for test #26.

<b>Prototype Water Surface Profile</b>		
Cross-Sectional Profile, $X_p = 20.3$ m - Step 18; 1/3 PMF		
<b>station</b>	<b>elev</b>	
<b><math>Y_p</math> (m)</b>	<b><math>Z_p</math>(m)</b>	<b>Comments</b>
46.00	287.57	top of wall - step 18
45.87	284.27	
45.26	284.20	
44.26	284.11	
42.25	284.55	TW
32.19	284.61	TW
18.78	284.67	TW
5.36	284.62	TW
-8.05	284.63	TW
-21.46	284.62	TW
-31.52	284.48	TW
-33.53	284.01	out of TW
-34.87	284.04	
-36.21	284.07	
-37.55	284.20	
-38.22	284.36	
-38.89	284.54	
-39.56	284.81	
-40.23	284.98	
-40.64	287.62	top of wall

Table A123. Model cross-sectional water surface profile at step 18, station 0.92 m for test #26.

<b>Model Water Surface Profile</b>		
Cross-Sectional Profile, $X_m = 0.92$ m - Step 18; 1/3 PMF		
<b>station</b> <b><math>Y_m</math> (m)</b>	<b>elev</b> <b><math>Z_m</math>(m)</b>	<b>Comments</b>
2.09	13.07	top of wall - step 18
2.08	12.92	
2.06	12.92	
2.01	12.91	
1.92	12.93	TW
1.46	12.94	TW
0.85	12.94	TW
0.24	12.94	TW
-0.37	12.94	TW
-0.98	12.94	TW
-1.43	12.93	TW
-1.52	12.91	out of TW
-1.58	12.91	
-1.65	12.91	
-1.71	12.92	
-1.74	12.93	
-1.77	12.93	
-1.80	12.95	
-1.83	12.95	
-1.85	13.07	top of wall

Table A124. Prototype cross-sectional water surface profile at step 21, station 23.1 m for test #26.

<b>Prototype Water Surface Profile</b>		
Cross-Sectional Profile, $X_p = 23.1$ m - Step 21; 1/3 PMF - Low TW		
<b>station</b>	<b>elev</b>	
<b><math>Y_p</math> (m)</b>	<b><math>Z_p</math>(m)</b>	<b>Comments</b>
45.33	287.15	top of wall - step 21
45.13	283.40	
44.59	283.33	
43.59	283.21	
42.25	283.07	
40.90	283.01	
39.56	282.97	
37.55	282.95	
35.54	282.92	
32.19	282.93	
25.48	282.92	
18.78	282.92	
12.07	282.92	
5.36	282.93	
0.00	282.93	
-8.05	282.92	
-14.75	282.92	
-21.46	282.93	
-28.16	282.98	
-31.52	283.06	
-32.86	283.08	
-34.20	283.16	
-35.54	283.31	
-36.88	283.50	
-38.22	283.97	
-38.89	284.16	
-39.09	287.22	top of wall

Table A125. Model cross-sectional water surface profile at step 21, station 1.05 m for test #26.

<b>Model Water Surface Profile</b>		
Cross-Sectional Profile, $X_m = 1.05$ m - Step 21; 1/3 PMF - Low TW		
<b>station</b>	<b>elev</b>	
<b><math>Y_m</math> (m)</b>	<b><math>Z_m</math> (m)</b>	<b>Comments</b>
2.06	13.05	top of wall - step 21
2.05	12.88	
2.03	12.88	
1.98	12.87	
1.92	12.87	
1.86	12.86	
1.80	12.86	
1.71	12.86	
1.62	12.86	
1.46	12.86	
1.16	12.86	
0.85	12.86	
0.55	12.86	
0.24	12.86	
0.00	12.86	
-0.37	12.86	
-0.67	12.86	
-0.98	12.86	
-1.28	12.86	
-1.43	12.87	
-1.49	12.87	
-1.55	12.87	
-1.62	12.88	
-1.68	12.89	
-1.74	12.91	
-1.77	12.92	
-1.78	13.06	top of wall

Table A126. Prototype cross-sectional water surface profile at step 25, station 26.8 m for test #26.

<b>Prototype Water Surface Profile</b>		
Cross-Sectional Profile, $X_p = -26.8$ m - Step 25; 1/3 PMF - Low TW		
<b>station</b> <b><math>Y_p</math> (m)</b>	<b>elev</b> <b><math>Z_p</math> (m)</b>	<b>Comments</b>
44.32	287.14	top of wall - step 25
44.12	282.15	
43.59	282.06	
42.92	281.96	
41.57	281.88	
40.23	281.78	
38.89	281.75	
36.88	281.69	
34.87	281.68	
32.19	281.67	
25.48	281.68	
18.78	281.68	
12.07	281.69	
5.36	281.68	
0.00	281.68	
-8.05	281.68	
-14.75	281.67	
-21.46	281.69	
-24.81	281.74	
-28.16	281.80	
-31.52	281.92	
-32.86	282.08	
-34.20	282.29	
-35.54	282.49	
-36.21	282.77	
-36.75	282.94	
-36.95	287.17	top of wall

Table A127. Model cross-sectional water surface profile at step 25, station 1.22 m for test #26.

<b>Model Water Surface Profile</b>		
Cross-Sectional Profile, $X_m = 1.22$ m - Step 25; 1/3 PMF - Low TW		
<b>station</b> <b><math>Y_m</math> (m)</b>	<b>elev</b> <b><math>Z_m</math> (m)</b>	<b>Comments</b>
2.01	13.05	top of wall - step 25
2.01	12.82	
1.98	12.82	
1.95	12.82	
1.89	12.81	
1.83	12.81	
1.77	12.81	
1.68	12.80	
1.58	12.80	
1.46	12.80	
1.16	12.80	
0.85	12.80	
0.55	12.80	
0.24	12.80	
0.00	12.80	
-0.37	12.80	
-0.67	12.80	
-0.98	12.80	
-1.13	12.81	
-1.28	12.81	
-1.43	12.81	
-1.49	12.82	
-1.55	12.83	
-1.62	12.84	
-1.65	12.85	
-1.67	12.86	
-1.68	13.05	top of wall

Table A128. Prototype centerline water surface profile for test #27.

<b>Prototype Water Surface Profile</b>		
Centerline Profile, $Y_p = 0.0$ m; 1/6 PMF		
<b>station</b>	<b>elev</b>	
$X_p$ (m)	$Z_p$ (m)	Comments
-113.12	290.86	centerline profile
-99.71	290.86	
-86.30	290.86	
-72.89	290.86	
-59.48	290.86	
-46.07	290.86	
-32.66	290.86	
-19.25	290.86	
-5.83	290.82	
-4.49	290.82	
-3.15	290.82	
-1.81	290.81	
-0.47	290.74	
0.20	290.61	
0.87	290.33	
1.54	290.06	
2.21	289.80	
2.88	289.54	
3.55	289.23	
4.22	289.07	
5.90	288.54	
7.58	287.91	
9.25	287.38	
10.93	286.87	
12.61	286.25	
14.28	285.73	
15.96	285.17	
17.64	284.62	
18.84	284.20	
20.99	283.55	
21.93	283.23	edge TW
23.00	283.52	TW
24.34	283.51	TW
27.69	283.59	TW
31.05	283.65	
34.40	283.65	
47.81	283.64	
61.22	283.64	
74.63	283.65	
88.04	283.65	
101.46	283.66	
141.69	283.65	TW reading d.s.

Table A129. Model centerline water surface profile for test #27.

Model Water Surface Profile		
Run #: 27		Centerline profile, $Y_m = 0.0$ m; 1/6 PMF
Date: 10 Dec 2004		
station	elev	Comments
$X_m$ (m)	$Z_m$ (m)	
-5.14	13.22	centerline profile
-4.53	13.22	
-3.92	13.22	
-3.31	13.22	
-2.70	13.22	
-2.09	13.22	
-1.48	13.22	
-0.87	13.22	
-0.27	13.22	
-0.20	13.22	
-0.14	13.22	
-0.08	13.22	
-0.02	13.22	
0.01	13.21	
0.04	13.20	
0.07	13.18	
0.10	13.17	
0.13	13.16	
0.16	13.15	
0.19	13.14	
0.27	13.12	
0.34	13.09	
0.42	13.06	
0.50	13.04	
0.57	13.01	
0.65	12.99	
0.73	12.96	
0.80	12.94	
0.86	12.92	
0.95	12.89	
1.00	12.87	edge TW
1.05	12.89	TW
1.11	12.89	TW
1.26	12.89	TW
1.41	12.89	
1.56	12.89	
2.17	12.89	
2.78	12.89	
3.39	12.89	
4.00	12.89	
4.61	12.89	
6.44	12.89	TW reading d.s.

Table A130. Prototype water surface profile along right wall looking downstream for test #27.

<b>Prototype Water Surface Profile</b>			
WS along Rt. Wall looking d.s. 1/6 PMF, $\phi = 30$ on rt, 15 on lt			
<b>station <math>X_p</math> (m)</b>	<b>station <math>Y_p</math> (m)</b>	<b>elev <math>Z_p</math>(m)</b>	<b>Comments</b>
-12.54	-49.62	290.85	rt wall look ds
-9.19	-49.62	290.82	
-7.85	-49.62	290.82	
-6.50	-49.62	290.83	
-5.83	-49.62	290.83	
-2.48	-49.62	290.82	
-1.14	-49.62	290.80	
0.87	-49.62	290.31	
3.69	-49.62	289.27	joint wall begins conv
4.90	-49.29	289.36	
7.58	-47.61	288.60	
10.93	-45.80	287.44	
14.28	-43.85	286.45	
17.64	-41.91	285.40	
21.46	-39.83	284.07	wall begins level off
24.21	-38.29	283.17	edge of TW
25.68	-37.35	283.55	TW
27.69	-36.21	283.69	TW
31.05	-35.14	283.71	stilling basin
34.40	-35.14	283.75	stilling basin
38.22	-35.14	283.79	stilling basin end

Table A131. Model water surface profile along right wall looking downstream for test #27.

<b>Model Water Surface Profile</b>			
WS along Rt. Wall looking d.s. 1/6 PMF, $\phi = 30$ on rt, 15 on lt			
<b>station X<sub>m</sub> (m)</b>	<b>station Y<sub>m</sub> (m)</b>	<b>elev Z<sub>m</sub>(m)</b>	<b>Comments</b>
-0.57	-2.26	13.22	rt wall look ds
-0.42	-2.26	13.22	
-0.36	-2.26	13.22	
-0.30	-2.26	13.22	
-0.27	-2.26	13.22	
-0.11	-2.26	13.22	
-0.05	-2.26	13.22	
0.04	-2.26	13.20	
0.17	-2.26	13.15	joint wall begins conv
0.22	-2.24	13.15	
0.34	-2.16	13.12	
0.50	-2.08	13.07	
0.65	-1.99	13.02	
0.80	-1.91	12.97	
0.98	-1.81	12.91	wall begins level off
1.10	-1.74	12.87	edge of TW
1.17	-1.70	12.89	TW
1.26	-1.65	12.89	TW
1.41	-1.60	12.90	stilling basin
1.56	-1.60	12.90	stilling basin
1.74	-1.60	12.90	stilling basin end

Table A132. Prototype cross-sectional water surface profile at step 1, station 4.6 m for test #27.

<b>Prototype Water Surface Profile</b>		
Cross-Sectional Profile, $X_p = 4.6$ m - Step 1; 1/6 PMF		
<b>station</b>	<b>elev</b>	
<b><math>Y_p</math> (m)</b>	<b><math>Z_p</math> (m)</b>	<b>Comments</b>
50.09	292.86	top of wall - step 1
49.89	289.11	
49.62	288.94	
48.95	288.94	
48.28	288.93	
46.94	288.94	
45.60	288.94	
38.89	288.98	
32.19	288.98	
25.48	288.96	
18.78	288.94	
12.07	288.93	
5.36	288.93	
0.00	288.94	
-8.05	288.95	
-14.75	288.94	
-21.46	288.94	
-28.16	288.94	
-34.87	288.95	
-41.57	288.94	
-44.93	288.92	
-46.27	288.92	
-47.61	288.94	
-48.28	288.94	
-48.95	288.98	
-49.42	289.42	
-49.69	292.88	top of wall

Table A133. Model cross-sectional water surface profile at step 1, station 0.21 m looking downstream for test #27.

<b>Model Water Surface Profile</b>		
Cross-Sectional Profile, $X_m = 0.21$ m - Step 1; 1/6 PMF		
<b>station</b> <b><math>Y_m</math> (m)</b>	<b>elev</b> <b><math>Z_m</math>(m)</b>	<b>Comments</b>
2.28	13.31	top of wall - step 1
2.27	13.14	
2.26	13.13	
2.23	13.13	
2.19	13.13	
2.13	13.13	
2.07	13.13	
1.77	13.14	
1.46	13.14	
1.16	13.13	
0.85	13.13	
0.55	13.13	
0.24	13.13	
0.00	13.13	
-0.37	13.13	
-0.67	13.13	
-0.98	13.13	
-1.28	13.13	
-1.58	13.13	
-1.89	13.13	
-2.04	13.13	
-2.10	13.13	
-2.16	13.13	
-2.19	13.13	
-2.23	13.14	
-2.25	13.16	
-2.26	13.31	top of wall

Table A134. Prototype cross-sectional water surface profile at step 8, station 11 m for test #27.

<b>Prototype Water Surface Profile</b>		
Cross-Sectional Profile, $X_p = 11$ m - Step 8; 1/6 PMF		
<b>station</b> <b><math>Y_p</math> (m)</b>	<b>elev</b> <b><math>Z_p</math> (m)</b>	<b>Comments</b>
48.41	290.70	top of wall - step 8
48.28	287.05	
47.61	286.99	
46.94	286.87	
46.27	286.80	
45.60	286.78	
44.26	286.83	
42.25	286.82	
38.89	286.80	
32.19	286.82	
25.48	286.79	
18.78	286.79	
12.07	286.81	
5.36	286.83	
0.00	286.82	
-8.05	286.83	
-14.75	286.81	
-21.46	286.82	
-28.16	286.82	
-34.87	286.82	
-38.22	286.79	
-40.23	286.77	
-41.57	286.83	
-42.92	286.85	
-44.26	287.01	
-44.93	287.26	
-45.67	287.40	
-45.93	290.74	top of wall

Table A135. Model cross-sectional water surface profile at step 8, station 0.5 m for test #27.

<b>Model Water Surface Profile</b>		
Cross-Sectional Profile, $X_m = 0.5$ m - Step 8; 1/6 PMF		
<b>station</b>	<b>elev</b>	
<b><math>Y_m</math> (m)</b>	<b><math>Z_m</math> (m)</b>	<b>Comments</b>
2.20	13.21	top of wall - step 8
2.19	13.05	
2.16	13.04	
2.13	13.04	
2.10	13.04	
2.07	13.04	
2.01	13.04	
1.92	13.04	
1.77	13.04	
1.46	13.04	
1.16	13.04	
0.85	13.04	
0.55	13.04	
0.24	13.04	
0.00	13.04	
-0.37	13.04	
-0.67	13.04	
-0.98	13.04	
-1.28	13.04	
-1.58	13.04	
-1.74	13.04	
-1.83	13.04	
-1.89	13.04	
-1.95	13.04	
-2.01	13.05	
-2.04	13.06	
-2.08	13.06	
-2.09	13.22	top of wall

Table A136. Prototype cross-sectional water surface profile at step 12, station 14.8 m for test #27.

<b>Prototype Water Surface Profile</b>		
Cross-Sectional Profile, $X_p = 14.8$ m - Step 12; 1/6 PMF		
<b>station</b>	<b>elev</b>	
<b><math>Y_p</math> (m)</b>	<b><math>Z_p</math> (m)</b>	<b>Comments</b>
47.48	289.45	top of wall - step 12
47.27	285.84	
46.60	285.71	
45.60	285.63	
44.93	285.58	
44.26	285.58	
42.92	285.59	
41.57	285.58	
38.89	285.55	
32.19	285.56	
25.48	285.54	
18.78	285.57	
12.07	285.59	
5.36	285.59	
0.00	285.59	
-8.05	285.59	
-14.75	285.61	
-21.46	285.56	
-28.16	285.56	
-34.87	285.56	
-38.22	285.58	
-40.23	285.63	
-41.57	285.73	
-42.25	285.92	
-42.92	286.10	
-43.65	286.37	
-43.79	289.48	top of wall

Table A137. Model cross-sectional water surface profile at step 12, station 0.67 m for test #27.

<b>Model Water Surface Profile</b>		
Cross-Sectional Profile, $X_m = 0.67$ m - Step 12; 1/6 PMF		
<b>station</b>	<b>elev</b>	
<b><math>Y_m</math> (m)</b>	<b><math>Z_m</math> (m)</b>	<b>Comments</b>
2.16	13.16	top of wall - step 12
2.15	12.99	
2.12	12.99	
2.07	12.98	
2.04	12.98	
2.01	12.98	
1.95	12.98	
1.89	12.98	
1.77	12.98	
1.46	12.98	
1.16	12.98	
0.85	12.98	
0.55	12.98	
0.24	12.98	
0.00	12.98	
-0.37	12.98	
-0.67	12.98	
-0.98	12.98	
-1.28	12.98	
-1.58	12.98	
-1.74	12.98	
-1.83	12.98	
-1.89	12.99	
-1.92	13.00	
-1.95	13.00	
-1.98	13.02	
-1.99	13.16	top of wall

Table A138. Prototype cross-sectional water surface profile at step 18, station 20.3 m for test #27.

<b>Prototype Water Surface Profile</b>		
Cross-Sectional Profile, $X_p = 20.3$ m - Step 18; 1/6 PMF		
<b>station</b>	<b>elev</b>	
<b><math>Y_p</math> (m)</b>	<b><math>Z_p</math> (m)</b>	<b>Comments</b>
46.07	287.60	top of wall - step 18
45.87	284.03	
45.26	283.92	
44.59	283.88	
43.59	283.80	
42.25	283.72	
40.23	283.75	
38.89	283.73	
32.19	283.75	
25.48	283.75	
18.78	283.77	
12.07	283.78	
5.36	283.78	
0.00	283.77	
-8.05	283.80	
-14.75	283.77	
-21.46	283.76	
-28.16	283.73	
-31.52	283.71	
-34.87	283.80	
-36.21	283.82	
-37.55	283.89	
-38.89	284.20	
-39.56	284.20	
-40.43	284.42	
-40.64	287.62	top of wall

Table A139. Model cross-sectional water surface profile at step 18, station 0.92 m for test #27.

<b>Model Water Surface Profile</b>		
Cross-Sectional Profile, $X_m = 0.92$ m - Step 18; 1/6 PMF		
<b>station</b> <b><math>Y_m</math> (m)</b>	<b>elev</b> <b><math>Z_m</math>(m)</b>	<b>Comments</b>
2.09	13.07	top of wall - step 18
2.08	12.91	
2.06	12.91	
2.03	12.90	
1.98	12.90	
1.92	12.90	
1.83	12.90	
1.77	12.90	
1.46	12.90	
1.16	12.90	
0.85	12.90	
0.55	12.90	
0.24	12.90	
0.00	12.90	
-0.37	12.90	
-0.67	12.90	
-0.98	12.90	
-1.28	12.90	
-1.43	12.90	
-1.58	12.90	
-1.65	12.90	
-1.71	12.90	
-1.77	12.92	
-1.80	12.92	
-1.84	12.93	
-1.85	13.07	top of wall

Table A140. Prototype cross-sectional water surface profile at step 21, station 23.1 m for test #27.

<b>Prototype Water Surface Profile</b>		
Cross-Sectional Profile, $X_p = 23.1$ m - Step 21; 1/6 PMF - Low TW		
<b>station</b>	<b>elev</b>	
<b><math>Y_p</math> (m)</b>	<b><math>Z_p</math> (m)</b>	<b>Comments</b>
45.33	287.16	top of wall - step 21
45.13	283.08	
44.59	283.00	
43.59	282.94	
42.25	282.86	
40.90	282.82	
38.89	282.82	
32.19	282.82	
25.48	282.84	
18.78	282.82	
12.07	282.84	
5.36	282.85	
0.00	282.83	
-8.05	282.84	
-14.75	282.81	
-21.46	282.82	
-28.16	282.82	
-31.52	282.84	
-34.87	282.93	
-36.21	283.02	
-36.88	283.25	
-37.55	283.33	
-38.22	283.37	
-38.89	283.52	
-39.09	287.23	top of wall

Table A141. Model cross-sectional water surface profile at step 21, station 1.05 m for test #27.

<b>Model Water Surface Profile</b>		
Cross-Sectional Profile, $X_m = 1.05$ m - Step 21; 1/6 PMF - Low TW		
<b>station</b>	<b>elev</b>	
<b><math>Y_m</math> (m)</b>	<b><math>Z_m</math> (m)</b>	<b>Comments</b>
2.06	13.05	top of wall - step 21
2.05	12.87	
2.03	12.86	
1.98	12.86	
1.92	12.86	
1.86	12.86	
1.77	12.86	
1.46	12.86	
1.16	12.86	
0.85	12.86	
0.55	12.86	
0.24	12.86	
0.00	12.86	
-0.37	12.86	
-0.67	12.85	
-0.98	12.86	
-1.28	12.86	
-1.43	12.86	
-1.58	12.86	
-1.65	12.86	
-1.68	12.87	
-1.71	12.88	
-1.74	12.88	
-1.77	12.89	
-1.78	13.06	top of wall

Table A142. Prototype cross-sectional water surface profile at step 25, station 26.8 m for test #27.

<b>Prototype Water Surface Profile</b>		
Cross-Sectional Profile, $X_p = 26.8$ m - Step 25; 1/6 PMF - Low TW		
<b>station</b>	<b>elev</b>	
<b><math>Y_p</math> (m)</b>	<b><math>Z_p</math> (m)</b>	<b>Comments</b>
45.33	287.16	top of wall - step 25
45.13	283.08	
44.59	283.00	
43.59	282.94	
42.25	282.86	
40.90	282.82	
38.89	282.82	
32.19	282.82	
25.48	282.84	
18.78	282.82	
12.07	282.84	
5.36	282.85	
0.00	282.83	
-8.05	282.84	
-14.75	282.81	
-21.46	282.82	
-28.16	282.82	
-31.52	282.84	
-34.87	282.93	
-36.21	283.02	
-36.88	283.25	
-37.55	283.33	
-38.22	283.37	
-38.89	283.52	
-39.09	287.23	top of wall

Table A143. Model cross-sectional water surface profile at step 25, station 1.22 m for test #27.

<b>Model Water Surface Profile</b>		
Cross-Sectional Profile, $X_m = 1.22$ m - Step 25; 1/6 PMF - Low TW		
<b>station</b>	<b>elev</b>	
<b><math>Y_m</math> (m)</b>	<b><math>Z_m</math> (m)</b>	<b>Comments</b>
2.06	13.05	top of wall - step 25
2.05	12.87	
2.03	12.86	
1.98	12.86	
1.92	12.86	
1.86	12.86	
1.77	12.86	
1.46	12.86	
1.16	12.86	
0.85	12.86	
0.55	12.86	
0.24	12.86	
0.00	12.86	
-0.37	12.86	
-0.67	12.85	
-0.98	12.86	
-1.28	12.86	
-1.43	12.86	
-1.58	12.86	
-1.65	12.86	
-1.68	12.87	
-1.71	12.88	
-1.74	12.88	
-1.77	12.89	
-1.78	13.06	top of wall

Table A144. Prototype centerline water surface profile for test #32.

<b>Prototype Water Surface Profile</b>		
Centerline Profile, $Y_p = 0.0$ m; 1/6 PMF		
<b>station</b>	<b>elev</b>	
<b><math>X_p</math> (m)</b>	<b><math>Z_p</math> (m)</b>	<b>Comments</b>
0.00	290.66	Centerline profile with respect
0.87	290.37	to stilling basin
4.22	289.12	
7.58	287.97	
10.93	286.86	
14.28	285.71	
17.64	284.59	
20.99	283.49	
21.66	283.76	TW edge
24.34	283.73	TW
27.69	283.81	TW
31.05	283.80	TW - stilling basin
34.40	283.82	TW - stilling basin
37.75	283.90	edge of stilling basin
41.11	283.70	
47.81	283.55	
61.22	283.55	
74.63	283.56	
88.04	283.55	
101.46	283.55	
141.69	283.55	

Table A145. Model centerline water surface profile for test #32.

<b>Model Water Surface Profile</b>		
Run #: Run 32		Centerline profile, $Y_m = 0.0$ m; 1/6 PMF
Date: 3 Feb 2005		
<b>station</b>	<b>elev</b>	<b>Comments</b>
<b><math>X_m</math> (m)</b>	<b><math>Z_m</math> (m)</b>	
0.00	13.21	Centerline profile with respect
0.04	13.20	to stilling basin
0.19	13.14	
0.34	13.09	
0.50	13.04	
0.65	12.99	
0.80	12.94	
0.95	12.89	
0.98	12.90	TW edge
1.11	12.90	TW
1.26	12.90	TW
1.41	12.90	TW - stilling basin
1.56	12.90	TW - stilling basin
1.72	12.90	edge of stilling basin
1.87	12.90	
2.17	12.89	
2.78	12.89	
3.39	12.89	
4.00	12.89	
4.61	12.89	
6.44	12.89	

Table A146. Prototype centerline water surface profile along right wall looking downstream for test #32.

<b>Prototype Water Surface Profile</b>			
WS along Rt. Wall looking d.s. 1/6 PMF; $\phi = 70$ deg rt; 0 deg lt			
<b>station <math>X_p</math> (m)</b>	<b>station <math>Y_p</math> (m)</b>	<b>elev <math>Z_p</math>(m)</b>	<b>Comments</b>
-12.54	-49.62	290.86	
-9.19	-49.62	290.83	
-7.85	-49.62	290.83	
-6.50	-49.62	290.84	
-5.83	-49.62	290.84	
-2.48	-49.62	290.82	
-0.80	-49.62	290.78	
0.87	-49.62	290.33	
1.81	-49.62	289.94	edge of smooth water
3.08	-49.62	290.34	
3.72	-49.62	290.62	pt of conv wall jnt
4.90	-46.27	290.37	
6.84	-40.97	289.92	
8.99	-34.87	289.36	
11.33	-28.16	288.76	
13.95	-21.46	288.00	
16.40	-14.75	287.26	
18.81	-8.05	286.45	
21.19	-1.34	285.80	
23.67	5.36	285.04	
26.15	12.07	284.32	
28.63	18.78	283.67	
29.10	19.98	283.58	wall jnt @ basin
29.81	20.12	283.41	basin
34.53	20.32	283.46	basin
38.59	20.32	283.47	basin end

Table A147. Model centerline water surface profile along right wall looking downstream for test #32.

Model Water Surface Profile			
WS along Rt. Wall looking d.s. 1/6 PMF; $\phi = 70$ deg rt; 0 deg lt			
station $X_m$ (m)	station $Y_m$ (m)	elev $Z_m$ (m)	Comments
-0.57	-2.26	13.22	
-0.42	-2.26	13.22	
-0.36	-2.26	13.22	
-0.30	-2.26	13.22	
-0.27	-2.26	13.22	
-0.11	-2.26	13.22	
-0.04	-2.26	13.22	
0.04	-2.26	13.20	
0.08	-2.26	13.18	edge of smooth water
0.14	-2.26	13.20	
0.17	-2.26	13.21	pt of conv wall jnt
0.22	-2.10	13.20	
0.31	-1.86	13.18	
0.41	-1.58	13.15	
0.52	-1.28	13.13	
0.63	-0.98	13.09	
0.75	-0.67	13.06	
0.85	-0.37	13.02	
0.96	-0.06	12.99	
1.08	0.24	12.96	
1.19	0.55	12.92	
1.30	0.85	12.89	
1.32	0.91	12.89	wall jnt @ basin
1.35	0.91	12.88	basin
1.57	0.92	12.88	basin
1.75	0.92	12.88	basin end

Table A148. Prototype centerline water surface profile along left wall looking downstream for test #32.

<b>Prototype Water Surface Profile</b>			
WS along Lt. Wall looking d.s. 1/6 PMF; $\phi = 70$ deg rt; 0 deg lt			
<b>station X<sub>p</sub> (m)</b>	<b>station Y<sub>p</sub> (m)</b>	<b>elev Z<sub>p</sub>(m)</b>	<b>Comments</b>
-12.54	49.62	290.84	
-9.19	49.62	290.82	
-7.85	49.62	290.82	
-6.50	49.62	290.83	
-5.83	49.62	290.82	
-2.48	49.62	290.82	
-0.80	49.62	290.78	
0.00	49.62	290.66	
0.87	49.62	290.35	
2.21	49.62	289.80	
3.55	49.62	289.31	
4.90	49.62	288.88	
6.24	49.62	288.44	
7.58	49.62	288.00	
10.93	49.62	286.92	
14.28	49.62	285.75	
17.64	49.62	284.63	
20.99	49.62	283.51	
21.59	49.62	283.70	TW
22.33	49.62	283.67	TW
24.34	49.62	283.71	TW
27.69	49.62	283.97	TW
29.10	49.62	283.99	TW, wall joint @ basin
31.05	49.62	284.04	basin
34.40	49.62	284.22	basin
38.59	49.62	284.00	basin end

Table A149. Model centerline water surface profile along left wall looking downstream for test #32.

<b>Model Water Surface Profile</b>			
WS along Lt. Wall looking d.s. 1/6 PMF; $\phi = 70$ deg rt; 0 deg lt			
<b>station</b> <b>X<sub>m</sub> (m)</b>	<b>station</b> <b>Y<sub>m</sub> (m)</b>	<b>elev</b> <b>Z<sub>m</sub> (m)</b>	<b>Comments</b>
-0.57	2.26	13.22	
-0.42	2.26	13.22	
-0.36	2.26	13.22	
-0.30	2.26	13.22	
-0.27	2.26	13.22	
-0.11	2.26	13.22	
-0.04	2.26	13.22	
0.00	2.26	13.21	
0.04	2.26	13.20	
0.10	2.26	13.17	
0.16	2.26	13.15	
0.22	2.26	13.13	
0.28	2.26	13.11	
0.34	2.26	13.09	
0.50	2.26	13.04	
0.65	2.26	12.99	
0.80	2.26	12.94	
0.95	2.26	12.89	
0.98	2.26	12.90	TW
1.01	2.26	12.89	TW
1.11	2.26	12.90	TW
1.26	2.26	12.91	TW
1.32	2.26	12.91	TW, wall joint @ basin
1.41	2.26	12.91	basin
1.56	2.26	12.92	basin
1.75	2.26	12.91	basin end

Table A150. Prototype cross-sectional water surface profile at step 1, station 4.6 m for test #32.

<b>Prototype Water Surface Profile</b>		
Cross-Sectional Profile, $X_p = 4.6$ m - Step 1; 1/6 PMF		
<b>station</b>	<b>elev</b>	
<b><math>Y_p</math> (m)</b>	<b><math>Z_p</math> (m)</b>	<b>Comments</b>
-47.61	295.38	top of wall - step 1
-47.61	290.49	
-45.60	290.19	
-43.92	289.86	
-42.58	289.88	
-40.23	289.57	
-35.41	289.10	end of rough water
-34.53	288.98	smooth
-31.52	288.96	
-28.16	288.95	
-24.81	288.96	
-21.46	288.94	
-14.75	288.94	
-8.05	288.96	
-1.34	288.93	
5.36	288.94	
12.07	288.94	
18.78	288.94	
25.48	288.96	
32.19	288.98	
38.89	288.99	
45.60	288.93	
48.28	288.92	
49.62	288.94	
50.22	288.96	
50.43	292.89	top of wall

Table A151. Model cross-sectional water surface profile at step 1, station 0.21 m for test #32.

<b>Model Water Surface Profile</b>		
Cross-Sectional Profile, $X_m = 0.21$ m - Step 1; 1/6 PMF		
<b>station</b> $Y_m$ (m)	<b>elev</b> $Z_m$ (m)	<b>Comments</b>
-2.16	13.43	top of wall - step 1
-2.16	13.20	
-2.07	13.19	
-2.00	13.18	
-1.94	13.18	
-1.83	13.16	
-1.61	13.14	end of rough water
-1.57	13.14	smooth
-1.43	13.13	
-1.28	13.13	
-1.13	13.13	
-0.98	13.13	
-0.67	13.13	
-0.37	13.13	
-0.06	13.13	
0.24	13.13	
0.55	13.13	
0.85	13.13	
1.16	13.13	
1.46	13.14	
1.77	13.14	
2.07	13.13	
2.19	13.13	
2.26	13.13	
2.28	13.13	
2.29	13.31	top of wall

Table A152. Prototype cross-sectional water surface profile at step 8, station 11 m for test #32.

<b>Prototype Water Surface Profile</b>		
Cross-Sectional Profile, $X_p = 11$ m - Step 8; 1/6 PMF		
<b>station</b> <b><math>Y_p</math> (m)</b>	<b>elev</b> <b><math>Z_p</math>(m)</b>	<b>Comments</b>
-30.18	293.21	top of wall - step 8
-29.84	288.97	
-28.16	288.70	
-25.48	288.27	
-23.47	288.13	
-20.79	287.83	
-17.43	287.44	
-15.36	287.15	end of rough water
-14.42	286.91	smooth water
-12.07	286.83	
-8.05	286.79	
-4.69	286.80	
-1.34	286.80	
5.36	286.78	
12.07	286.78	
18.78	286.81	
25.48	286.77	
32.19	286.80	
38.89	286.83	
45.60	286.76	
47.61	286.79	
48.95	286.77	
50.09	286.75	
50.43	290.74	top of wall

Table A153. Model cross-sectional water surface profile at step 8, station 0.5 m for test #32.

<b>Model Water Surface Profile</b>		
Cross-Sectional Profile, $X_m = 0.5$ m - Step 8; 1/6 PMF		
<b>station</b> <b><math>Y_m</math> (m)</b>	<b>elev</b> <b><math>Z_m</math>(m)</b>	<b>Comments</b>
-1.37	13.33	top of wall - step 8
-1.36	13.13	
-1.28	13.12	
-1.16	13.10	
-1.07	13.10	
-0.94	13.08	
-0.79	13.07	
-0.70	13.05	end of rough water
-0.66	13.04	smooth water
-0.55	13.04	
-0.37	13.04	
-0.21	13.04	
-0.06	13.04	
0.24	13.04	
0.55	13.04	
0.85	13.04	
1.16	13.04	
1.46	13.04	
1.77	13.04	
2.07	13.03	
2.16	13.04	
2.23	13.03	
2.28	13.03	
2.29	13.22	top of wall

Table A154. Prototype cross-sectional water surface profile at step 12, station 14.8 m for test #32.

<b>Prototype Water Surface Profile</b>		
Cross-Sectional Profile, $X_p = 14.8$ m - Step 12; 1/6 PMF		
<b>station</b> <b><math>Y_p</math> (m)</b>	<b>elev</b> <b><math>Z_p</math>(m)</b>	<b>Comments</b>
-20.25	293.09	top of wall - step 12
-19.78	287.84	
-17.43	287.52	
-15.42	287.30	
-12.74	287.04	
-8.05	286.50	
-4.02	286.00	end of rough water
-2.68	285.63	smooth water
-1.34	285.61	
2.01	285.55	
5.36	285.55	
12.07	285.56	
18.78	285.59	
25.48	285.56	
32.19	285.56	
38.89	285.55	
45.60	285.53	
48.28	285.55	
50.16	285.54	
50.49	289.50	top of wall

Table A155. Model cross-sectional water surface profile at step 12, station 0.67 m for test #32.

<b>Model Water Surface Profile</b>		
Cross-Sectional Profile, $X_m = 0.67$ m - Step 12; 1/6 PMF		
<b>station</b> <b><math>Y_m</math> (m)</b>	<b>elev</b> <b><math>Z_m</math>(m)</b>	<b>Comments</b>
-0.92	13.32	top of wall - step 12
-0.90	13.08	
-0.79	13.07	
-0.70	13.06	
-0.58	13.05	
-0.37	13.02	
-0.18	13.00	end of rough water
-0.12	12.98	smooth water
-0.06	12.98	
0.09	12.98	
0.24	12.98	
0.55	12.98	
0.85	12.98	
1.16	12.98	
1.46	12.98	
1.77	12.98	
2.07	12.98	
2.19	12.98	
2.28	12.98	
2.30	13.16	top of wall

Table A156. Prototype cross-sectional water surface profile at step 18, station 20.3 m for test #32.

<b>Prototype Water Surface Profile</b>		
Cross-Sectional Profile, $X_p = 20.3$ m - Step 18; 1/6 PMF		
<b>station</b>	<b>elev</b>	
<b><math>Y_p</math> (m)</b>	<b><math>Z_p</math> (m)</b>	<b>Comments</b>
-5.03	291.26	top of wall - step 18
-4.36	286.12	
-2.01	285.83	
1.34	285.56	
5.36	285.16	
9.05	284.63	
12.07	284.28	end of rough water
14.08	283.82	smooth
16.76	285.29	
18.78	285.22	
22.13	285.02	
25.48	283.82	
32.19	283.75	
38.89	283.75	
45.60	283.65	
48.95	283.70	
50.29	283.69	
50.43	287.62	top of wall

Table A157. Model cross-sectional water surface profile at step 18, station 0.92 m for test #32.

<b>Model Water Surface Profile</b>		
Cross-Sectional Profile, $X_m = 0.92$ m - Step 18; 1/6 PMF		
<b>station</b> $Y_m$ (m)	<b>elev</b> $Z_m$ (m)	<b>Comments</b>
-0.23	13.24	top of wall - step 18
-0.20	13.01	
-0.09	12.99	
0.06	12.98	
0.24	12.96	
0.41	12.94	
0.55	12.92	end of rough water
0.64	12.90	smooth
0.76	12.97	
0.85	12.96	
1.01	12.96	
1.16	12.90	
1.46	12.90	
1.77	12.90	
2.07	12.89	
2.23	12.90	
2.29	12.90	
2.29	13.07	top of wall

Table A158. Prototype cross-sectional water surface profile at step 21, station 23.1 m for test #32.

<b>Prototype Water Surface Profile</b>		
Cross-Sectional Profile, $X_p = 23.1$ m - Step 21; 1/6 PMF - Low TW		
<b>station</b> $Y_p$ (m)	<b>elev</b> $Z_p$ (m)	<b>Comments</b>
2.48	290.33	top of wall - step 21
3.35	285.32	
5.36	285.10	
8.72	284.76	
12.07	284.43	
15.42	284.07	
18.78	283.63	edge of rough water
20.79	283.08	smooth water
22.80	282.90	
25.48	282.81	
28.83	282.74	
32.19	282.78	
38.89	282.77	
45.60	282.80	
48.95	282.78	
50.22	282.81	
50.56	287.11	top of wall - step 21

Table A159. Model cross-sectional water surface profile at step 21, station 1.05 m for test #32.

<b>Model Water Surface Profile</b>		
Cross-Sectional Profile, $X_m = 1.05$ m - Step 21; 1/6 PMF - Low TW		
<b>station</b>	<b>elev</b>	
<b><math>Y_m</math> (m)</b>	<b><math>Z_m</math> (m)</b>	<b>Comments</b>
0.11	13.20	top of wall - step 21
0.15	12.97	
0.24	12.96	
0.40	12.94	
0.55	12.93	
0.70	12.91	
0.85	12.89	edge of rough water
0.94	12.87	smooth water
1.04	12.86	
1.16	12.85	
1.31	12.85	
1.46	12.85	
1.77	12.85	
2.07	12.85	
2.23	12.85	
2.28	12.85	
2.30	13.05	top of wall - step 21

Table A160. Prototype cross-sectional water surface profile at step 25, station 23.1 m for test #32.

<b>Prototype Water Surface Profile</b>		
Cross-Sectional Profile, $X_p = 26.8$ m - Step 25; 1/6 PMF - Low TW		
<b>station</b>	<b>elev</b>	
<b><math>Y_p</math> (m)</b>	<b><math>Z_p</math> (m)</b>	<b>Comments</b>
12.74	289.07	top of wall - step 25
13.55	284.14	
15.42	284.00	
18.78	283.69	
22.13	283.22	
25.48	282.88	
28.83	282.24	edge of rough water
32.19	281.68	smooth water
35.54	281.56	
38.89	281.53	
42.25	281.54	
45.60	281.57	
50.09	281.57	
50.49	287.11	top of wall - step 25

Table A161. Prototype cross-sectional water surface profile at step 25, station 1.22 m for test #32.

<b>Model Water Surface Profile</b>		
Cross-Sectional Profile, $X_m = 1.22$ m - Step 25; 1/6 PMF - Low TW		
<b>station</b> <b><math>Y_m</math> (m)</b>	<b>elev</b> <b><math>Z_m</math> (m)</b>	<b>Comments</b>
0.58	13.14	top of wall - step 25
0.62	12.92	
0.70	12.91	
0.85	12.89	
1.01	12.87	
1.16	12.86	
1.31	12.83	edge of rough water
1.46	12.80	smooth water
1.62	12.80	
1.77	12.80	
1.92	12.80	
2.07	12.80	
2.28	12.80	
2.30	13.05	top of wall - step 25

Table A162. Prototype centerline water surface profile for test #33.

<b>Prototype Water Surface Profile</b>		
Centerline Profile, $Y_p = 0.0$ m; 1/3 PMF		
<b>station</b> <b><math>X_p</math> (m)</b>	<b>elev</b> <b><math>Z_p</math> (m)</b>	<b>Comments</b>
0.00	290.98	
0.87	290.61	
4.22	289.35	
7.58	288.14	
10.93	286.97	
14.28	285.83	
17.17	284.87	edge of TW
18.31	285.24	TW
20.99	285.16	TW
24.34	285.22	TW
27.69	285.24	TW
31.05	285.24	TW - u.s. edge of stilling basin
34.40	285.28	TW - stilling basin
37.75	285.30	TW - d.s. edge of stilling basin
41.11	285.20	
47.81	285.06	
61.22	284.98	
74.63	284.98	
88.04	284.98	
101.46	285.00	
141.69	284.98	

Table A163. Model centerline water surface profile for test #33.

<b>Model Water Surface Profile</b>		
Run #: Run 32		Centerline profile, $Y_m = 0.0$ m; 1/3 PMF
Date: 4 Feb 2005		
station	elev	Comments
$X_m$ (m)	$Z_m$ (m)	
0.00	13.23	
0.04	13.21	
0.19	13.15	
0.34	13.10	
0.50	13.04	
0.65	12.99	
0.78	12.95	edge of TW
0.83	12.97	TW
0.95	12.96	TW
1.11	12.96	TW
1.26	12.97	TW
1.41	12.97	TW - u.s. edge of stilling basin
1.56	12.97	TW - stilling basin
1.72	12.97	TW - d.s. edge of stilling basin
1.87	12.96	
2.17	12.96	
2.78	12.95	
3.39	12.95	
4.00	12.95	
4.61	12.95	
6.44	12.95	

Table A164. Prototype water surface profile along the right wall looking downstream for test #33.

<b>Prototype Water Surface Profile</b>			
WS along Rt. Wall looking d.s. 1/3 PMF; $\phi = 70$ deg rt; 0 deg lt			
<b>station <math>X_p</math> (m)</b>	<b>station <math>Y_p</math> (m)</b>	<b>elev <math>Z_p</math> (m)</b>	<b>Comments</b>
-12.54	-49.62	291.27	Rt wall looking d.s.
-9.19	-49.62	291.22	
-7.85	-49.62	291.16	
-6.50	-49.62	291.22	
-5.83	-49.62	291.22	
-2.48	-49.62	291.20	
-0.80	-49.62	291.14	
0.00	-49.62	291.06	
0.67	-49.62	290.97	edge of rough water
4.22	-49.62	291.11	elevated water
2.62	-49.62	291.10	
3.76	-49.62	291.21	pt of conv wall - joint
4.90	-46.60	291.15	
6.84	-40.97	290.86	
8.99	-34.87	290.41	
11.33	-28.16	289.84	
13.95	-21.46	289.18	
16.40	-14.75	288.51	
18.81	-8.05	287.80	
21.19	-1.34	287.03	
23.67	5.36	286.49	
26.15	12.07	285.78	
28.63	18.78	285.26	
29.10	19.98	285.14	wall - joint @ basin
29.81	20.12	284.87	stilling basin
34.53	20.32	284.84	stilling basin
38.59	20.32	284.89	stilling basin end

Table A165. Model water surface profile along the right wall looking downstream for test #33.

<b>Model Water Surface Profile</b>			
WS along Rt. Wall looking d.s. 1/3 PMF; $\phi = 70$ deg rt; 0 deg lt			
<b>station</b> <b>X<sub>m</sub> (m)</b>	<b>station</b> <b>Y<sub>m</sub> (m)</b>	<b>elev</b> <b>Z<sub>m</sub>(m)</b>	<b>Comments</b>
-0.57	-2.26	13.24	Rt wall looking d.s.
-0.42	-2.26	13.24	
-0.36	-2.26	13.23	
-0.30	-2.26	13.24	
-0.27	-2.26	13.24	
-0.11	-2.26	13.24	
-0.04	-2.26	13.23	
0.00	-2.26	13.23	
0.03	-2.26	13.23	edge of rough water
0.19	-2.26	13.23	elevated water
0.12	-2.26	13.23	
0.17	-2.26	13.24	pt of conv wall - joint
0.22	-2.12	13.23	
0.31	-1.86	13.22	
0.41	-1.58	13.20	
0.52	-1.28	13.17	
0.63	-0.98	13.14	
0.75	-0.67	13.11	
0.85	-0.37	13.08	
0.96	-0.06	13.05	
1.08	0.24	13.02	
1.19	0.55	12.99	
1.30	0.85	12.97	
1.32	0.91	12.96	wall - joint @ basin
1.35	0.91	12.95	stilling basin
1.57	0.92	12.95	stilling basin
1.75	0.92	12.95	stilling basin end

Table A166. Prototype water surface profile along the left wall looking downstream for test #33.

<b>Prototype Water Surface Profile</b>			
WS along Lt. Wall looking d.s. 1/3 PMF; $\phi = 70$ deg rt; 0 deg lt			
<b>station</b> <b>X<sub>p</sub> (m)</b>	<b>station</b> <b>Y<sub>p</sub> (m)</b>	<b>elev</b> <b>Z<sub>p</sub>(m)</b>	<b>Comments</b>
-12.54	49.62	291.26	Lt wall looking d.s.
-9.19	49.62	291.17	
-7.85	49.62	291.15	
-6.50	49.62	291.18	
-5.83	49.62	291.19	
-2.48	49.62	291.18	
-0.80	49.62	291.10	
0.00	49.62	290.96	
0.87	49.62	290.66	
2.21	49.62	290.07	
3.55	49.62	289.57	
4.90	49.62	289.07	
6.24	49.62	288.63	
7.58	49.62	288.15	
10.93	49.62	287.00	
14.28	49.62	285.87	
17.64	49.62	284.74	edge of TW
18.31	49.62	285.09	TW
20.99	49.62	284.96	TW
24.34	49.62	285.61	TW
27.69	49.62	285.79	TW
29.10	49.62	285.91	TW - wall joint - basin
31.05	49.62	286.25	stilling basin
34.40	49.62	286.33	stilling basin
38.59	49.62	286.26	stilling basin end

Table A167. Model water surface profile along the left wall looking downstream for test #33.

Model Water Surface Profile			
WS along Lt. Wall looking d.s. 1/3 PMF; $\phi = 70$ deg rt; 0 deg lt			
station	station	elev	Comments
$X_m$ (m)	$Y_m$ (m)	$Z_m$ (m)	
-0.57	2.26	13.24	Lt wall looking d.s.
-0.42	2.26	13.24	
-0.36	2.26	13.23	
-0.30	2.26	13.24	
-0.27	2.26	13.24	
-0.11	2.26	13.24	
-0.04	2.26	13.23	
0.00	2.26	13.23	
0.04	2.26	13.21	
0.10	2.26	13.19	
0.16	2.26	13.16	
0.22	2.26	13.14	
0.28	2.26	13.12	
0.34	2.26	13.10	
0.50	2.26	13.05	
0.65	2.26	12.99	
0.80	2.26	12.94	edge of TW
0.83	2.26	12.96	TW
0.95	2.26	12.95	TW
1.11	2.26	12.98	TW
1.26	2.26	12.99	TW
1.32	2.26	13.00	TW - wall joint - basin
1.41	2.26	13.01	stilling basin
1.56	2.26	13.01	stilling basin
1.75	2.26	13.01	stilling basin end

Table A168. Prototype cross-sectional water surface profile at step 1, station 4.6 m for test #33.

<b>Prototype Water Surface Profile</b>		
Cross-Sectional Profile, $X_p = 4.6$ m - Step 1; 1/3 PMF		
<b>station</b> <b><math>Y_p</math> (m)</b>	<b>elev</b> <b><math>Z_p</math>(m)</b>	<b>Comments</b>
-47.61	295.38	top of wall - step 1
-47.61	291.18	
-45.60	291.04	
-42.92	290.97	
-39.56	290.22	
-37.55	290.19	
-34.20	289.88	
-30.18	289.55	
-27.49	289.21	edge of rough water
-26.82	289.18	smooth water
-24.81	289.17	
-21.46	289.16	
-18.11	289.15	
-14.75	289.15	
-8.05	289.15	
-1.34	289.15	
5.36	289.14	
12.07	289.14	
18.78	289.14	
25.48	289.15	
32.19	289.17	
38.89	289.17	
45.60	289.13	
48.95	289.13	
50.16	289.15	
50.36	292.90	top of wall

Table A169. Model cross-sectional water surface profile at step 1, station 0.21 m for test #33.

<b>Model Water Surface Profile</b>		
Cross-Sectional Profile, $X_m = 0.21$ m - Step 1; 1/3 PMF		
<b>station</b> $Y_m$ (m)	<b>elev</b> $Z_m$ (m)	<b>Comments</b>
-2.16	13.43	top of wall - step 1
-2.16	13.24	
-2.07	13.23	
-1.95	13.23	
-1.80	13.19	
-1.71	13.19	
-1.55	13.18	
-1.37	13.16	
-1.25	13.15	edge of rough water
-1.22	13.14	smooth water
-1.13	13.14	
-0.98	13.14	
-0.82	13.14	
-0.67	13.14	
-0.37	13.14	
-0.06	13.14	
0.24	13.14	
0.55	13.14	
0.85	13.14	
1.16	13.14	
1.46	13.14	
1.77	13.14	
2.07	13.14	
2.23	13.14	
2.28	13.14	
2.29	13.31	top of wall

Table A170. Prototype cross-sectional water surface profile at step 8, station 11 m for test #33.

<b>Prototype Water Surface Profile</b>		
Cross-Sectional Profile, $X_p = 11$ m - Step 8; 1/3 PMF		
<b>station</b> $Y_p$ (m)	<b>elev</b> $Z_p$ (m)	<b>Comments</b>
-30.18	293.20	top of wall - step 8
-30.18	290.06	
-28.16	289.82	
-24.81	289.38	
-21.46	289.00	
-18.11	288.53	
-14.75	288.15	
-11.40	287.75	
-8.72	287.39	edge of rough water
-7.38	286.95	smooth water
-5.36	286.93	
-3.35	286.93	
-1.34	286.93	
2.01	286.92	
5.36	286.93	
12.07	286.91	
18.78	286.94	
25.48	286.94	
32.19	286.93	
38.89	286.91	
45.60	286.91	
48.28	286.94	
50.16	286.93	
50.36	290.74	top of wall

Table A171. Model cross-sectional water surface profile at step 8, station 0.5 m for test #33.

<b>Model Water Surface Profile</b>		
Cross-Sectional Profile, $X_m = 0.5$ m - Step 8; 1/3 PMF		
<b>station</b>	<b>elev</b>	
<b><math>Y_m</math> (m)</b>	<b><math>Z_m</math> (m)</b>	<b>Comments</b>
-1.37	13.33	top of wall - step 8
-1.37	13.18	
-1.28	13.17	
-1.13	13.15	
-0.98	13.14	
-0.82	13.11	
-0.67	13.10	
-0.52	13.08	
-0.40	13.06	edge of rough water
-0.34	13.04	smooth water
-0.24	13.04	
-0.15	13.04	
-0.06	13.04	
0.09	13.04	
0.24	13.04	
0.55	13.04	
0.85	13.04	
1.16	13.04	
1.46	13.04	
1.77	13.04	
2.07	13.04	
2.19	13.04	
2.28	13.04	
2.29	13.22	top of wall

Table A172. Prototype cross-sectional water surface profile at step 12, station 14.8 m for test #33.

<b>Prototype Water Surface Profile</b>		
Cross-Sectional Profile, $X_p = 14.8$ m - Step 12; 1/3 PMF		
<b>station</b>	<b>elev</b>	
<b><math>Y_p</math> (m)</b>	<b><math>Z_p</math>(m)</b>	<b>Comments</b>
-20.25	293.10	top of wall - step 12
-20.25	289.03	
-18.11	288.83	
-14.75	288.48	
-11.40	288.04	
-8.05	287.68	
-4.69	287.20	
-1.34	286.77	
2.68	286.26	edge of rough water
4.02	285.78	smooth water
5.36	285.73	
7.38	285.71	
9.39	285.68	
12.07	285.67	
15.42	285.67	
18.78	285.65	
25.48	285.67	
32.19	285.69	
38.89	285.66	
45.60	285.67	
48.95	285.68	
50.16	285.67	
50.43	289.50	top of wall

Table A173. Model cross-sectional water surface profile at step 12, station 0.67 m for test #33.

<b>Model Water Surface Profile</b>		
Cross-Sectional Profile, $X_m = 0.67$ m - Step 12; 1/3 PMF		
<b>station</b>	<b>elev</b>	
<b><math>Y_m</math> (m)</b>	<b><math>Z_m</math> (m)</b>	<b>Comments</b>
-0.92	13.32	top of wall - step 12
-0.92	13.14	
-0.82	13.13	
-0.67	13.11	
-0.52	13.09	
-0.37	13.08	
-0.21	13.05	
-0.06	13.03	
0.12	13.01	edge of rough water
0.18	12.99	smooth water
0.24	12.99	
0.34	12.99	
0.43	12.99	
0.55	12.98	
0.70	12.99	
0.85	12.98	
1.16	12.98	
1.46	12.99	
1.77	12.98	
2.07	12.99	
2.23	12.99	
2.28	12.98	
2.29	13.16	top of wall

Table A174. Prototype cross-sectional water surface profile at step 18, station 20.3 m for test #33.

<b>Prototype Water Surface Profile</b>		
Cross-Sectional Profile, $X_p = 20.3$ m - Step 18; 1/3 PMF; Low TW		
<b>station</b>	<b>elev</b>	
<b><math>Y_p</math> (m)</b>	<b><math>Z_p</math> (m)</b>	<b>Comments</b>
-5.03	291.27	top of wall - step 18
-5.03	287.40	
-1.34	287.00	
2.01	286.69	
5.36	286.33	
8.72	285.91	
12.07	285.54	
15.42	284.94	
18.78	284.49	
20.79	284.30	edge of rough water
21.46	283.96	smooth water
23.47	283.88	
25.48	283.86	
28.83	283.83	
32.19	283.82	
38.89	283.82	
45.60	283.82	
48.95	283.83	
50.16	283.84	
50.43	287.64	top of wall

Table A175. Model cross-sectional water surface profile at step 18, station 0.92 m for test #33.

<b>Model Water Surface Profile</b>		
Cross-Sectional Profile, $X_m = 0.92$ m - Step 18; 1/3 PMF; Low TW		
<b>station</b>	<b>elev</b>	
<b><math>Y_m</math> (m)</b>	<b><math>Z_m</math> (m)</b>	<b>Comments</b>
-0.23	13.24	top of wall - step 18
-0.23	13.06	
-0.06	13.05	
0.09	13.03	
0.24	13.01	
0.40	13.00	
0.55	12.98	
0.70	12.95	
0.85	12.93	
0.94	12.92	edge of rough water
0.98	12.91	smooth water
1.07	12.90	
1.16	12.90	
1.31	12.90	
1.46	12.90	
1.77	12.90	
2.07	12.90	
2.23	12.90	
2.28	12.90	
2.29	13.07	top of wall

Table A176. Prototype cross-sectional water surface profile at step 21, station 23.1 m for test #33.

<b>Prototype Water Surface Profile</b>		
Cross-Sectional Profile, $X_p = 23.1$ m - Step 21; 1/3 PMF - Low TW		
<b>station</b>	<b>elev</b>	
$Y_p$ (m)	$Z_p$ (m)	<b>Comments</b>
2.62	290.33	top of wall - step 21
2.62	286.69	
5.36	286.38	
8.72	286.08	
12.07	285.69	
15.42	285.27	
18.78	284.82	
22.13	284.22	
25.48	283.73	edge of rough water
28.83	283.18	smooth water
32.19	282.96	
35.54	282.92	
38.89	282.90	
42.25	282.89	
45.60	282.91	
48.95	282.92	
50.16	282.85	
50.43	287.11	top of wall

Table A177. Model cross-sectional water surface profile at step 21, station 1.05 m for test #33.

<b>Model Water Surface Profile</b>		
Cross-Sectional Profile, $X_m = 1.05$ m - Step 21; 1/3 PMF - Low TW		
<b>station</b>	<b>elev</b>	
$Y_m$ (m)	$Z_m$ (m)	<b>Comments</b>
0.12	13.20	top of wall - step 21
0.12	13.03	
0.24	13.02	
0.40	13.00	
0.55	12.99	
0.70	12.97	
0.85	12.95	
1.01	12.92	
1.16	12.90	edge of rough water
1.31	12.87	smooth water
1.46	12.86	
1.62	12.86	
1.77	12.86	
1.92	12.86	
2.07	12.86	
2.23	12.86	
2.28	12.86	
2.29	13.05	top of wall

Table A178. Prototype cross-sectional water surface profile at step 25, station 26.8 m for test #33.

<b>Prototype Water Surface Profile</b>		
Cross-Sectional Profile, $X_p = 26.8$ m - Step 25; 1/3 PMF - Low TW		
station $Y_p$ (m)	elev $Z_p$ (m)	Comments
12.74	289.07	top of wall - step 25
12.74	285.53	
15.42	285.37	
18.78	284.87	
22.13	284.23	
25.48	283.90	
28.83	283.80	
32.19	282.96	edge of rough water
35.54	282.09	smooth water
38.89	281.82	
42.25	282.34	TW
45.60	282.43	TW
48.95	282.66	TW
50.16	282.58	TW
50.43	287.12	top of wall

Table A179. Prototype cross-sectional water surface profile at step 25, station 1.22 m for test #33.

<b>Model Water Surface Profile</b>		
Cross-Sectional Profile, $X_m = 1.22$ m - Step 25; 1/3 PMF - Low TW		
station $Y_m$ (m)	elev $Z_m$ (m)	Comments
0.58	13.14	top of wall - step 25
0.58	12.98	
0.70	12.97	
0.85	12.95	
1.01	12.92	
1.16	12.90	
1.31	12.90	
1.46	12.86	edge of rough water
1.62	12.82	smooth water
1.77	12.81	
1.92	12.83	TW
2.07	12.84	TW
2.23	12.85	TW
2.28	12.84	TW
2.29	13.05	top of wall

Table A180. Prototype centerline bed surface profile.

Prototype Bed Surface Profile		
Centerline Profile, $Y_p = 0.0$ m		
station $X_p$ (m)	elev $Z_p$ (m)	Comments
-116.48	282.96	
-113.12	282.96	
-106.42	282.94	
-99.71	282.93	
-93.01	282.91	
-86.30	282.90	
-79.60	282.93	
-76.24	282.78	edge of rock
-72.89	283.85	
-66.18	284.62	
-59.48	284.67	
-52.77	284.38	
-46.07	284.38	
-39.36	284.35	
-32.66	284.44	
-25.95	284.33	
-21.93	284.32	break in slope
-19.25	284.87	
-12.54	287.19	
-7.17	288.87	edge of rock
-6.97	289.07	edge of approach (wood)
-5.83	289.00	
-2.48	288.94	
-0.60	289.78	us edge of ogee
-0.47	289.93	
-0.34	290.01	
-0.13	290.06	
0.00	290.08	centerpoint of ogee
0.20	290.08	
0.54	290.03	
0.87	289.90	
1.54	289.68	
2.21	289.47	
2.88	289.26	
3.55	289.09	
3.76	289.00	ds edge of ogee
4.63	288.70	step 1
5.63	288.40	step 2
6.50	288.09	step 3
7.38	287.79	step 4
8.31	287.48	step 5
9.25	287.20	step 6
10.19	286.87	step 7
11.06	286.56	step 8
12.00	286.26	step 9
12.87	285.95	step 10
13.81	285.65	step 11
14.75	285.33	step 12
15.62	285.03	step 13
16.56	284.71	step 14
17.50	284.41	step 15
18.44	284.11	step 16
19.38	283.82	step 17
20.32	283.52	step 18
21.26	283.19	step 19
22.13	282.90	step 20
23.07	282.59	step 21
23.94	282.29	step 22
24.88	281.97	step 23
25.75	281.66	step 24
26.76	281.35	step 25
27.63	281.07	step 26
28.63	280.70	step 27
28.50	280.40	floor (us edge of basin)
31.05	280.40	basin
34.40	280.39	
37.95	280.42	basin floor ds edge
37.95	281.04	top of end sill (us)
38.56	281.04	top of end sill ds

Table A181. Model centerline bed surface profile.

Model Bed Surface Profile				
Run #: Pre-Test		Centerline bed surface profile		
Date: 13 Oct 2004		BM-0 rd. x=7.52 y=19.82 z=0.875		
Time	X (m)	Y (m)	Z (m)	Comments
9:44 a.m.	2.29	22.92	0.31	centerline profile
	2.44	22.92	0.31	
	2.74	22.92	0.31	
	3.05	22.92	0.31	
	3.35	22.92	0.31	
	3.66	22.92	0.31	
	3.96	22.92	0.31	
	4.11	22.92	0.30	Edge of rock
	4.27	22.92	0.35	
	4.57	22.92	0.38	
	4.88	22.92	0.39	
	5.18	22.92	0.37	
	5.49	22.92	0.37	
	5.79	22.92	0.37	
	6.10	22.92	0.37	
	6.40	22.92	0.37	
	6.58	22.92	0.37	Breaking Slope
	6.71	22.92	0.39	
	7.01	22.92	0.50	
	7.25	22.92	0.58	Edge of rock
	7.26	22.92	0.59	Edge of approach (wood)
	7.32	22.92	0.58	
	7.47	22.92	0.58	
	7.55	22.92	0.62	Upstream edge of ogee
	7.56	22.92	0.62	
	7.57	22.92	0.63	
	7.57	22.92	0.63	
	7.58	22.92	0.63	Centerpoint on ogee
	7.59	22.92	0.63	
	7.60	22.92	0.63	
	7.62	22.92	0.62	
	7.65	22.92	0.61	
	7.68	22.92	0.60	
	7.71	22.92	0.59	
	7.74	22.92	0.59	
	7.75	22.92	0.58	d.s. edge of ogee
	7.79	22.92	0.57	centerline profile D.S. of step 1
	7.84	22.92	0.55	D.S. of step 2
	7.88	22.92	0.54	step 3
	7.92	22.92	0.53	step 4
	7.96	22.92	0.51	step 5
	8.00	22.92	0.50	step 6
	8.04	22.92	0.49	step 7
	8.08	22.92	0.47	step 8
	8.13	22.92	0.46	step 9
	8.17	22.92	0.44	step 10
	8.21	22.92	0.43	step 11
	8.25	22.92	0.42	step 12
	8.29	22.92	0.40	step 13
	8.33	22.92	0.39	step 14
	8.38	22.92	0.37	step 15
	8.42	22.92	0.36	step 16
	8.46	22.92	0.35	step 17
	8.50	22.92	0.33	step 18
	8.55	22.92	0.32	step 19
	8.59	22.92	0.30	step 20
	8.63	22.92	0.29	step 21
	8.67	22.92	0.28	step 22
	8.71	22.92	0.26	step 23
	8.75	22.92	0.25	step 24
	8.80	22.92	0.23	step 25
	8.84	22.92	0.22	step 26
	8.88	22.92	0.21	step 27
	8.88	22.92	0.19	Floor (upstream edge of basin)
	8.99	22.92	0.19	Basin
	9.14	22.92	0.19	
	9.31	22.92	0.19	Basin Floor (D.S. edge)
	9.31	22.92	0.22	top of end sill (upstream edge)
	9.33	22.92	0.22	top of end sill (D.S. edge)

Table A182. Prototype bed surface profile along the right wall looking downstream.

Pre-Test Runs 1-4 Bed Surface Profile along right wall			
station $X_p$ m	station $Y_p$ m	Top of Wall elev $Z_p$ m	Bed elev $Z_p$ m
-9.72	-50.36	290.76	
-9.72	-50.36		289.02
-2.68	-50.33	293.15	
-2.68	-50.33		288.94
0.00	-50.26	293.16	
0.00	-50.26		290.08
3.69	-50.16	293.19	
3.69	-50.16		288.99
21.52	-28.06	287.28	
21.52	-28.06		282.89
29.37	-18.24	287.15	
29.37	-18.24		280.42
38.56	-15.15	287.16	
38.56	-15.15		281.03

Table A183. Model bed surface profile along the right wall looking downstream.

Pre-Test Runs 1-4 Model Bed Surface Profile along right wall			
station $X_m$ m	station $Y_m$ m	Top of Wall elev $Z_m$ m	Bed elev $Z_m$ m
-0.44	-2.29	13.22	
-0.44	-2.29		13.14
-0.12	-2.29	13.32	
-0.12	-2.29		13.13
0.00	-2.28	13.33	
0.00	-2.28		13.19
0.17	-2.28	13.33	
0.17	-2.28		13.14
0.98	-1.28	13.06	
0.98	-1.28		12.86
1.34	-0.83	13.05	
1.34	-0.83		12.75
1.75	-0.69	13.05	
1.75	-0.69		12.77

Table A184. Prototype bed surface profile along the left wall looking downstream.

Pre-Test Runs 1-4 Bed Surface Profile along left wall			
station $X_p$ m	station $Y_p$ m	Top of Wall elev $Z_p$ m	Bed elev $Z_p$ m
-9.72	50.19	290.77	
-9.72	50.19		288.97
-2.48	50.19	293.14	
-2.48	50.19		288.93
0.00	50.22	293.16	
0.00	50.22		290.08
3.69	50.22	293.18	
3.69	50.22		289.01
21.52	28.20	287.28	
21.52	28.20		282.92
29.30	18.31	287.15	
29.30	18.31		280.40
38.49	15.46	287.17	
38.49	15.46		281.04

Table A185. Model bed surface profile along the left wall looking downstream.

Pre-Test Runs 1-4 Model Bed Surface Profile along left wall			
station $X_m$ m	station $Y_m$ m	Top of Wall elev $Z_m$ m	Bed elev $Z_m$ m
-0.44	2.28	13.22	
-0.44	2.28		13.13
-0.11	2.28	13.32	
-0.11	2.28		13.13
0.00	2.28	13.33	
0.00	2.28		13.19
0.17	2.28	13.33	
0.17	2.28		13.14
0.98	1.28	13.06	
0.98	1.28		12.86
1.33	0.83	13.05	
1.33	0.83		12.75
1.75	0.70	13.05	
1.75	0.70		12.77

**APPENDIX B**

## Example Design

To reinforce the application of this design information, example designs are presented for both the empirical and theoretical approaches. In most cases, the design discharge is known. In this scenario, the expected probable maximum unit discharge is  $7.6 \text{ m}^3/(\text{s}\cdot\text{m})$  (81.8 cfs/ft) that results in an expected centerline water surface profile presented in Table B1. The expected tailwater elevation is 286.2 m (939 ft). The design engineer has chosen a stepped spillway chute slope of 3(H):1(V) and step height of 0.3 m (1 ft) step height. The bed profile of the stepped spillway chute is provided in Table B2. The spillway entrance is an ogee crested weir set at an elevation of 290.1 m (951.8 ft) and has a width of approximately 100 m (330 ft). The stilling basin elevation is set at an elevation of 280.4 m (919.9 ft). To fit the topography downstream, the spillway chute must converge  $25^\circ$ . With the given information, the design engineer is to find the training wall height necessary to contain the expected flood event.

Table B1. Centerline water surface profile.

station $X_p$ (m)	elev $Z_p$ (m)
-9.19	292.38
-5.83	292.26
-2.48	292.22
-1.81	292.20
-1.14	292.11
-0.47	292.02
0.20	291.86
0.87	291.68
1.54	291.33
2.21	291.07
2.88	290.70
3.55	290.43
4.22	290.08
4.90	289.83
6.24	289.30
7.58	288.77
8.92	288.27
10.26	287.78
11.60	287.29
12.94	286.85
13.61	286.59
14.28	286.33
15.62	286.70
16.97	286.61
18.31	286.65
19.65	286.69
24.34	286.80
27.69	287.26
31.05	287.72
34.40	287.80
41.11	287.57
47.81	287.26

Table B2. Stepped spillway chute bed surface profile.

station X <sub>p</sub> (m)	elev Z <sub>p</sub> (m)
-0.69	288.95
-0.69	289.74
-0.61	289.86
-0.43	289.99
-0.21	290.05
0.00	290.08
0.15	290.07
0.30	290.05
0.46	290.02
0.61	289.98
0.76	289.93
3.72	288.95
3.72	288.65
4.63	288.65
4.63	288.34
5.54	288.34
5.54	288.04
6.46	288.04
6.46	287.73
7.37	287.73
7.37	287.43
8.29	287.43
8.29	287.12
9.20	287.12
9.20	286.82
10.12	286.82
10.12	286.51
11.03	286.51
11.03	286.21
11.95	286.21
11.95	285.90
12.86	285.90
12.86	285.60
13.77	285.60
13.77	285.29
14.69	285.29
14.69	284.99
15.60	284.99
15.60	284.68
16.52	284.68
16.52	284.38
17.43	284.38
17.43	284.07
18.35	284.07
18.35	283.77
19.26	283.77
19.26	283.46
20.17	283.46
20.17	283.16
21.09	283.16
21.09	282.85
22.00	282.85
22.00	282.55
22.92	282.55
22.92	282.24
23.83	282.24
23.83	281.94
24.75	281.94
24.75	281.64
25.66	281.64
25.66	281.33
26.58	281.33
26.58	281.03
27.49	281.03
27.49	280.72
28.40	280.72
28.40	280.42
29.32	280.42
37.85	280.42
37.85	281.03
38.46	281.03
38.46	280.42

Solution 1:

Empirical design aid approach.

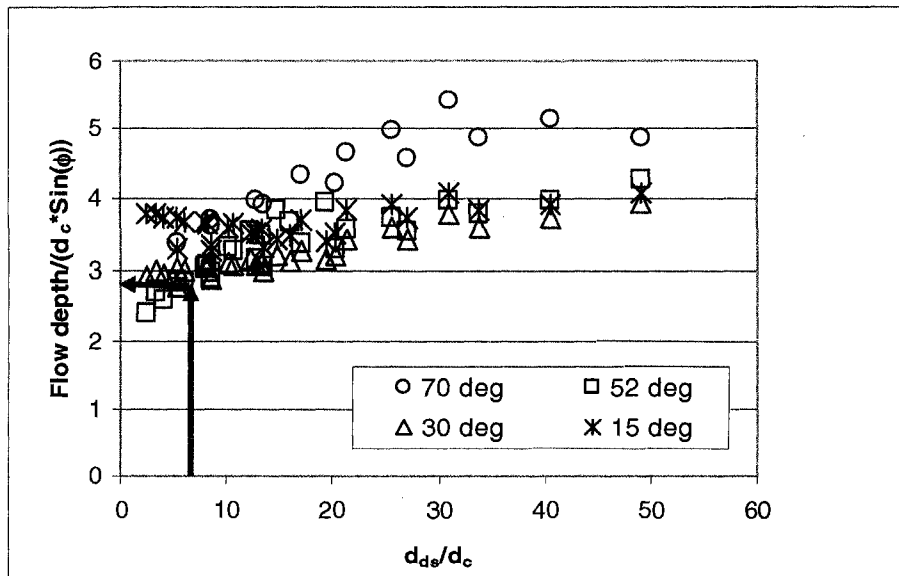


Figure 6.18. Flow depth at the training wall normalized by critical depth at the spillway crest divided by  $\sin(\phi)$  for all tested flows versus the normalized downstream distance ( $d_{sc}$ ) from the spillway crest.

This approach will yield the training wall height for the full length of the spillway chute, but in this example, the training wall height for a specific location was determined. For station, 15.6 m (51.2 ft), the flow depth is approximately 2.02 m (6.6 ft). Using Figure 6.18, the normalized distance down stream is approximately 7.7, which yields a normalized flow depth per  $\sin(\phi)$  of 2.9. With a convergence of  $25^\circ$  and a critical depth of 1.8 m (5.9 m), the flow depth is then calculated as

$$FlowDepth = 2.9d_c * \sin \phi = 2.2 \text{ m}$$

Therefore, the approximate training wall height at station 15.6 m (51.2 ft) should be 2.2 m (7.2 ft).

Solution 2:

Theoretical approach.

Using the same station and flow depth 15.6 m (51.2 ft) and 2.02 m (6.6 ft), respectively, the training wall height was estimated using the theoretical relationship presented in Equation 6.5.

$$H_w = \frac{(1 + 0.2 * \sin^2(\phi)) * \sqrt{\frac{\gamma d^2 \cos \theta}{2} + \rho v^2 d (\cos(\theta) \cos(\psi) \sin(\phi) + \sin(\theta) \sin(\phi))^2} * 2}{\gamma \cos(\psi_2) \cos(\psi) \cos(\psi_2)} \quad (6.5)$$

where the  $\gamma$  = specific weight of water,  $d$  = the flow depth in the center of spillway,  $\theta$  = chute slope,  $\rho$  = the density of water,  $v$  = velocity of the spillway flow as it descends the chute,  $\psi = \tan^{-1}(\sin(\phi) \tan(\theta))$ ,  $\phi$  = convergence angle, and  $\psi_2 = \tan^{-1}(\cos(\phi) \tan(\theta))$ .

The following parameters are required to apply Equation 6.5:

$\phi = 25^\circ$ ,  $\gamma = 9.8 \text{ kN/m}^3$  (64.4 lb/ft<sup>3</sup>),  $d = 2.02 \text{ m}$  (6.63 ft),  $\theta = 18.4^\circ$  (3H:1V),  $\rho = 999 \text{ kg/m}^3$  (1.94 slugs/ft<sup>3</sup>),  $v = q/d = (7.6 \text{ m}^3/(\text{s}\cdot\text{m}))/2.02 \text{ m} = 3.76 \text{ m/s}$  (12.3 ft/s),  $\psi = 8^\circ$ , and  $\psi_2 = 16.8^\circ$ .

With the above known parameters, the approximate training wall height necessary to retain the design flow is 2.6 m (8.6 ft).

As shown using both the empirical and theoretical methods, the training wall height necessary to retain the design flow at station 15.6 m (51.2 ft) is 2.2 m (7.2 ft) and 2.6 m (8.6 ft), respectively. Both the empirical and theoretical methods provide conservatism in the approaches because of the probable maximum flood used to design the training wall. Additionally, for this spillway chute design, aerated flow is not expected to fully develop in the spillway chute, so no additional conservatism should be required in the design of the training walls for this given example.